MARCH 2019 DIAGNOSIS LIST

19-0301: Rhinosporidiosis (sinonasal; ID pathology)
19-0302: cryptococcosis (lung; ID pathology)
19-0303: metastatic yolk sac tumor (bladder; GU pathology)
19-0304: primary intracranial sarcoma, DICER1-mutant (brain; neuropathology)
19-0305: de-differentiated liposarcoma (mediastinum; soft tissue pathology)
19-0306: atrophic kidney-like lesion (kidney; GU pathology)
19-0307: well-differentiated neuroendocrine tumor (carcinoid) (kidney/GU pathology)
19-0308: intrarenal ectopic adrenal tissue (kidney; GU pathology)
19-0309: c/w sporadic renal cell carcinoma with eosinophilic and vacuolated cytoplasm, with somatic TSC2/mTOR mutation (kidney; GU pathology)
19-0310: copper deficiency (bone marrow; hematopathology)

Disclosures
March 4, 2019

Dr. Ankur Sangoi has disclosed a financial relationship with Google (consultant). South Bay Pathology Society has determined that this relationship is not relevant to his role as planner and moderator and presenter of the clinical cases being presented.

The following planners and faculty had no financial relationships with commercial interests to disclose:

Presenters:

Nabeen Nayak, MD
Balaram Puligandla, MD
Jordan Taylor, MD
Emily Chan, MD
Jeffrey Hofmann, MD
Arie Perry, MD
Hannah Wang, MD
Gerald Berry, MD
Li Lei, MD
Megan Troxell, MD, PhD
Sharon Wu, MD

Activity Planners/Moderator:

Kristin Jensen, MD
Megan Troxell, MD, PhD

19-0301

Nabeen Nayak ; Sir Ganga Ram Hospital, New Dehli

68-year-old male presents with intermittent epistaxis for 2 weeks. Examination reveals irregular, partly polypoid, sessile soft tissue mass in left nasal cavity extending from medial meatus to nasopharynx.

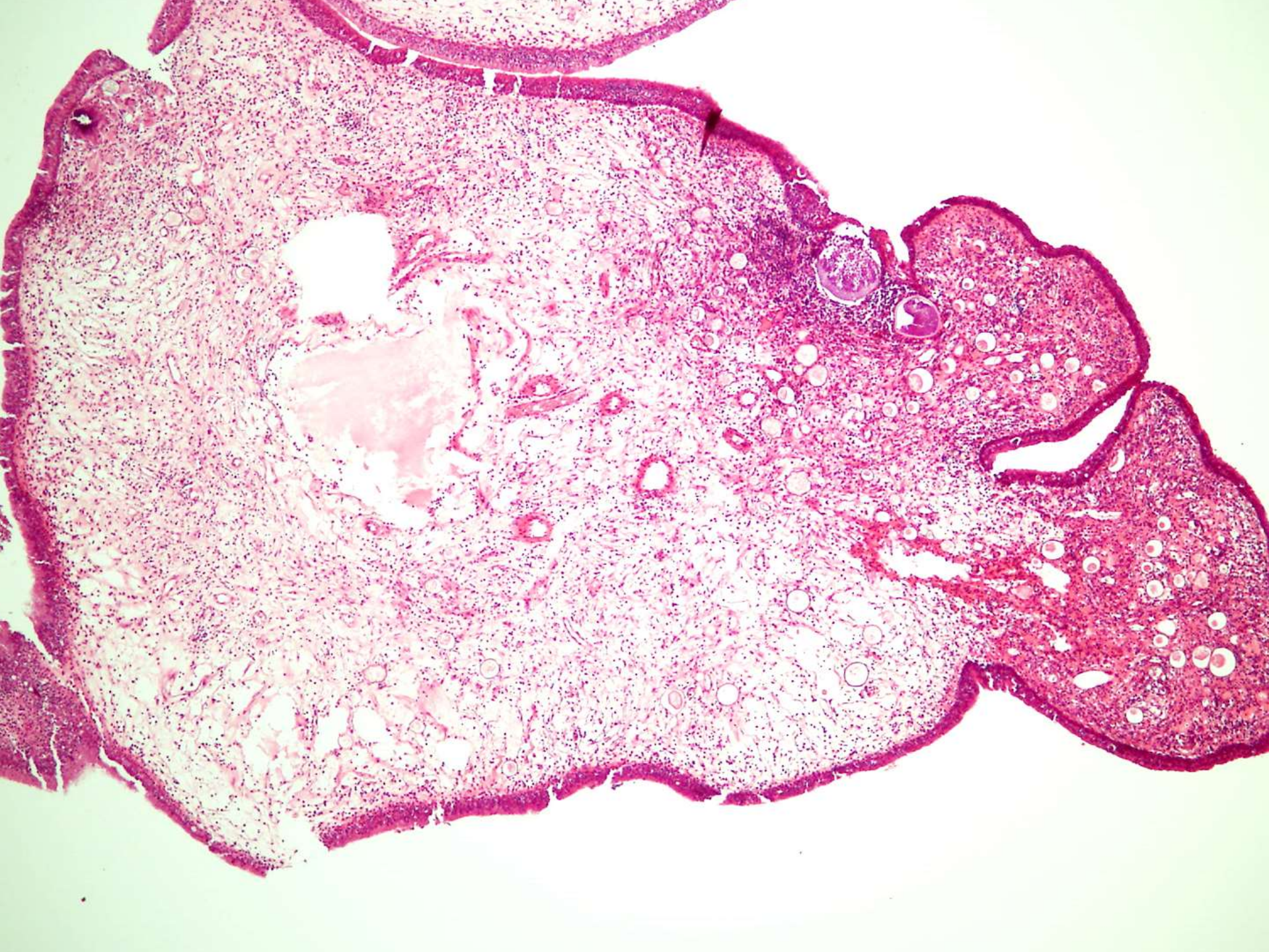

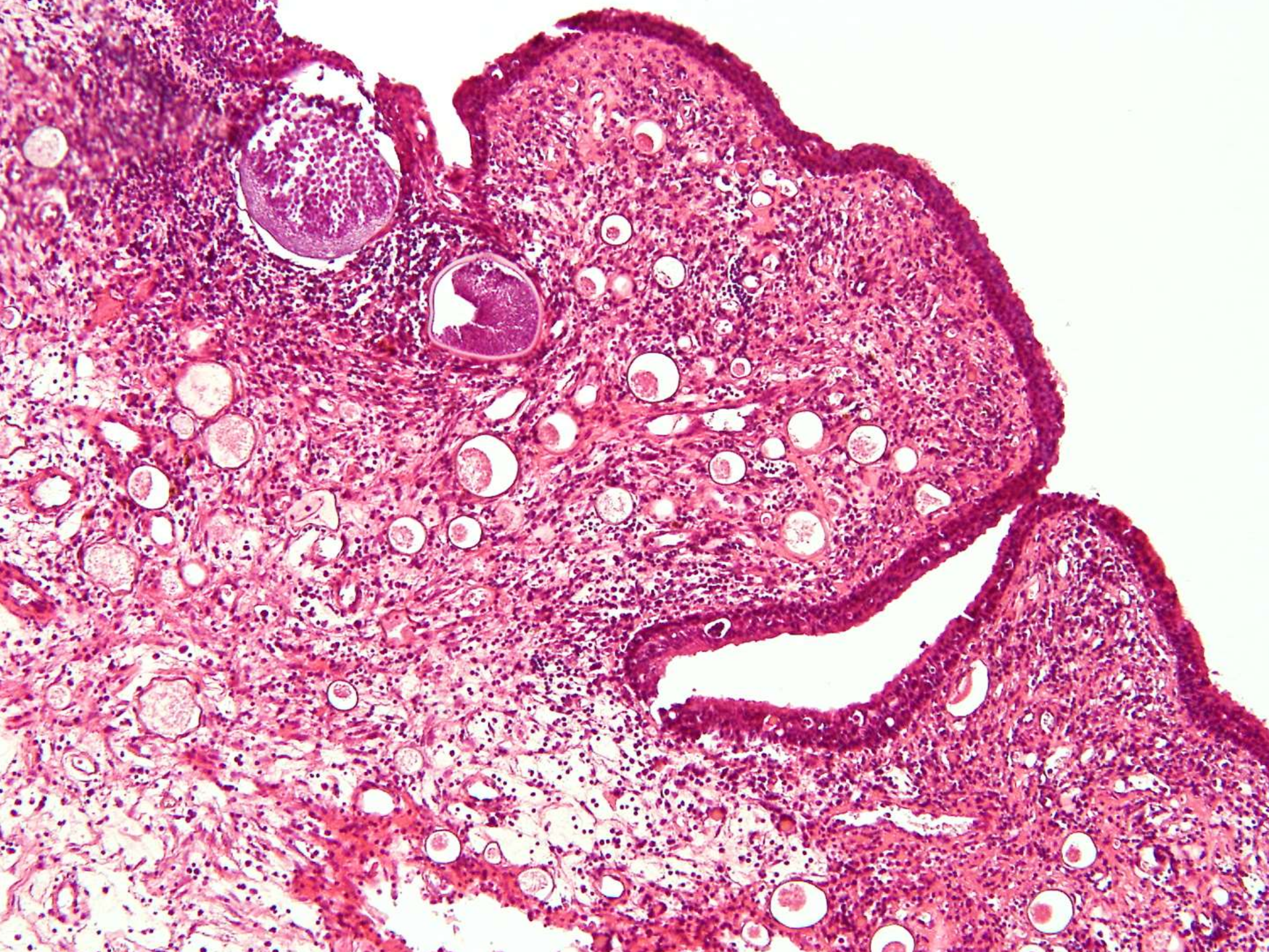

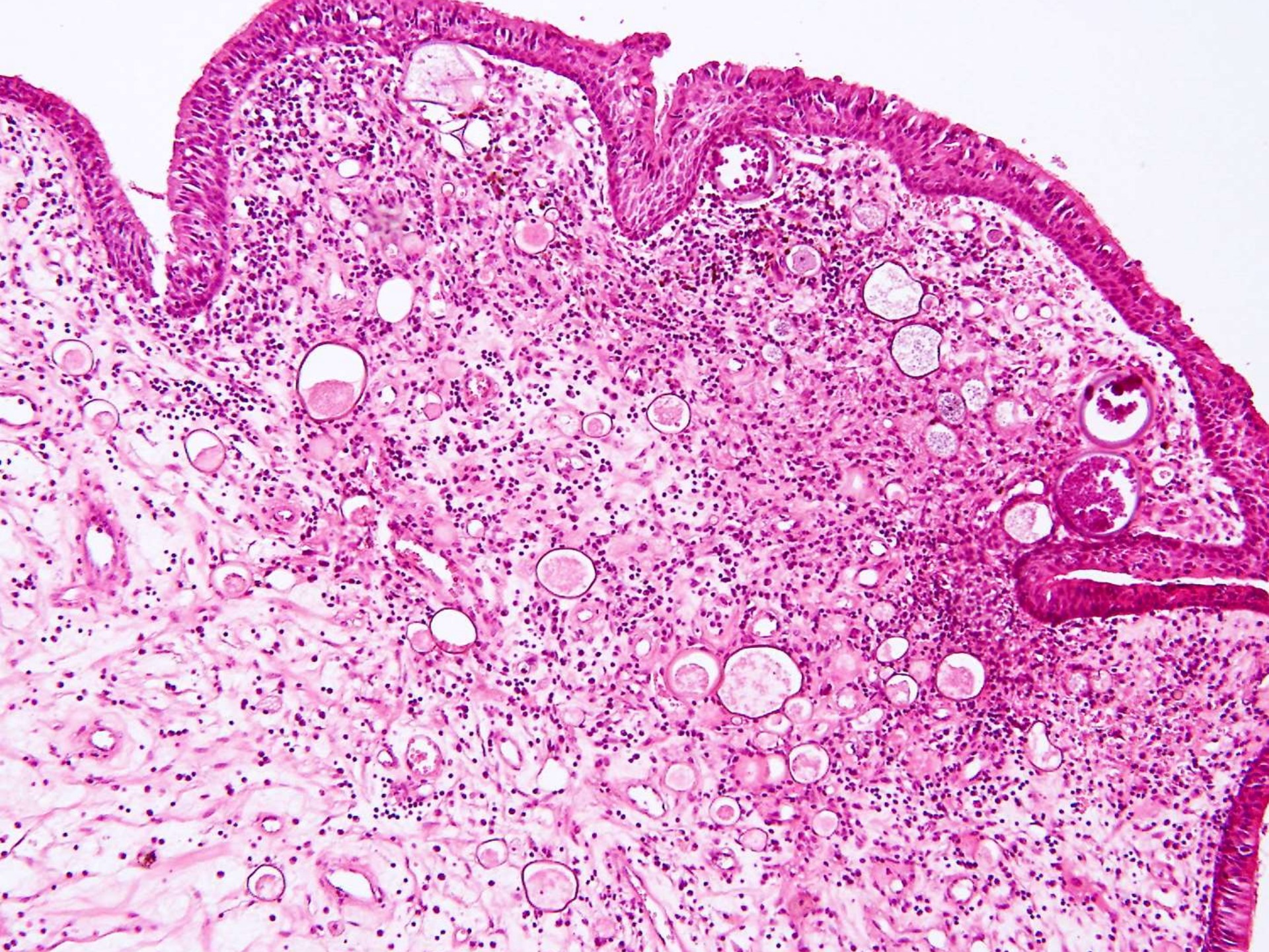

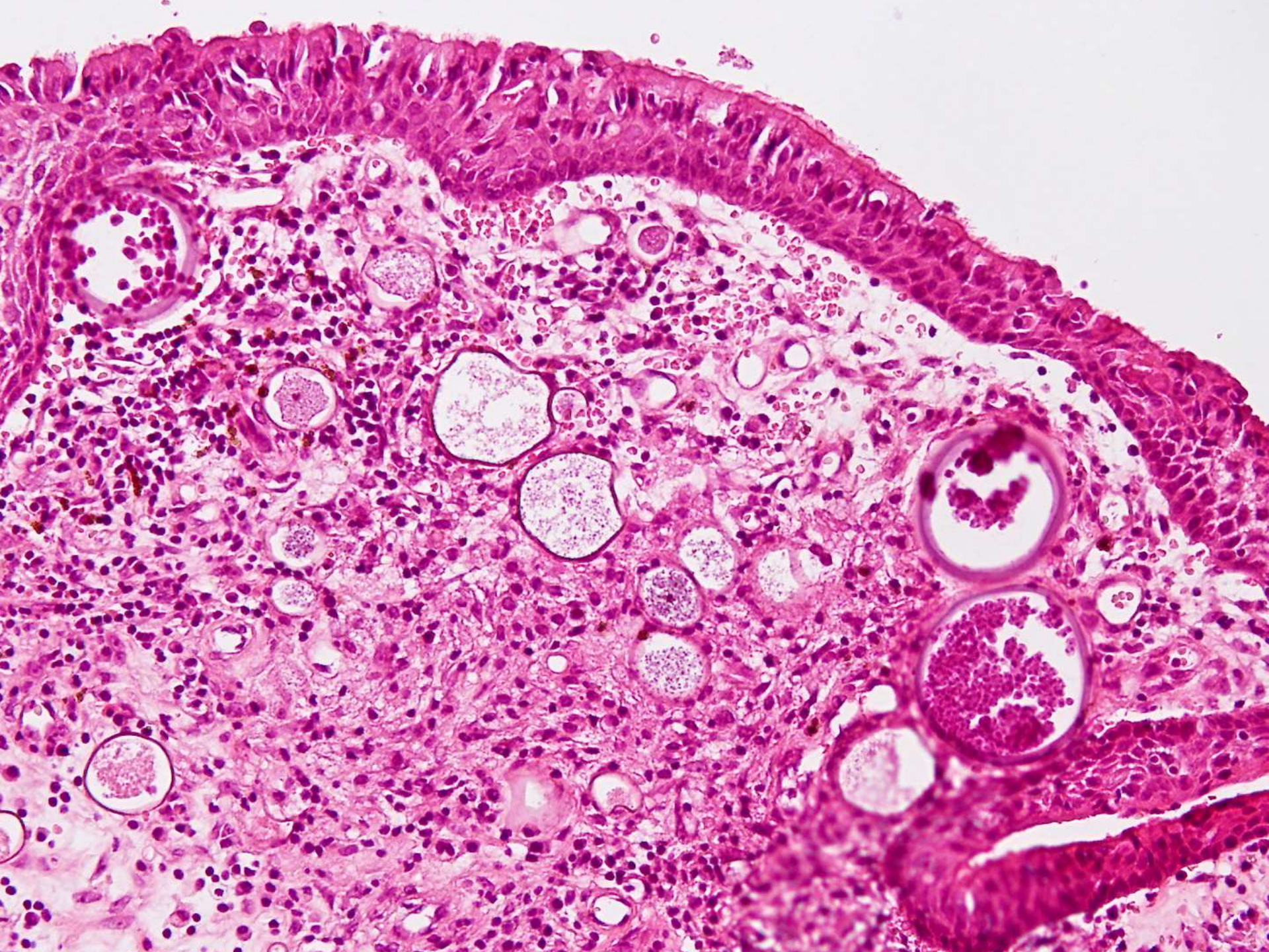

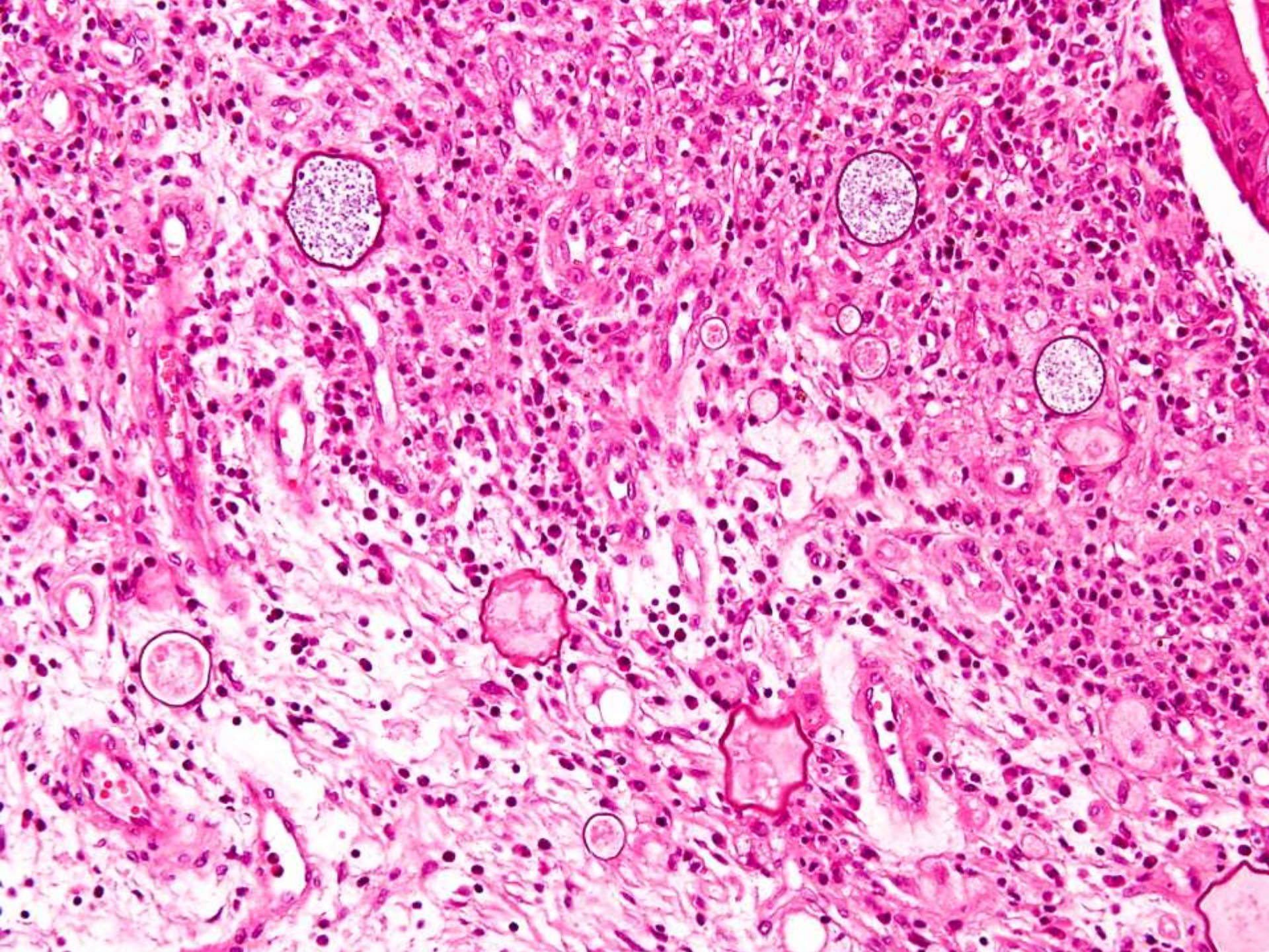

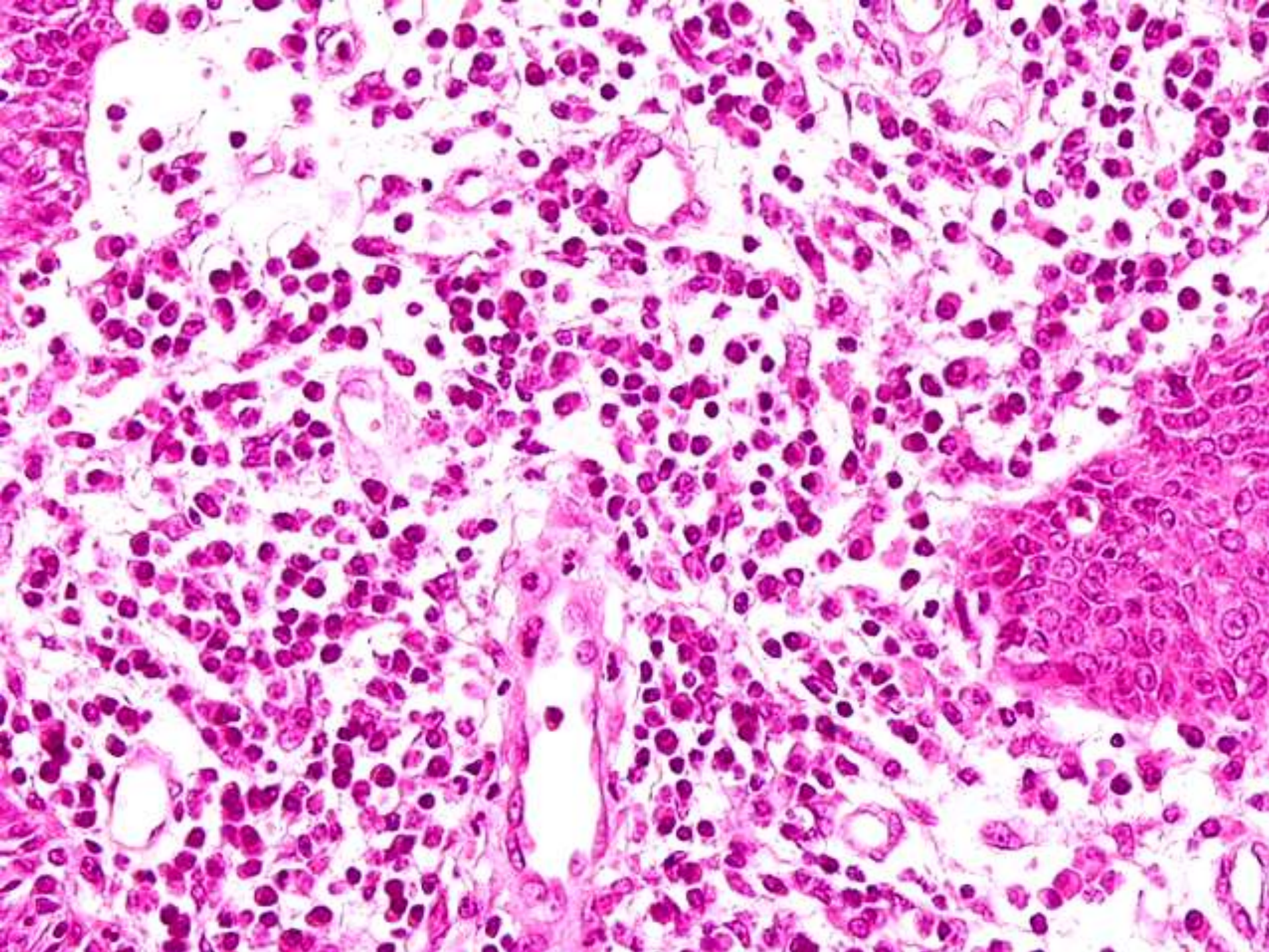

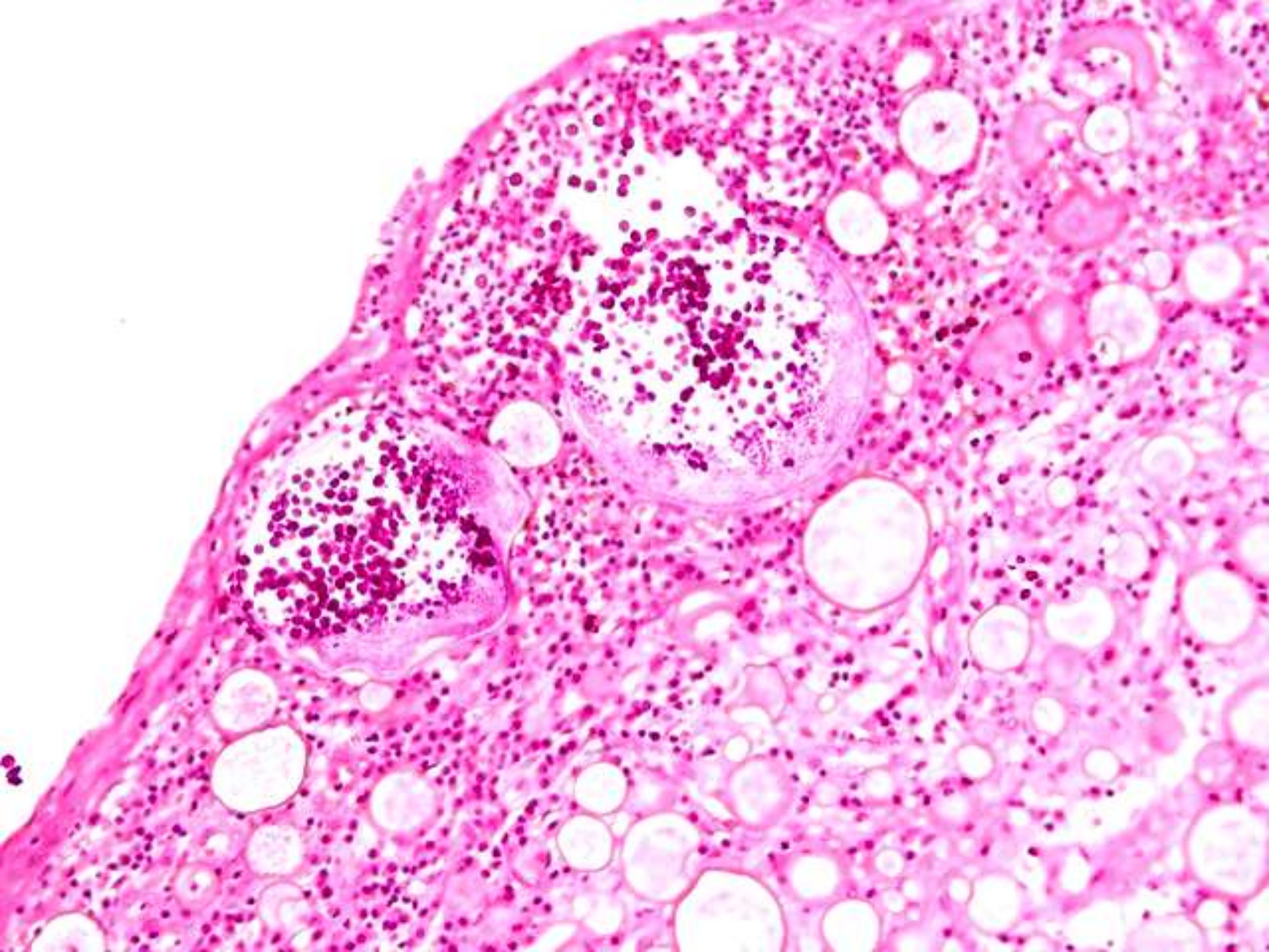

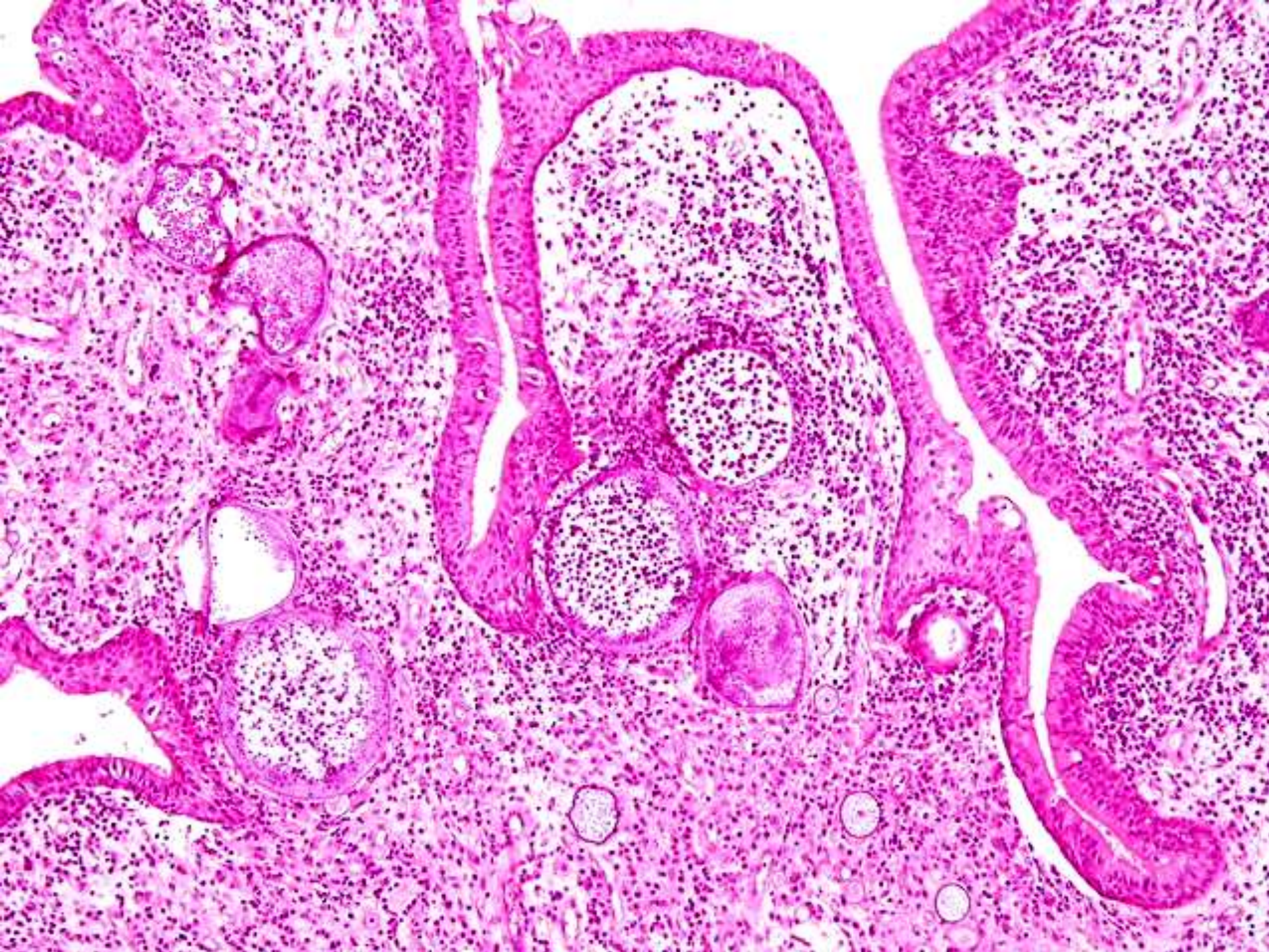

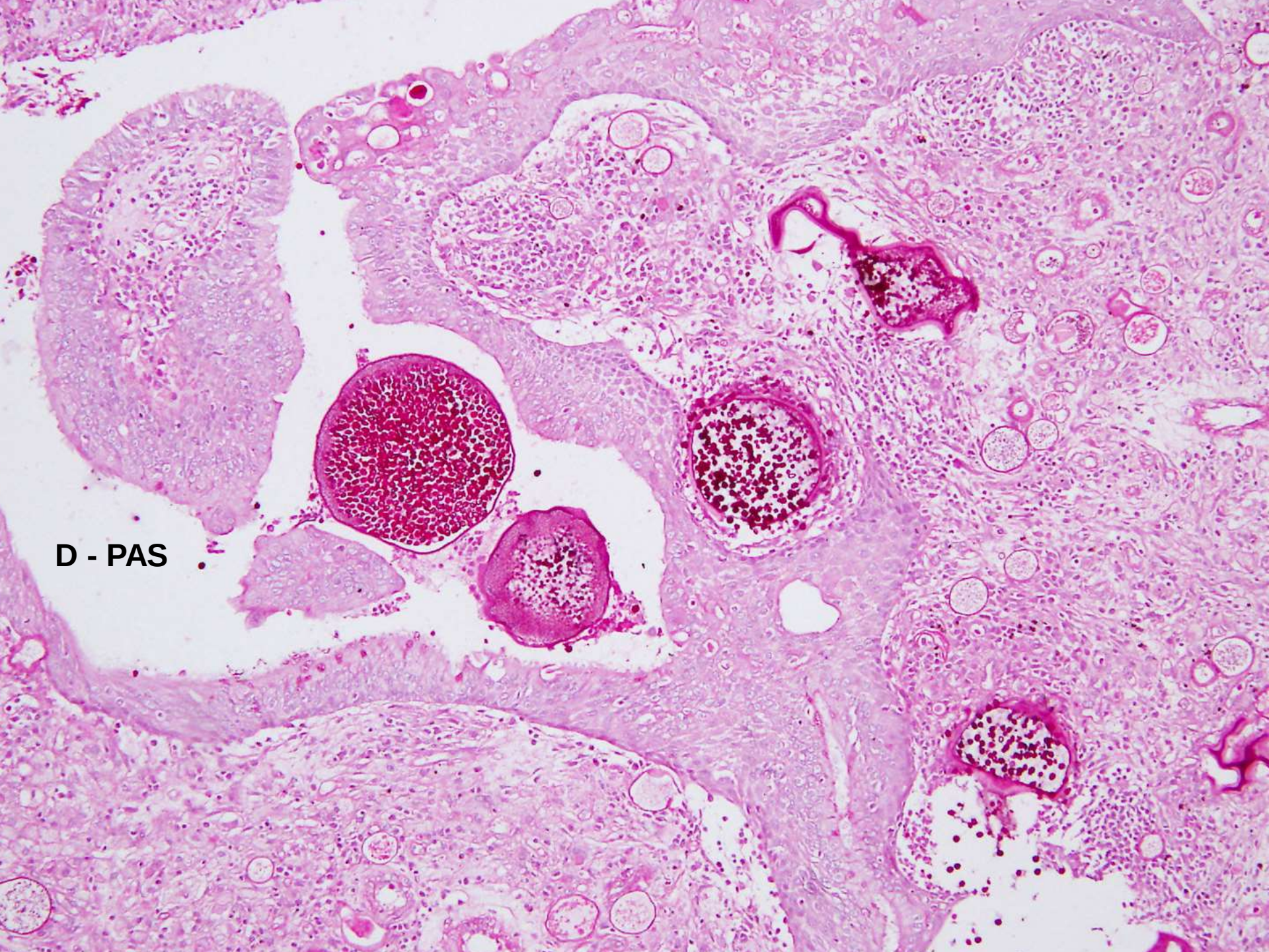
D - PAS

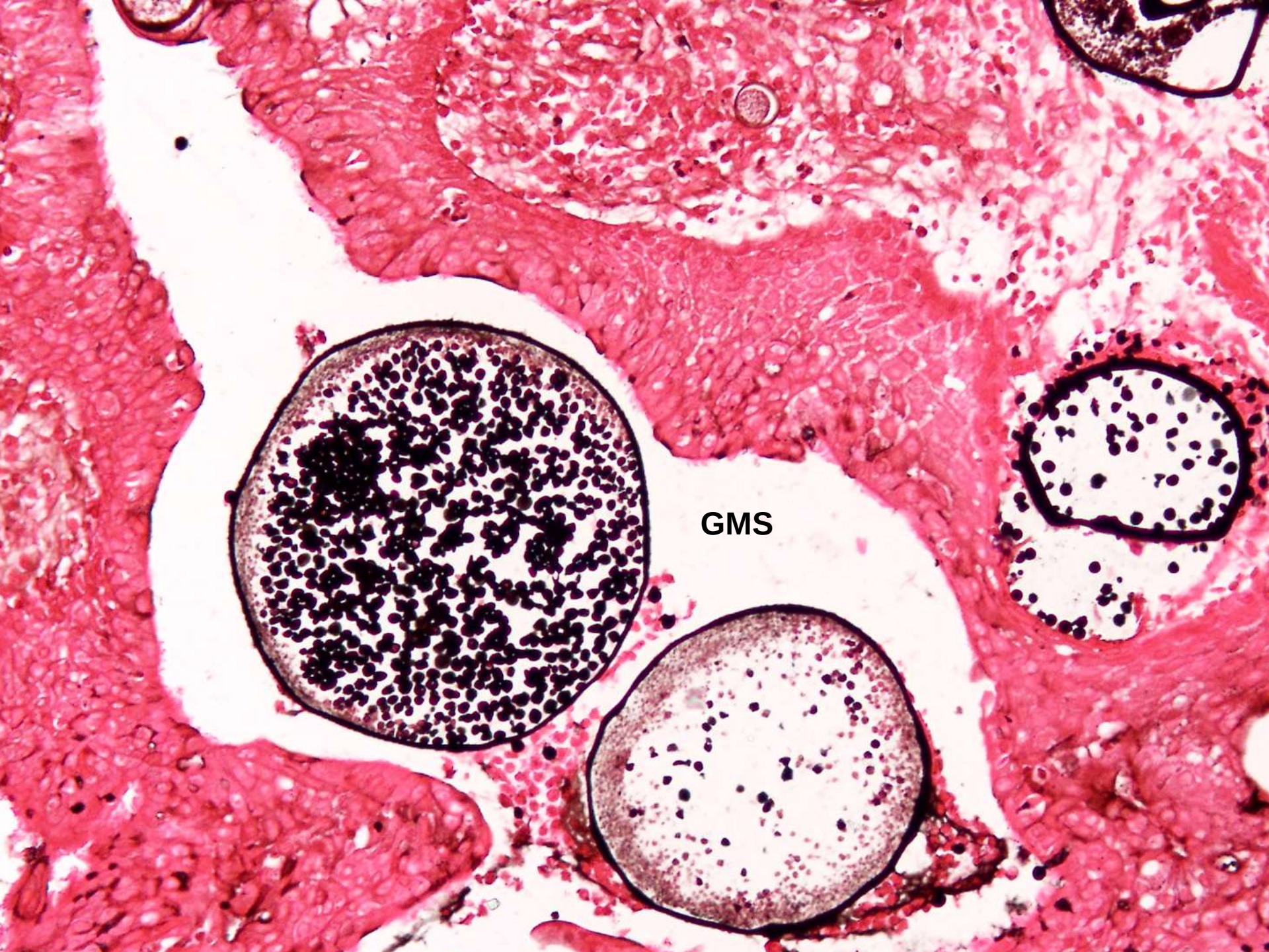
GMS

Diagnosis: Rhinosporidiosis, Nasal cavity

This disease is relatively simple to identify on histology but is very rarely encountered.

The phylogenic assignment of the causative agent, ***Rhinosporidium seeberi*** has remained uncertain for nearly a century, even though generally considered to have features of a fungus.

From early 2000 on molecular studies suggested it to belong to a novel class of Aquatic Protistan Parasites. More recent work using 18S rRNA gene sequencing however, seem to confirm that R. seeberi is some form of a low order Aquatic Fungus.

Natural Habitat: Non-flowing reservoir water as in Ponds

Even though reported from several mostly tropical and sub-tropical countries the vast majority of cases (95%) occur in India and Sri Lanka, the latter having the highest per-capita incidence rate globally.

Sites affected:

Nose & Nasopharynx (sometimes extending to the back of mouth)	- 90-95%
Eyes	- 3-5%
Skin & Genitalia	- very rare

Infection occurs through prolonged contact with stagnant water reservoir as Ponds / soil around them (confirmed on epidemiologic occurrence of cases in endemic, low socio-economic areas.)

19-0302
(scanned slide available)

Balaram Puligandlia; Kaiser Oakland

34-year-old male with h/o right orchiectomy in 2012 for seminoma. Now presents with pulmonary nodule. Right lower lobe of lung wedge resection performed.

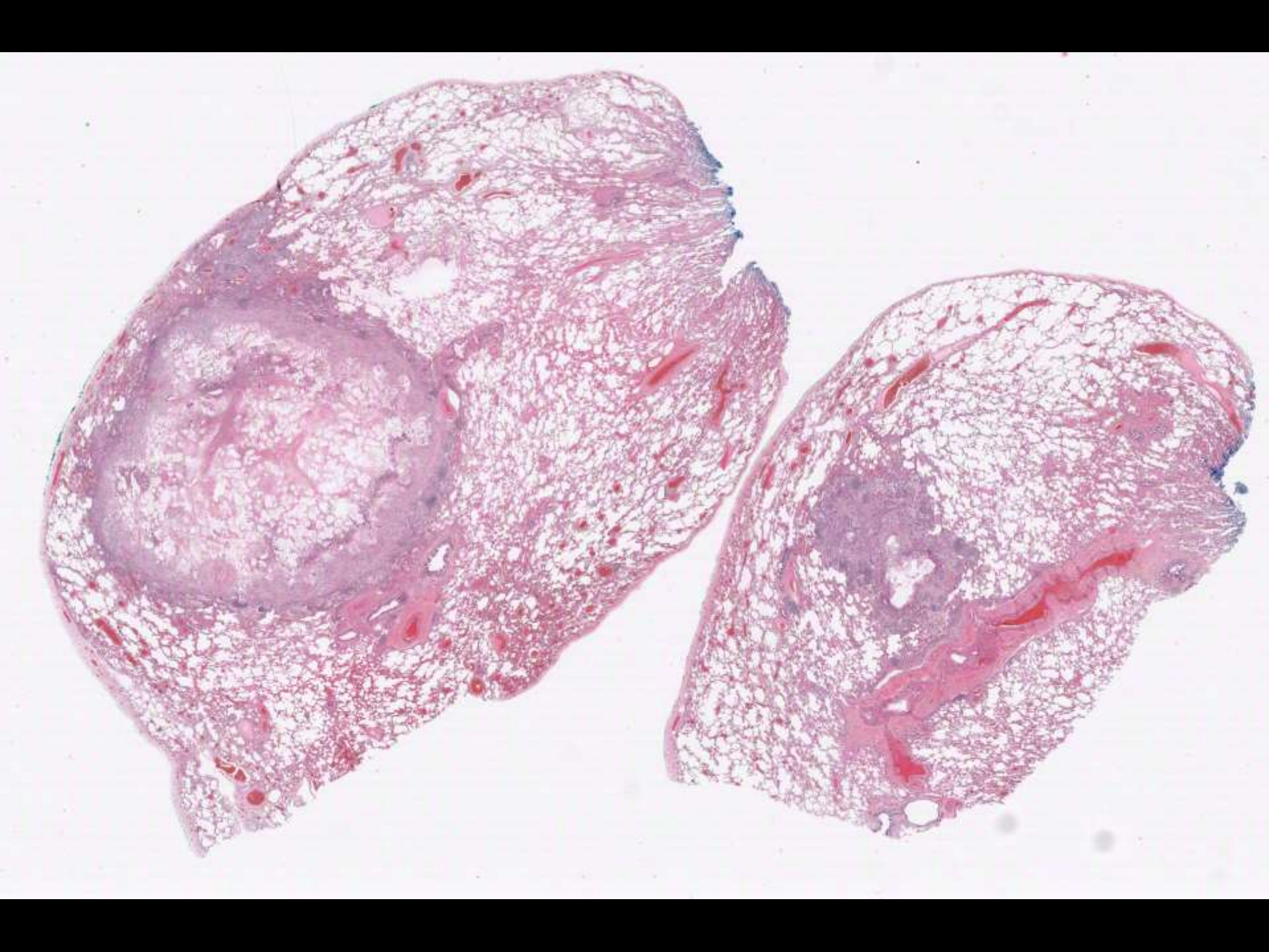

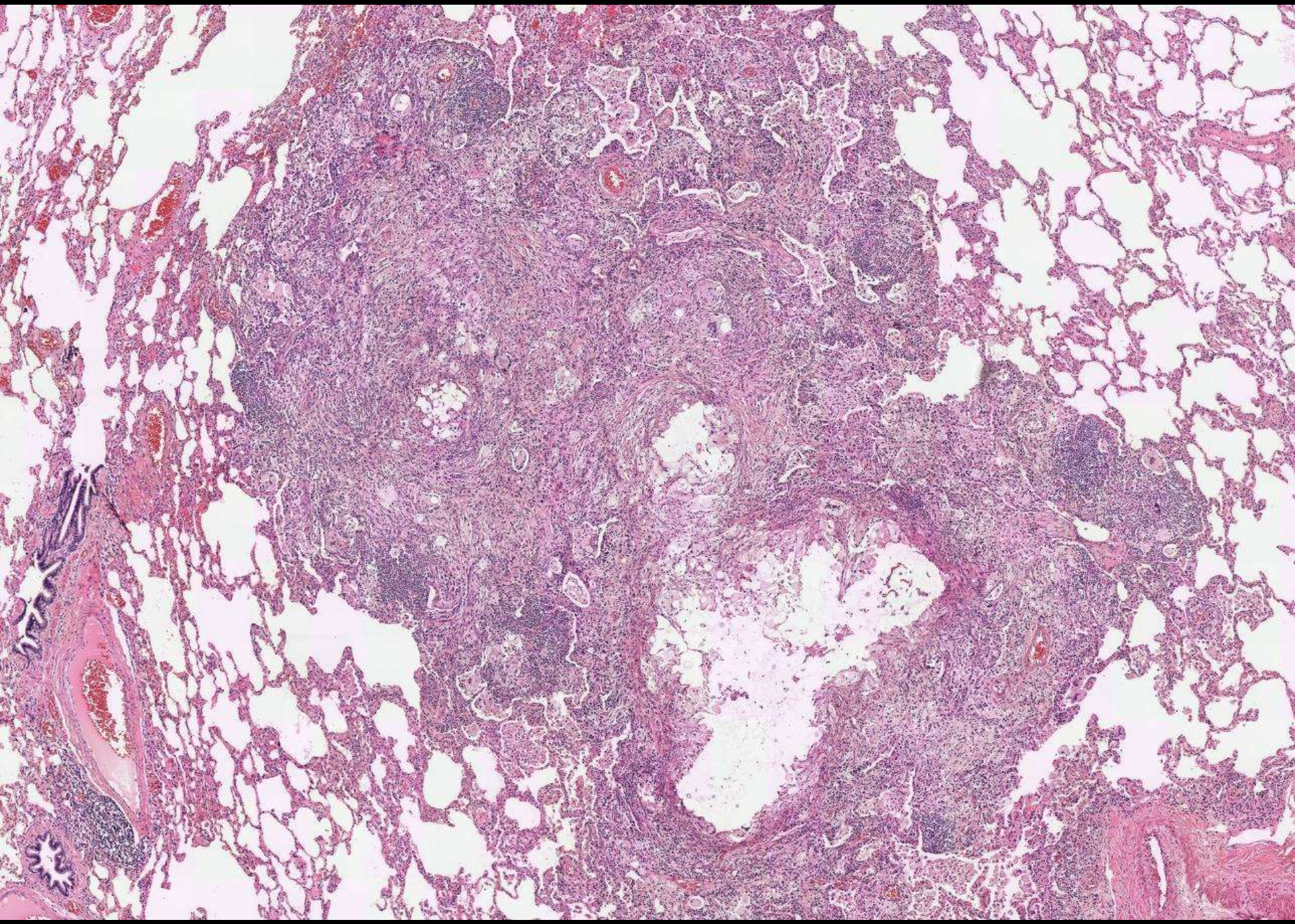

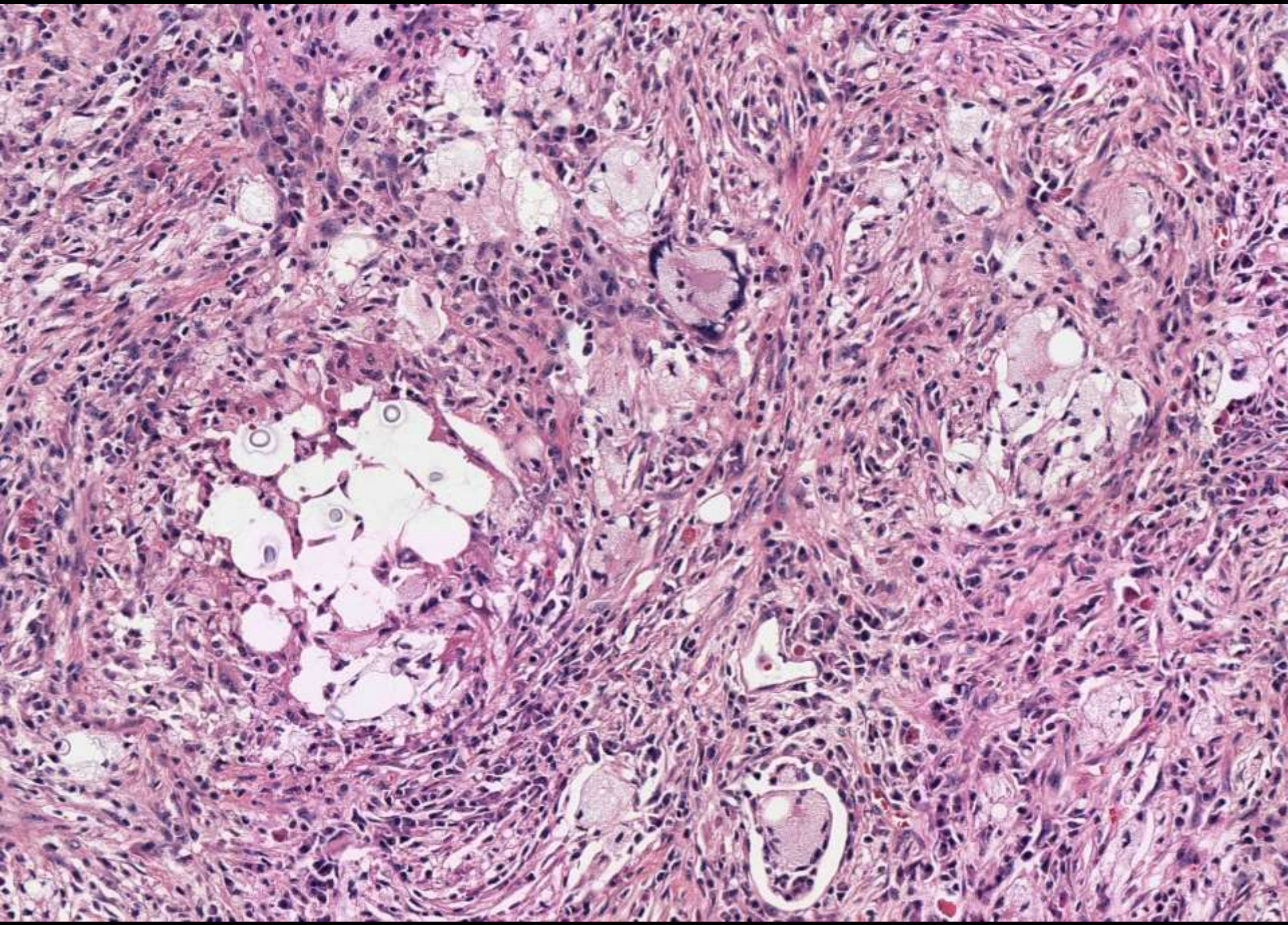

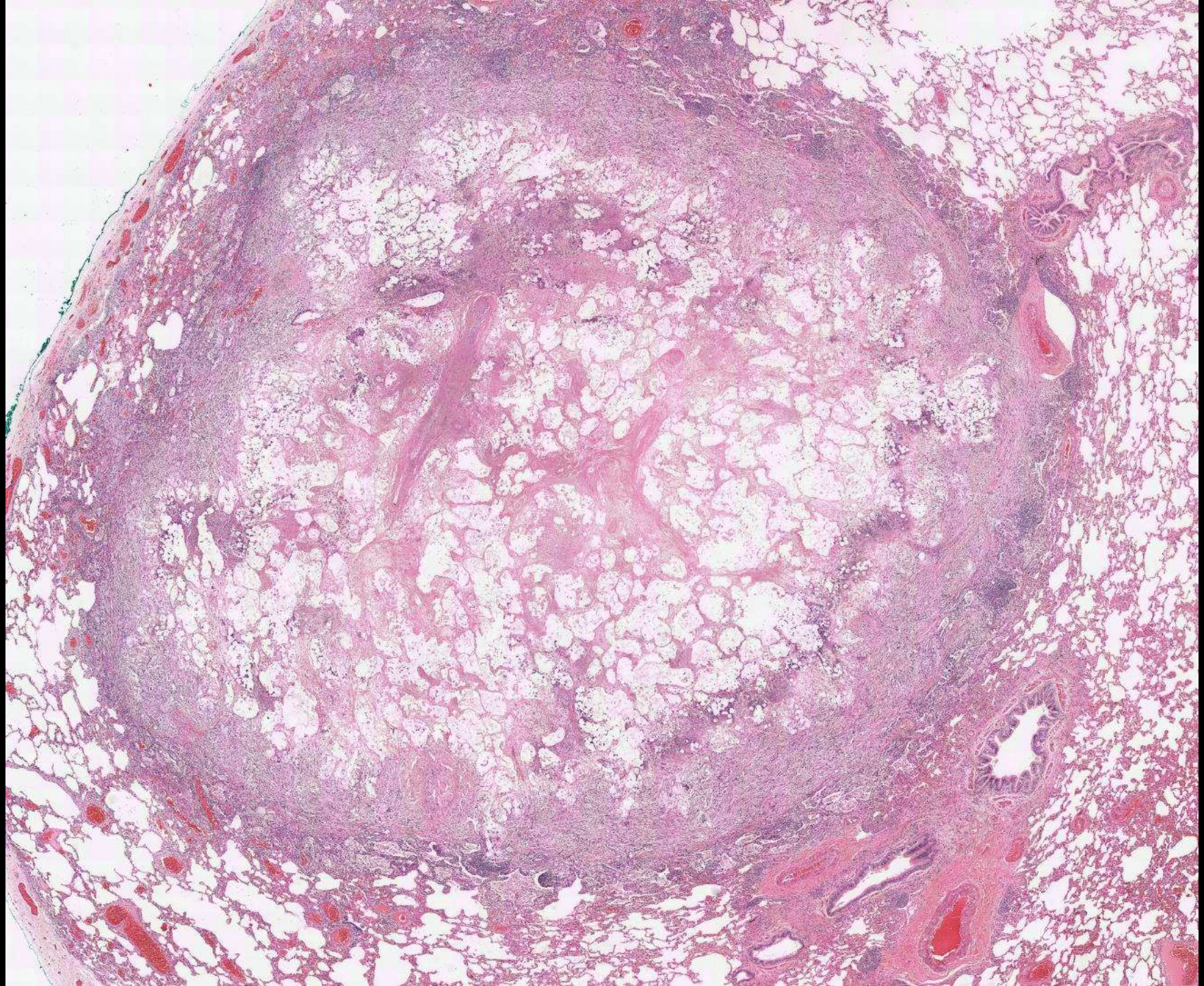

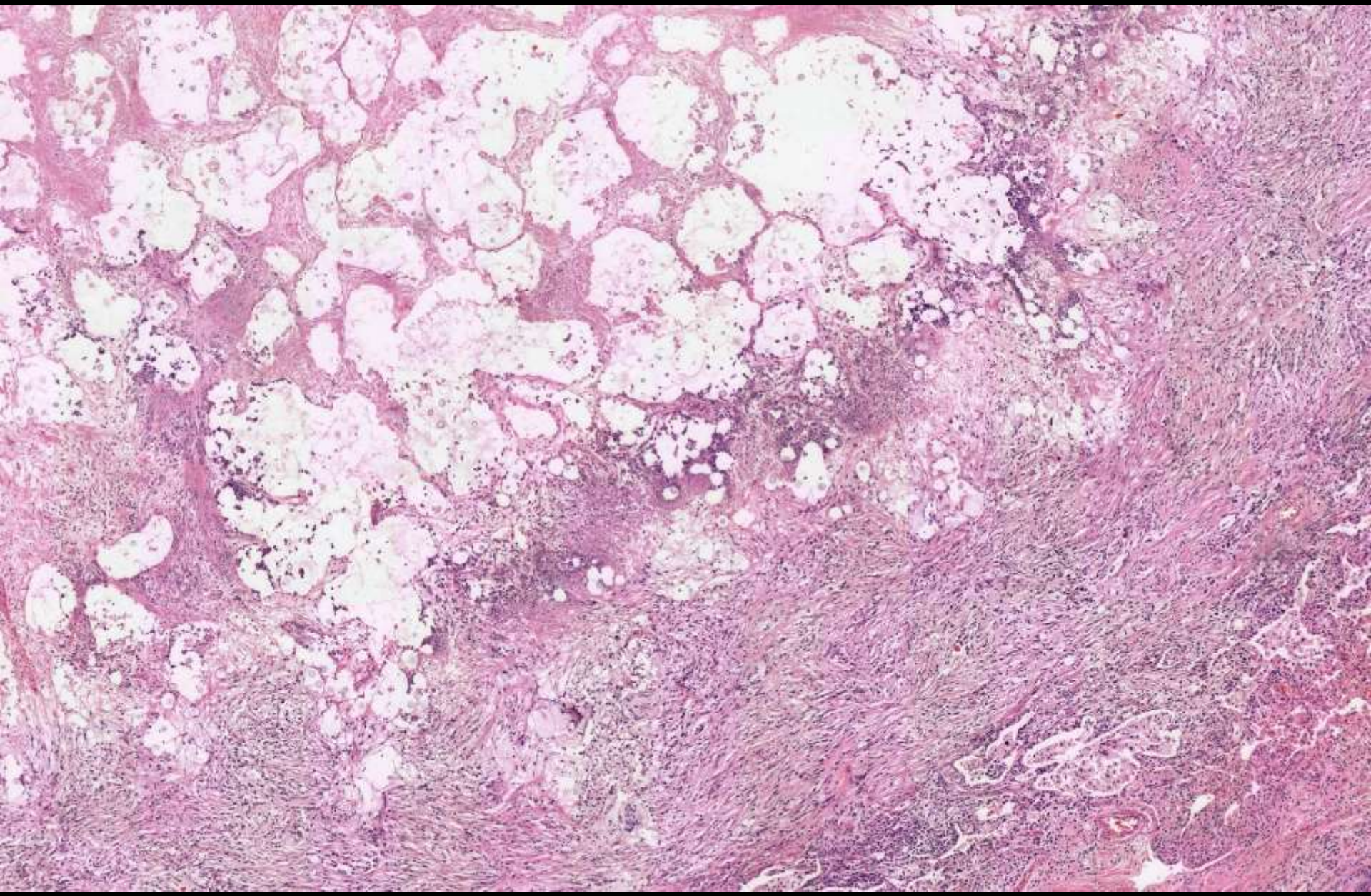

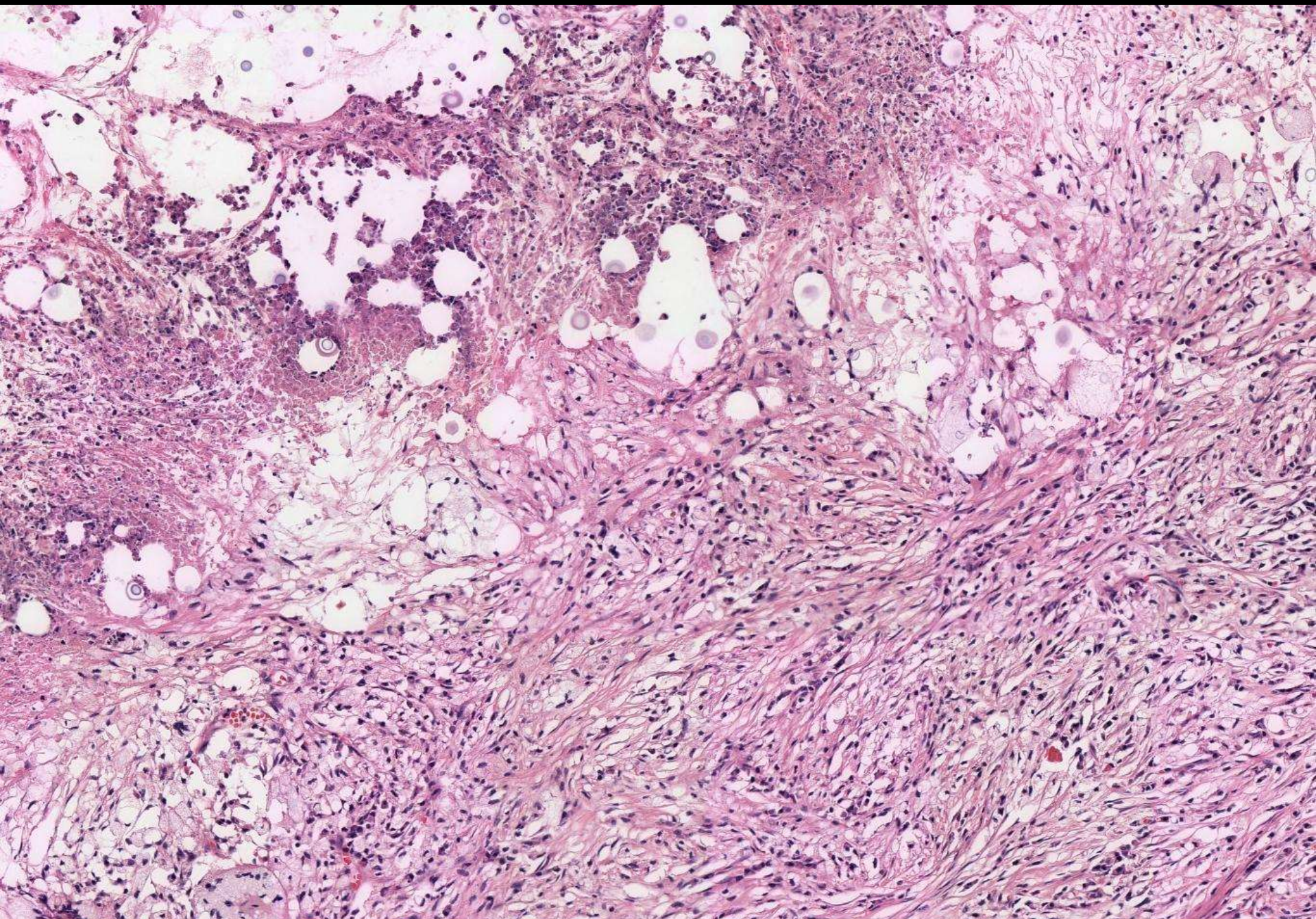

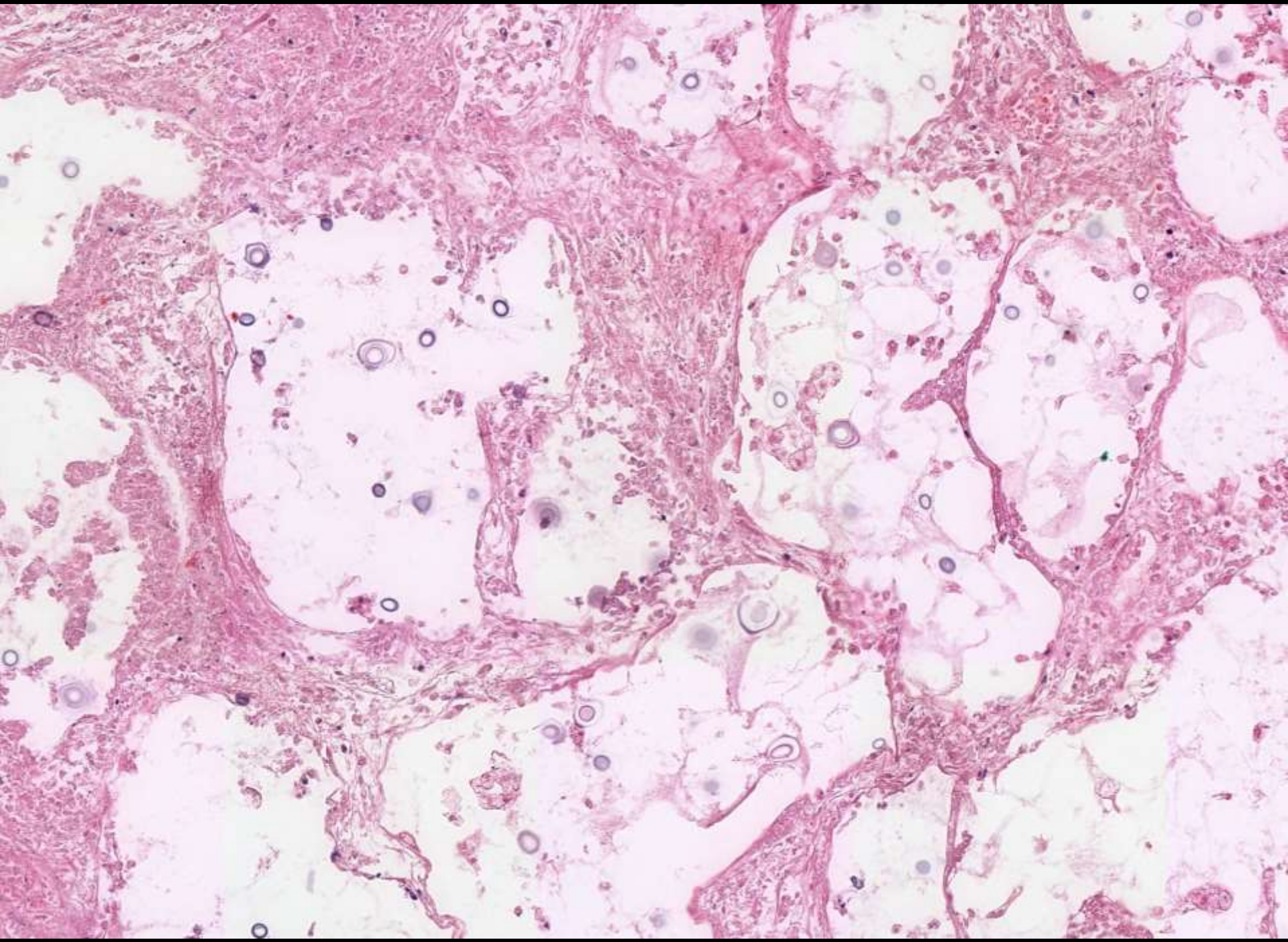

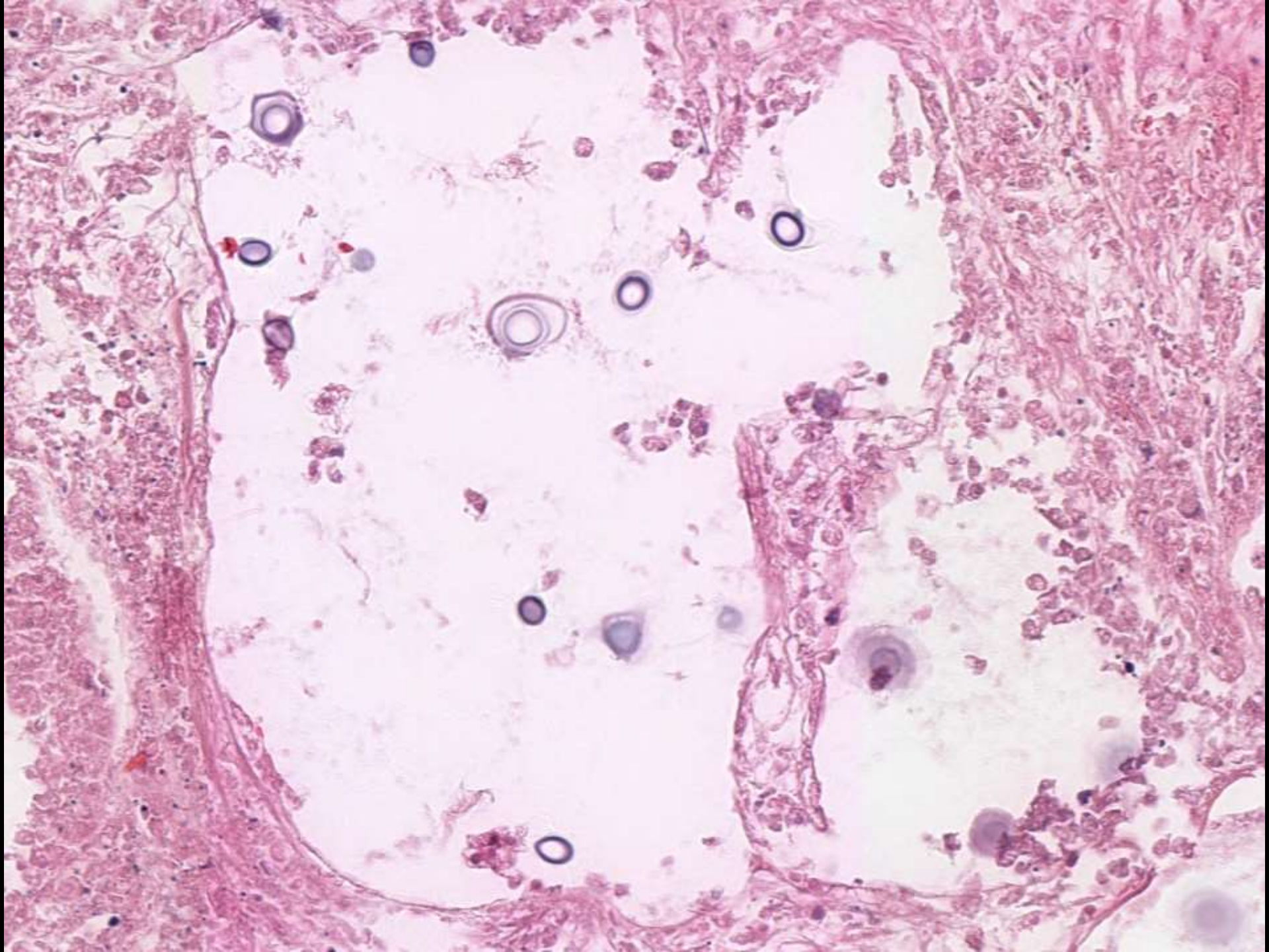

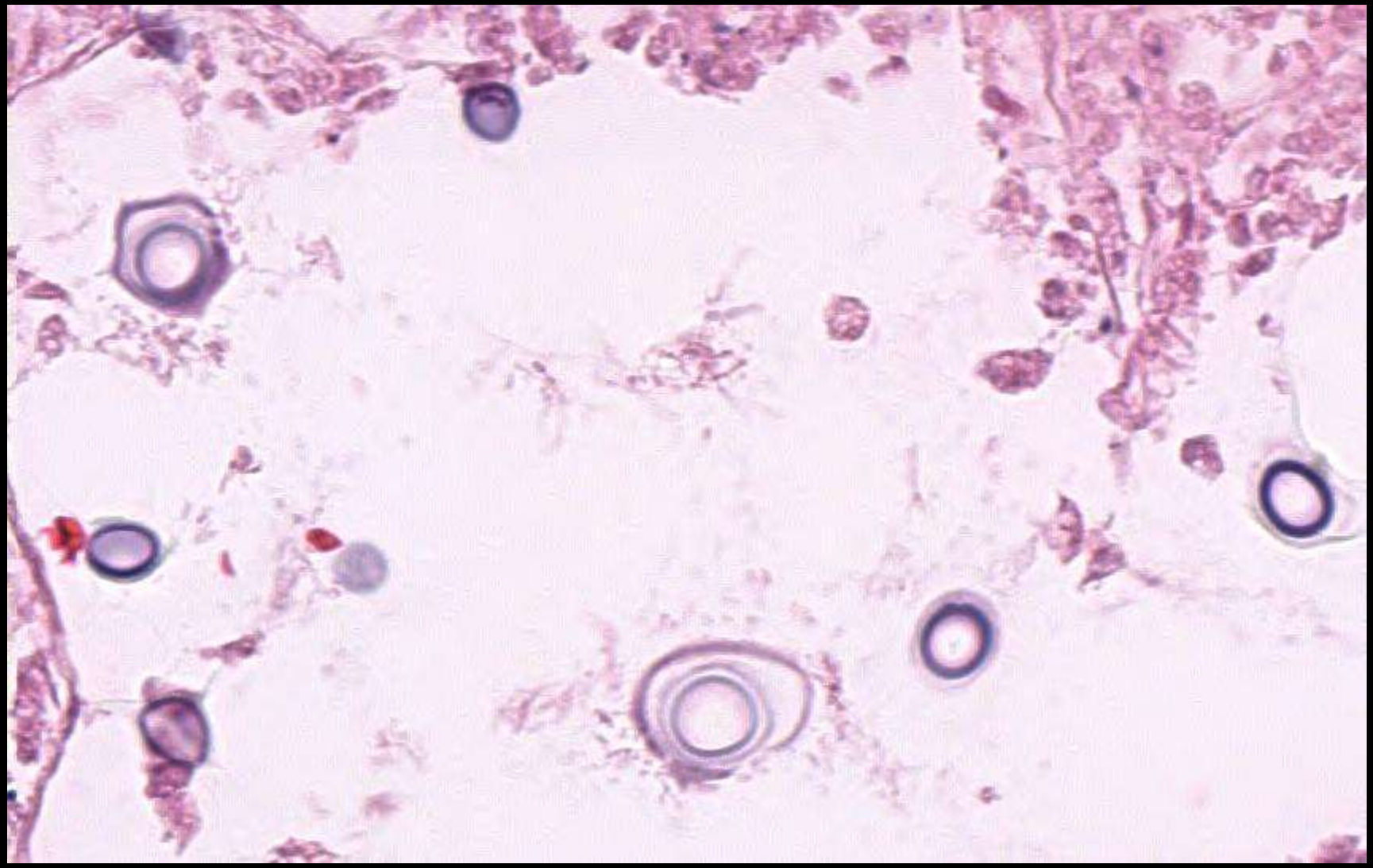

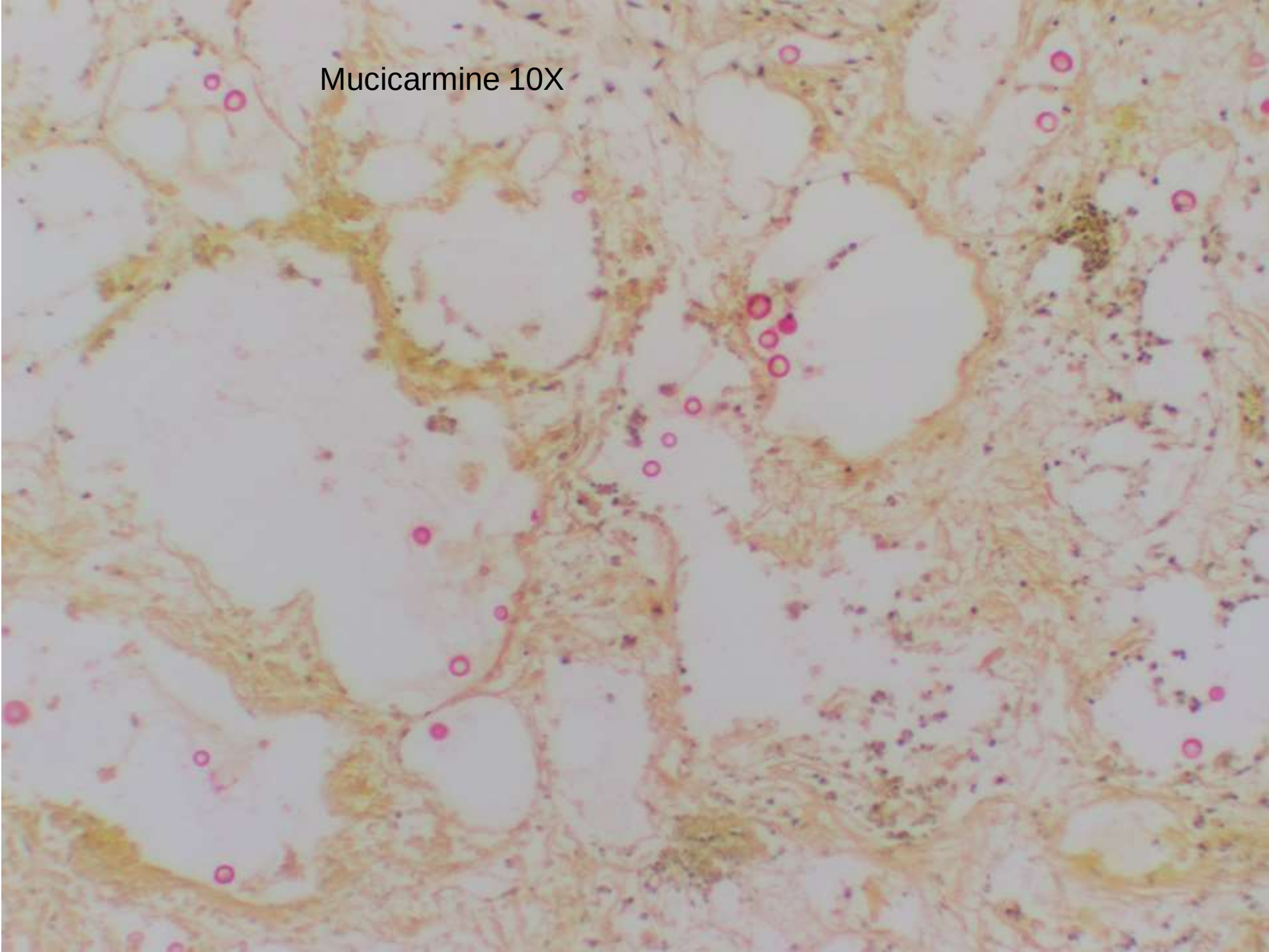
Mucicarmine 10X

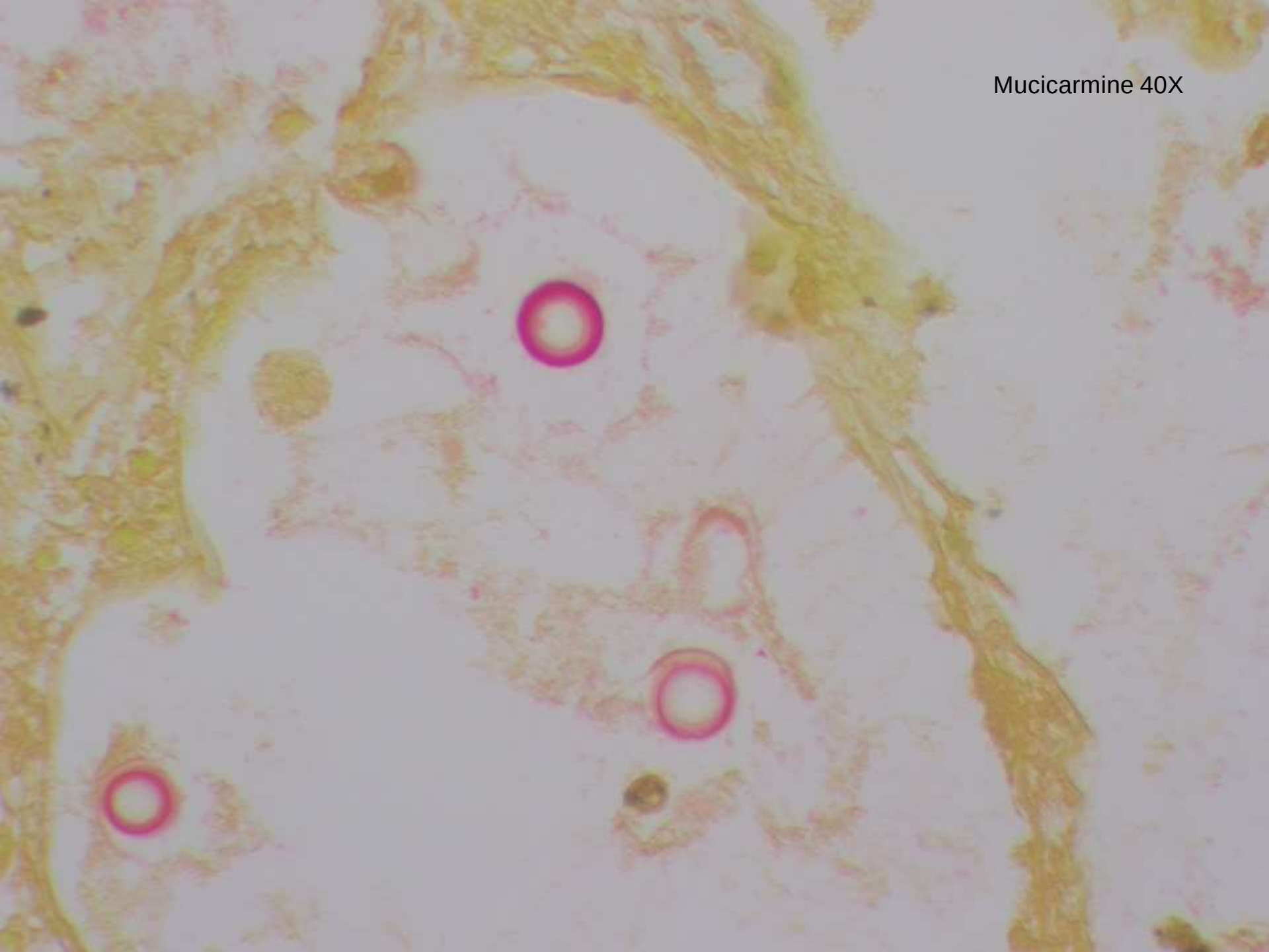
Mucicarmine 40X

CRYPTOCOCCOSIS

- World wide distribution, soil organism
- Infection occurs via inhalation of yeast cells or spores
- Cryptococcus is the only fungus with a mucicarmine-positive capsule.
- C. neoformans and C. gatti cause most of the infections

Semin Respir Crit Care Med 2011;32: 727-734:

CRYPTOCOCCOSIS

- 1 M cases and 625,000 deaths/year due to meningitis among HIV infected patients worldwide.
- Other risk factors: Long Term Corticosteroid Rx, Solid Organ Transplant, heme malignancies, sarcoidosis, dysfunction of cell mediated immunity and TNF-Alpha Rx.

Semin Respir Crit Care Med 2011;32: 727-734

CRYPTOCOCCOSIS

- Meningoencephalitis is the most frequent manifestation.
- Pneumonia is underdiagnosed, especially in non immuno compromised individuals
- Dx requires isolation by culture on blood agar or Sabouraud's Dextrose agar.
- Rx: Fluconazole 6-12 months. For severe disease induction with Amphotericin B for 2-4 weeks followed by Fluconazole.

Semin Respir Crit Care Med 2011;32: 727-734

19-0303
(scanned slide available)

Jordan Taylor/Emily Chan; UCSF

58-year-old male with incidental 1cm urinary bladder mass with thin stalk at bladder neck found.

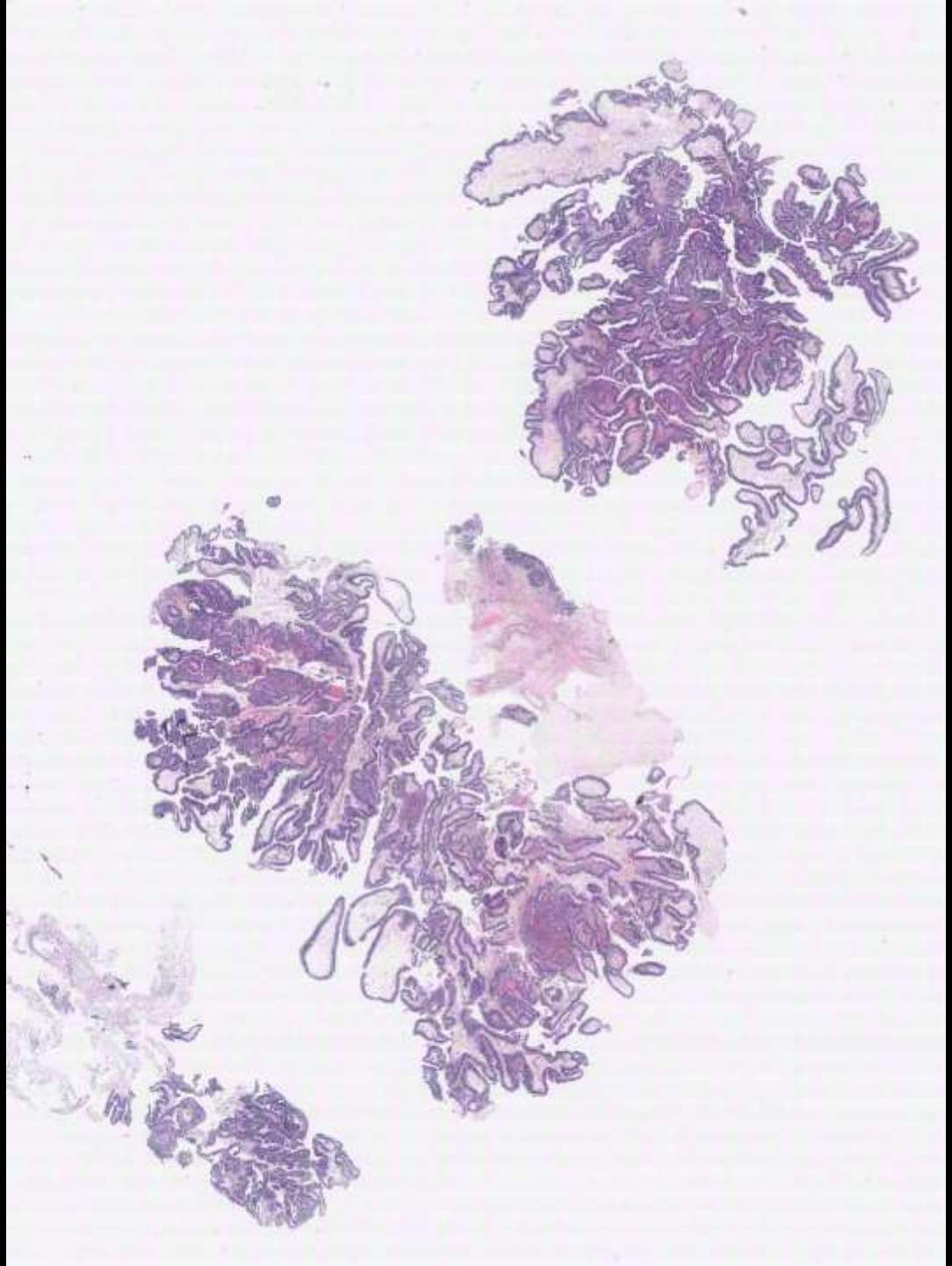

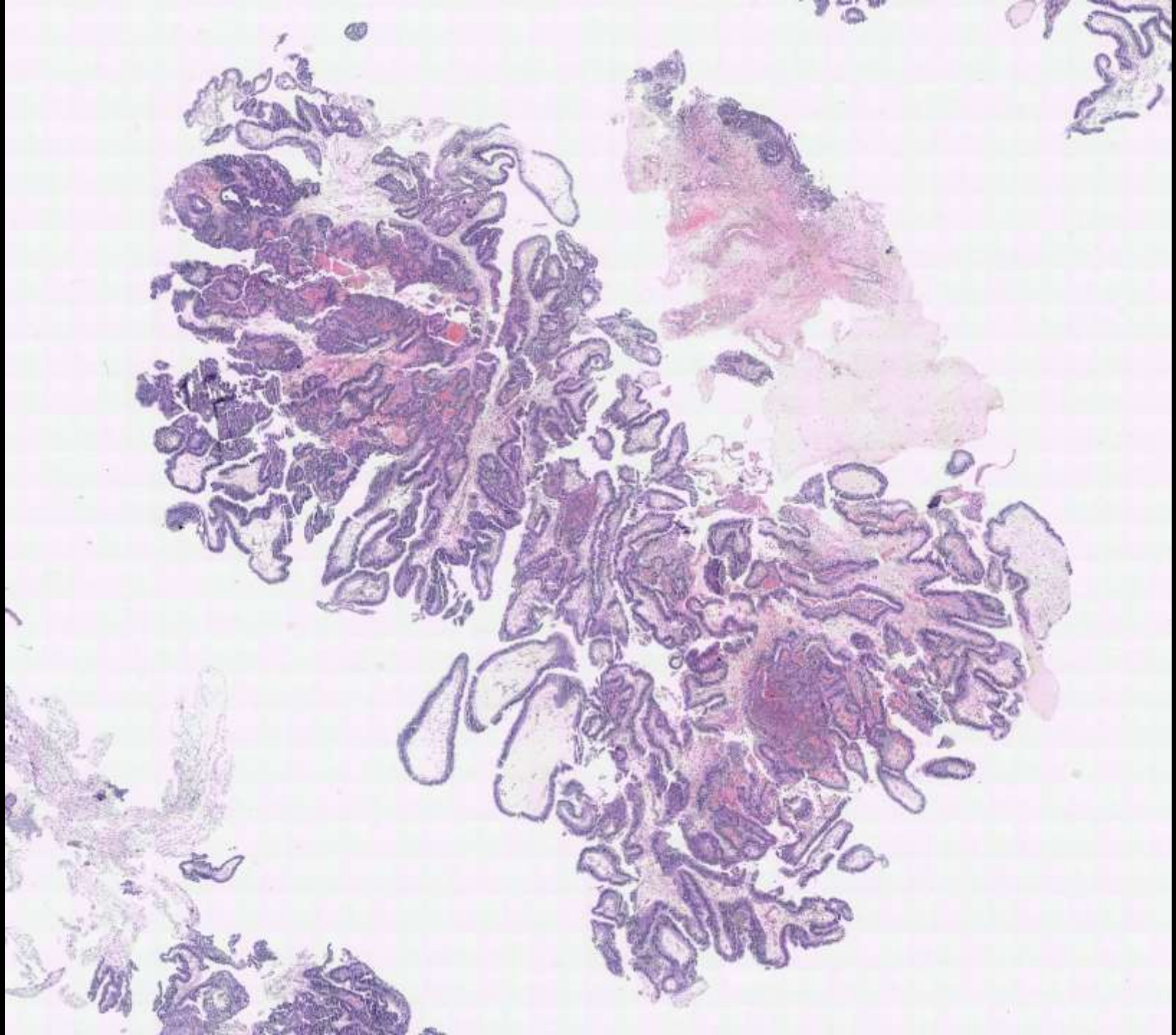

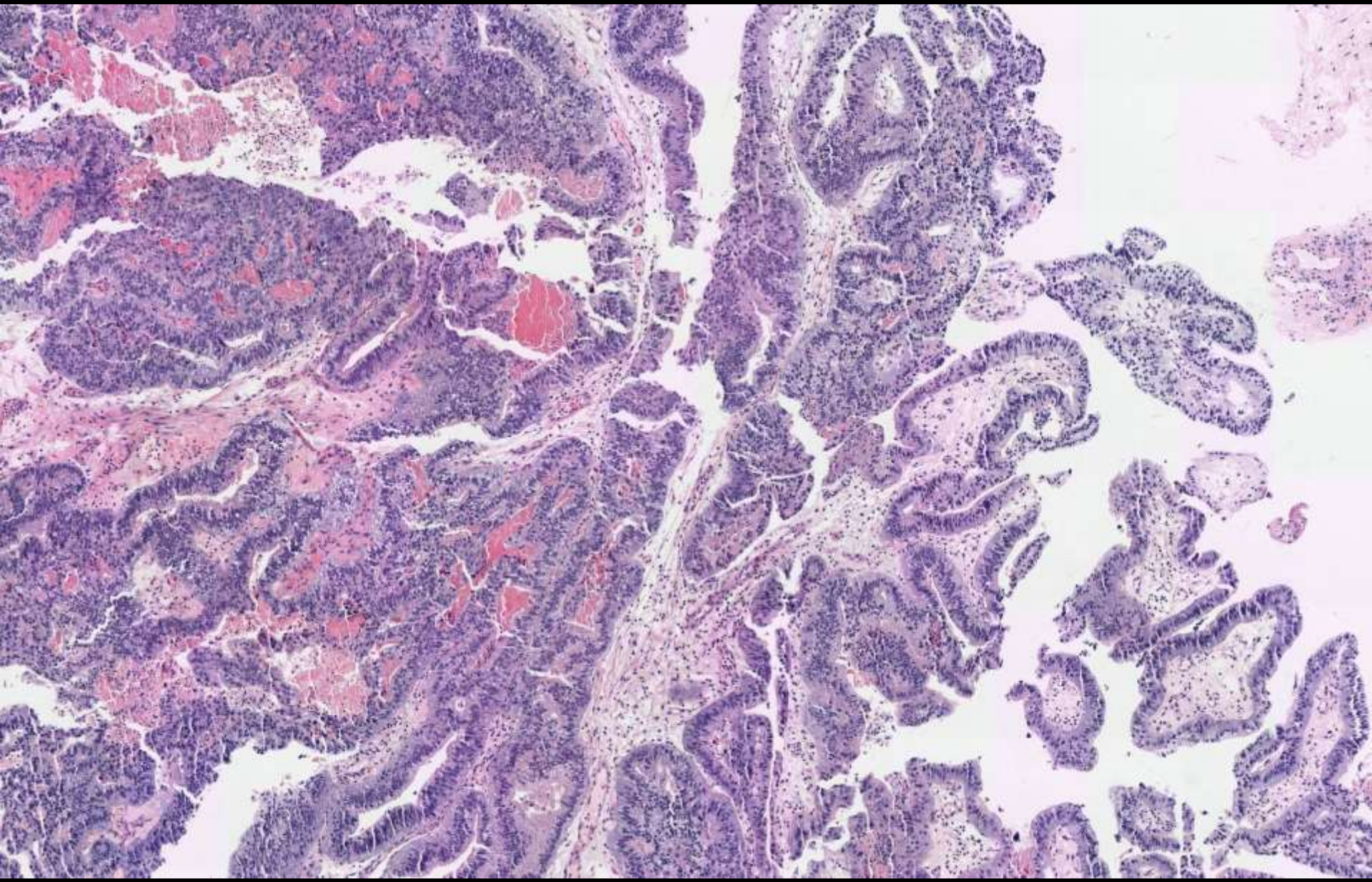

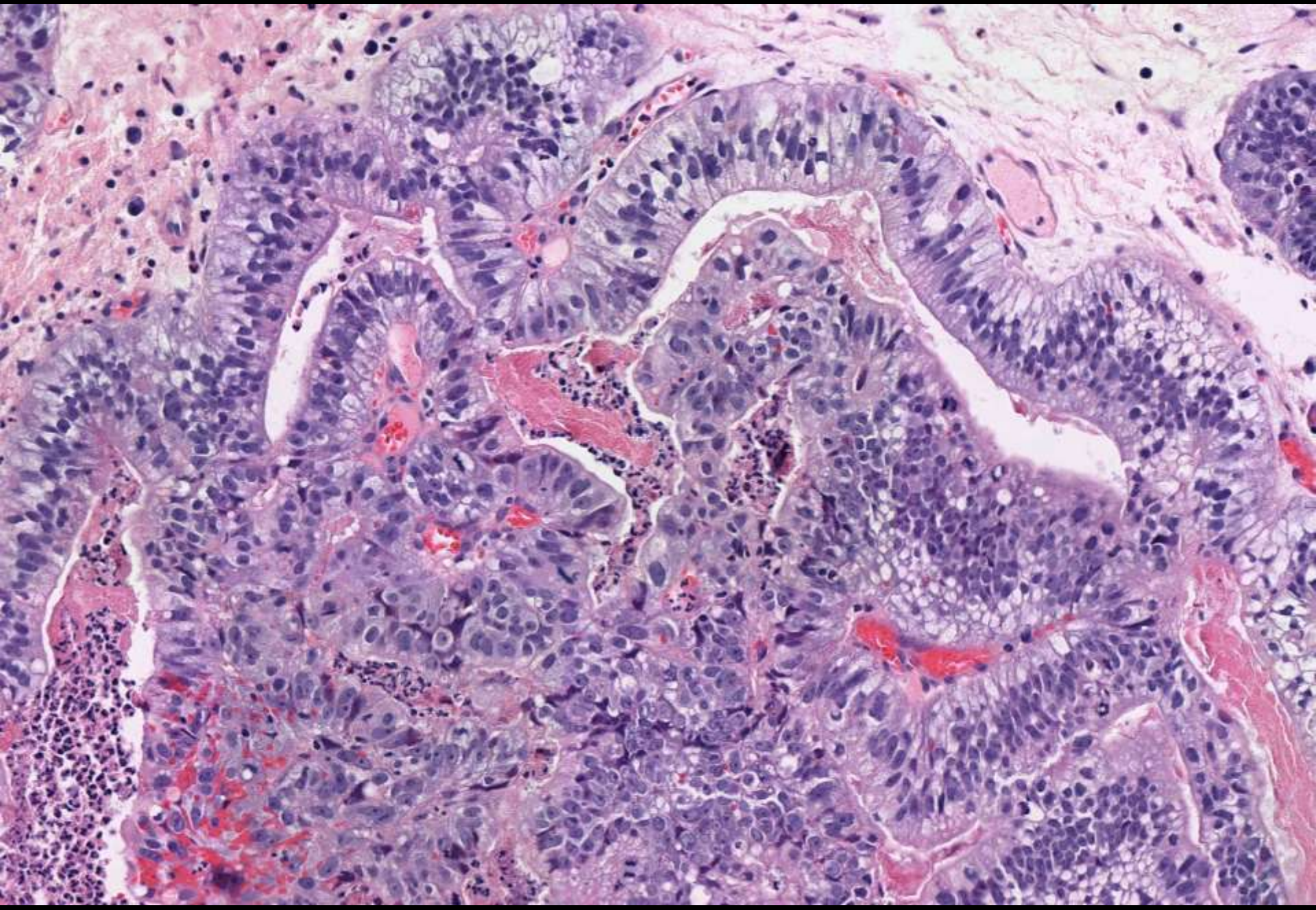

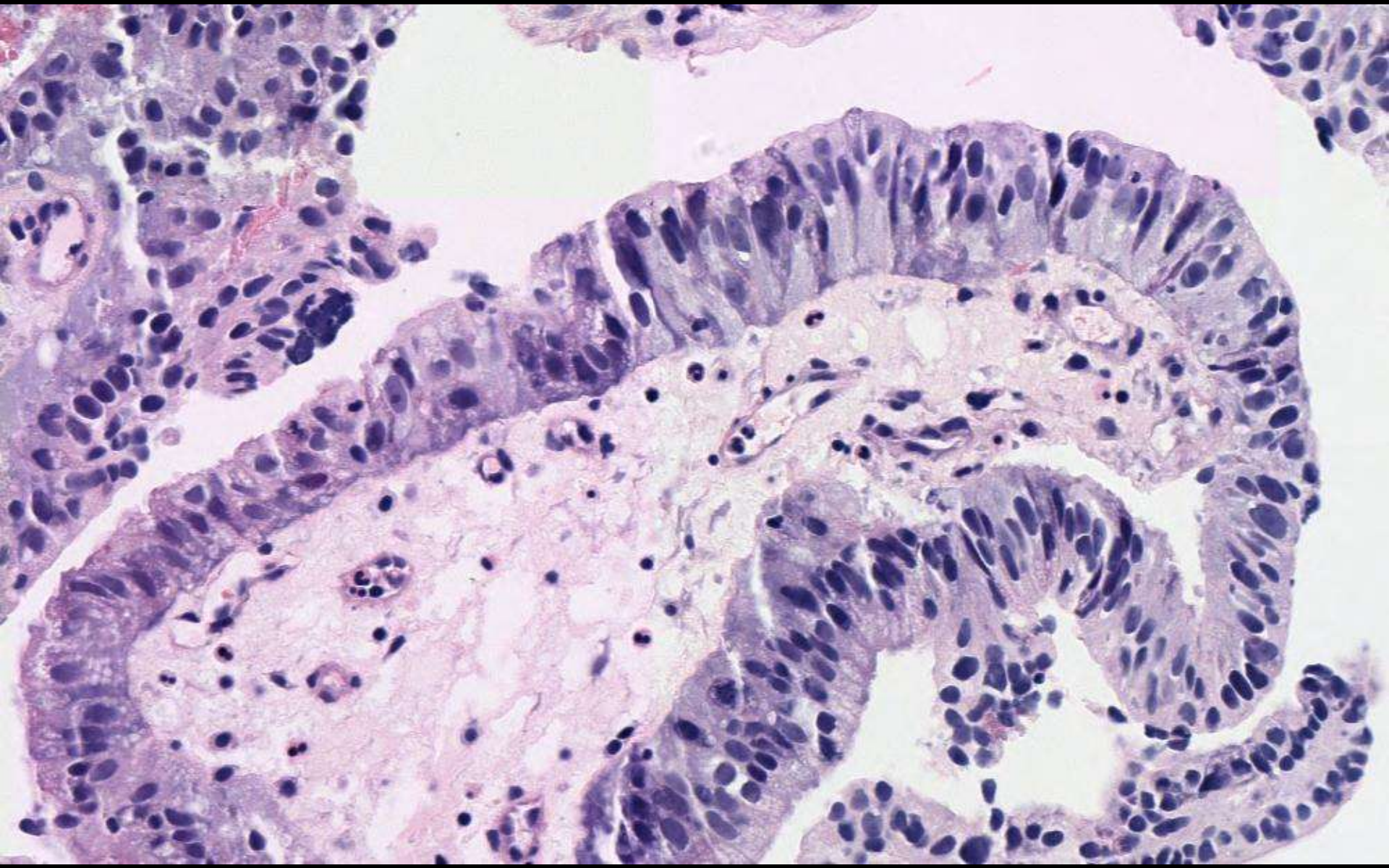

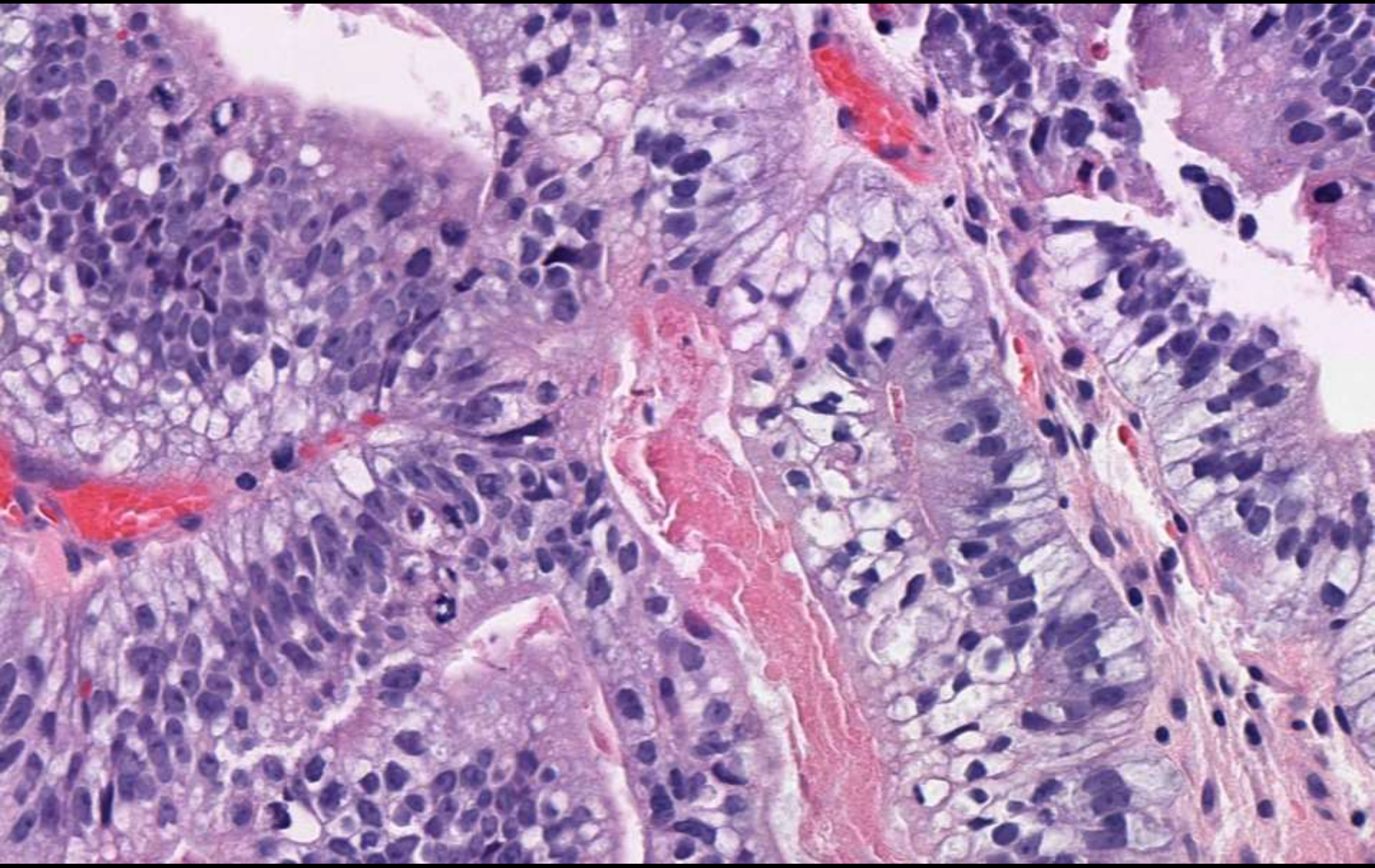

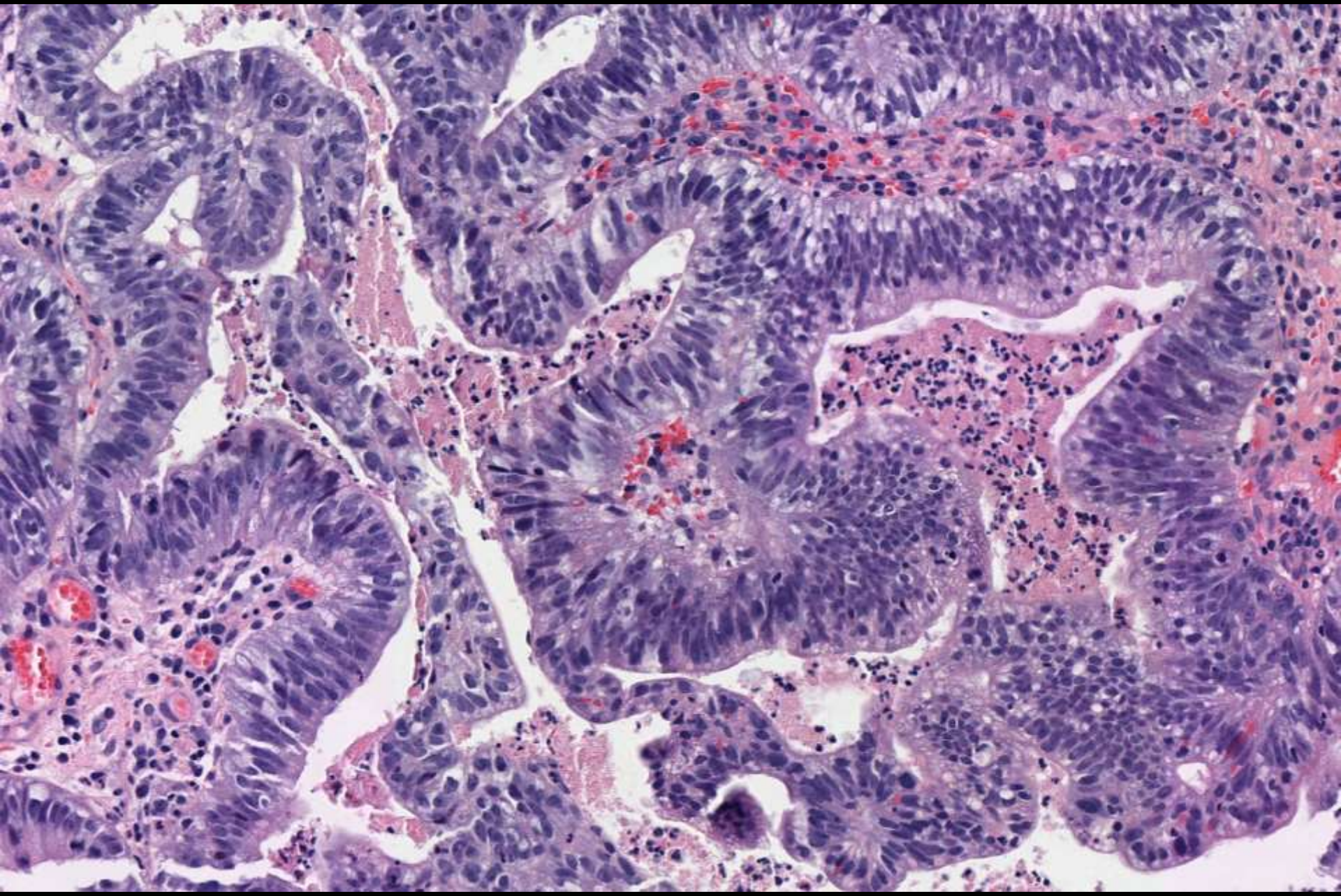

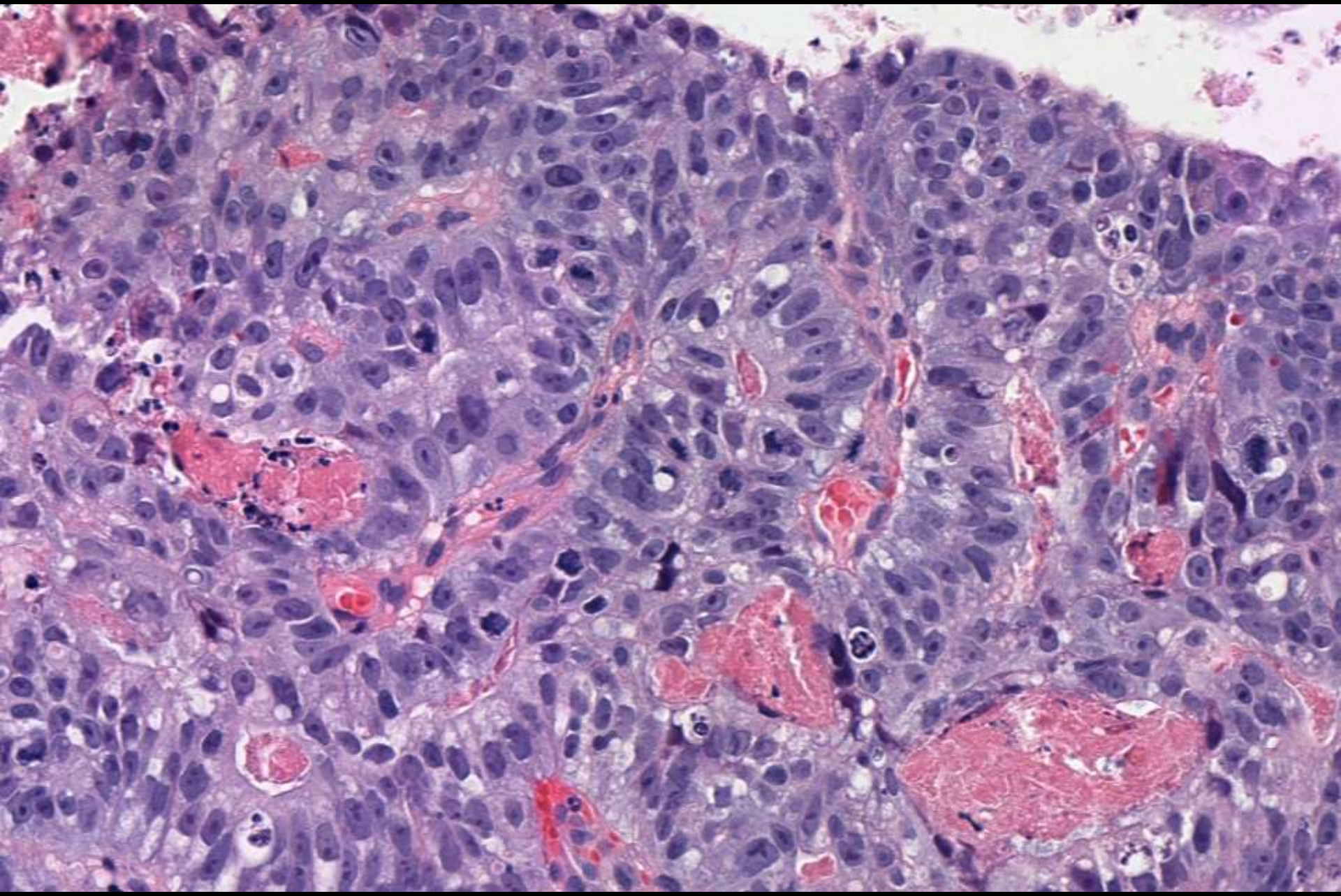

Differential diagnosis

- Villous adenoma
- Primary adenocarcinoma of the urinary bladder
- Urothelial carcinoma with glandular differentiation
- Prostatic ductal adenocarcinoma
- Metastasis
  - Gastrointestinal tract
  - Gynecologic tract

Immunohistochemistry

GATA3

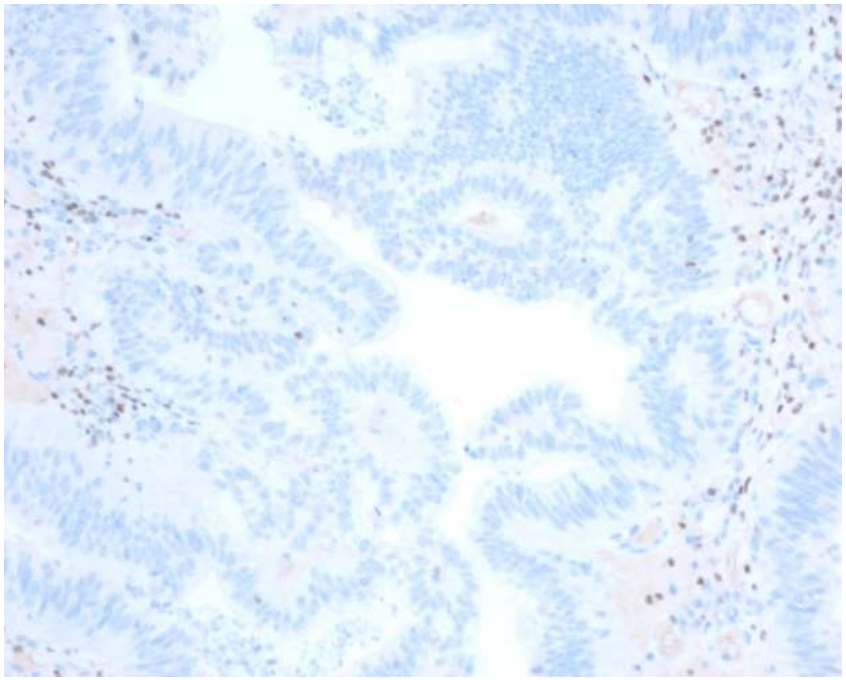

NKX3.1

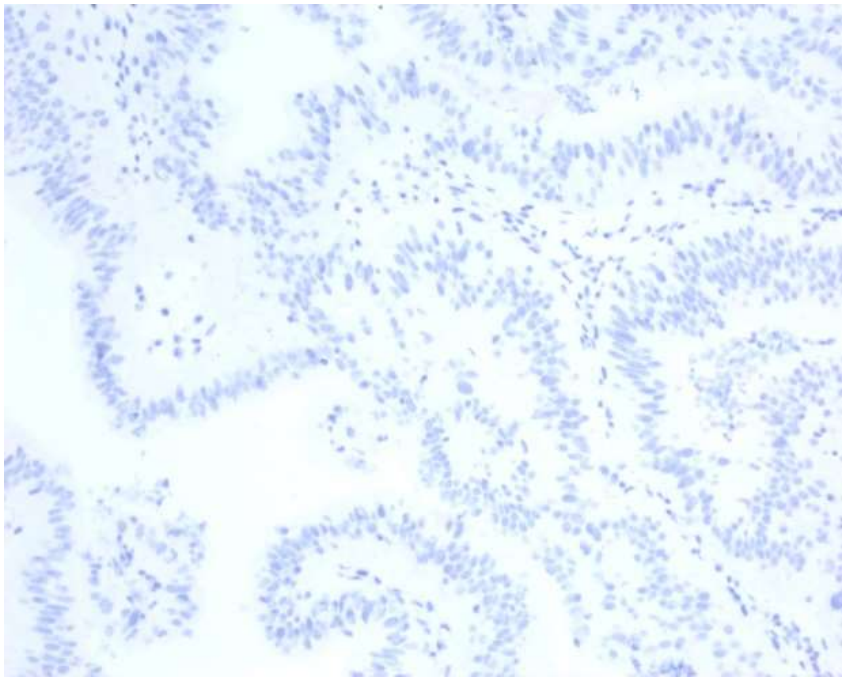

Immunohistochemistry

CDX2

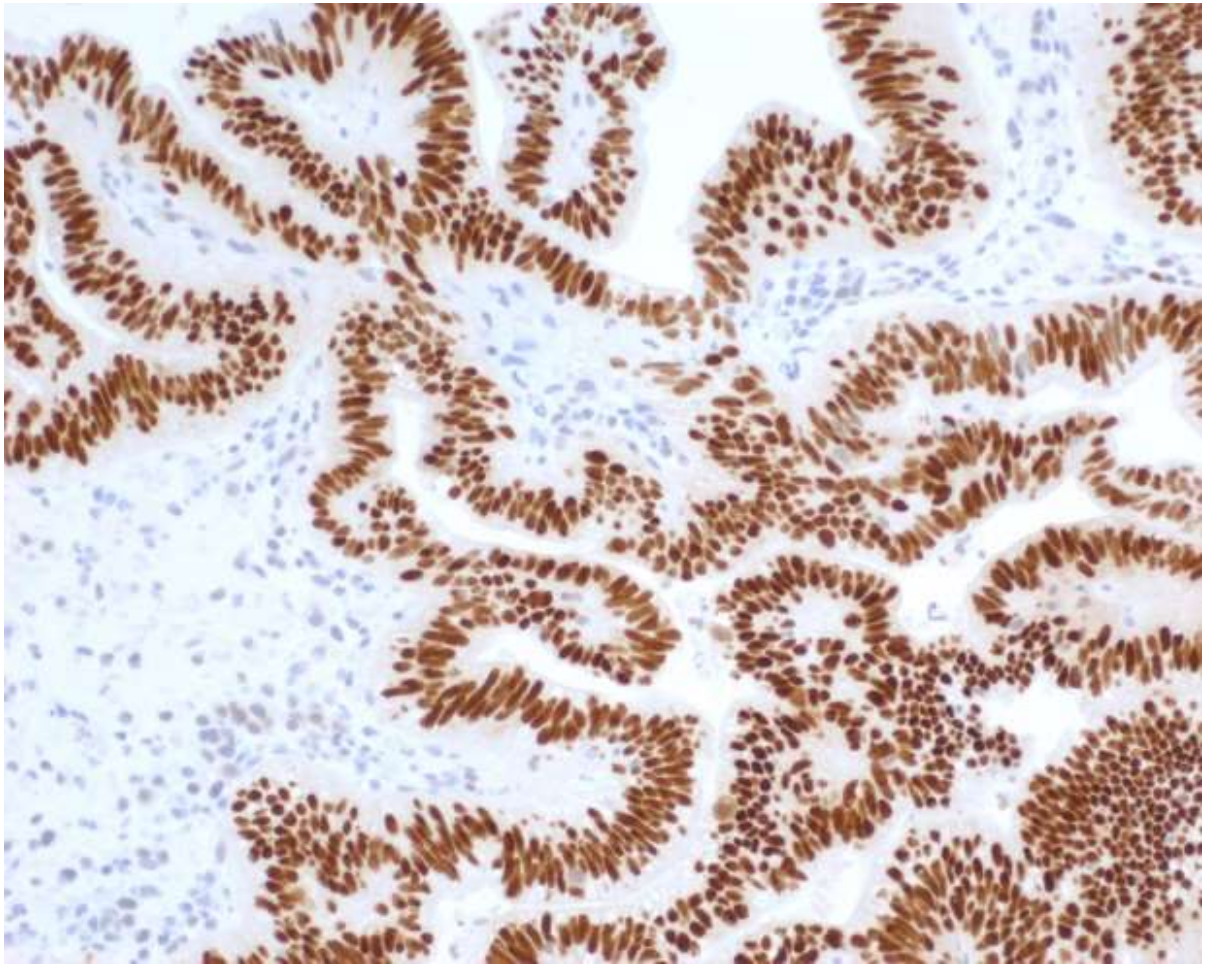

Patient history

- 2001: Left orchiectomy for mixed malignant germ cell tumor
  - Adjuvant chemotherapy
- 2013: Metastatic yolk sac tumor to the retroperitoneum
- 2016: Metastatic germ cell tumor to para and retro-aortic lymph nodes
- 2018: Presents with a 1 cm bladder mass at the bladder neck on a thin stalk

Immunohistochemistry

CDX2

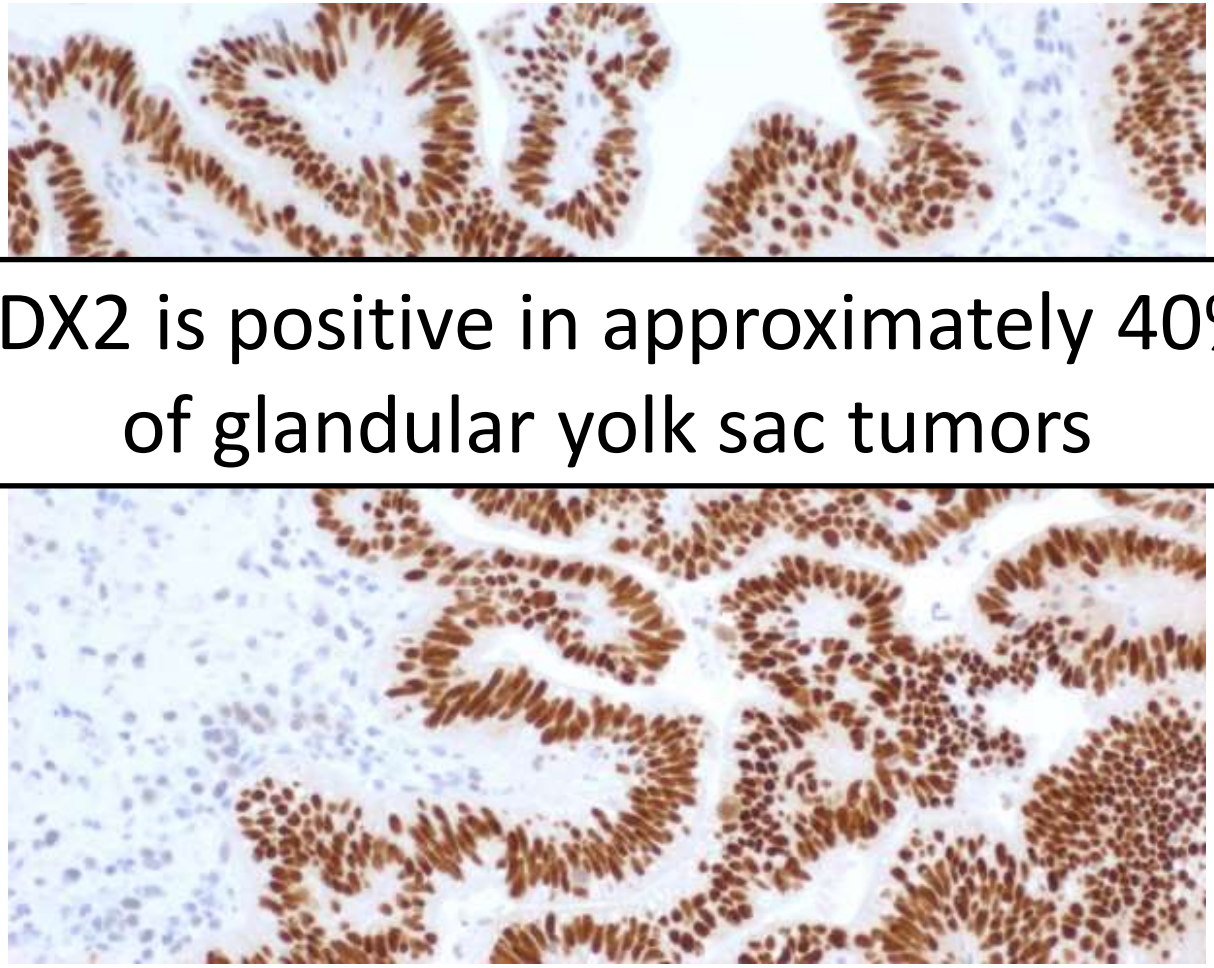

CDX2 is positive in approximately 40% of glandular yolk sac tumors

Nogales et al. Histopathology (2012)

Immunohistochemistry

SALL4

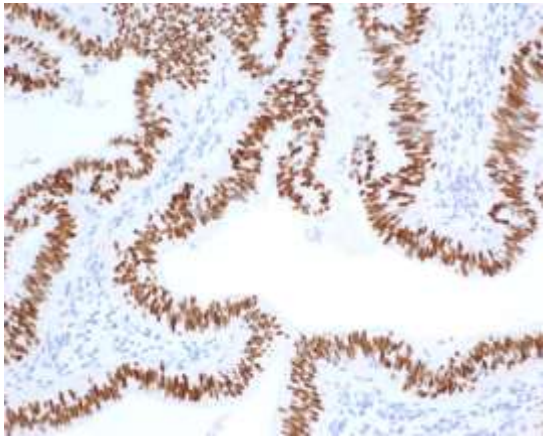

Glypican

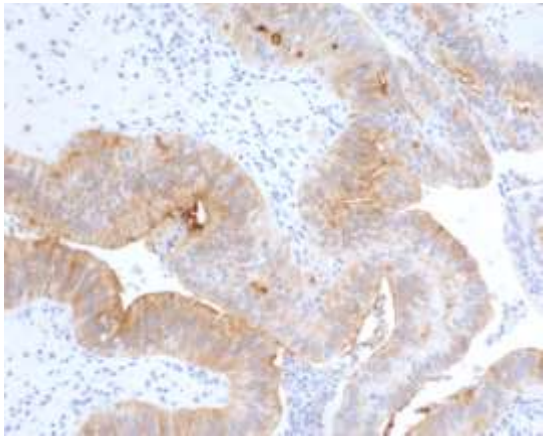

HNF-1

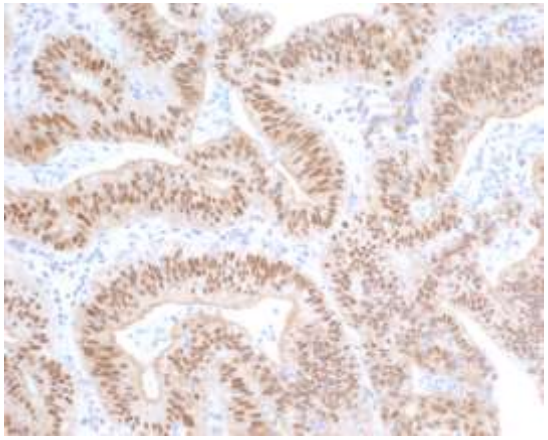

Additional stains

CK7: Rare patchy positive

CK20: Rare patchy positive

P63: Rare patchy positive

HNF-1: Strong positive

“Common” metastases to the urinary bladder

- Breast
- Genitourinary
- Gastrointestinal

- Yolk sac/germ cell tumor?
  - No reported cases in literature

Wang et al. Virchows Archiv (2019).
Xiao et al. Int J Surg Pathol. (2012).

19-0304
(scanned slide available)

Jeffrey Hoffman/Arie Perry; UCSF

43-year-old male with no prior medical history, presents with left parietal brain tumor.

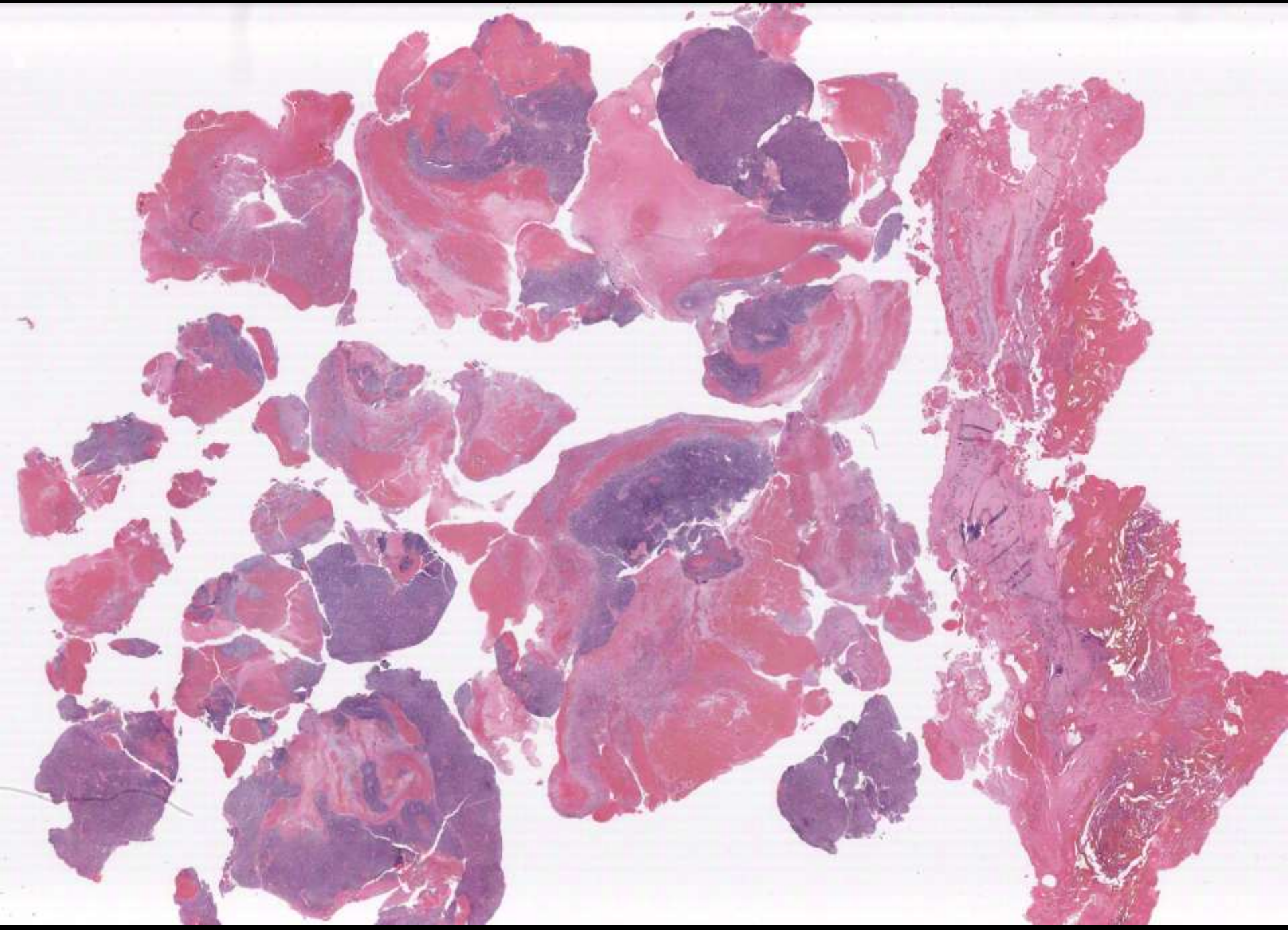

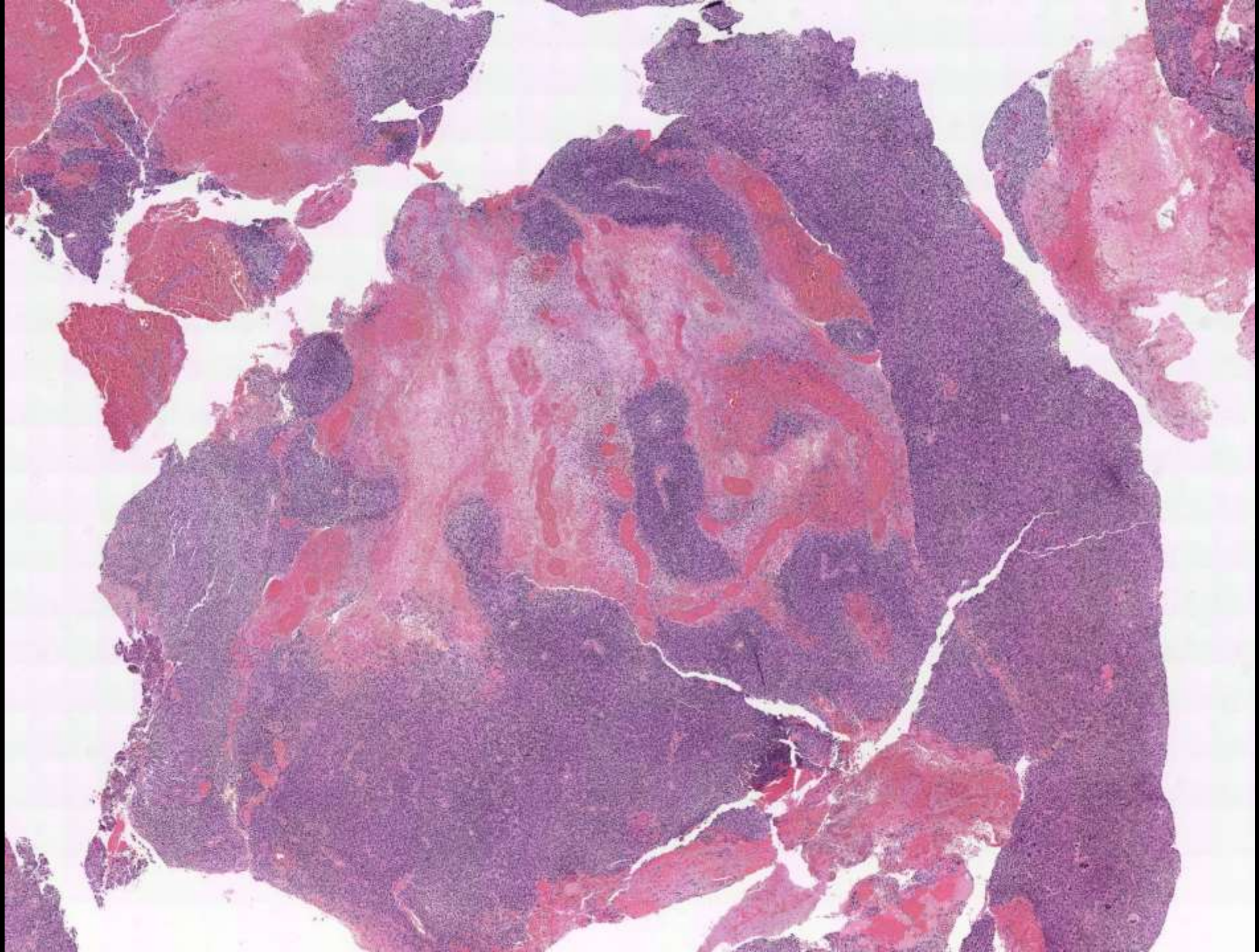

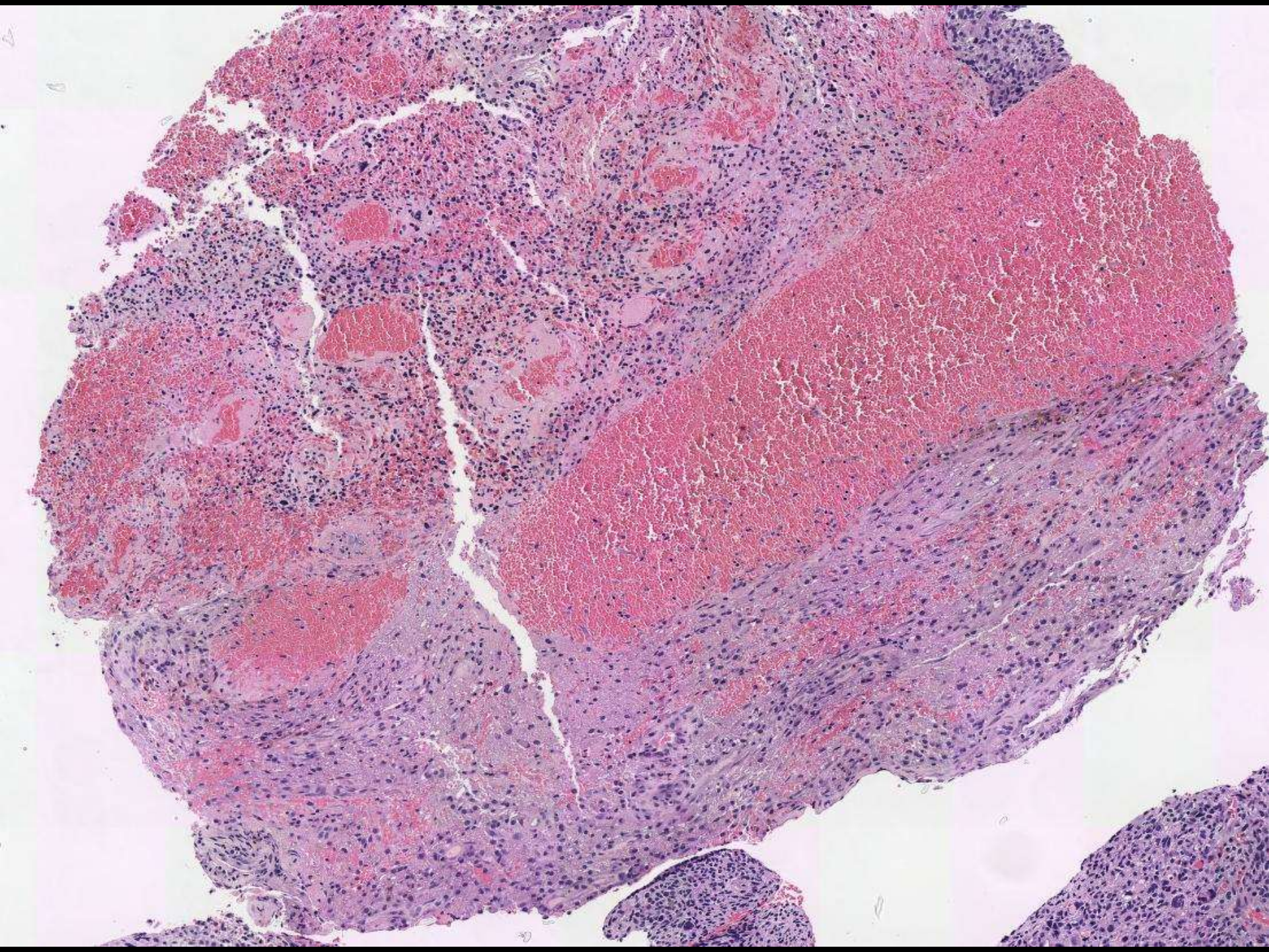

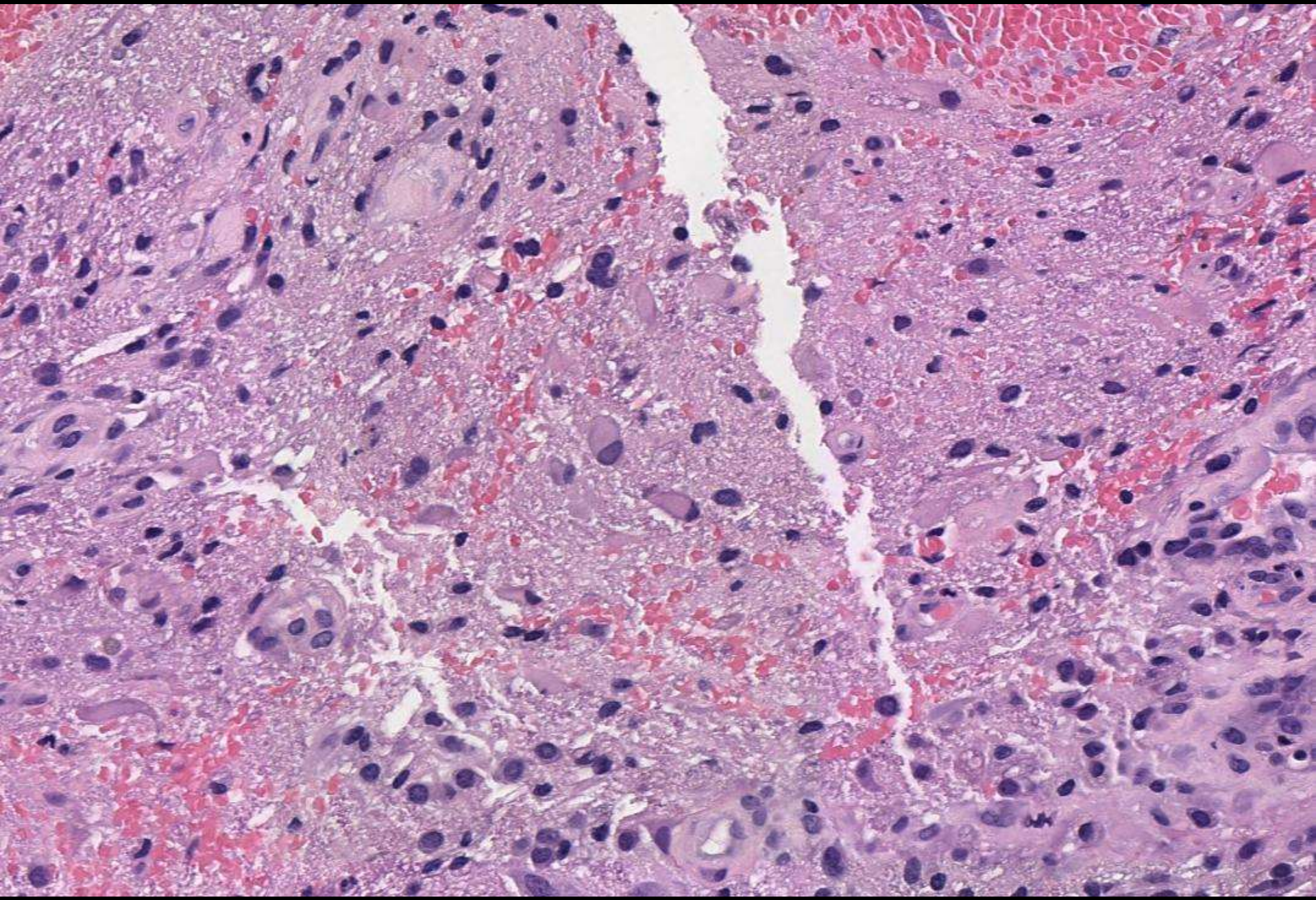

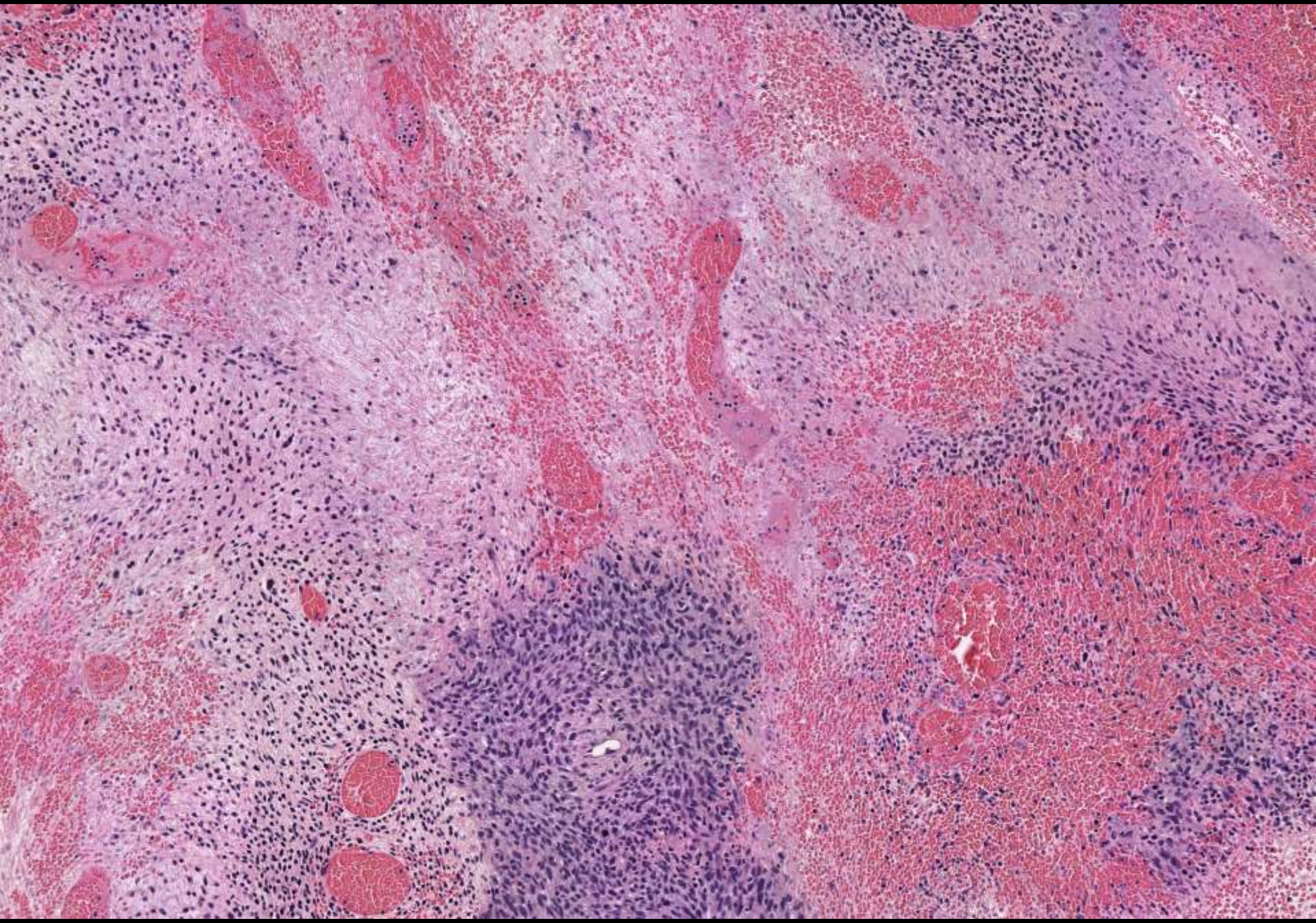

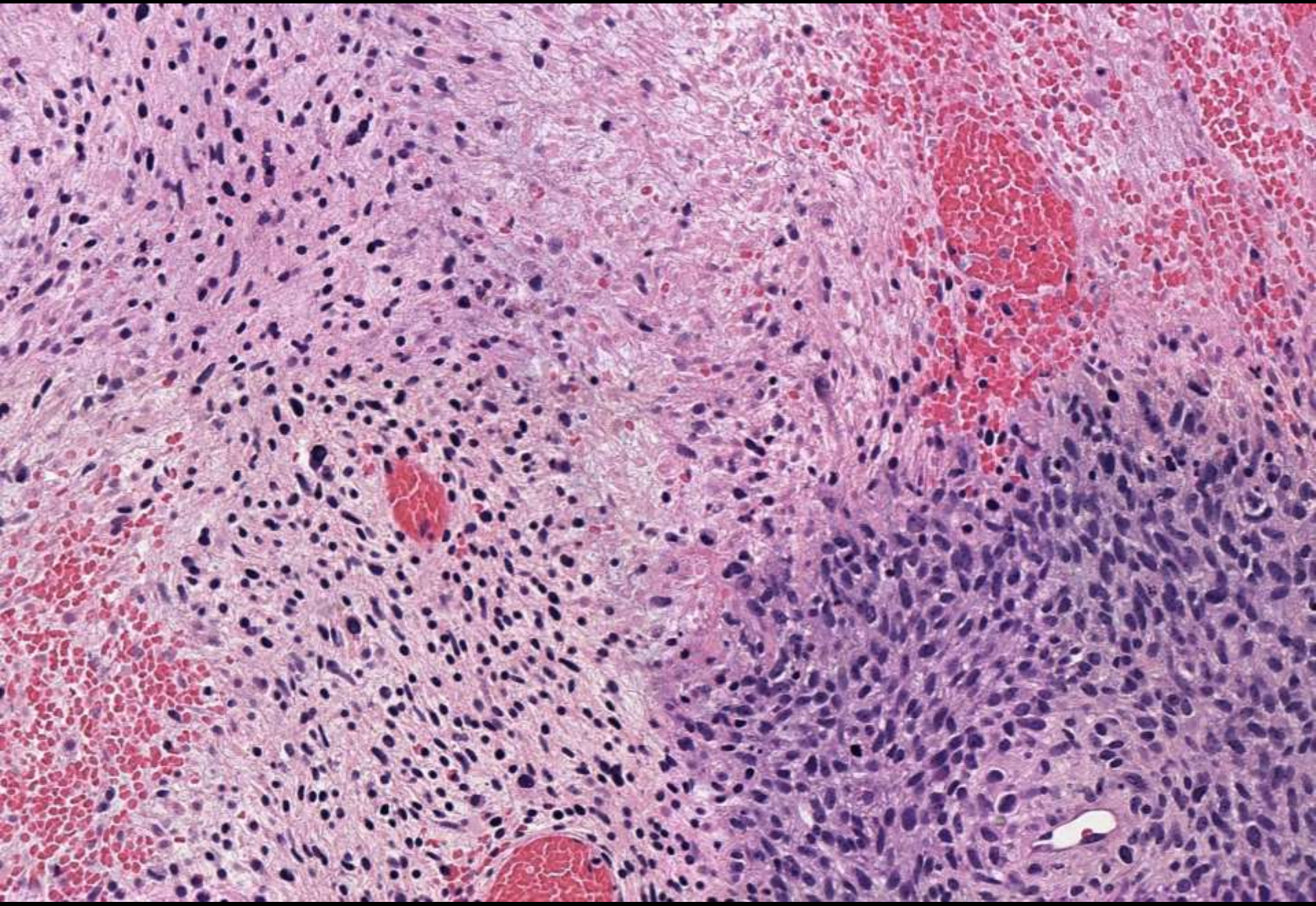

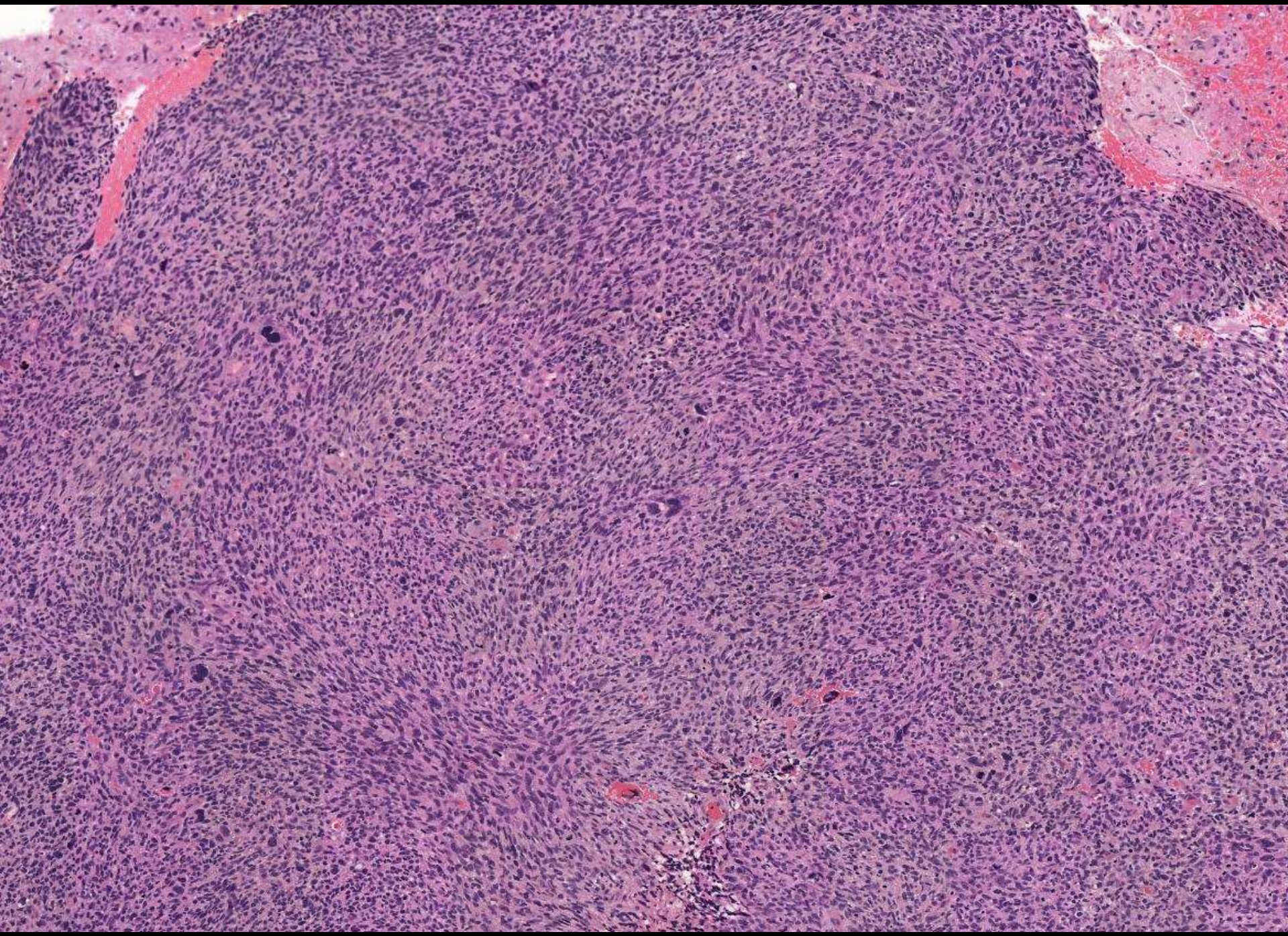

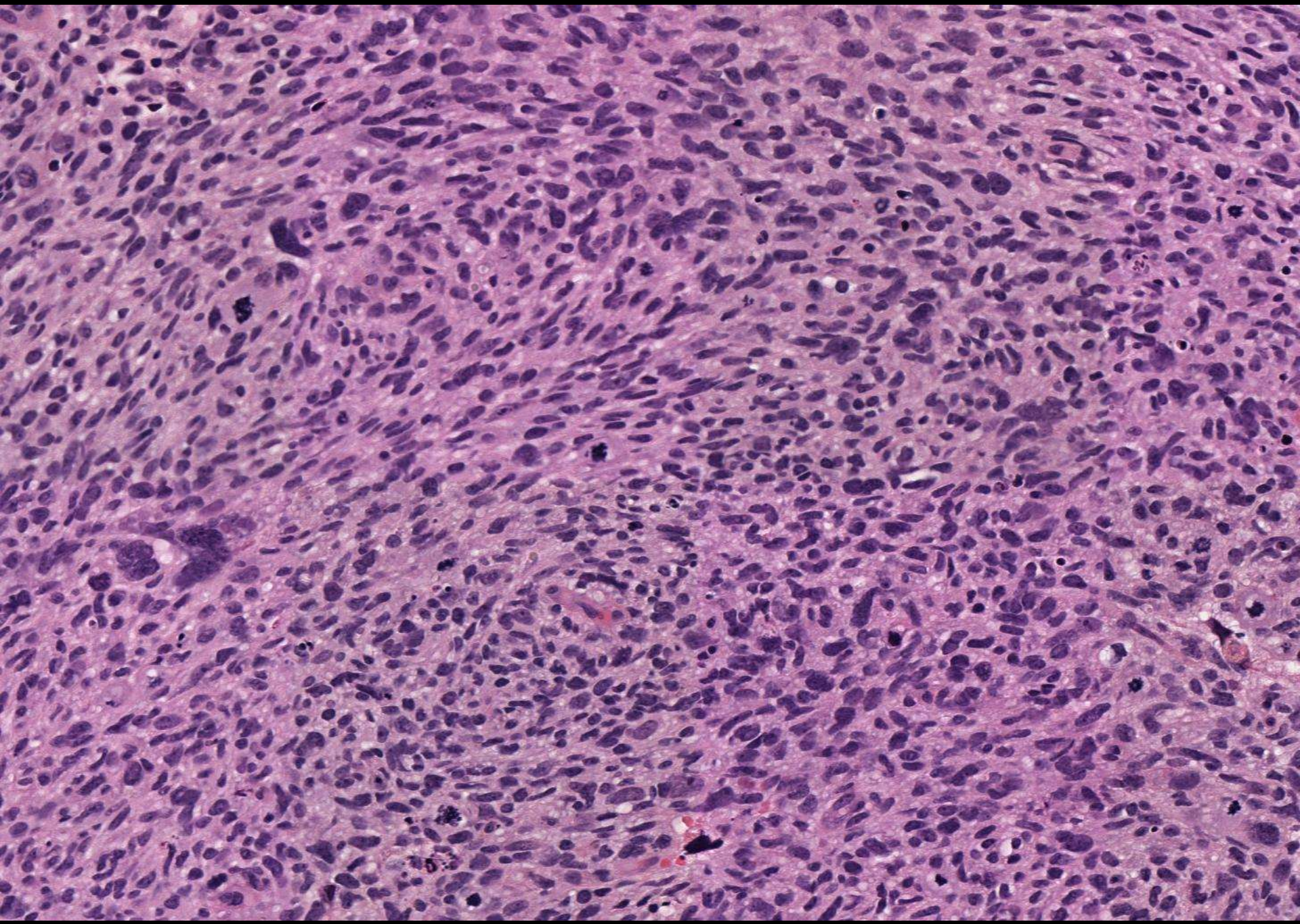

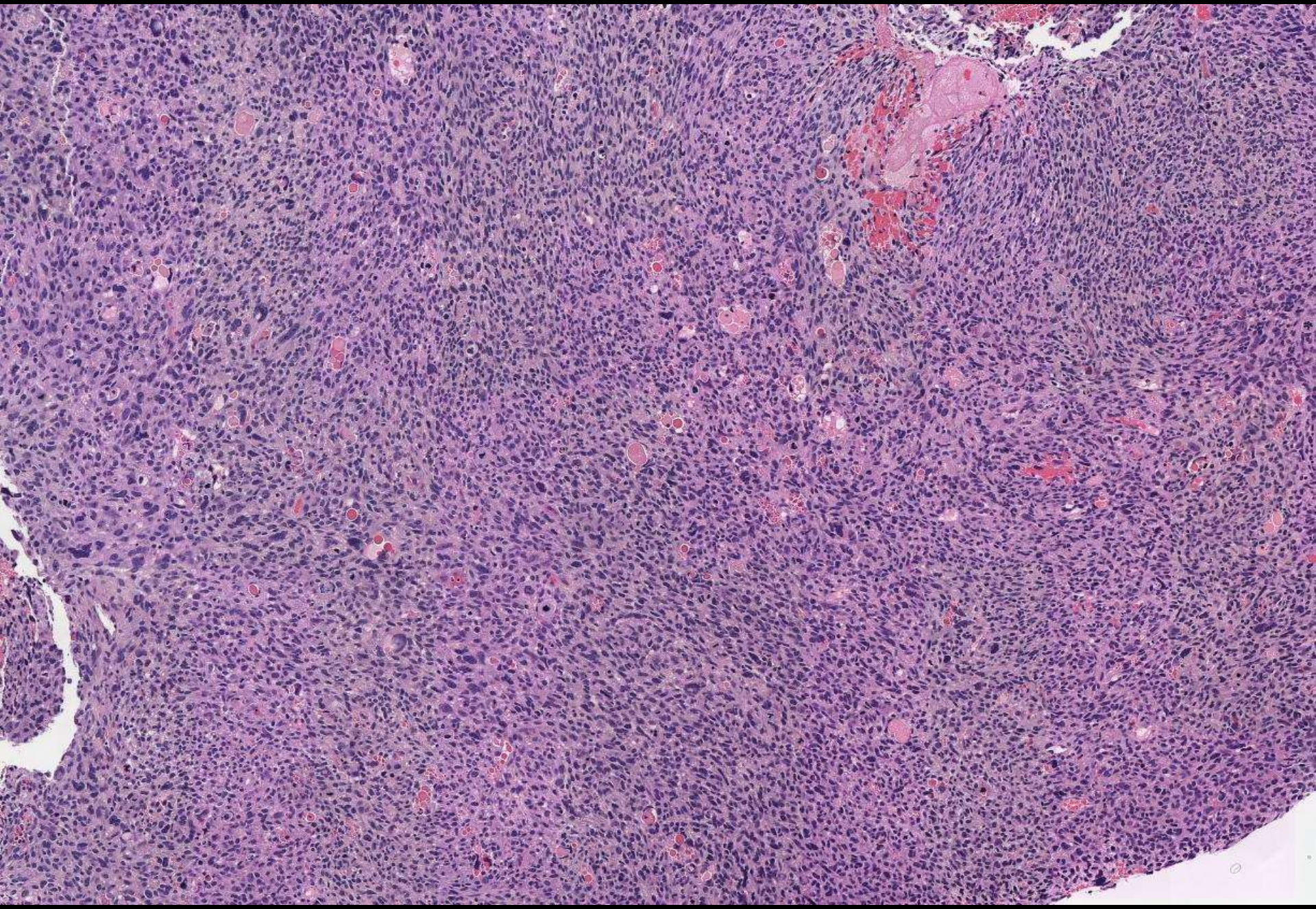

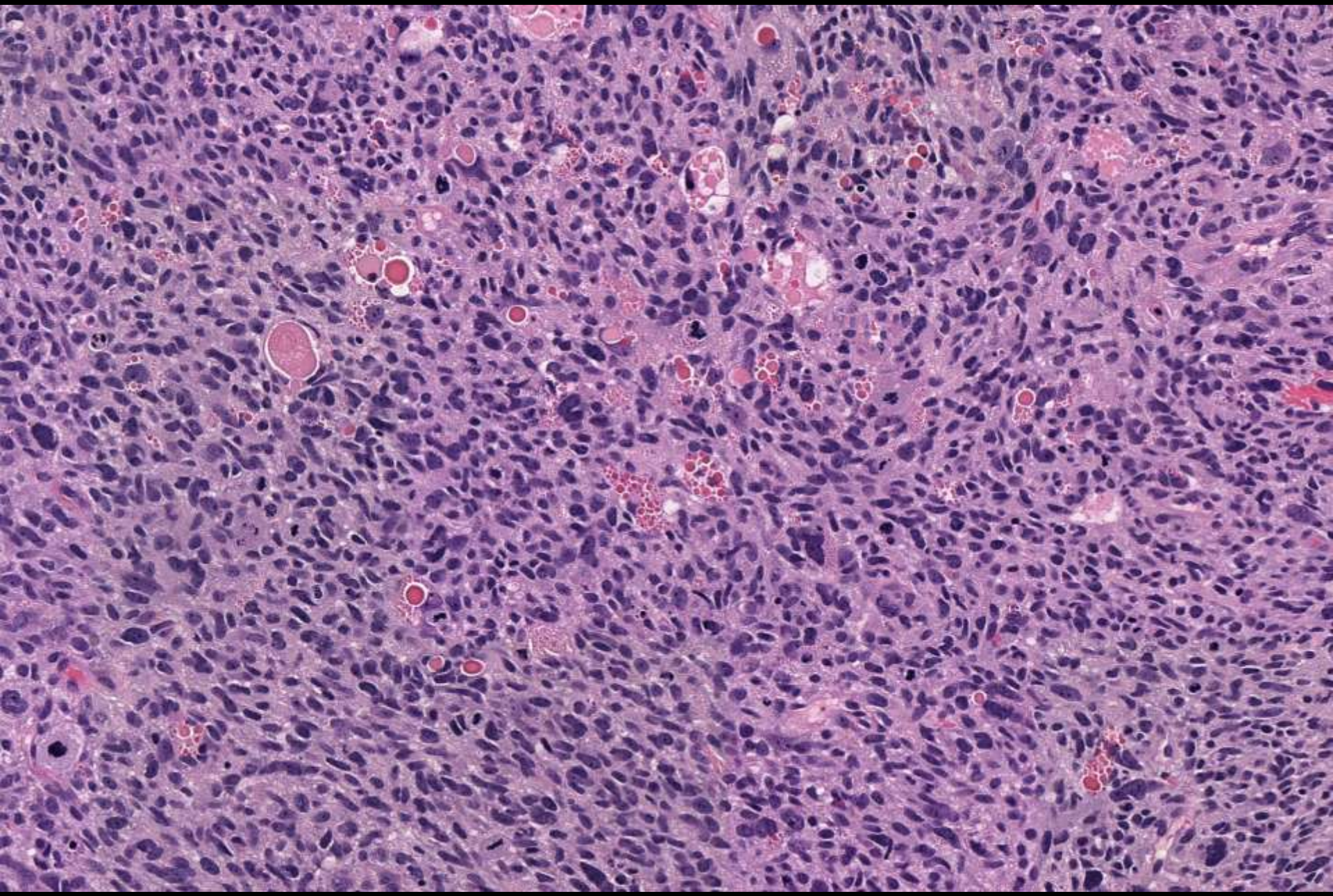

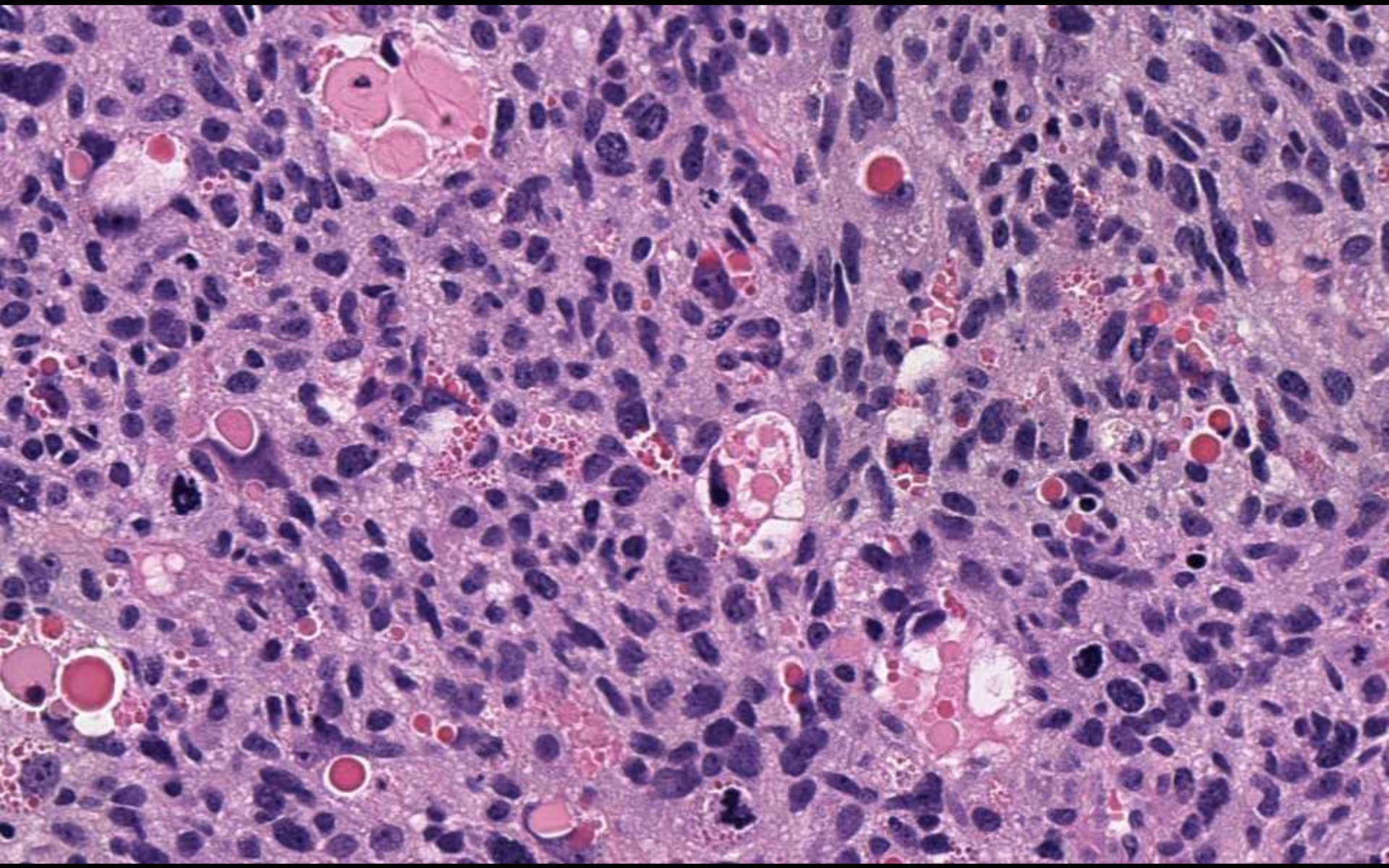

43-year-old man with a parietal lobe mass

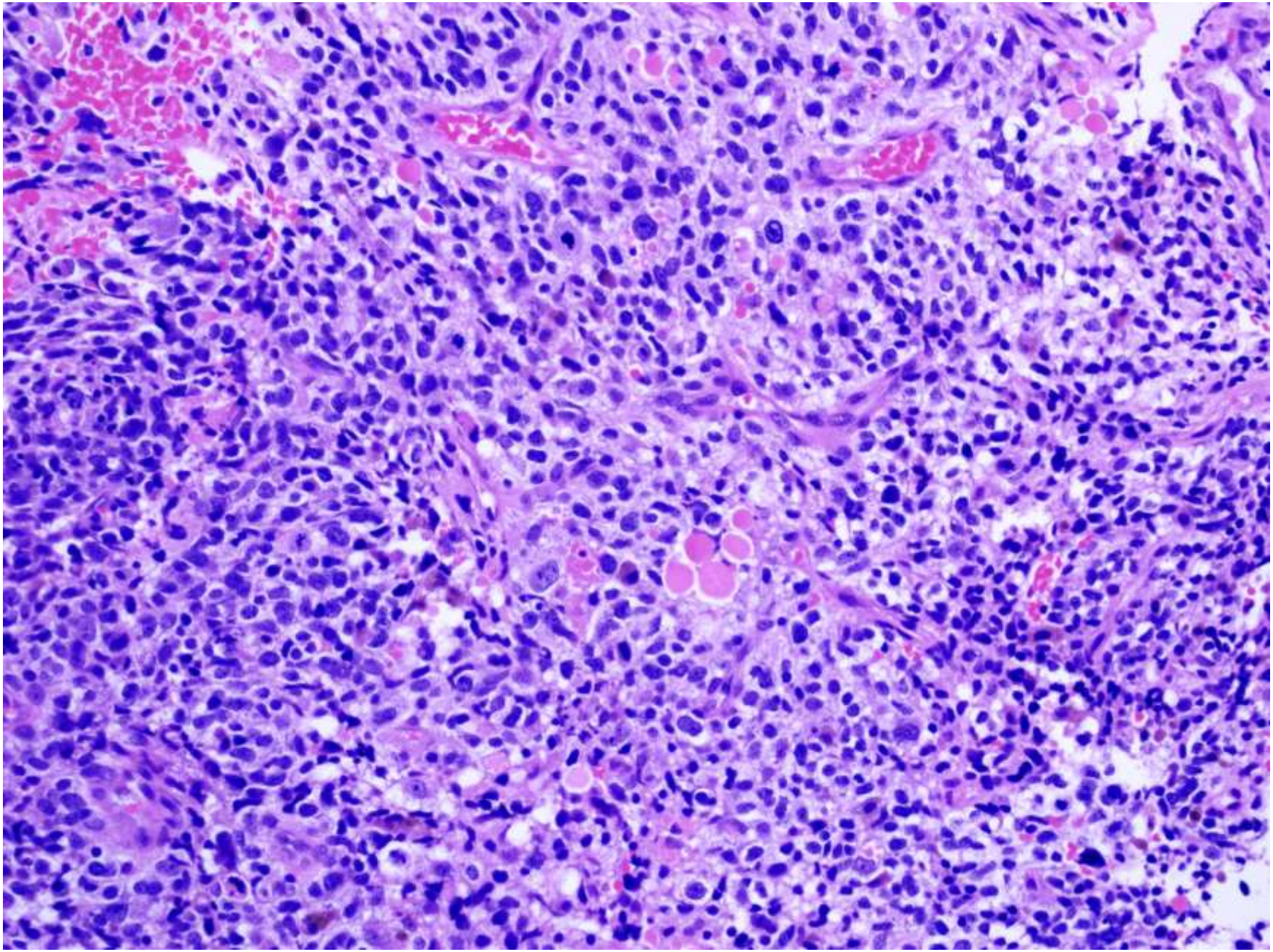

Pleomorphic, high mitotic activity, eosinophilic cytoplasmic globules

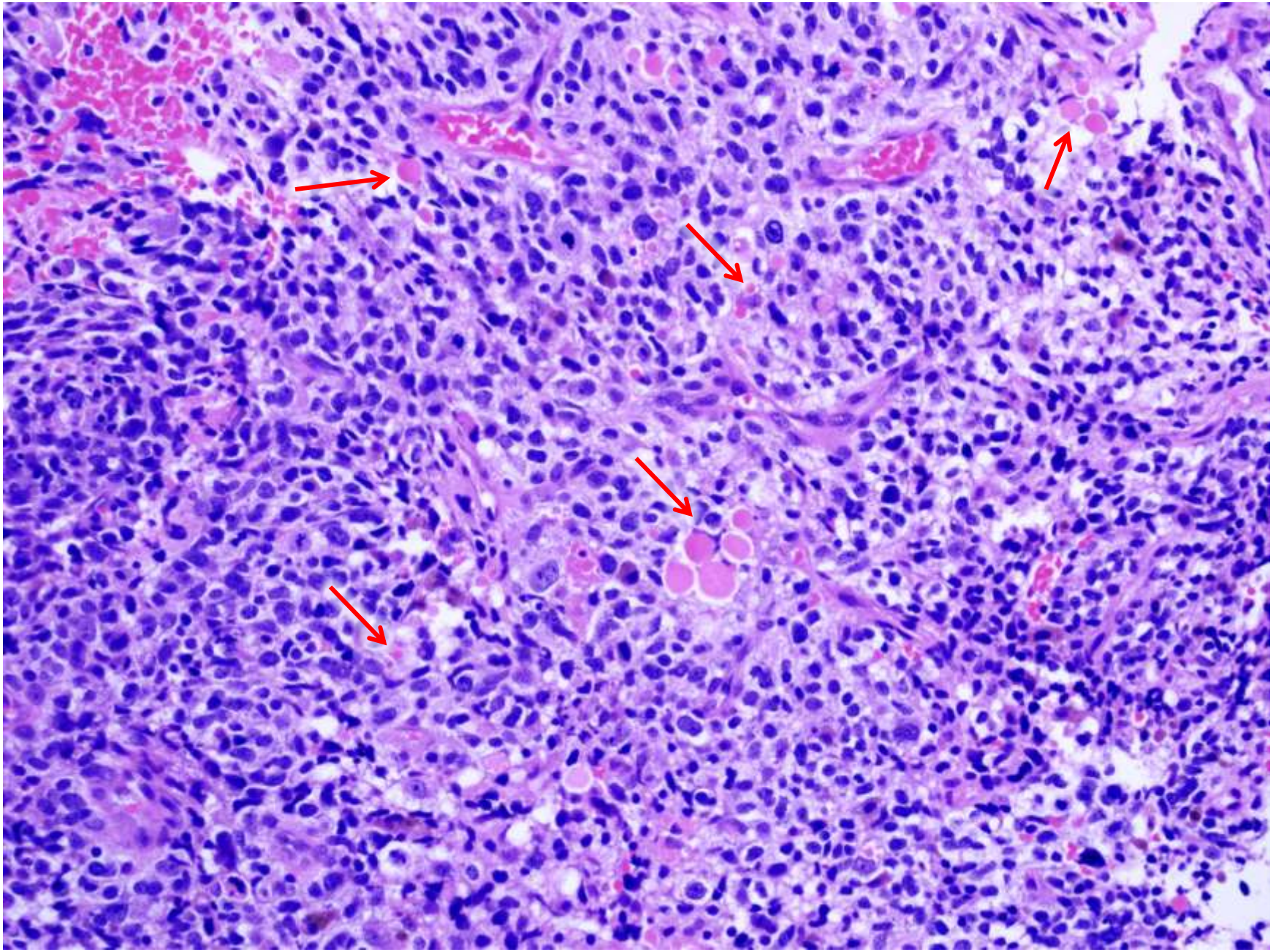

Pleomorphic, high mitotic activity, eosinophilic cytoplasmic globules

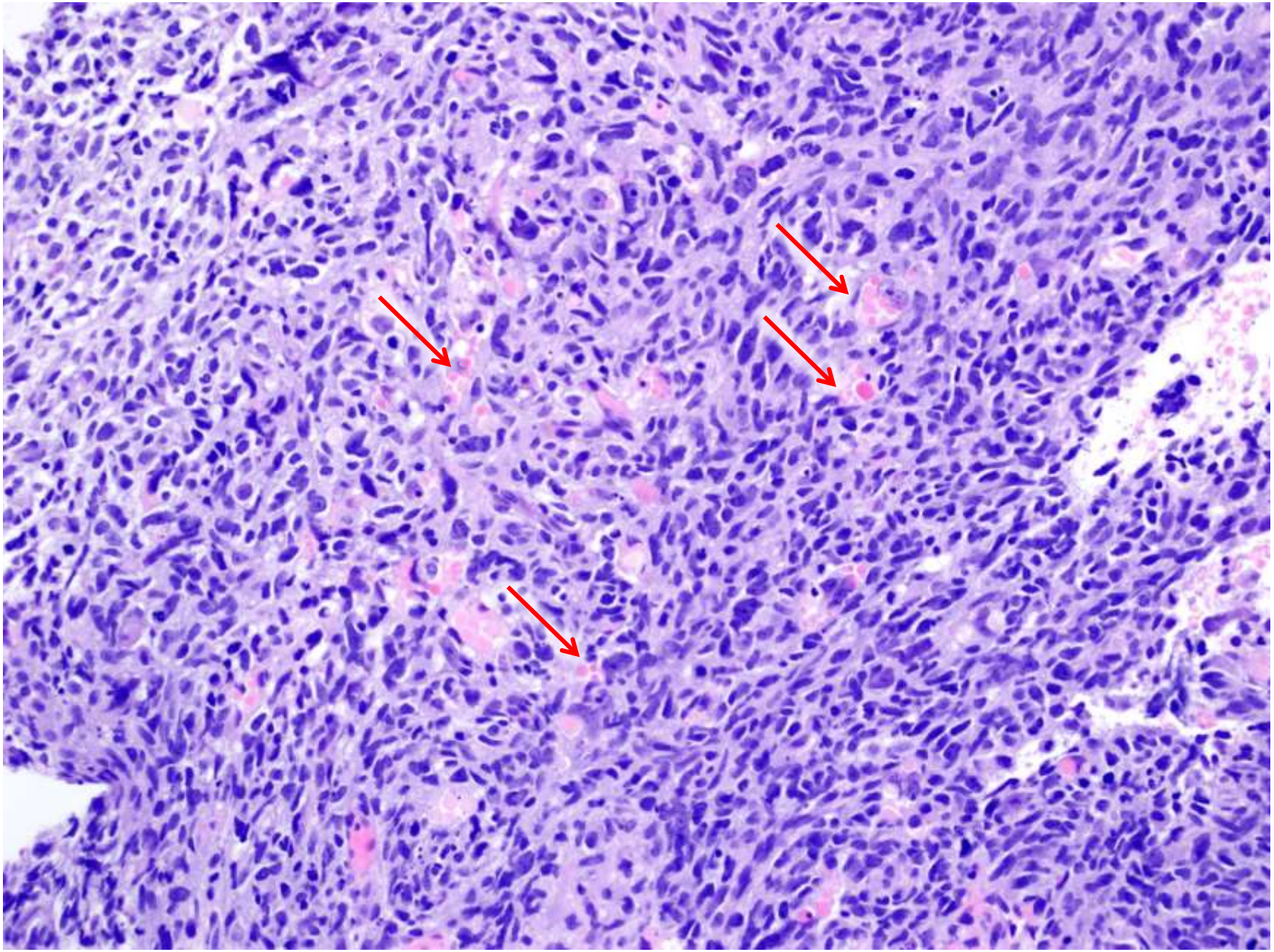

Spindled, somewhat fascicular, with scattered giant cells

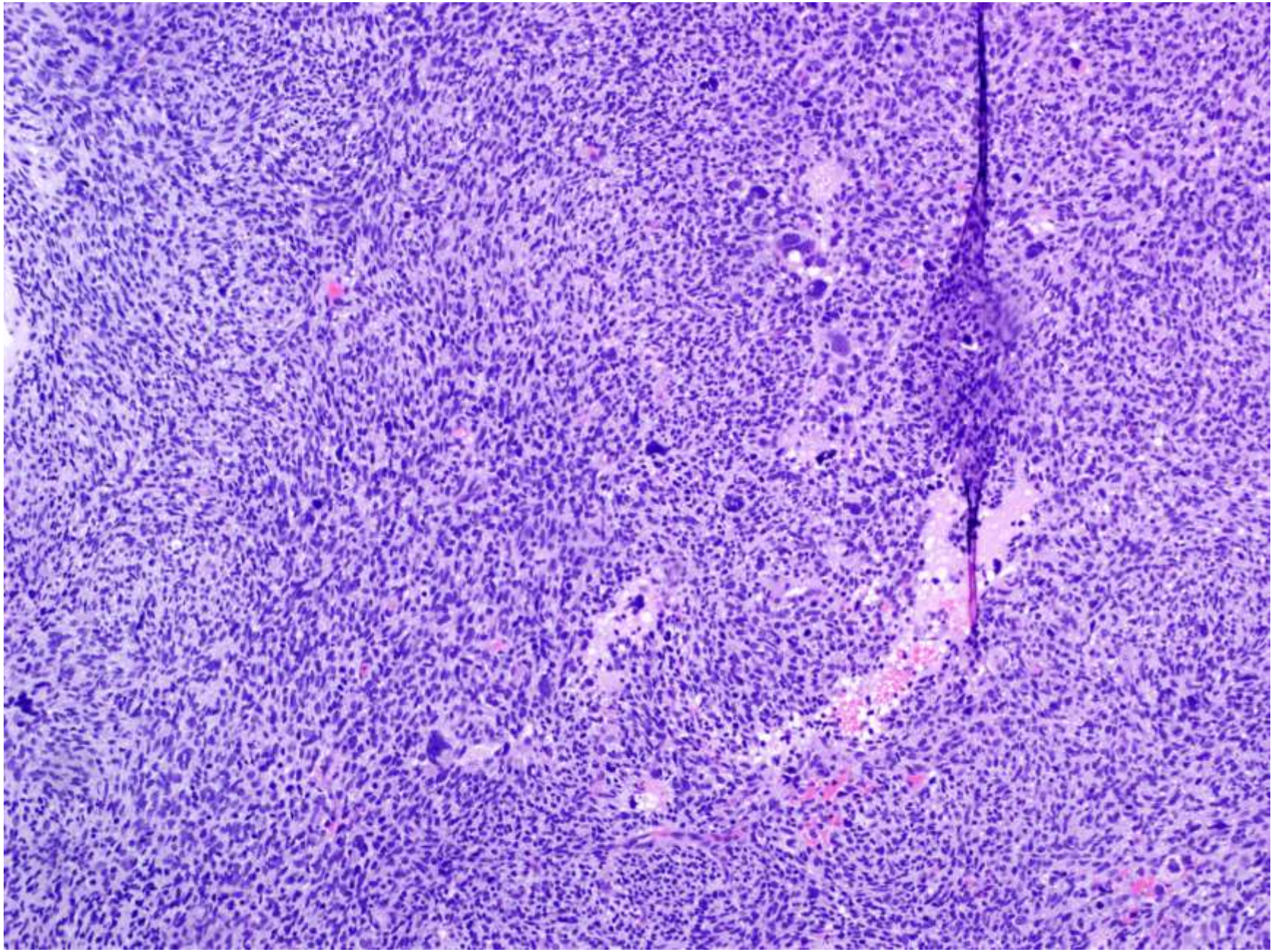

Subset of Desmin-positive cells

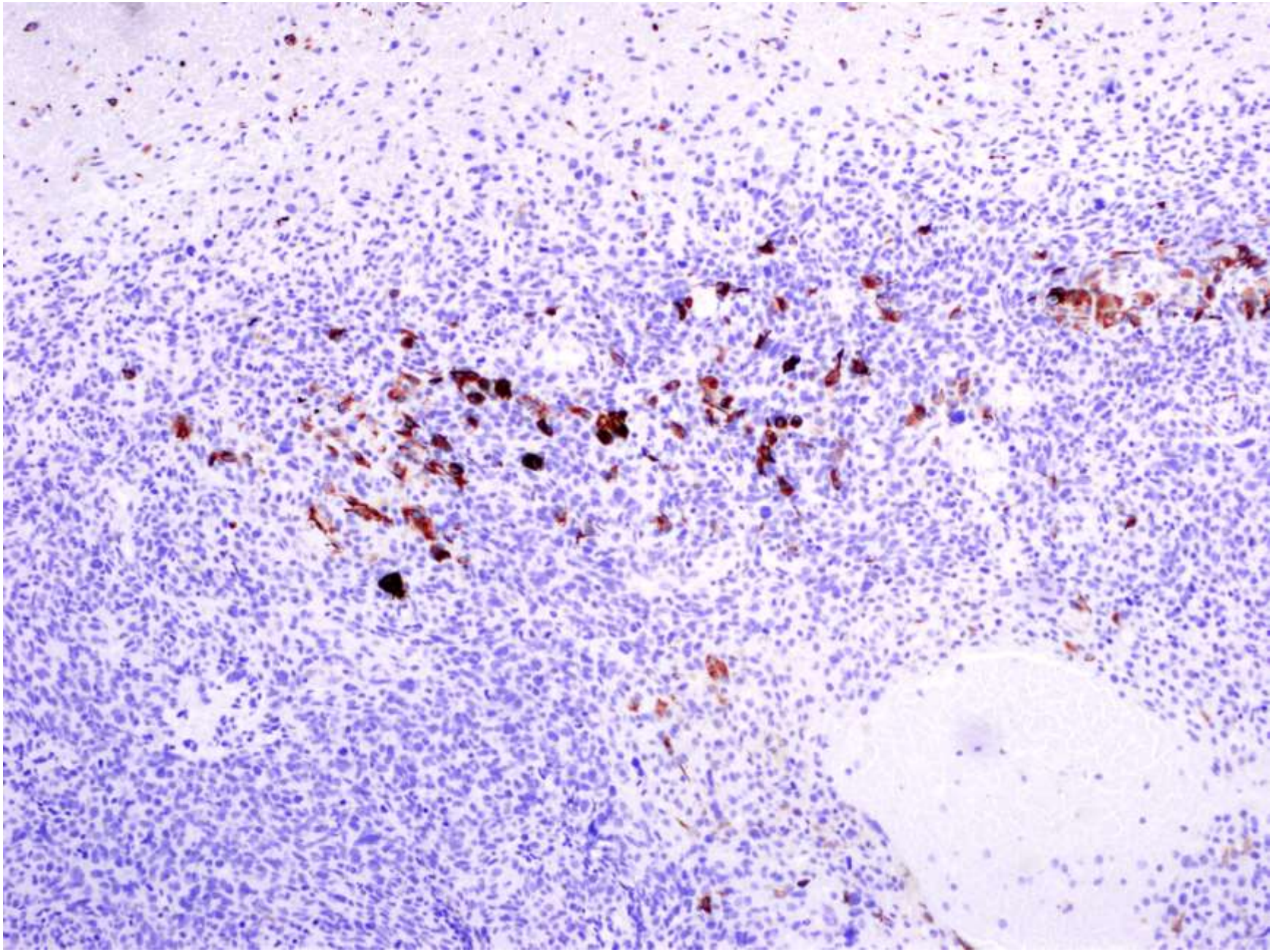

Subset of SMA-positive cells

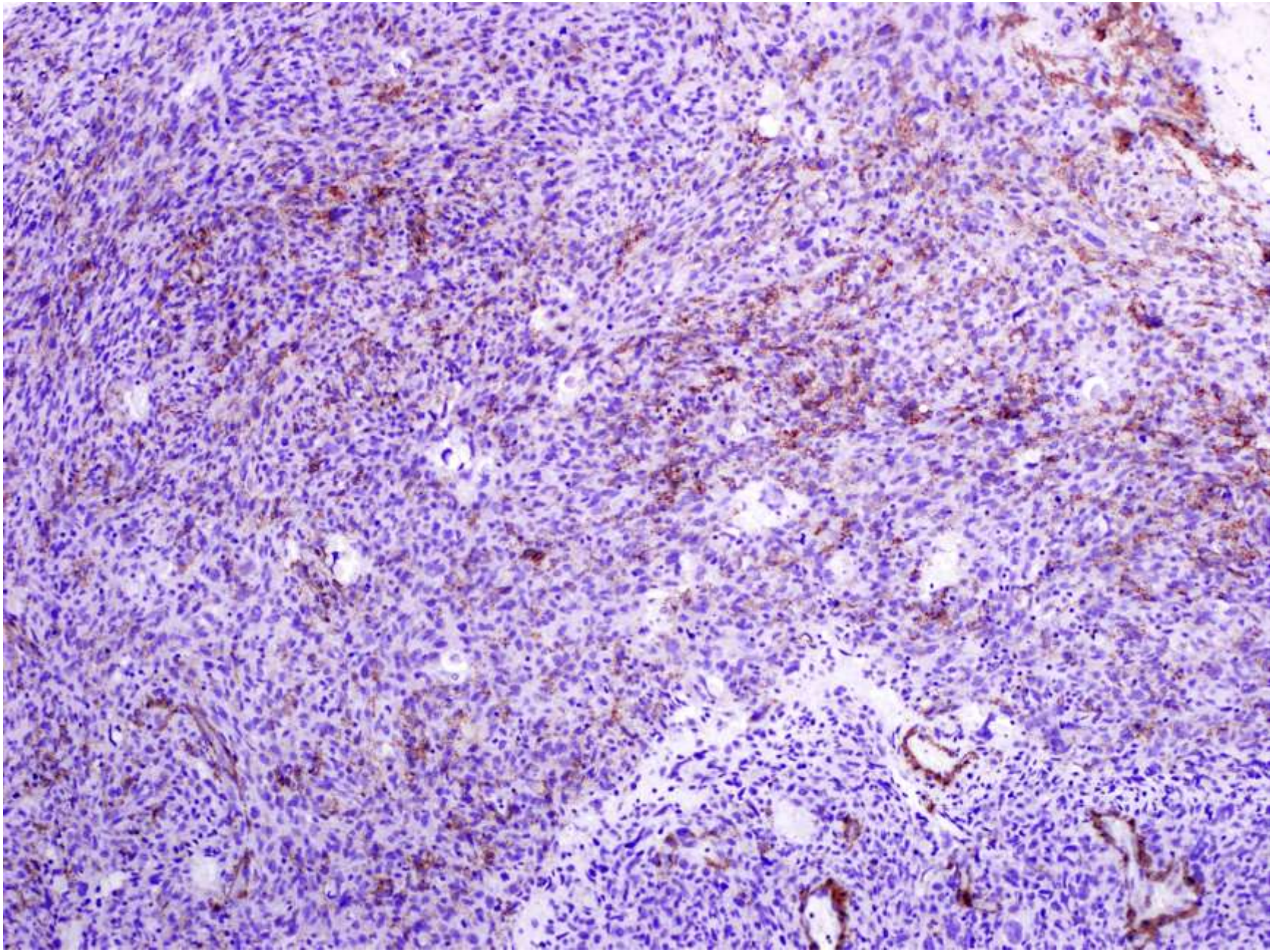

Sequencing shows mutations in DICER1, KRAS, TP53, and ATRX

PATHOGENIC AND LIKELY PATHOGENIC ALTERATIONS				
VARIANT	TRANSCRIPT ID	CLASSIFICATION	READS	MUTANT ALLELE FREQUENCY
DICER1 p.D1709N	NM_177438.2	Pathogenic	968	40%
DICER1 c.2988-1G>A	NM_177438.2	Pathogenic	505	47%
KRAS p.G12D	NM_004985.3	Pathogenic	591	46%
TP53 deep deletion	all	Pathogenic	N/A	N/A
ATRX p.G2120V	NM_000489.3	Likely Pathogenic	348	90%

Primary intracranial spindle cell sarcoma with rhabdomyosarcoma-like features share a highly distinct methylation profile and *DICER1* mutations

Christian Koelsche[1,2,3] · Martin Mynarek[4] · Daniel Schrimpf[1,2] · Luca Bertero[1,5] · Jonathan Serrano[6] · Felix Sahm[1,2] · David E. Reuss[1,2] · Yanghao Hou[1] · Daniel Baumhoer[7] · Christian Vokuhl[8] · Uta Flucke[9] · Iver Petersen[10] · Wolfgang Brück[11] · Stefan Rutkowski[4] · Sandro Casavilca Zambrano[12] · Juan Luis Garcia Leon[13,14,15] · Rosdali Yesenia Diaz Coronado[15] · Manfred Gessler[16,17] · Oscar M. Tirado[18] · Jaume Mora[19] · Javier Alonso[20] · Xavier Garcia del Muro[21] · Manel Esteller[22,23,24] · Dominik Sturm[25,26,27] · Jonas Ecker[25,27,28] · Till Milde[25,27,28] · Stefan M. Pfister[25,26,27] · Andrey Korshunov[1,2] · Matija Snuderl[6] · Gunhild Mechtersheimer[3] · Ulrich Schüller[4,29,30] · David T. W. Jones[25,31] · Andreas von Deimling[1,2]

Received: 13 May 2018 / Accepted: 2 June 2018 / Published online: 7 June 2018

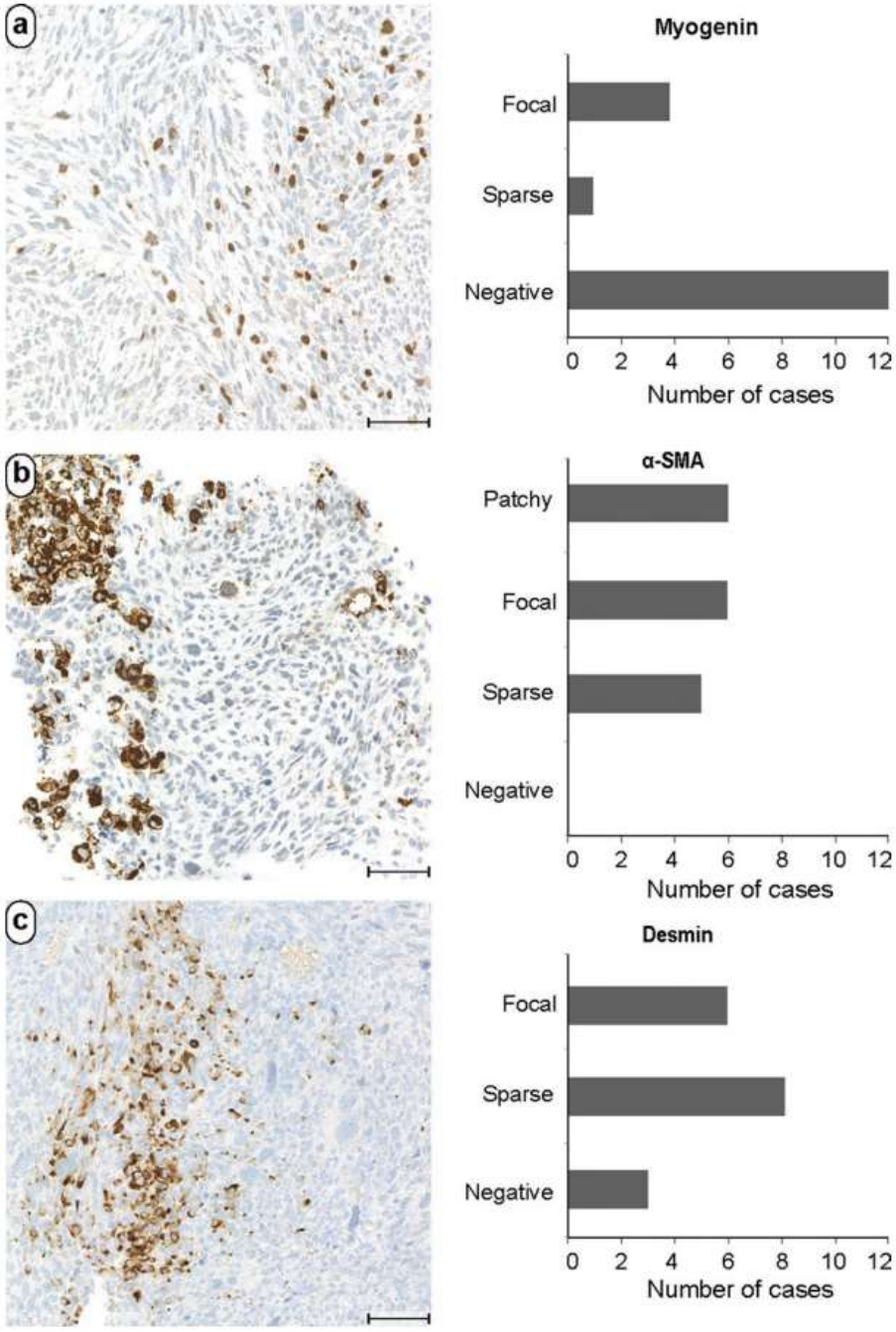
a
Myogenin
Focal
Sparse
Negative
0 2 4 6 8 10 12
Number of cases
b
α-SMA
Patchy
Focal
Sparse
Negative
0 2 4 6 8 10 12
Number of cases
c
Desmin
Focal
Sparse
Negative
0 2 4 6 8 10 12
Number of cases

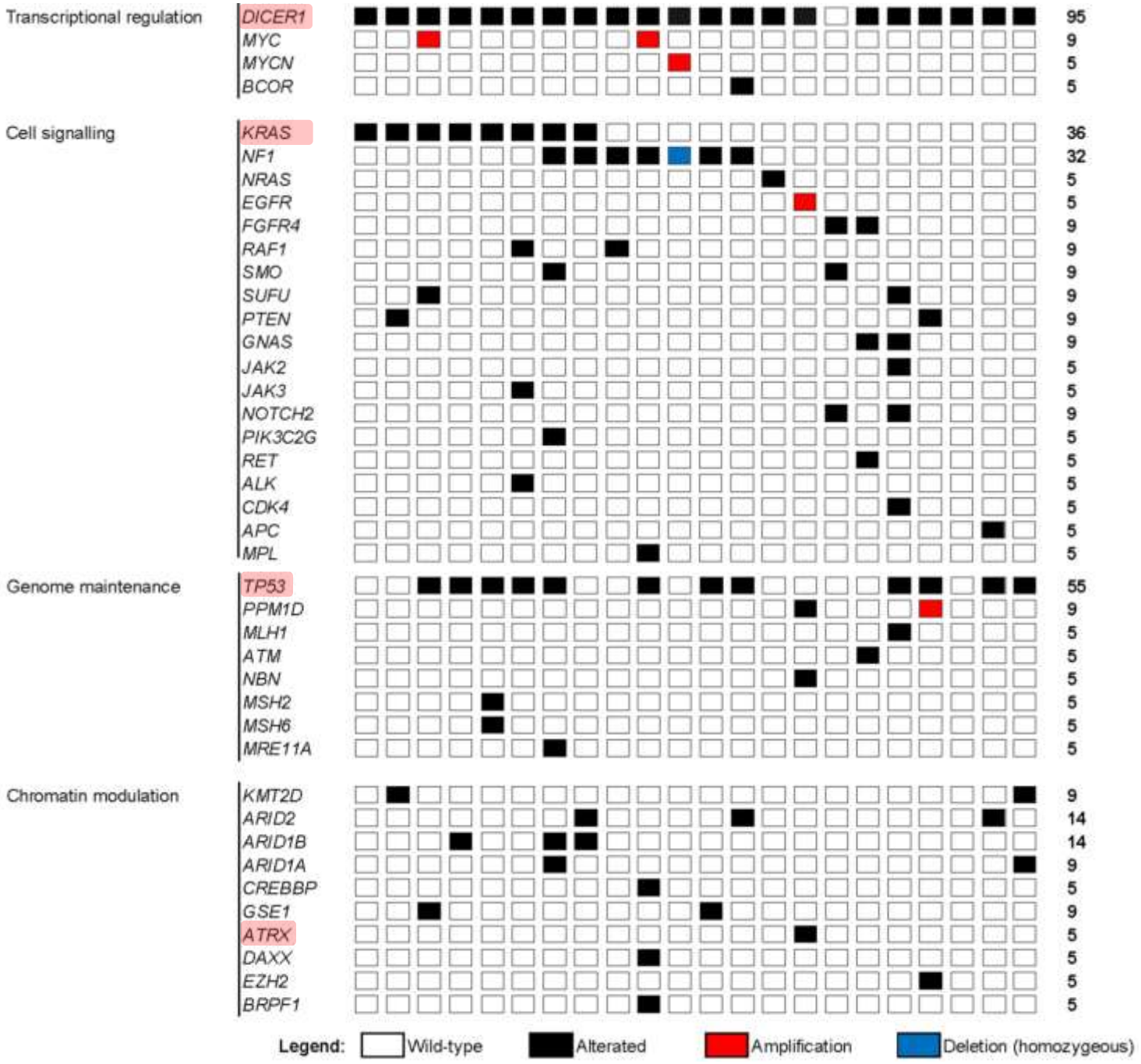
Transcriptional regulation
DICER1
MYC
MYCN
BCOR
95
9
5
5
Cell signalling
KRAS
NF1
NRAS
EGFR
FGFR4
RAF1
SMO
SUFU
PTEN
GNAS
JAK2
JAK3
NOTCH2
PIK3C2G
RET
ALK
CDK4
APC
MPL
36
32
5
5
9
9
9
9
9
9
5
5
9
5
5
5
5
5
5
Genome maintenance
TP53
PPM1D
MLH1
ATM
NBN
MSH2
MSH6
MRE11A
55
9
5
5
5
5
5
5
Chromatin modulation
KMT2D
ARID2
ARID1B
ARID1A
CREBBP
GSE1
ATRX
DAXX
EZH2
BRPF1
9
14
14
9
5
9
5
5
5
5
Legend:
Wild-type
Alterated
Amplification
Deletion (homozygeous)

19-0305

Hannah Wang/Gerald Berry; Stanford

37-year-old female with h/o left pneumonectomy on 2009 for a pleural-based tumor. She now presents with SOB, chest tightness. Imaging shows 12.9cm PET-avid posterior mediastinal mass with complex solid and cystic components.

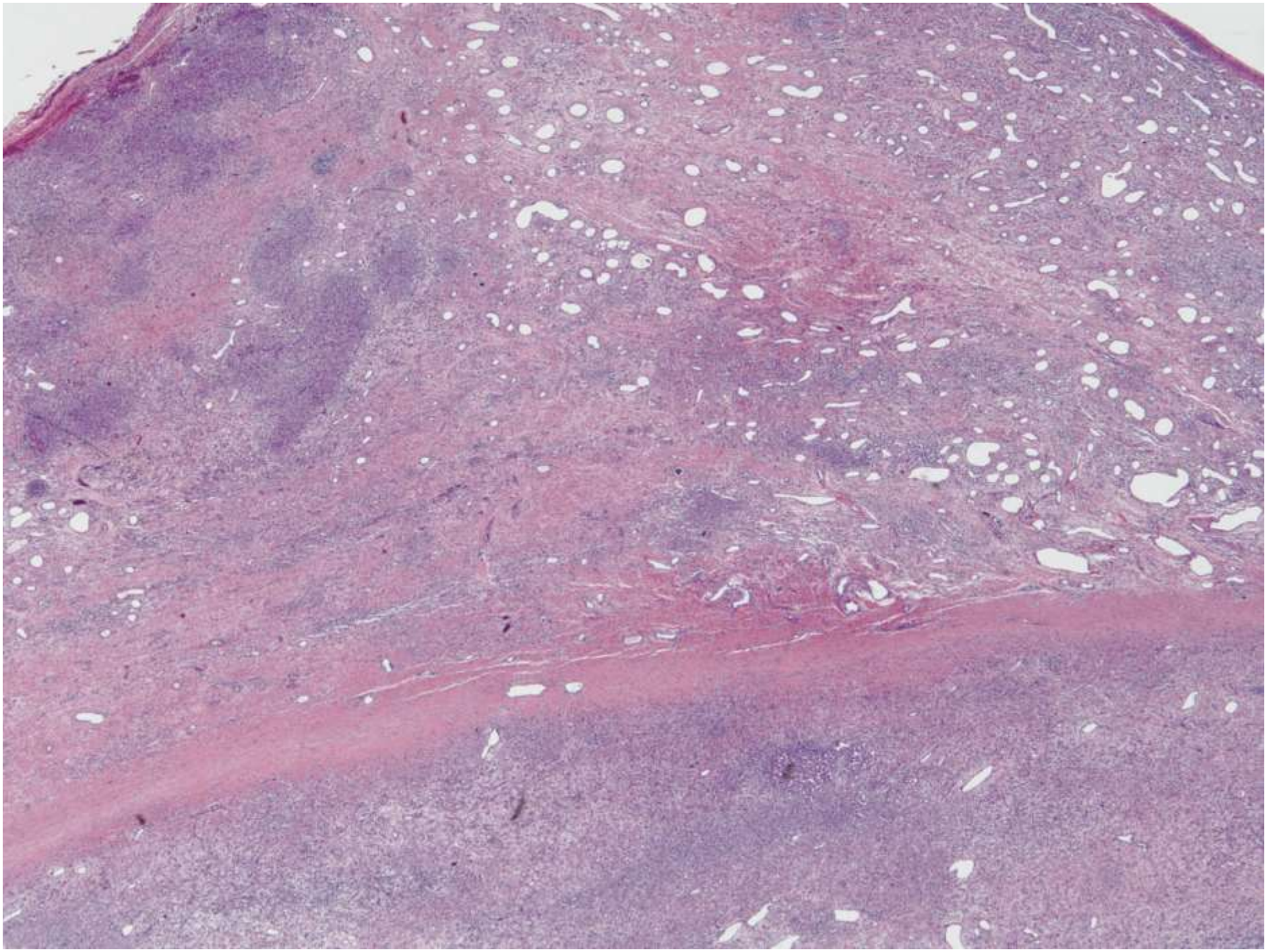

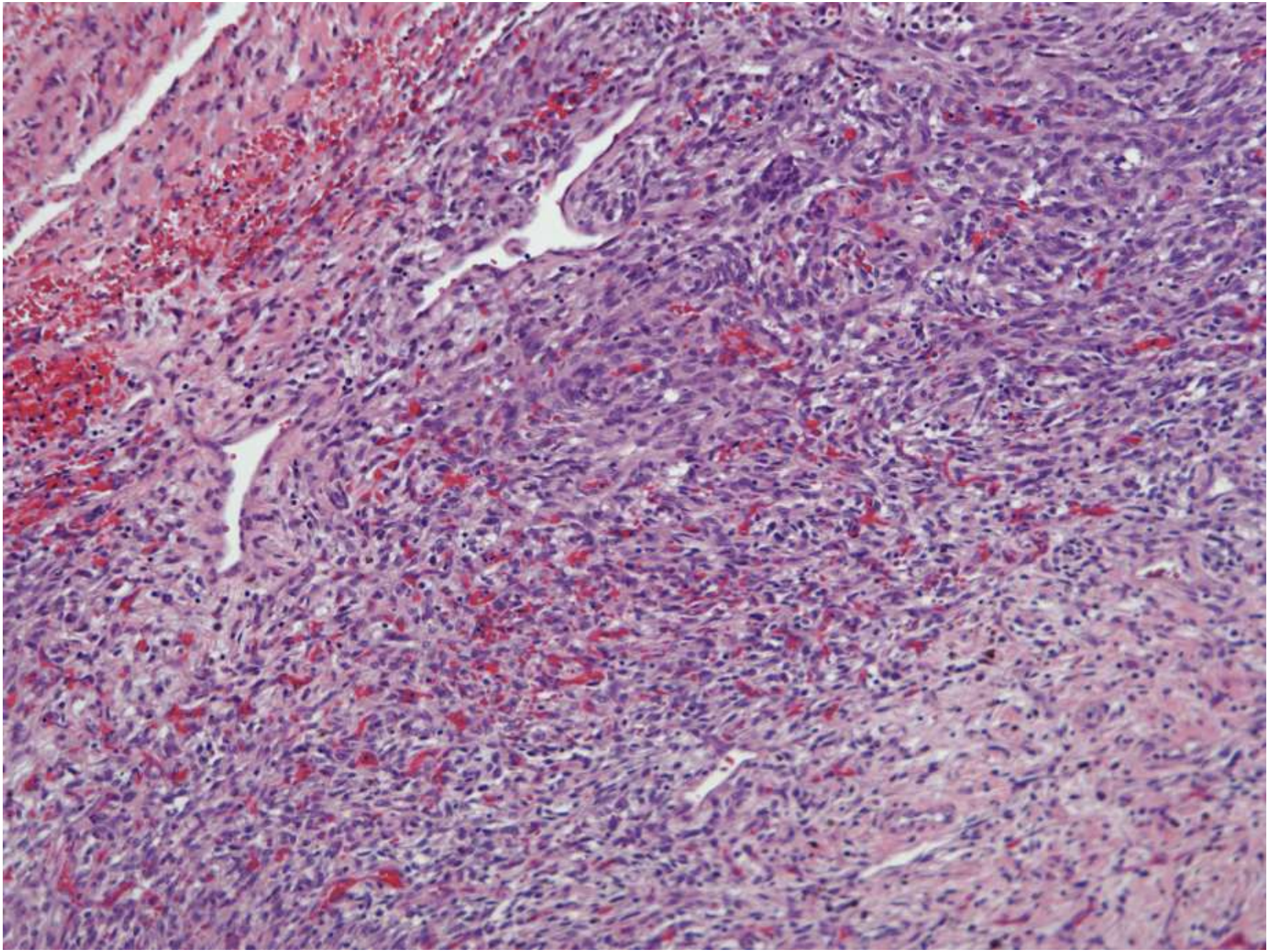

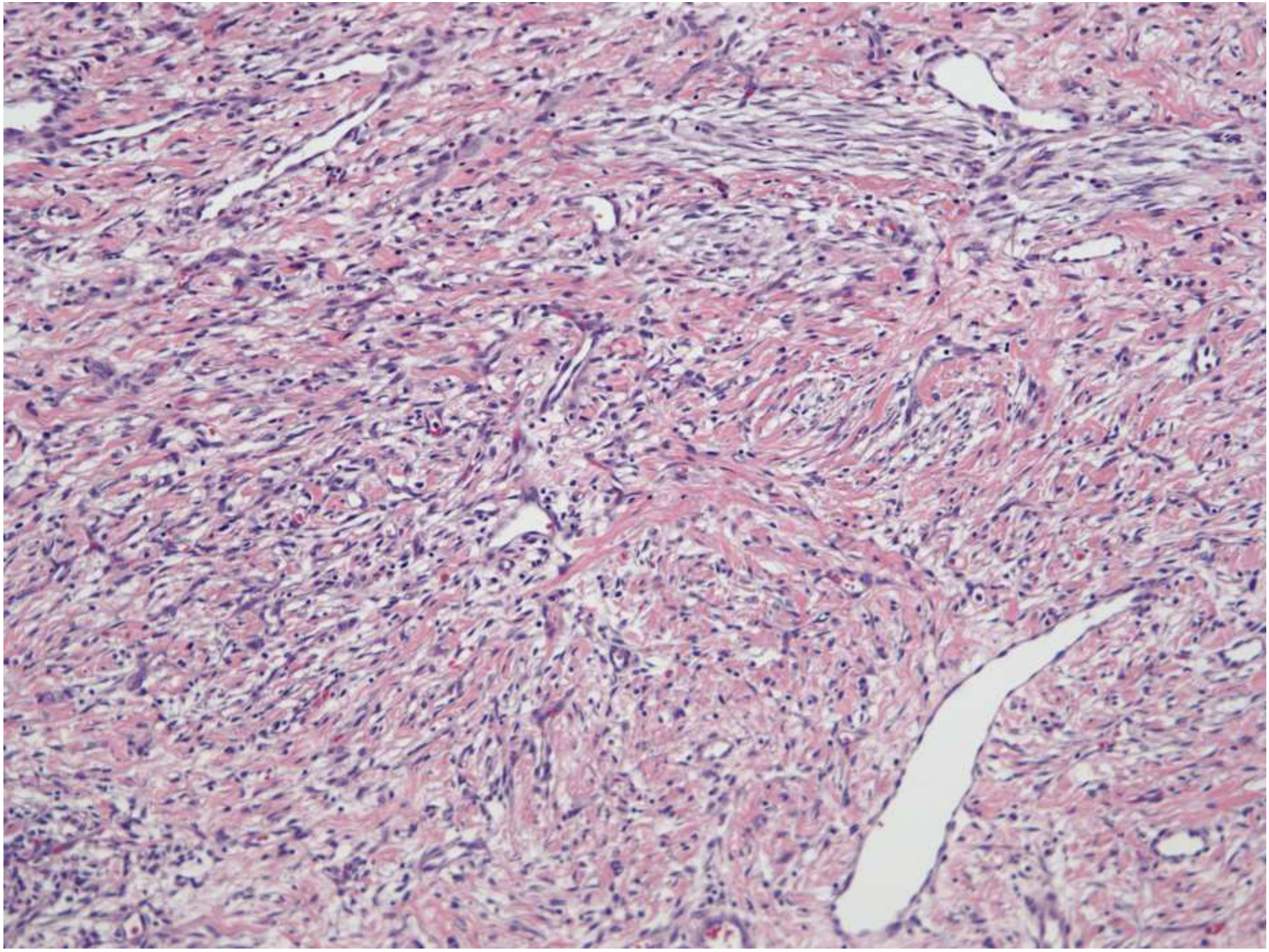

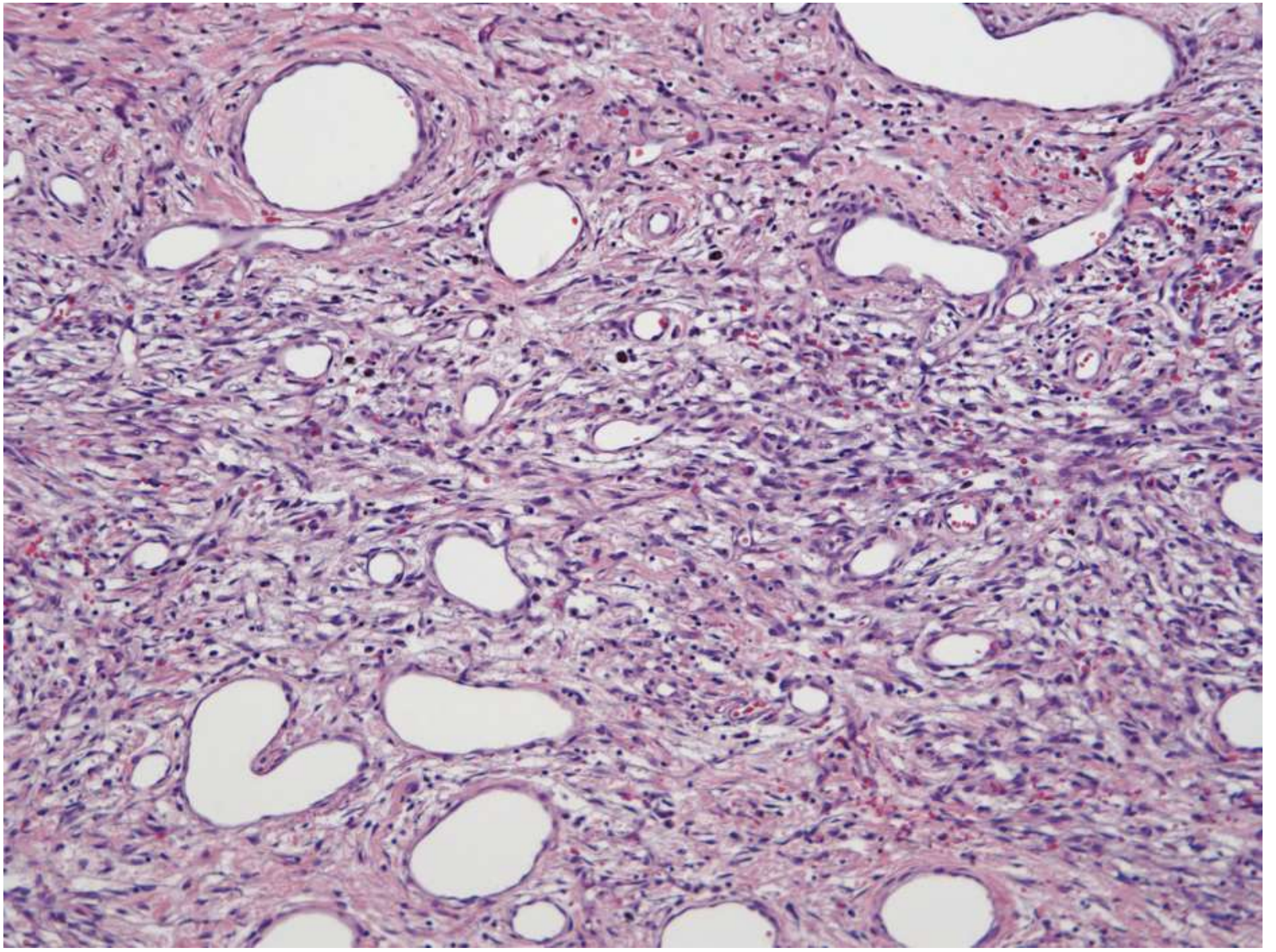

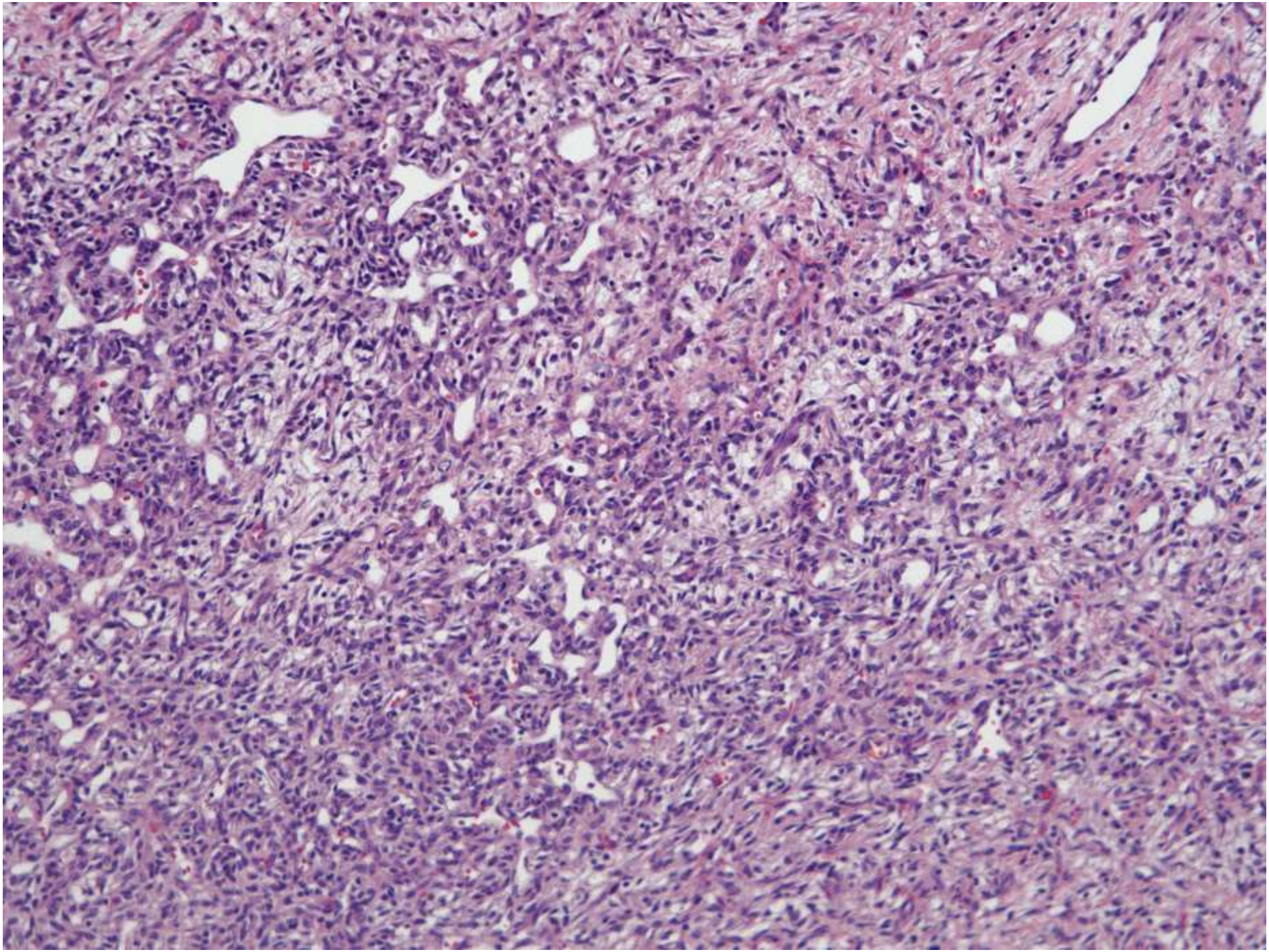

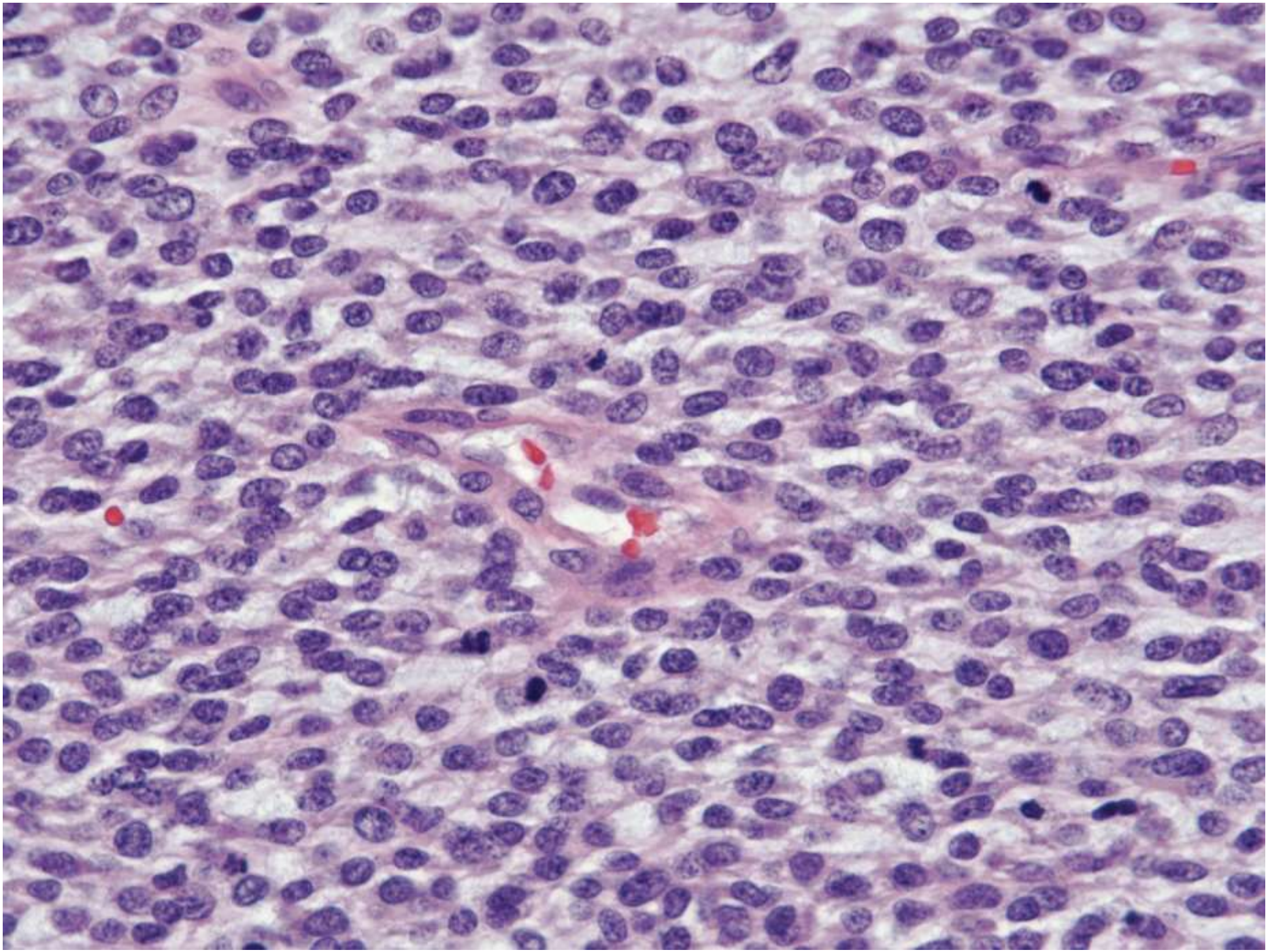

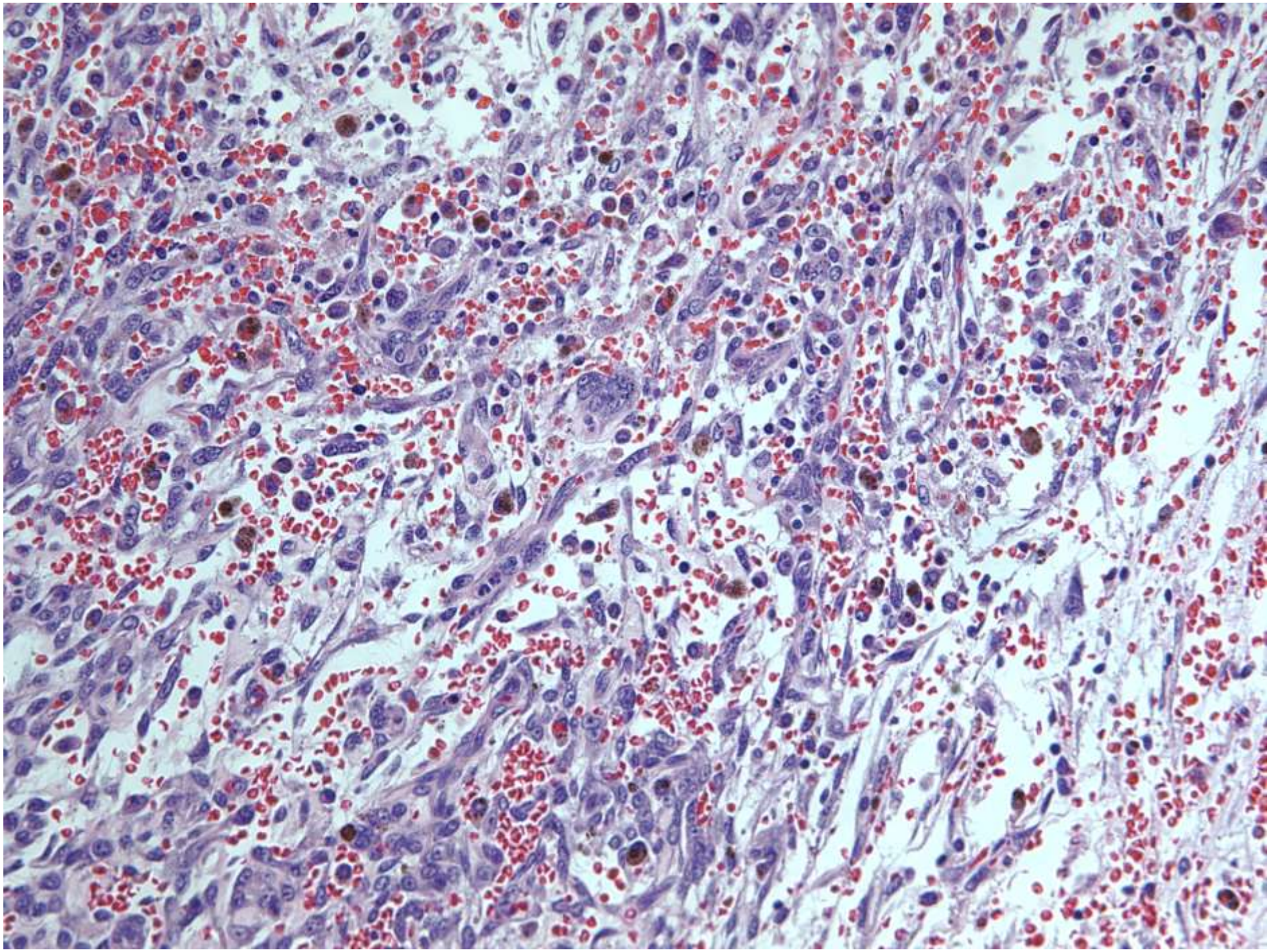

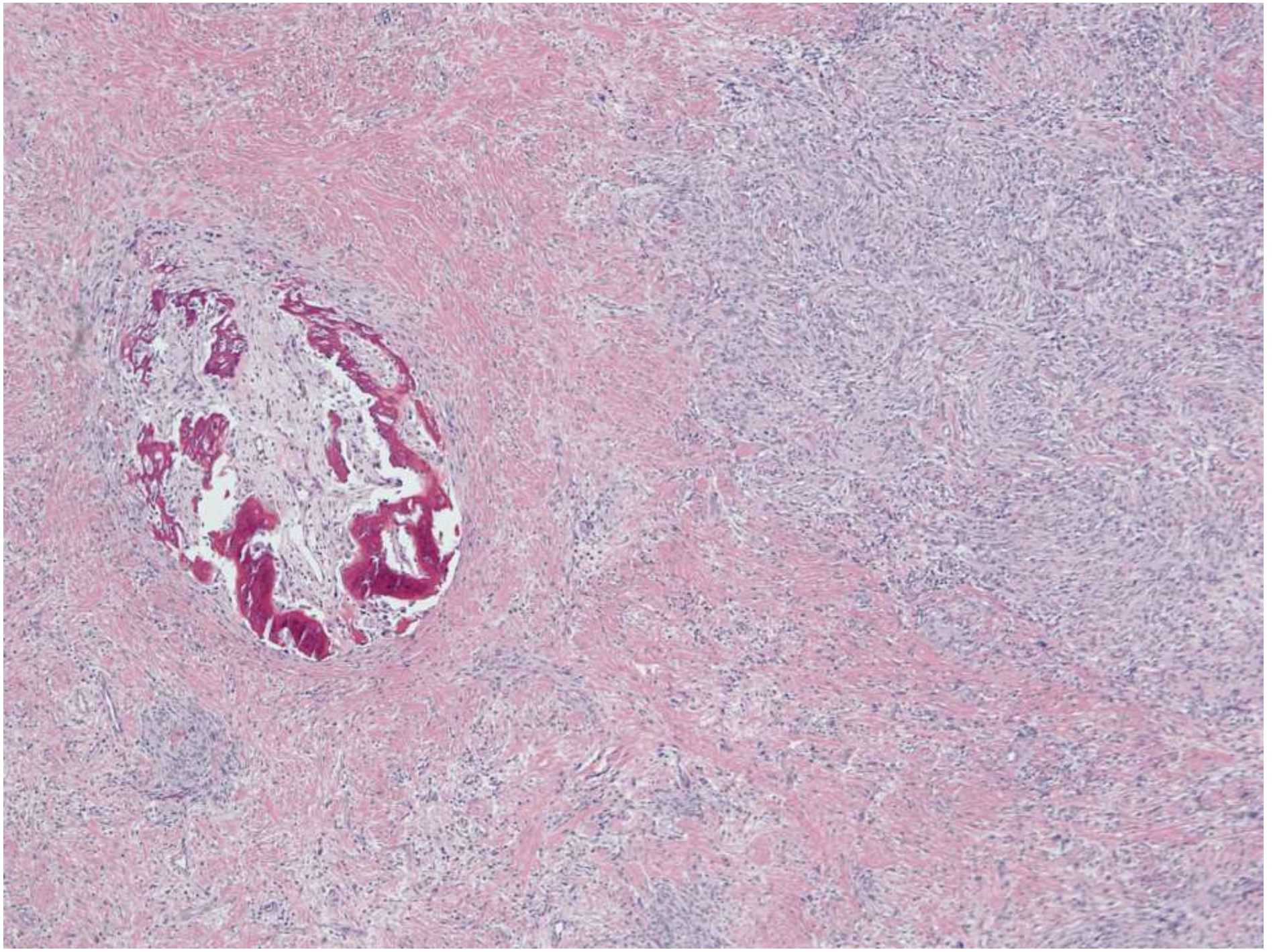

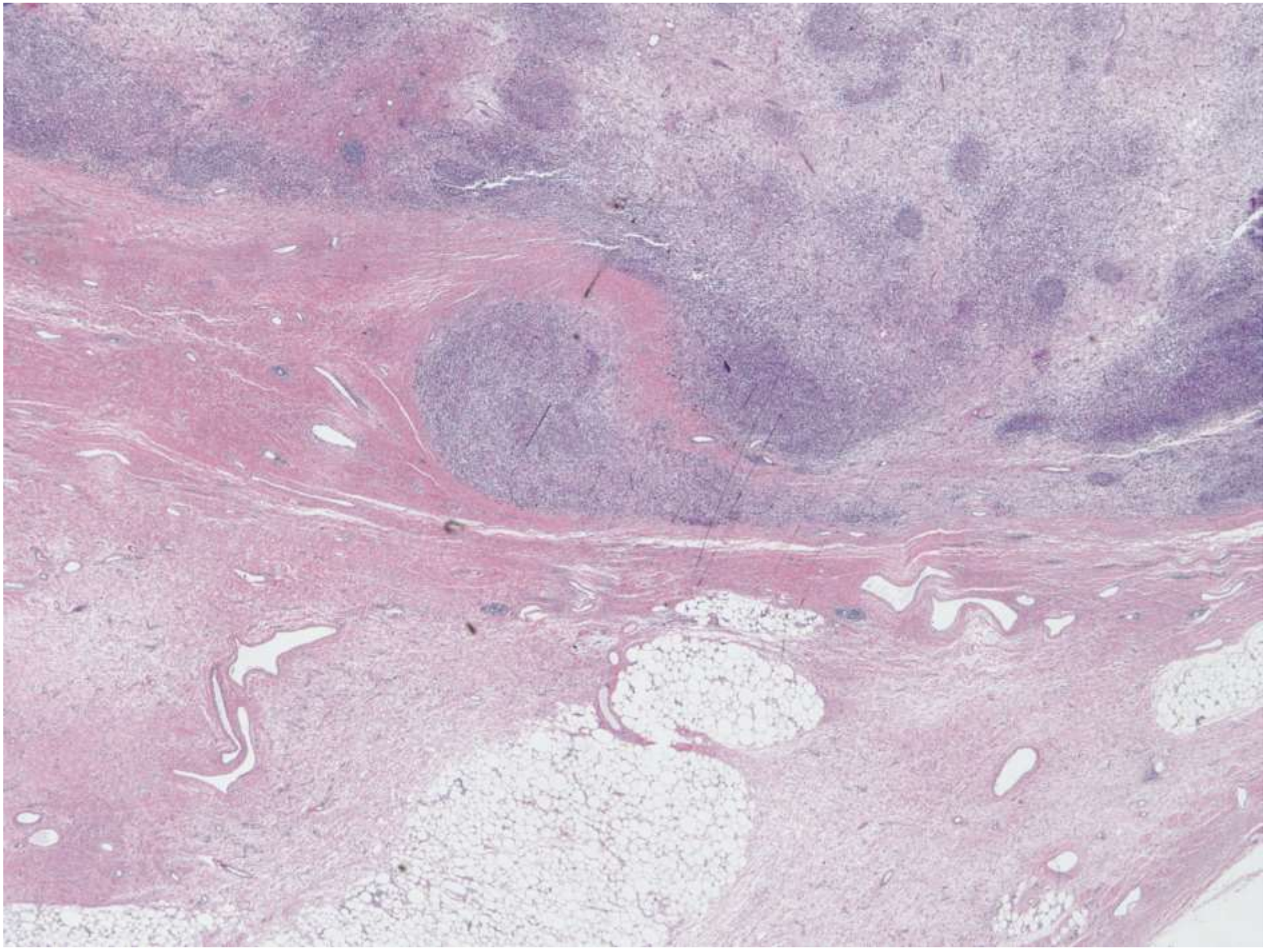

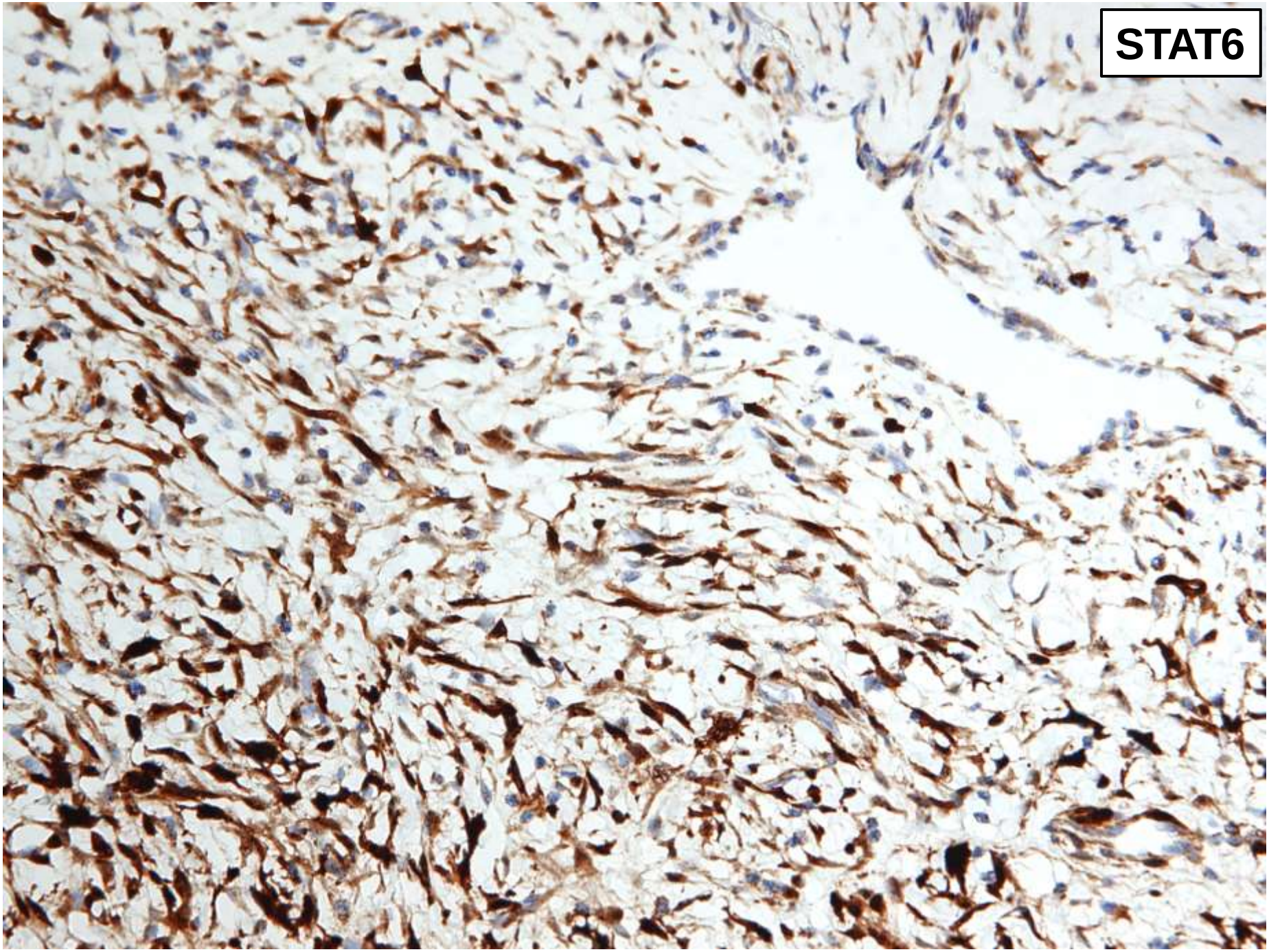
STAT6

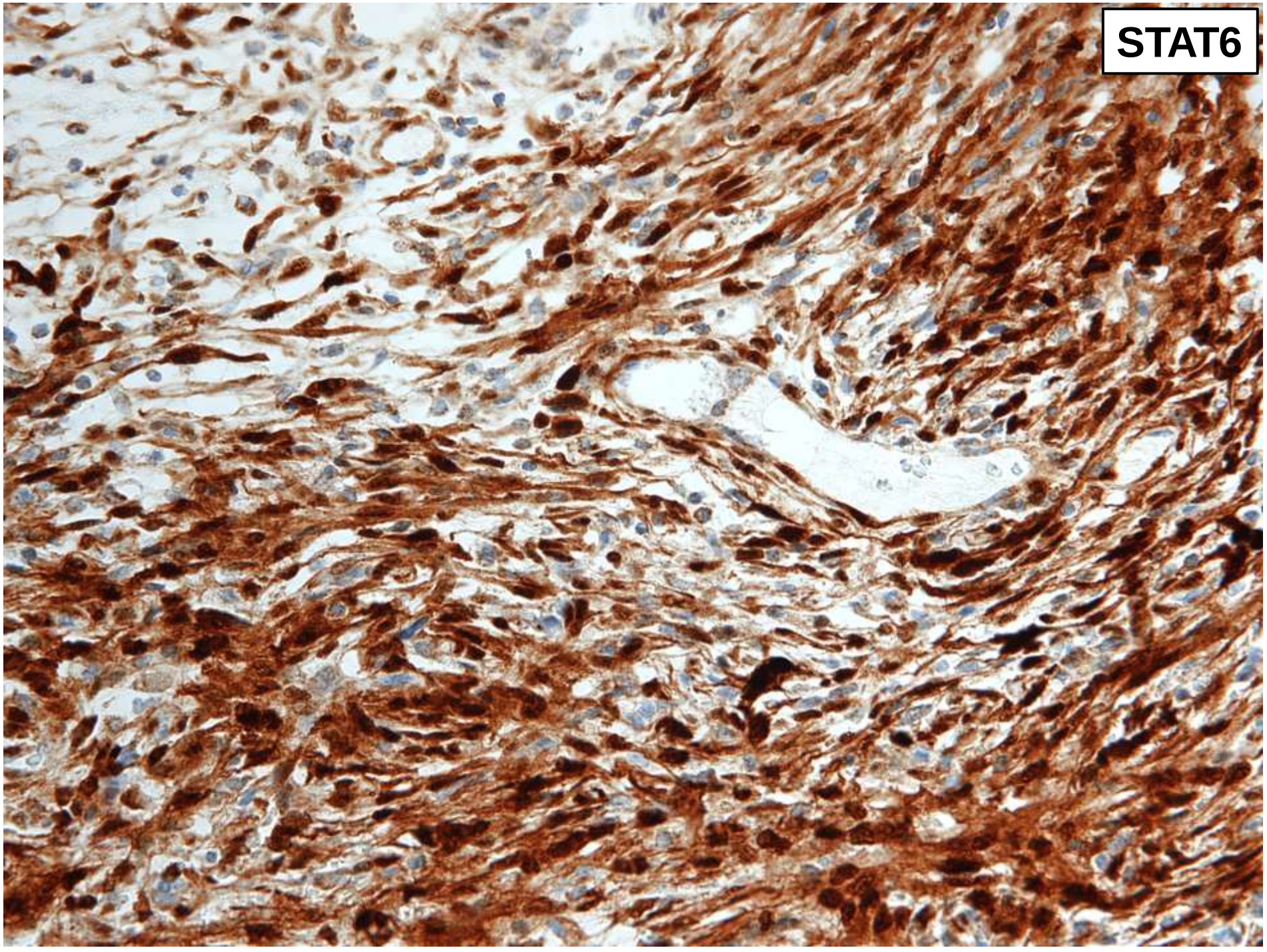
STAT6

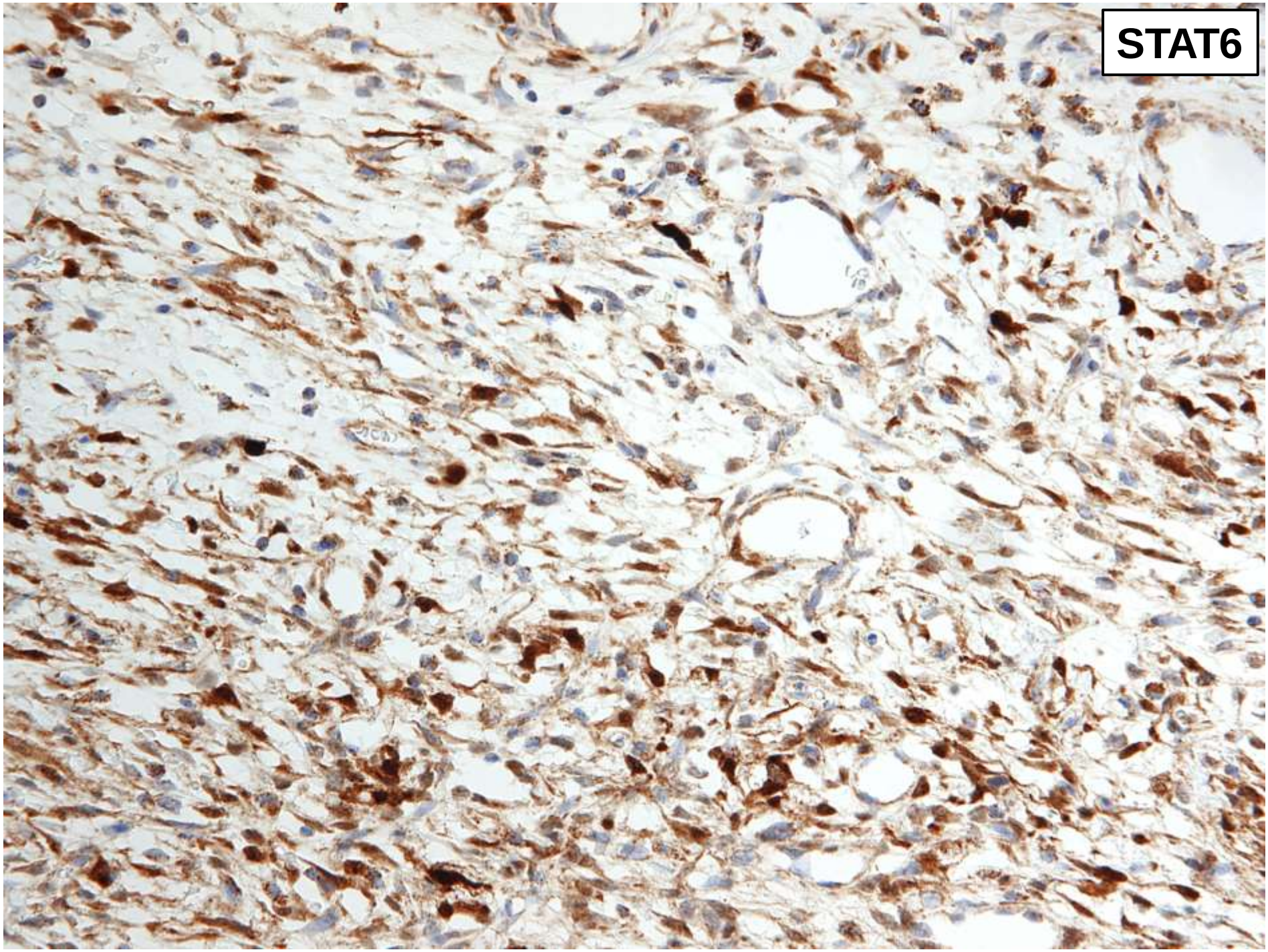
STAT6

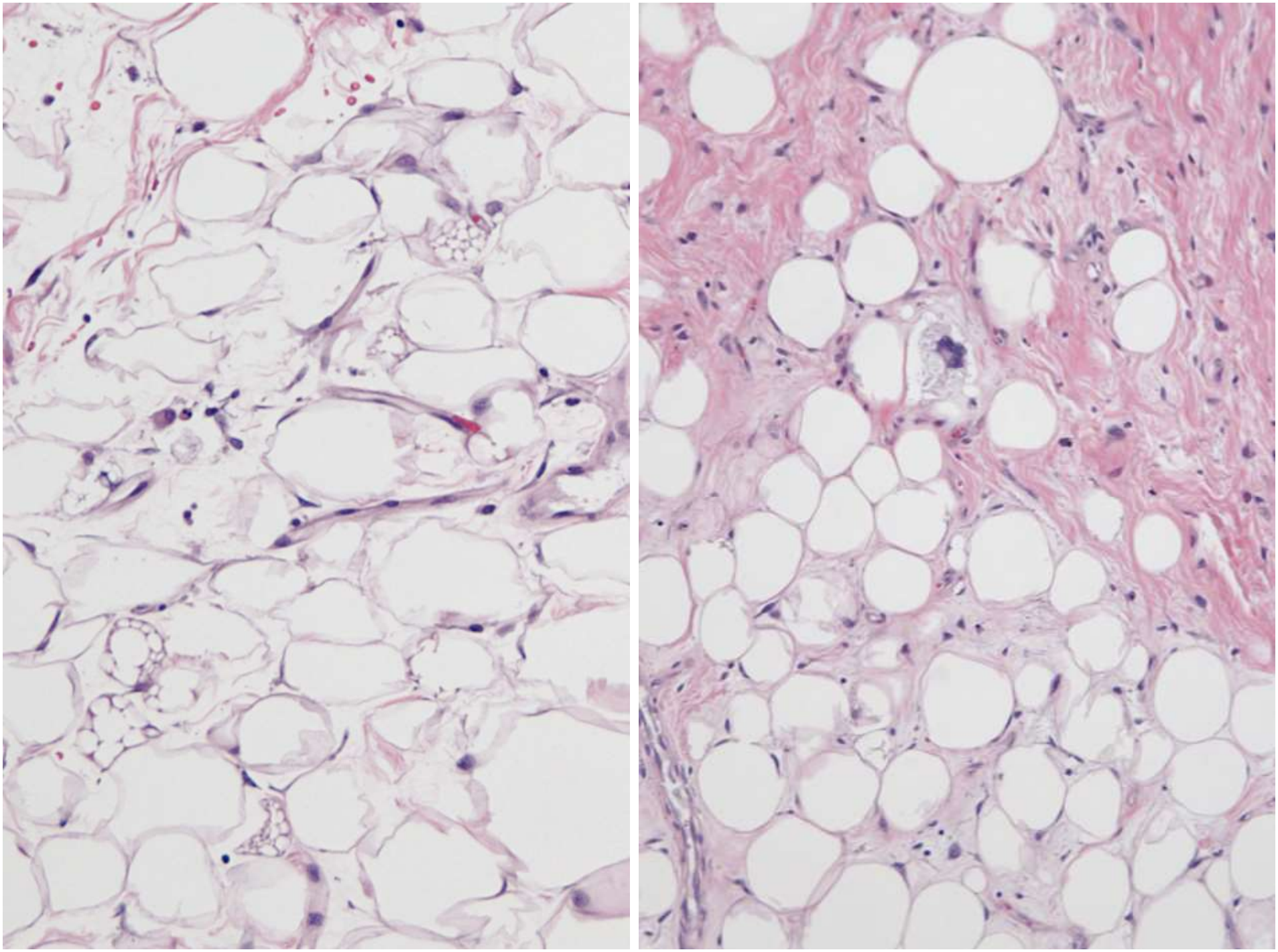

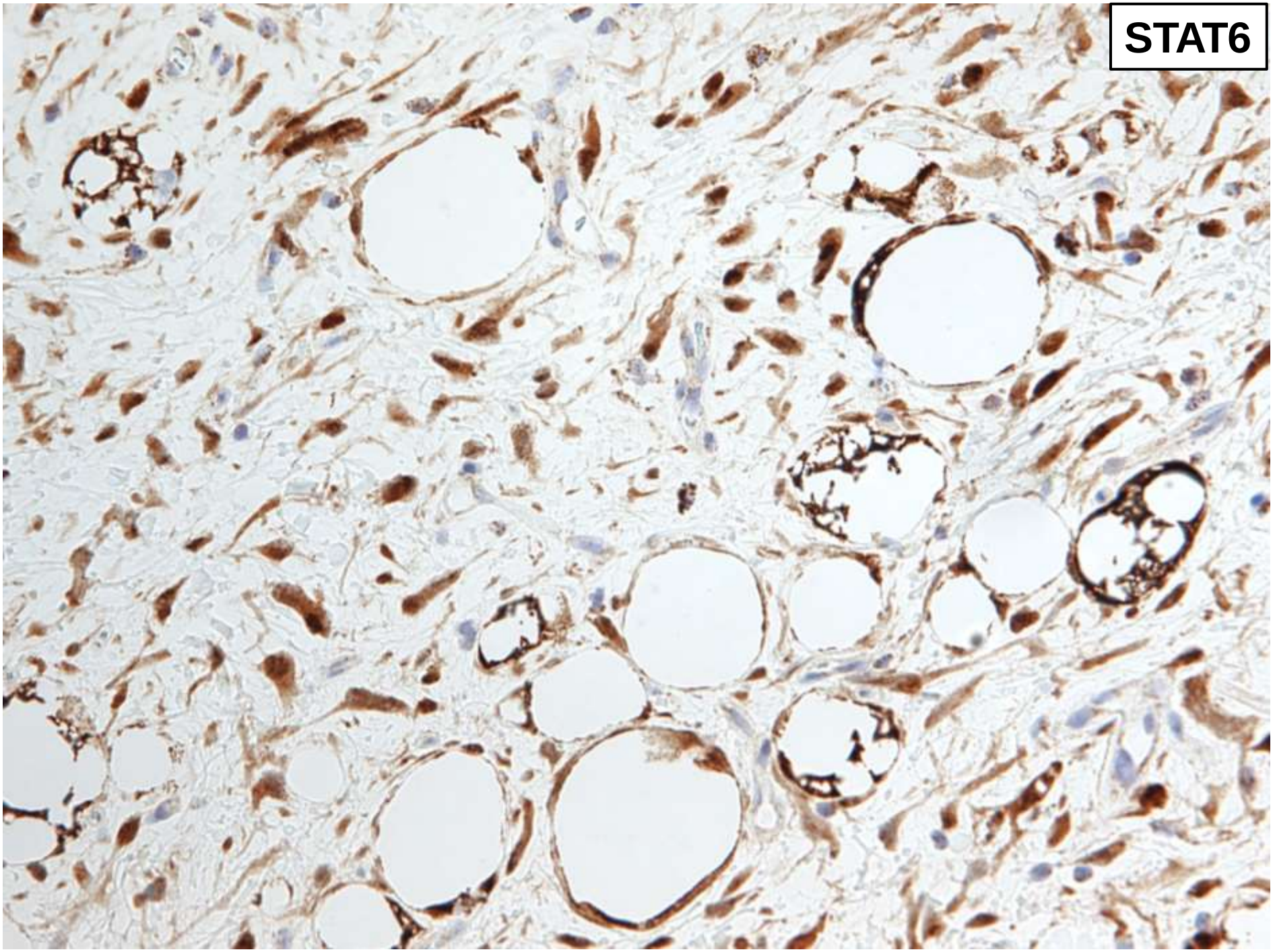
STAT6

Diagnosis:

-- Recurrent dedifferentiated liposarcoma
-- FISH positive for MDM2 gene amplification

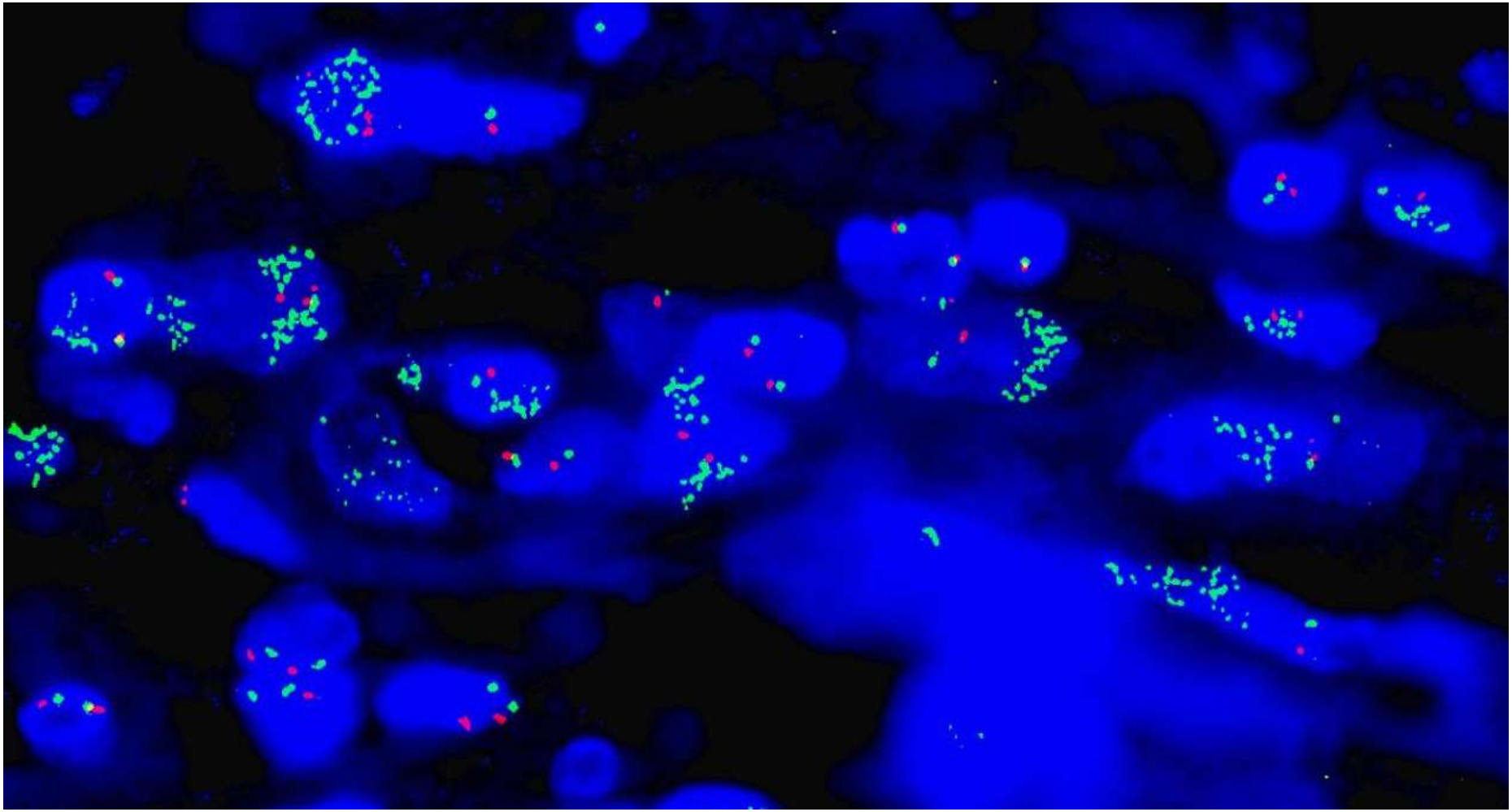

Diagnostic Pitfall:

Nuclear STAT6 expression is not specific to solitary fibrous tumor

Consider alternate diagnoses when stain is patchy or weak

STAT6 nuclear expression can be seen in benign scar or adipose tissue

Extensive Survey of STAT6 Expression in a Large Series of Mesenchymal Tumors

Elizabeth G. Demicco, MD, PhD,[1] Paul W. Harms, MD, PhD,[2] Rajiv M. Patel, MD,[2] Steven C. Smith, MD, PhD,[2] Davis Ingram,[3] Keila Torres, MD, PhD,[4,5] Shannon L. Carskadon, MS,[2] Sandra Camelo-Piragua, MD,[2] Jonathan B. McHugh, MD,[2] Javed Siddiqui, MS, MB (ASCP),[2] Nallasivam Palanisamy, PhD,[2] David R. Lucas, MD,[2] Alexander J. Lazar, MD, PhD,[3,4] and Wei-Lien Wang, MD[3]

From [1]Pathology, Icahn School of Medicine at Mount Sinai, New York, NY; [2]Pathology, University of Michigan Medical Center, Ann Arbor; and [3]Pathology, [4]Sarcoma Research Center, and [5]Surgical Oncology, The University of Texas MD Anderson Cancer Center, Houston.

Key Words: STAT6; Solitary fibrous tumor; Sarcoma; Immunohistochemistry

Am J Clin Pathol May 2015; 143:672-682

Table 1
Nuclear STAT6 Expression in Mesenchymal Tumors

Diagnosis	No. of Cases	Nuclear Expression 0-1+, No.	Equivocal, No.	2-3+, No. (%)
Solitary fibrous tumor	240	15	19	206 (86)
Unclassified sarcoma	65	55	2	8 (12)
ALT/WDL/DDLPS	409	359	1	49 (12)
Desmoid tumor	184	162	8	14 (8)
Neurofibroma	60	57	0	3 (5)
Clear cell sarcoma	19	18	0	1 (5)
Myxoid liposarcoma	108	106	0	2 (2)
Undifferentiated pleomorphic sarcoma	173	171	0	2 (1)

Table 2
STAT6 Expression in Selected Nonneoplastic Mesenchymal Tissues

Tissue	No. of Cases	Nuclear Expression 0-1+, No.	Equivocal, No.	2-3+, No. (%)
Scar	17	11	2	4 (24)
Adipose tissue	24	22	0	2 (8)
Bowel muscularis	4	4	0	0
Nerve	10	10	0	0
Uterine myometrium	6	6	0	0

Molecular Alterations Associated with Mesenchymal Tumors on Chromosome 12q

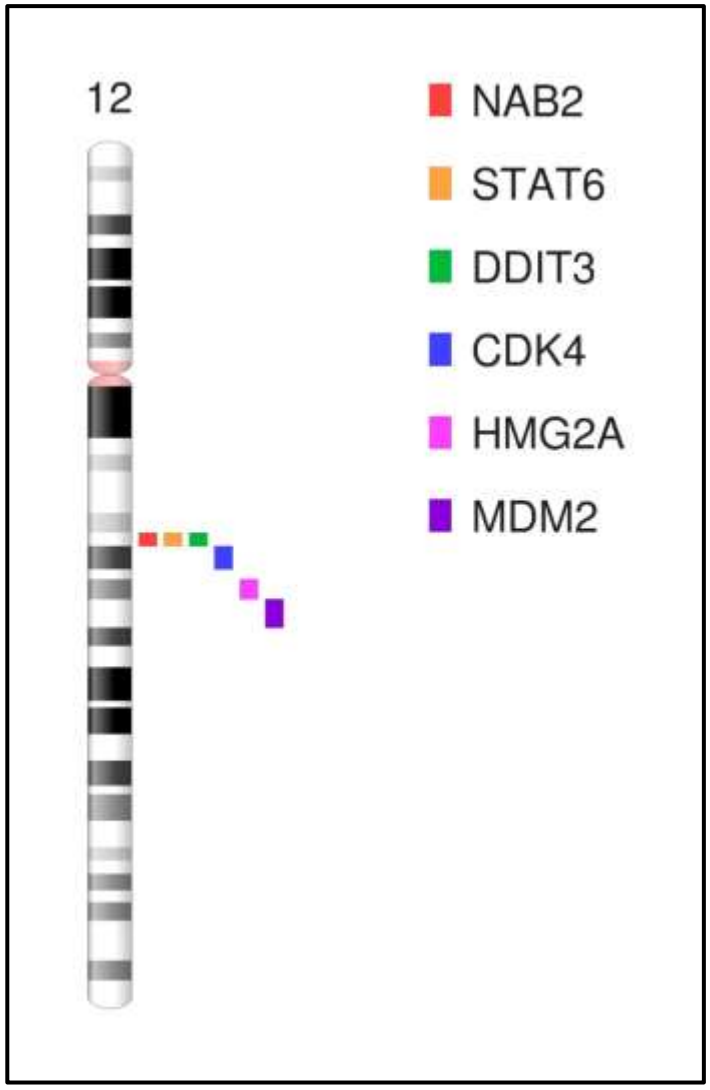

- ***Solitary fibrous tumor:*** NAB2-STAT6 fusion
- ***Myxoid liposarcoma:*** FUS-DDIT3 fusion
- ***Lipoma:*** HMG2A rearrangements
- ***Well differentiated/dedifferentiated liposarcoma:*** MDM2 and CDK4 amplification, some with HMG2A amplification, STAT6 amplification

Why Can Dedifferentiated Liposarcoma Have Solitary Fibrous Tumor-like Morphology?

MDM2 amplification in WDLPS/DDLPS happens through a complex series of events

Inherent to this process is a large degree of randomness, and thus, cell-to-cell heterogeneity

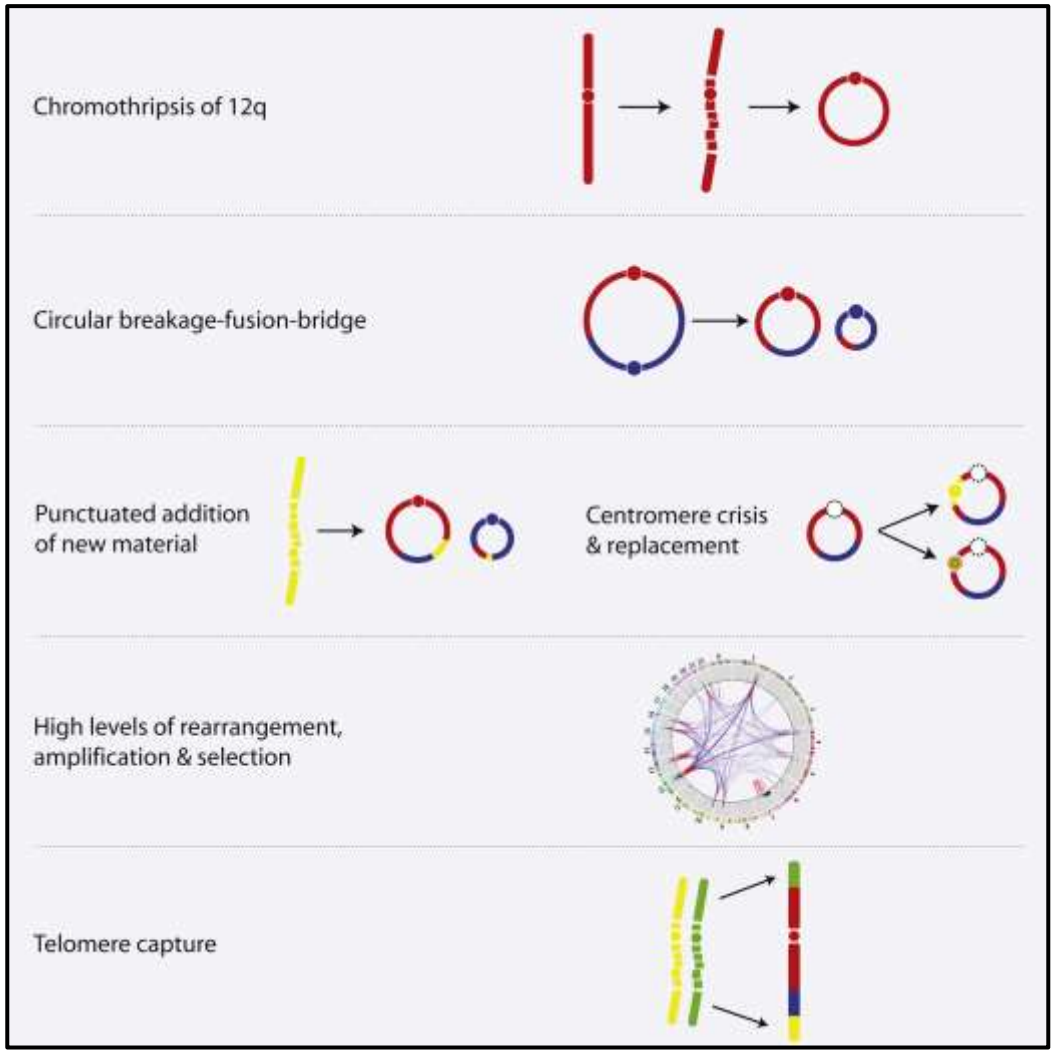

Cancer Cell
Article

The Architecture and Evolution of Cancer Neochromosomes

Dale W. Garsed, Owen J. Marshall, Vincent D.A. Corbin, Arthur Hsu, Leon Di Stefano, Jan Schröder, Jason Li, Zhi-Ping Feng, Bo W. Kim, Mark Kowarsky, Ben Lansdell, Ross Brookwell, Ola Myklebost, Leonardo Meza-Zepeda, Andrew J. Holloway, Florence Pedeutour, K.H. Andy Choo, Michael A. Damore, Andrew J. Deans, Anthony T. Papenfuss, and David M. Thomas

Can MDM2 Gene Amplification and NAB2-STAT6 Fusions Co-Occur?

Diamandis *et al. Diagnostic Pathology* (2016) 11:13
DOI 10.1186/s13000-016-0455-9

Diagnostic Pathology

CASE REPORT Open Access

Case Report: Next generation sequencing identifies a *NAB2-STAT6* fusion in Glioblastoma

Phedias Diamandis[1,2], Ruben Ferrer-Luna[3,4], Raymond Y. Huang[5], Rebecca D. Folkerth[2,6,7], Azra H. Ligon[2,6], Patrick Y. Wen[8], Rameen Beroukhim[3,4], Keith L. Ligon[2,3,6,7,8] and Shakti H. Ramkissoon[2,6,7,8*]

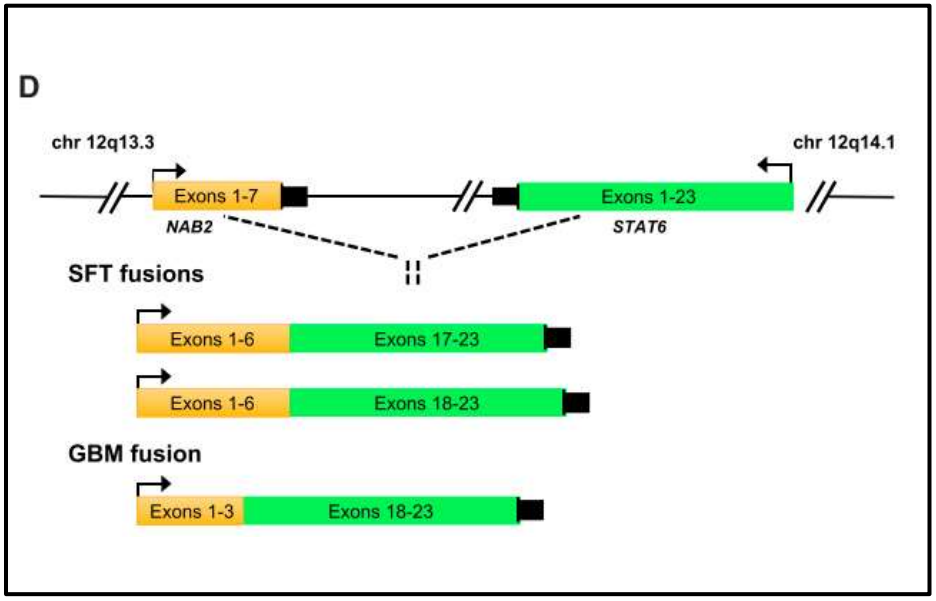

Single case of NAB2-STAT6 fusion identified in GBM, along with coamplification of NAB2, STAT6, CDK4

No NAB2-STAT6 fusions or other fusion events involving NAB2 or STAT6 found in TCGA database of adult low grade gliomas (n=361)

STAT6-CPM and HIPK2-STAT6 fusions each with co-amplification of CDK4 and MDM2 identified in GBM data set (n=206)

Summary

- Dedifferentiated liposarcoma can morphologically resemble solitary fibrous tumor, and can show diffuse STAT6 nuclear expression on IHC (though usually weak/patchy)
- Solitary fibrous tumors can rarely have fat-forming areas, as well as areas of heterologous differentiation
- STAT6 IHC is sensitive for detection of SFT, but not specific
- NAB2-STAT6 fusion (by sequencing) is “definitional” for SFT, at least for now
- MDM2 amplification helps in diagnosing WDLPS/DDLPS but can be seen in other sarcomas (low grade osteosarcoma, intimal sarcoma, up to 20% MPNSTs, up to 5% endometrial stromal sarcomas, rare sclerosing rhabdomyosarcoma)

19-0306
(scanned slide available)

Li Lei/Megan Troxell; Stanford

40-year-old male with a solid enhancing 3.5cm left mid renal cortical mass, most consistent with renal cell carcinoma on imaging.

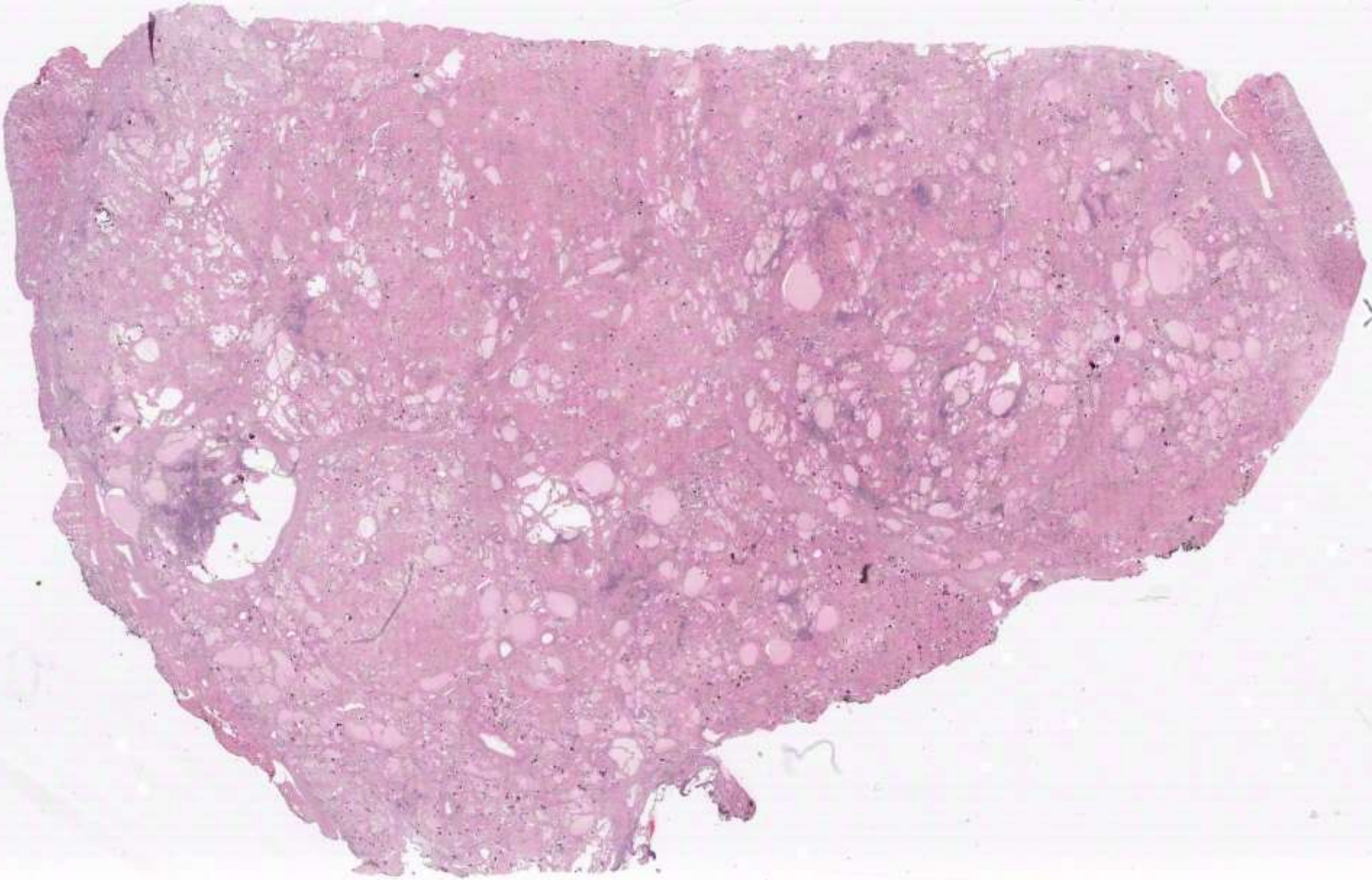

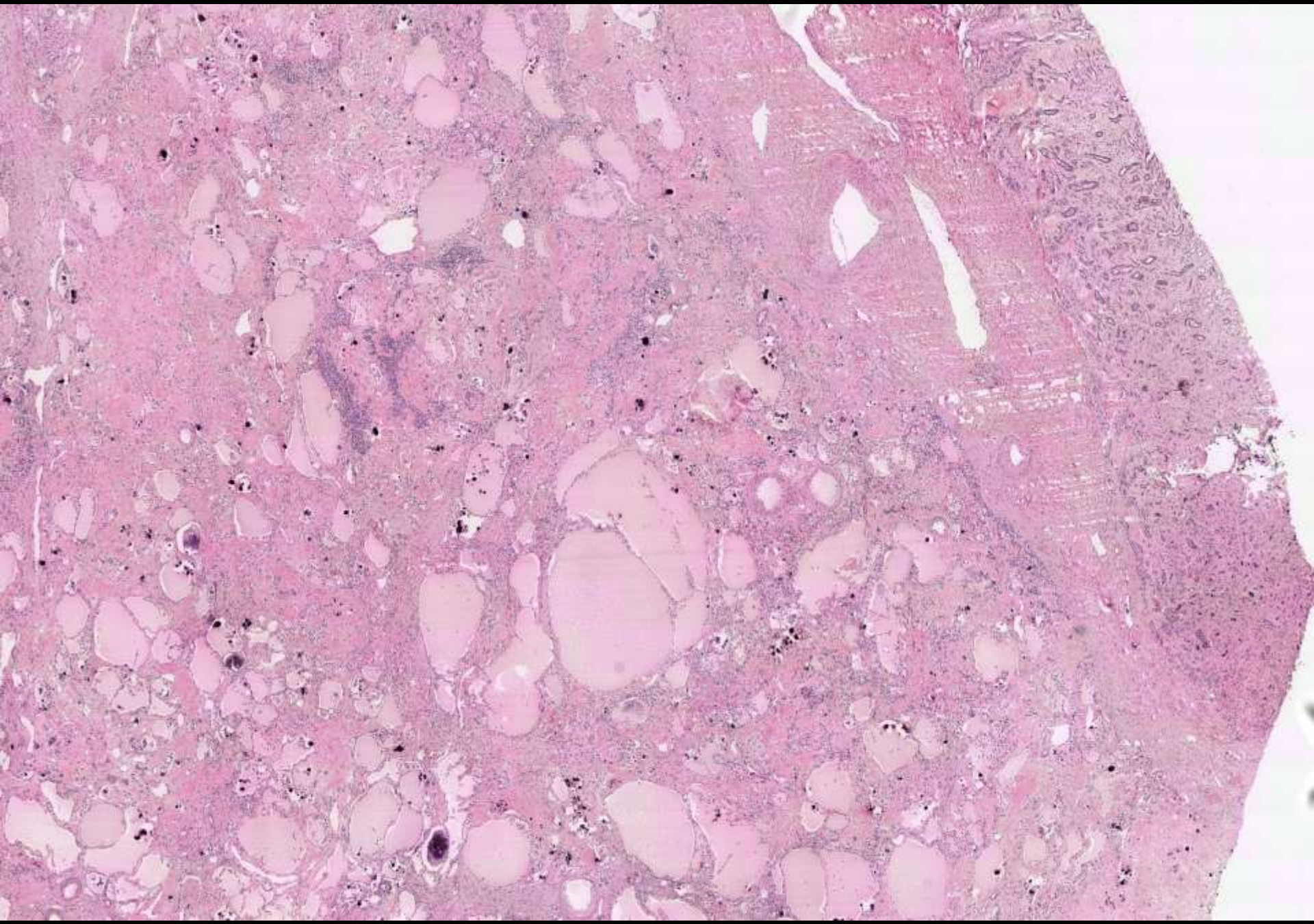

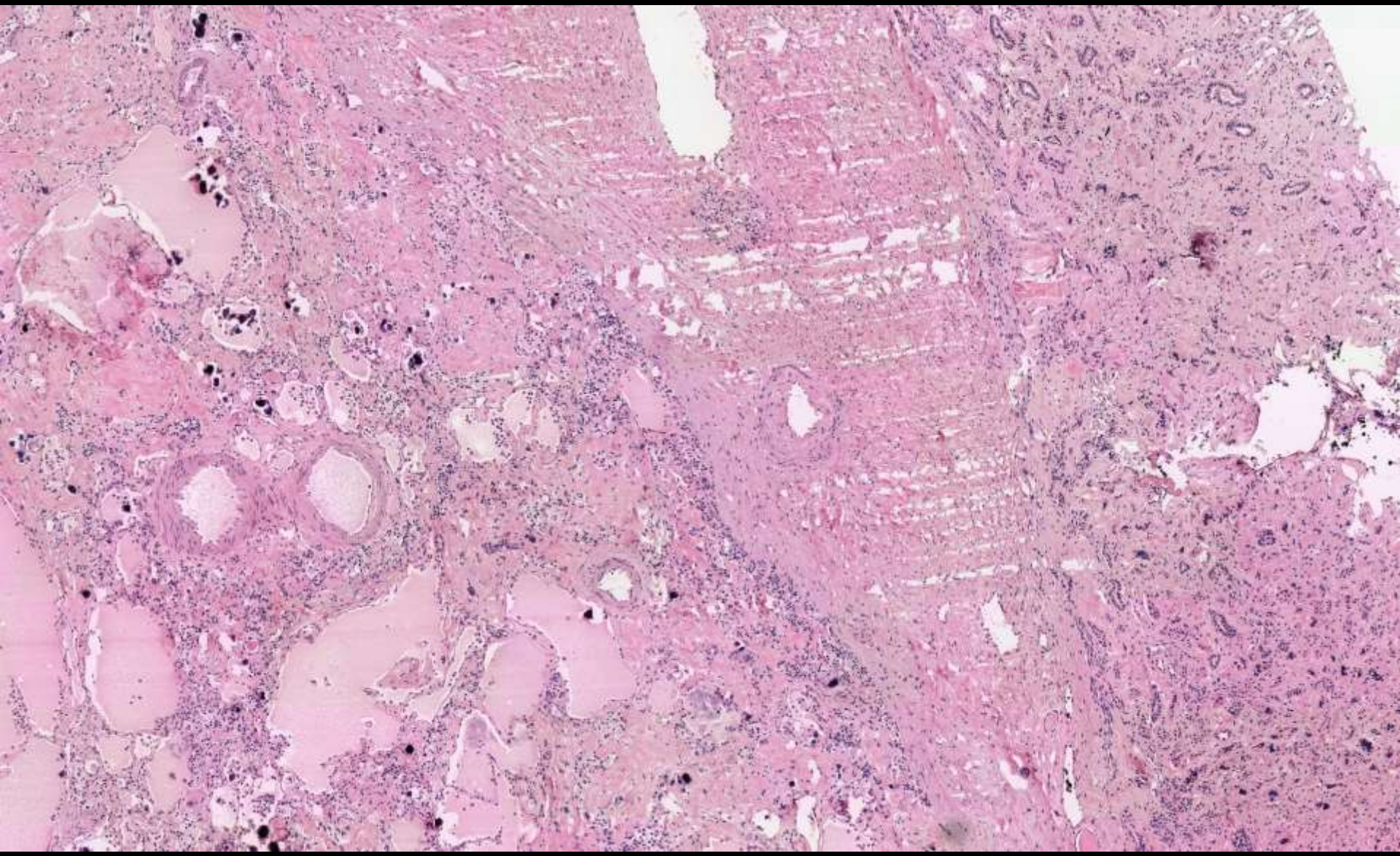

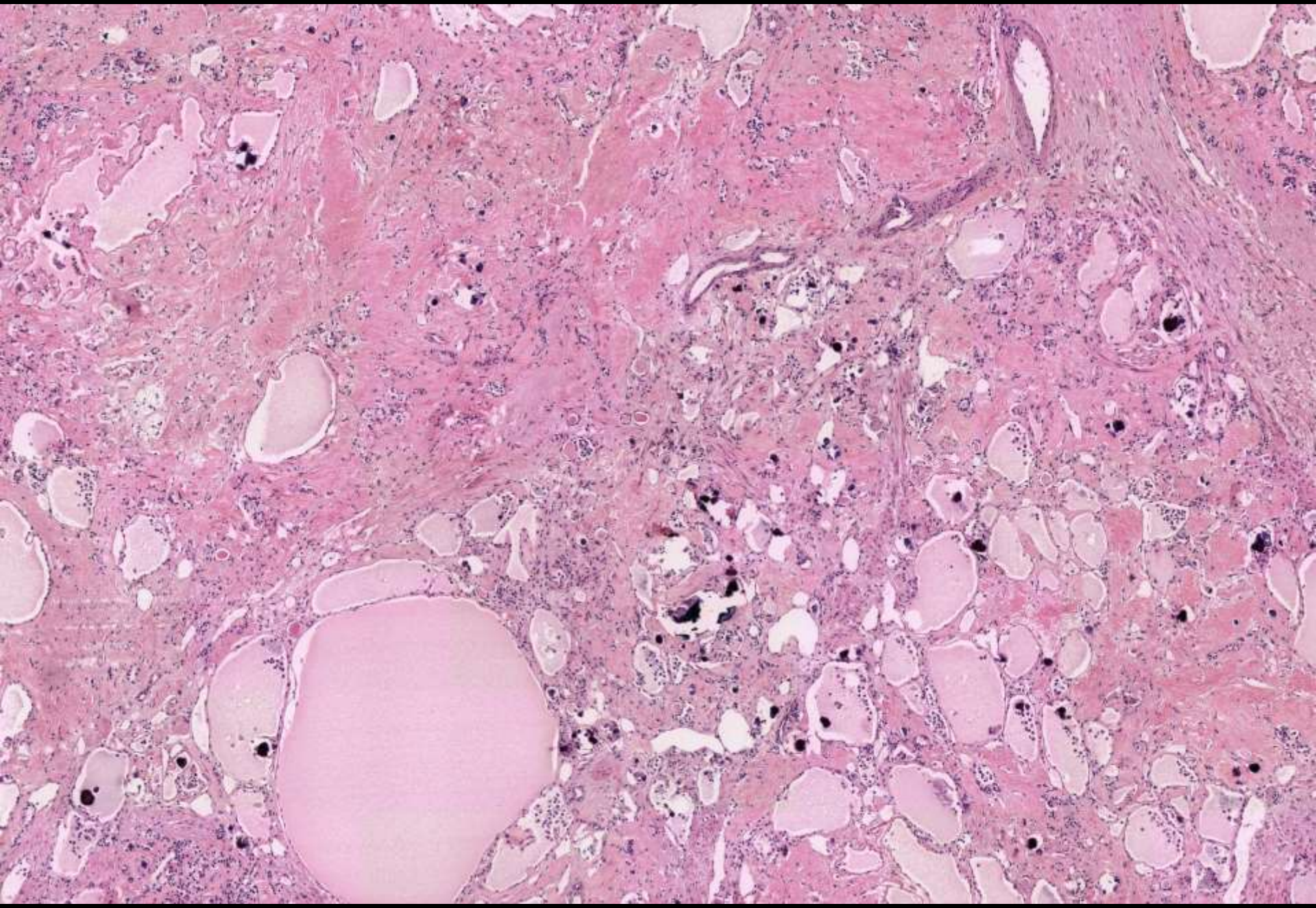

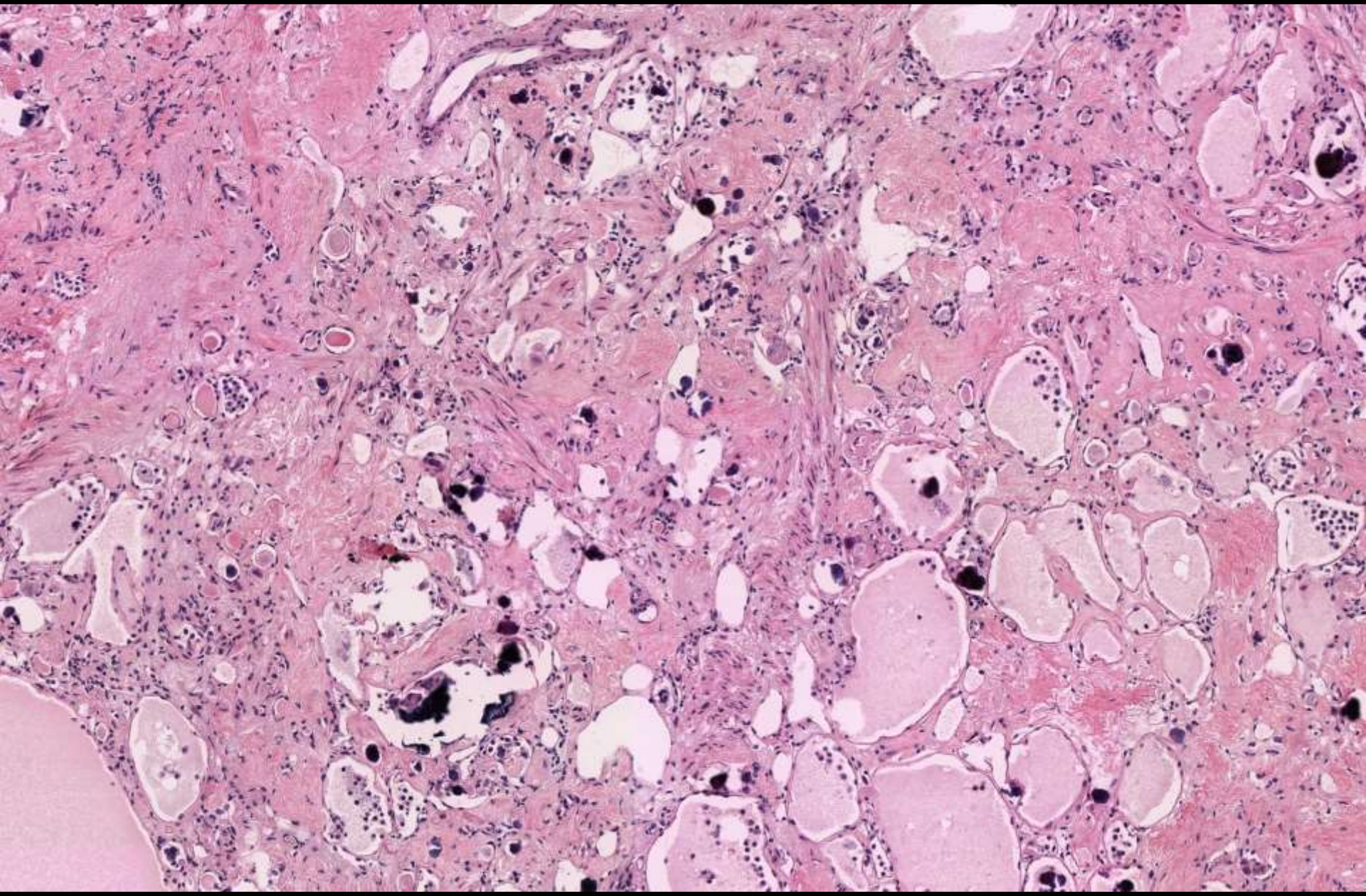

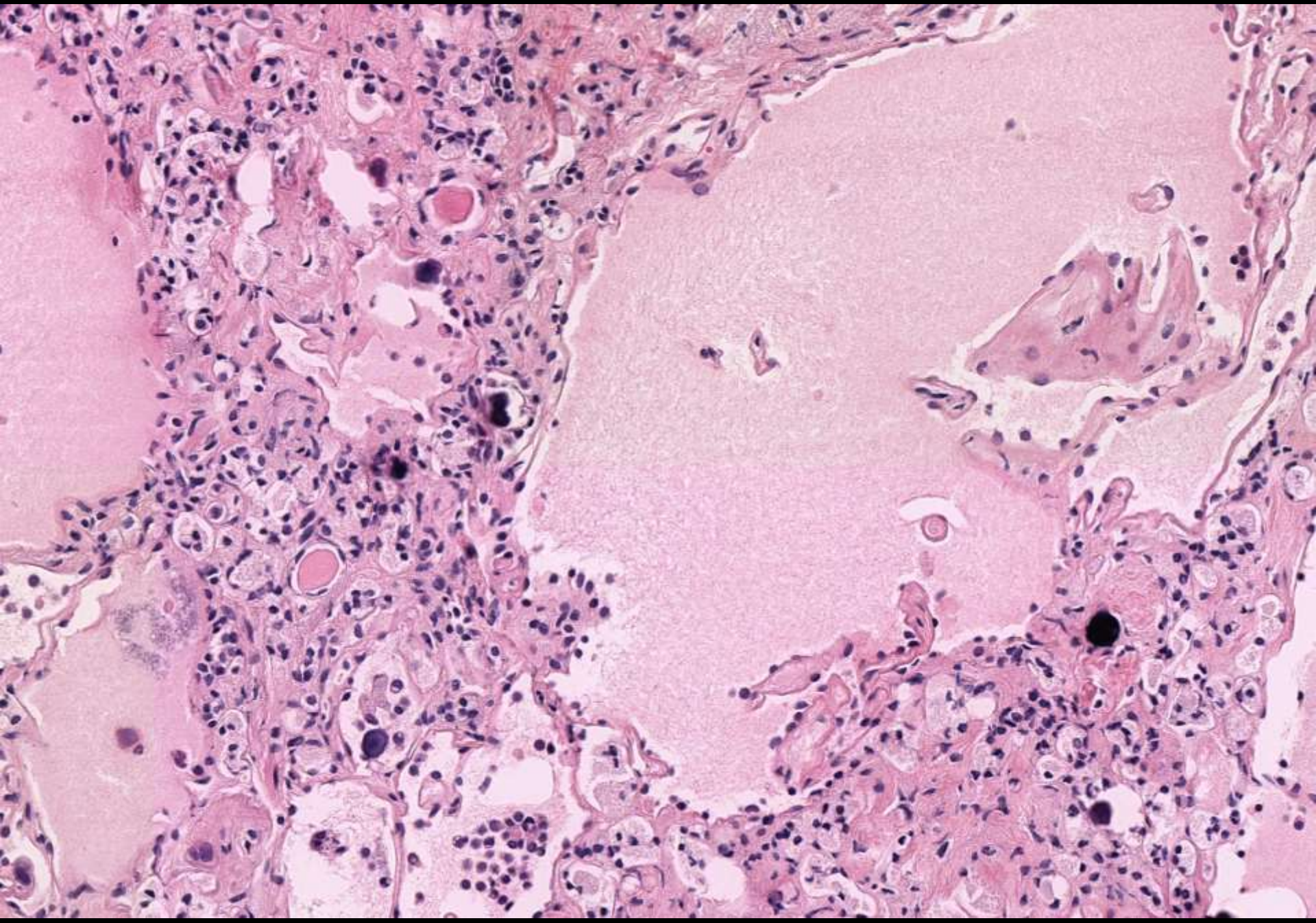

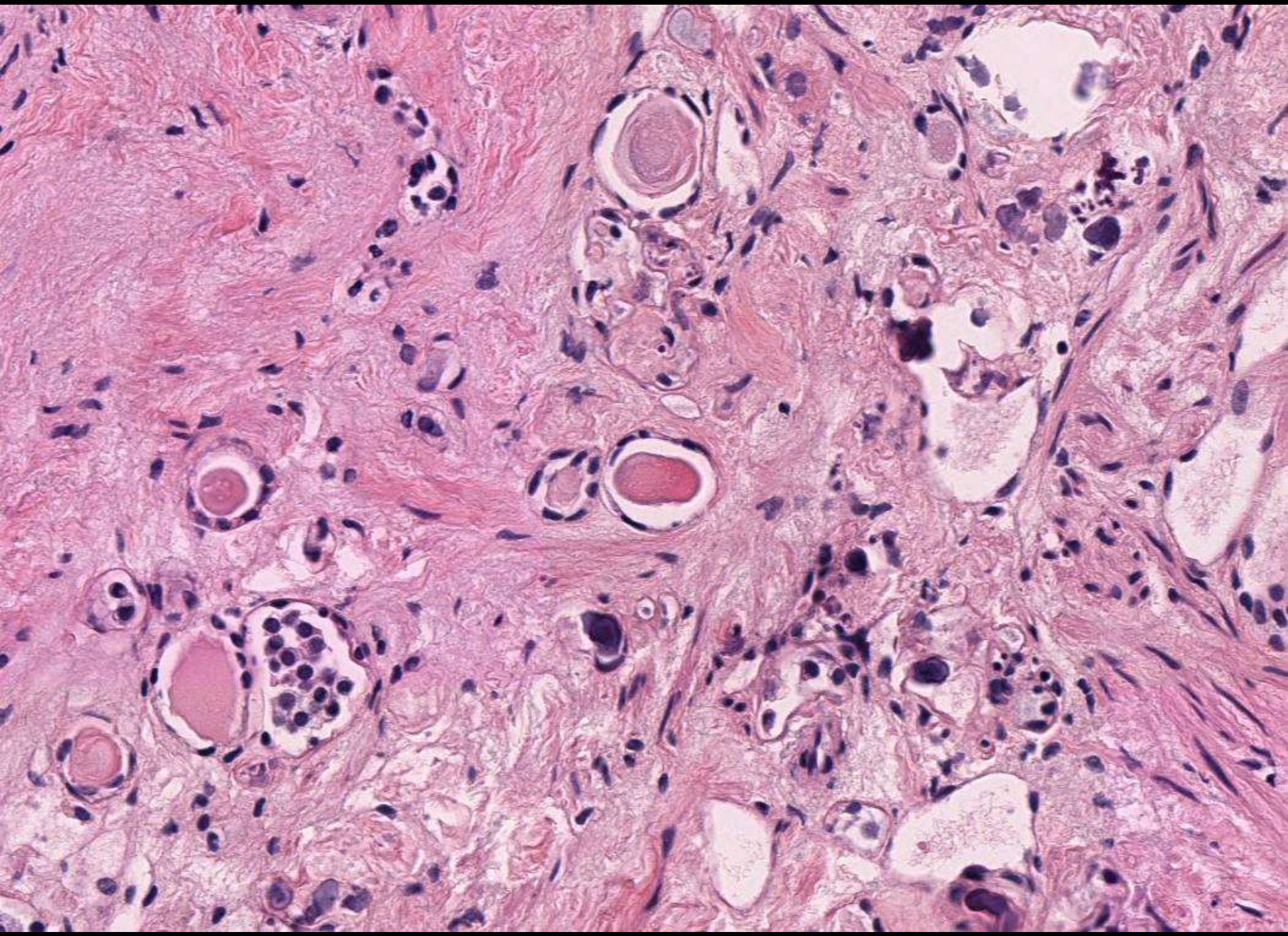

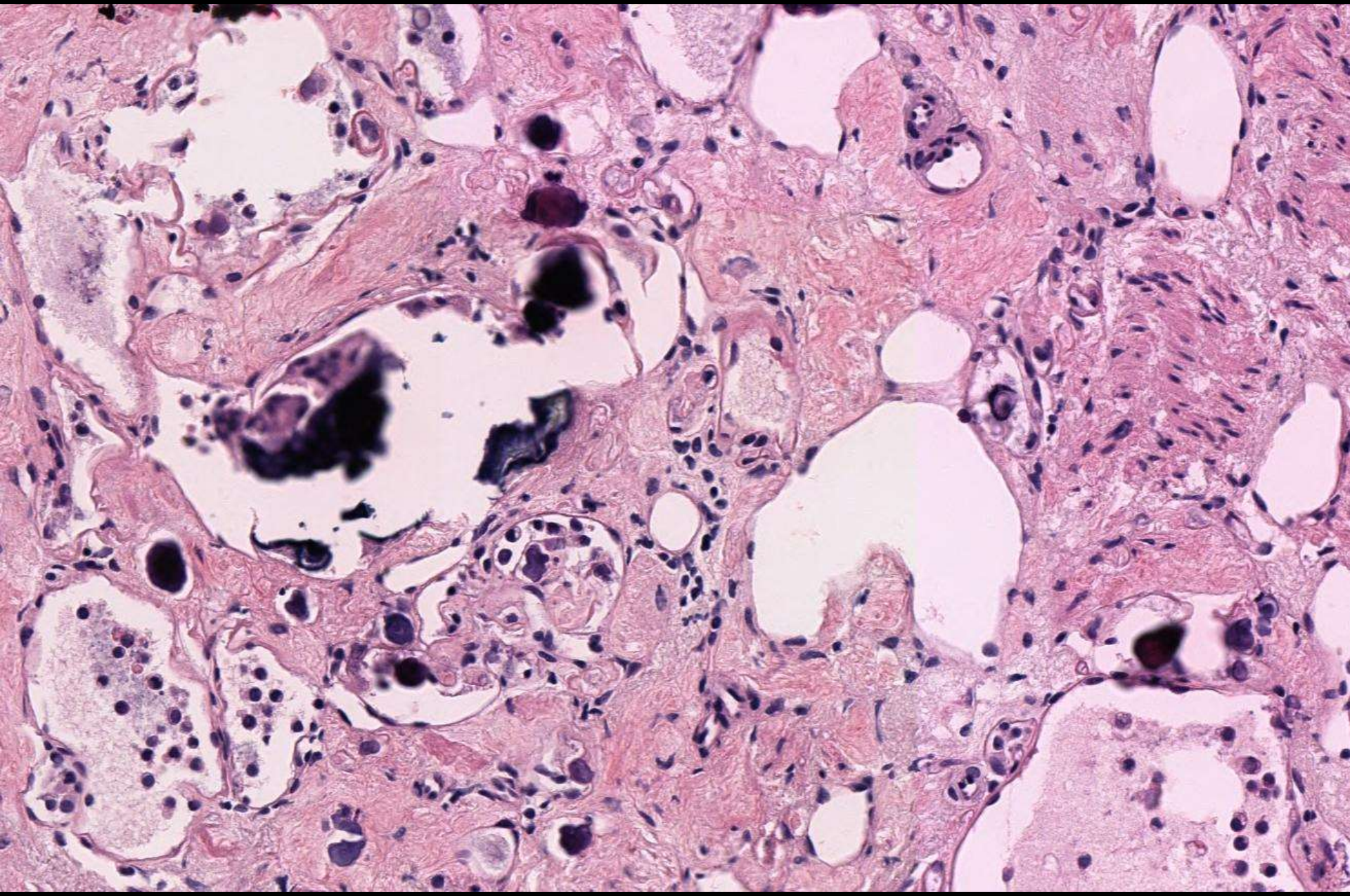

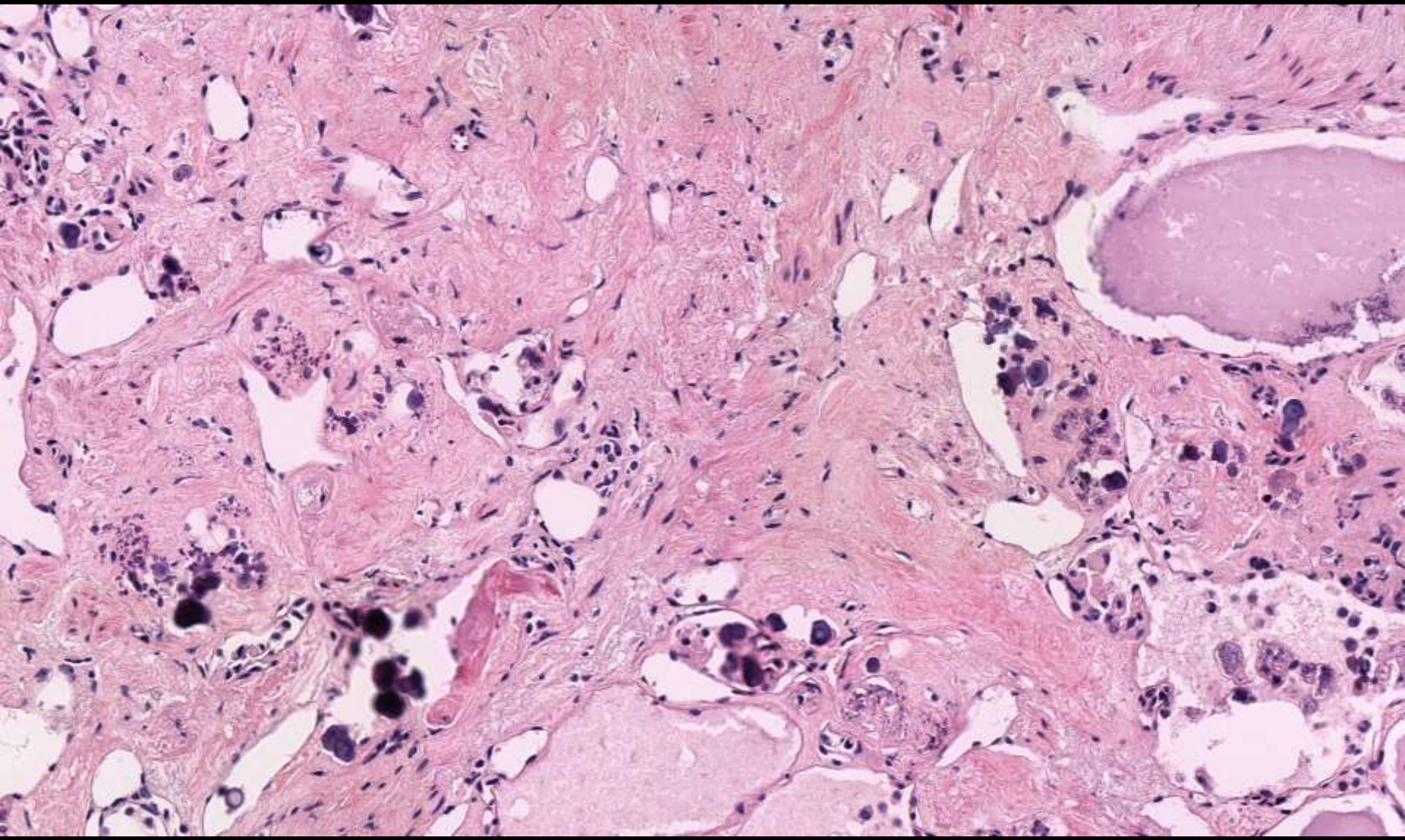

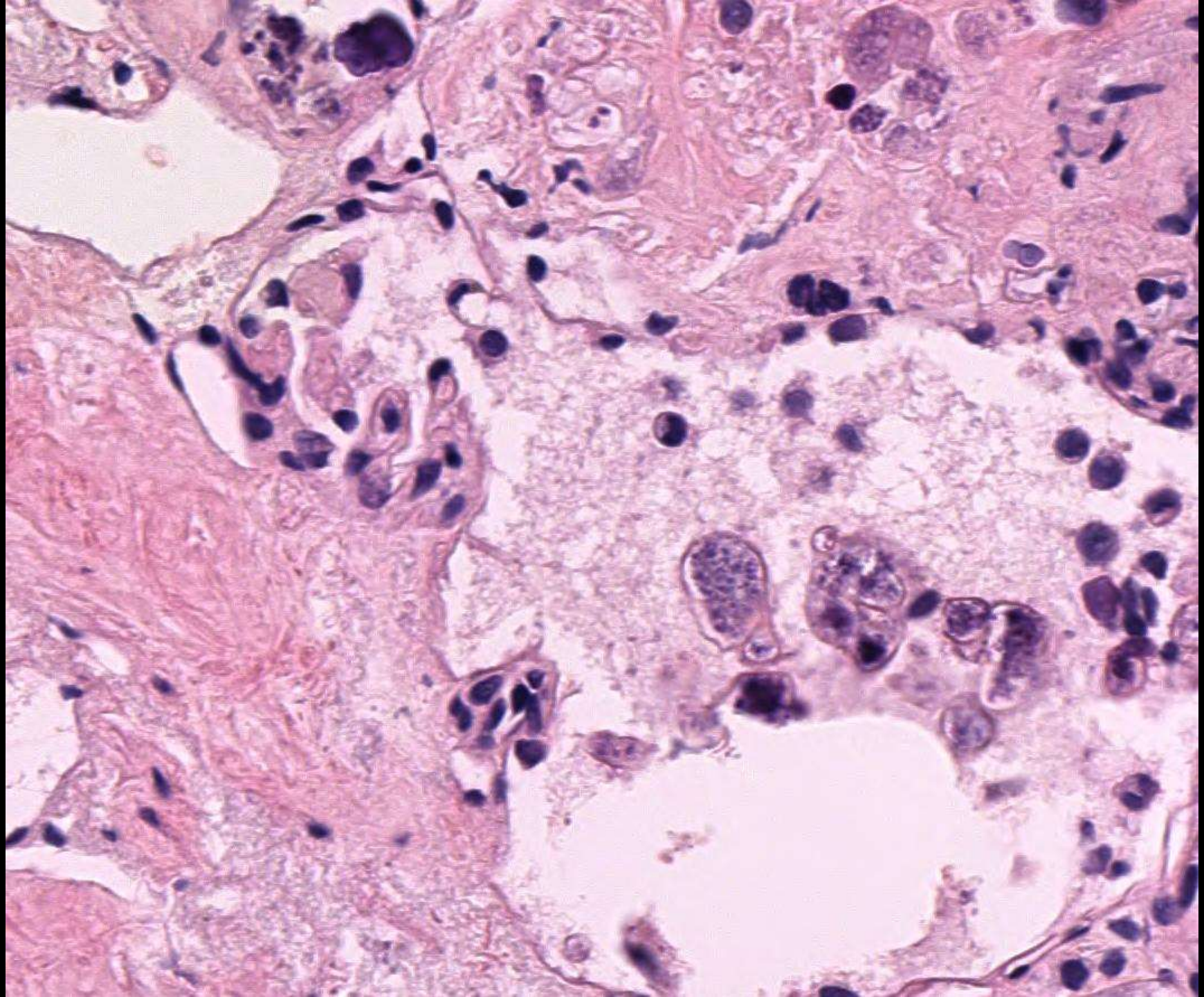

HPI

- CT: Solid enhancing left mid renal cortical mass measuring 3.5 cm, most consistent with a renal cell carcinoma
- Partial nephrectomy planned; Switched to radical nephrectomy due to positive margin on intraoperative consultation.
- Gross: encapsulated, bulging tan-white fibrous tumor

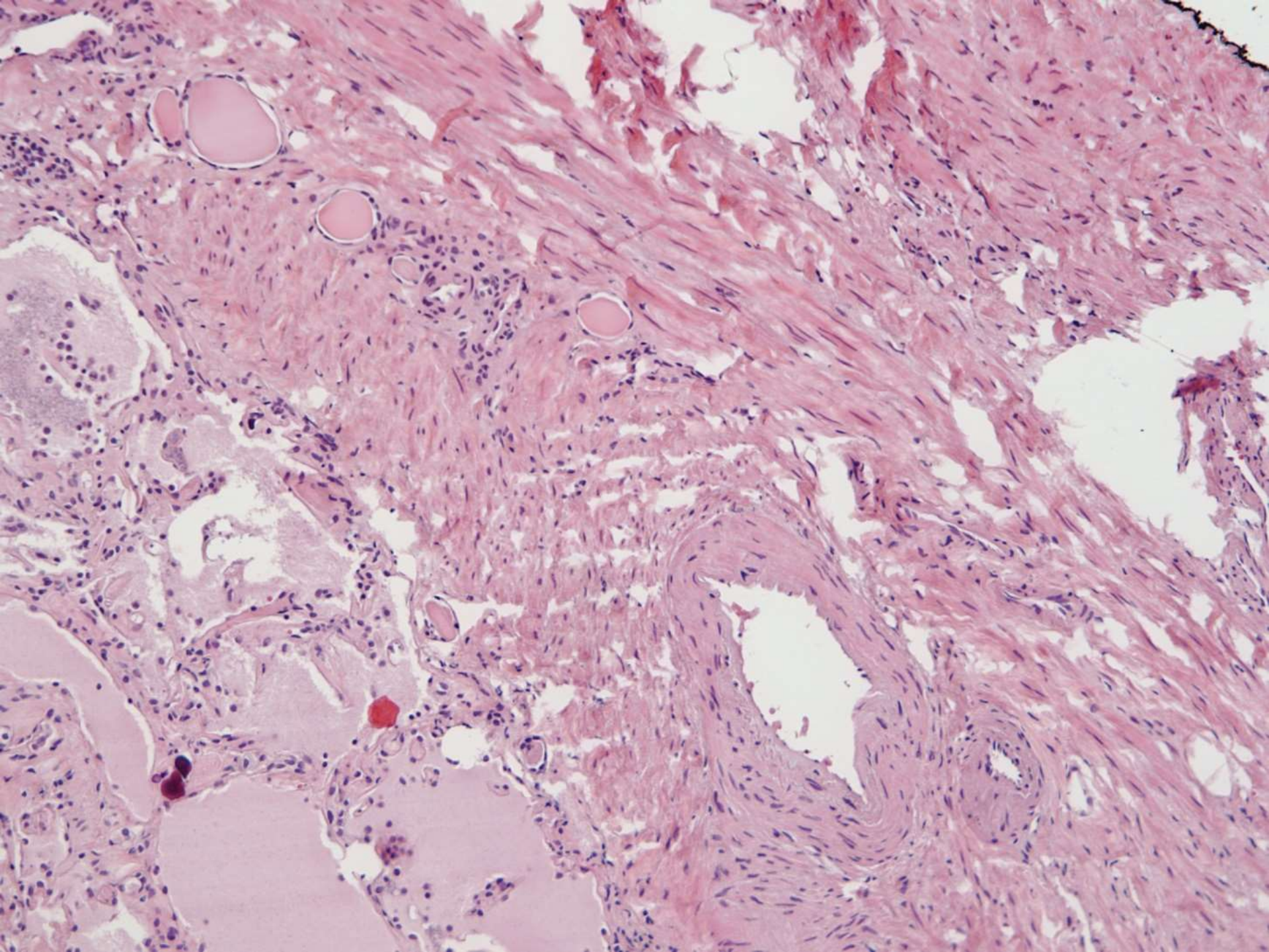

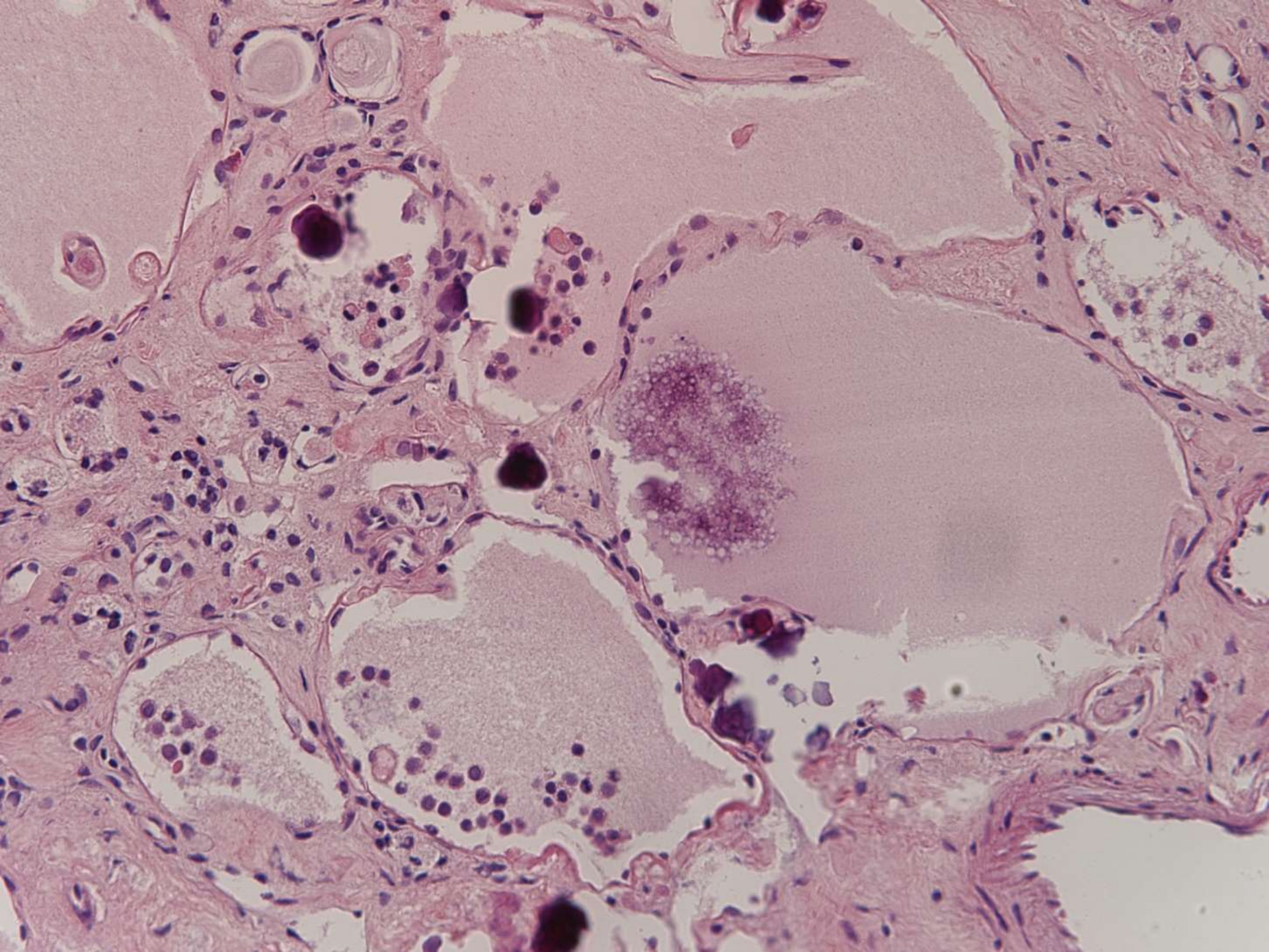

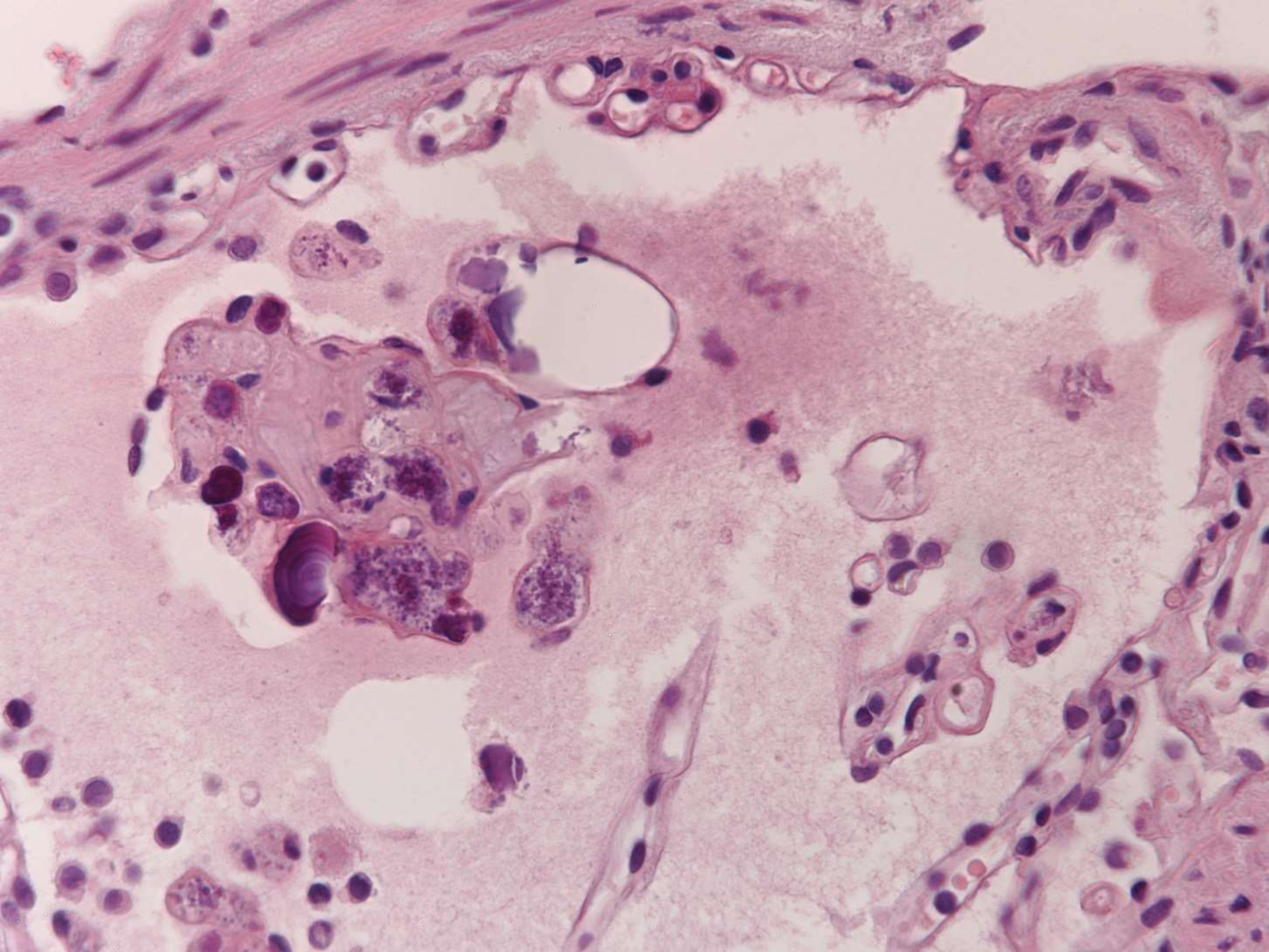

Ann Diagn Pathol. 2014 Apr;18(2):82-8. doi: 10.1016/j.anndiagpath.2013.12.003. Epub 2013 Dec 19.

Distinctive renal cell tumor simulating atrophic kidney with 2 types of microcalcifications. Report of 3 cases.

Hes O[1], de Souza TG[2], Pivovarcikova K[3], Grossmann P[3], Martinek P[3], Kuroda N[4], Kacerovska D[3], Svajdler M[5], Straka L[6], Petersson F[7], Hora M[8], Michal M[9].

Author information

Abstract

We report 3 cases of primary renal cell tumor simulating atrophic kidney with distinct gross, morphologic, immunohistochemical, and molecular genetic features. The tumors were retrieved out of more than 17 000 renal tumors from the Plzen Tumor Registry. Tissues for light microscopy had been fixed, embedded, and stained with hematoxylin and eosin using routine procedures. The tumors were further analyzed using immunohistochemistry, array comparative genomic hybridization, and human androgen receptor. Analyses of VHL gene and loss of heterozygosity (LOH) 3p were also performed. The patients were 2 women and 1 man, with ages ranging from 29 to 35 years (mean, 31.3 years). Grossly, the neoplasms were encapsulated and round with largest diameter of 3.5 cm (mean, 3.2 cm). Follow-up available for all patients ranged from 2 to 14 years (mean, 8 years). No aggressive behavior was noted. Histologically, akin to atrophic (postpyelonephritic) kidney parenchyma, the tumors were composed of follicles of varying sizes that were filled by eosinophilic secretion. Rare areas contained collapsed follicles. Each follicle was endowed with a small capillary. The stroma was loose, inconspicuous, and focally fibrotic. Two types of calcifications were noted: typical psammoma bodies and amorphous dark-blue stained calcified deposits. Immunohistochemically, tumors were strongly positive for cytokeratins (OSCAR), CD10, and vimentin, with weak immunopositivity for CAM5.2 and AE1-AE3. WT1 and cathepsin K were weakly to moderately focally to diffusely positive. Tumors were negative for cytokeratin 20, carbonic anhydrase IX, parvalbumin, HMB45, TTF1, TFE3, chromogranin A, thyroglobulin, PAX8, and ALK. Only 1 case was suitable for molecular genetic analyses. No mutations were found in the VHL gene; no methylation of VHL promoter was noted. No numerical aberrations were found by array comparative genomic hybridization analysis. LOH for chromosome 3p was not detected. Analysis of clonality (human androgen receptor) revealed the monoclonal nature of the tumor. We describe an unknown tumor of the kidney that (1) resembles renal atrophic kidney or nodular goiter of thyroidal gland; (2) contains a leiomyomatous capsule and 2 types of calcifications; (3) lacks mitoses, atypias, necroses, and hemorrhages and nearly lack Ki-67 positivity; and (4) so far showed benign biological behavior.

Am J Surg Pathol. 2018 Dec;42(12):1585-1595. doi: 10.1097/PAS.0000000000001157.

"Atrophic Kidney"-like Lesion: Clinicopathologic Series of 8 Cases Supporting a Benign Entity Distinct From Thyroid-like Follicular Carcinoma.

Herlitz L[1], Hes O[2], Michal M[2], Tretiakova M[3], Reyes-Múgica M[4], Nguyen JK[1], Troxell ML[5], Przybycin CG[1], Magi-Galluzzi C[1], McKenney JK[1].

Author information

Abstract

Renal mass lesions with a follicular architecture resembling atrophic kidney have been described, but their distinction from thyroid-like follicular carcinoma of the kidney remains controversial. We collected 8 cases of this purported "atrophic kidney"-like lesion to fully describe their clinical and histologic spectrum, their possible etiology, and to discuss their distinction from other renal neoplasms. Eight total cases were identified with patient ages ranging from 9 to 48 years (mean: 29 y; median: 28.5 y). Four patients were female and 4 were male. The tumors were unifocal and size ranged from 1.6 to 4.9 cm (mean: 3.4 cm; median: 3.4 cm). All 8 tumors had a remarkably similar histology. Each was enveloped by a smooth muscle rich capsule and had an overall low power "follicular" architecture. The luminal spaces of the "follicles" (or cysts) contained eosinophilic secretions and the lining epithelium was often flattened and atrophic, but some had more rounded cells with a distinctive hobnail arrangement. Many cysts contained discohesive round cells floating within the eosinophilic material, and some contained small intraluminal tufts with features of markedly atrophic glomeruli. Periodic acid-Schiff stains highlighted basement membrane material extending into these glomerular-like tufts, and some contained small distinct capillaries surrounded by endothelial cells, interspersed mesangial-like cells, and rare surrounding podocyte-like cells, providing additional evidence for glomerulocystic structures. Scattered calcifications were present within cysts (or within cyst walls) in varying numbers and were characterized by 2 types:

"Atrophic Kidney"-like Lesion

- Fibromuscular capsule with entrapped tubules
- Follicular architecture with eosinophilic secretion
- Features of markedly atrophic glomeruli
- Atrophic tubules: endocrine type, thyroidization
- Calcifications: psammoma bodies, amorphous

Herlitz L, et al. Am J Surg Pathol 2018

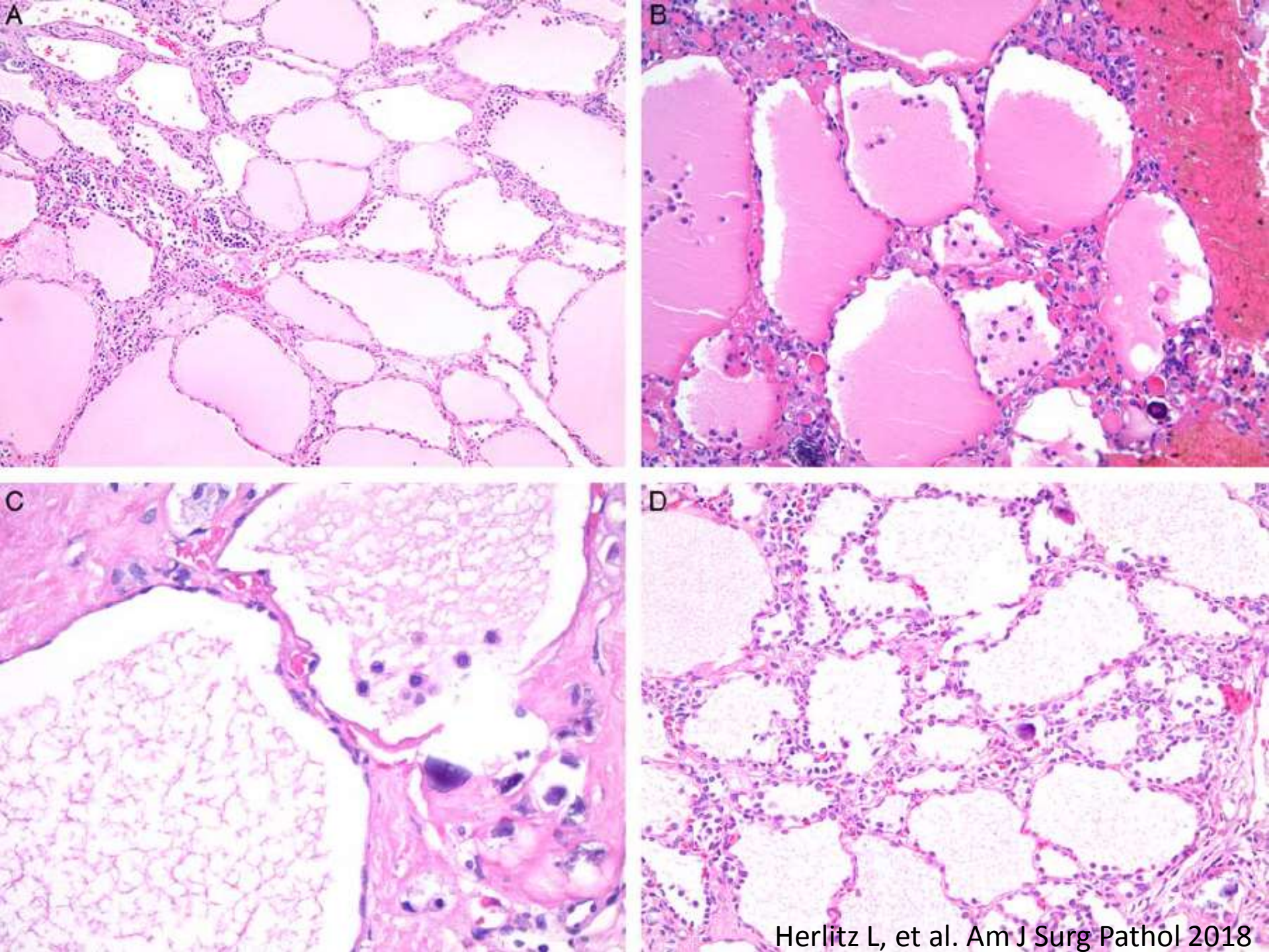

Herlitz L, et al. Am J Surg Pathol 2018

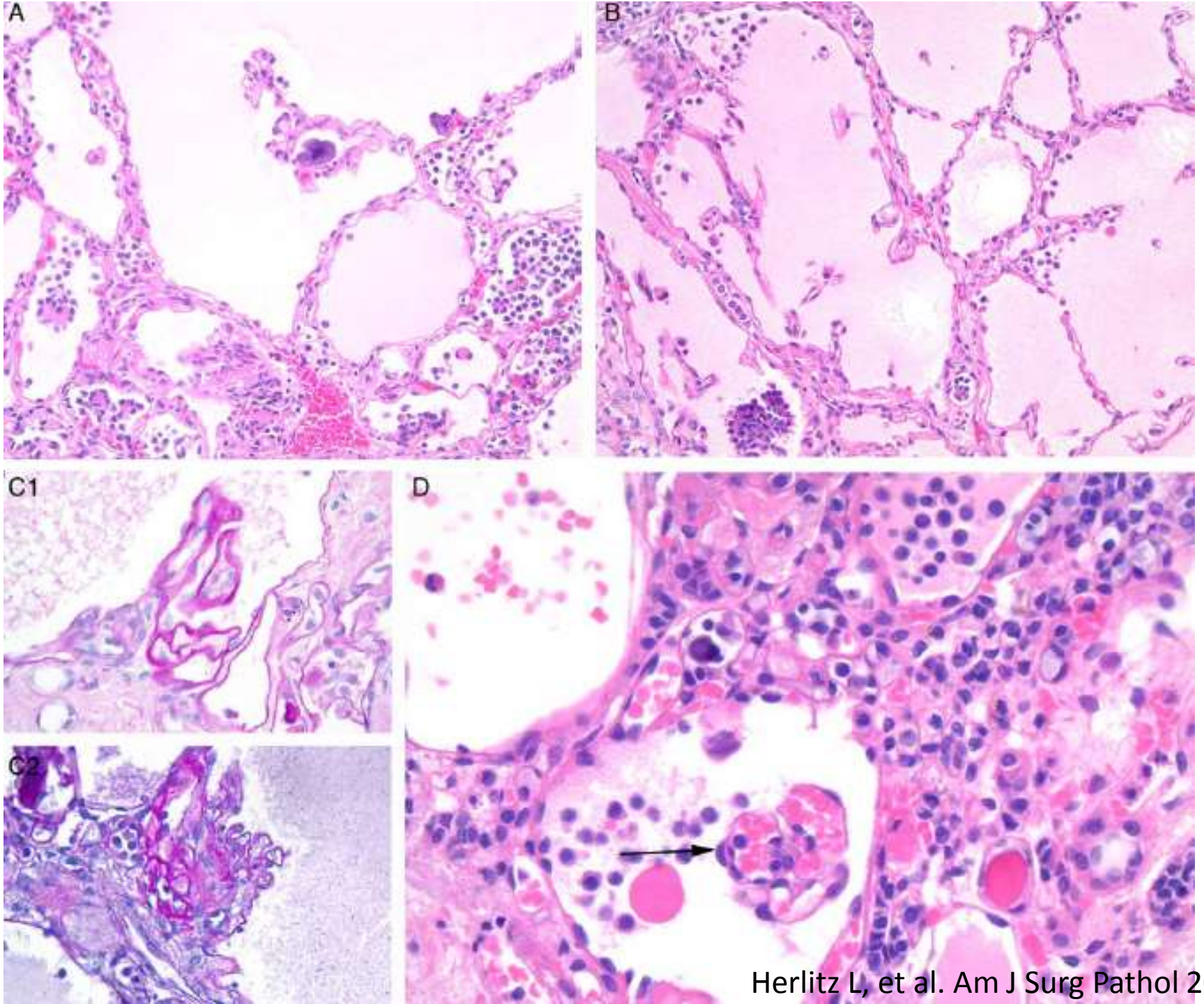

Herlitz L, et al. Am J Surg Pathol 2018

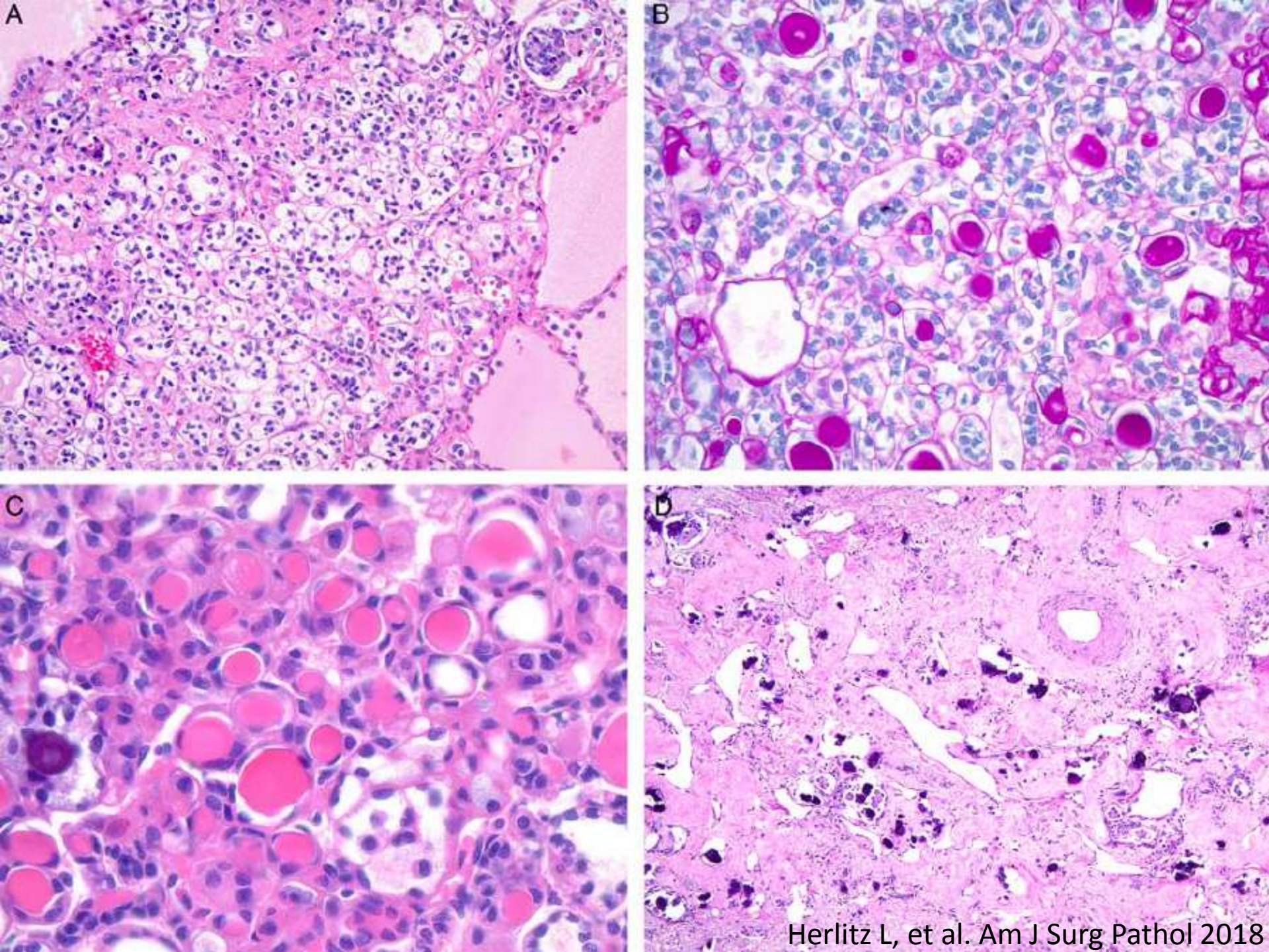

Herlitz L, et al. Am J Surg Pathol 2018

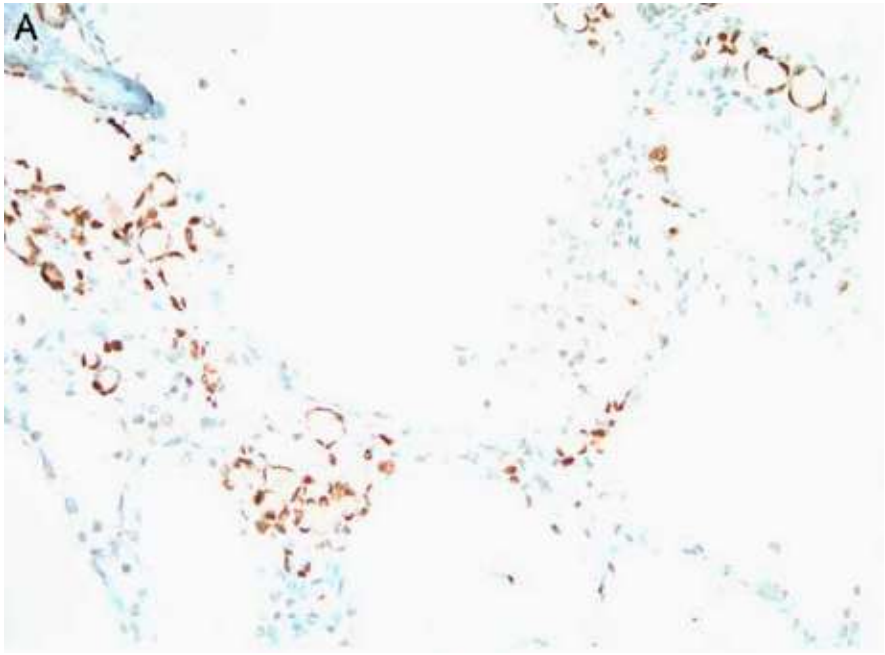

PAX8

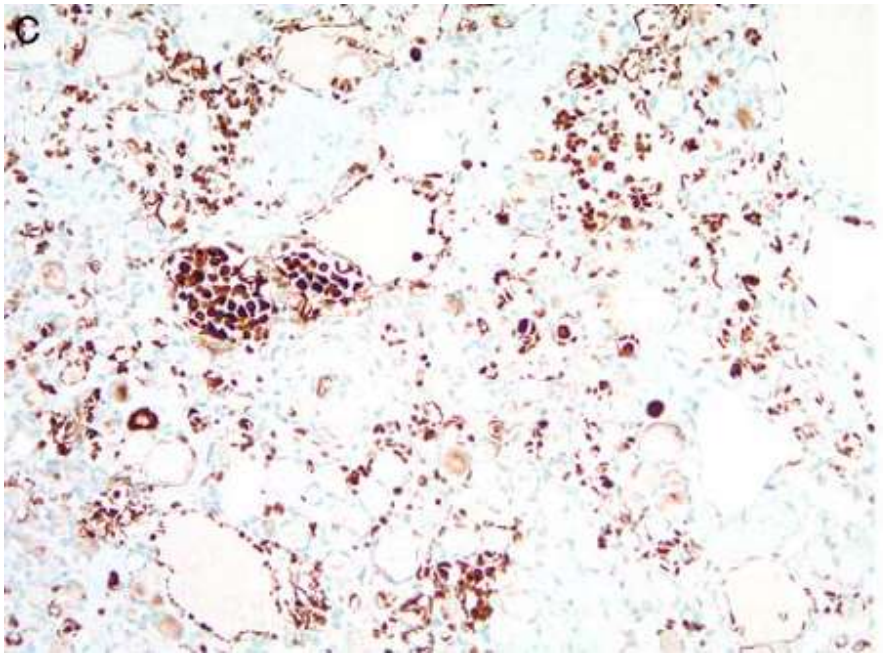

WT1

Herlitz L, et al. Am J Surg Pathol 2018

TABLE 2. Published Cases of Atrophic Kidney–like Tumor

Case	Age (y)	Sex	Size	Laterality	Stage	F/U (mo)	Publication
1	9	M	4.9	L	pT1b	NA*	Present study
2	28	F	4	R	pT1b	9 NED	Present study
3	27	M	2.5	L	pT1a	12.5 NED	Present study
4	21	F	3.2	R	pT1a	11 NED	Present study
5	39	M	4.5	L	pT1b	24 NED	Present study
6	48	M	1.6	L	pT1a	35 NED	Present study
7	29	F	3.5	L	pT1a	24 NED	Present study; Hes et al[1]
8	30	F	3	R	pT1a	168 NED	Present study; Hes et al[1]
9	58	M	3	L	pT1a	NA†	Berens et al[4]
10	19	M	4.4, 4	R, L	pT1b	156 NED	Oshiro et al[2]
11	27	M	6.5	L	pT1b	9 NED	Muscara et al[5]
12	29	F	1.9	R	pT1a	84 NED	Amin et al[6]
13	35	M	3	NA	pT1a	96 NED	Hes et al‡[1]

Herlitz L, et al. Am J Surg Pathol 2018

Conclusion

“Atrophic kidney"-like lesions may simply represent a non-neoplastic form of organizing tubular atrophy and glomerulocystic change.

Herlitz L, et al. Am J Surg Pathol 2018

19-0307
(scanned slide available)

Emily Chan; UCSF

60-year-old female with 3.3cm left renal mass.

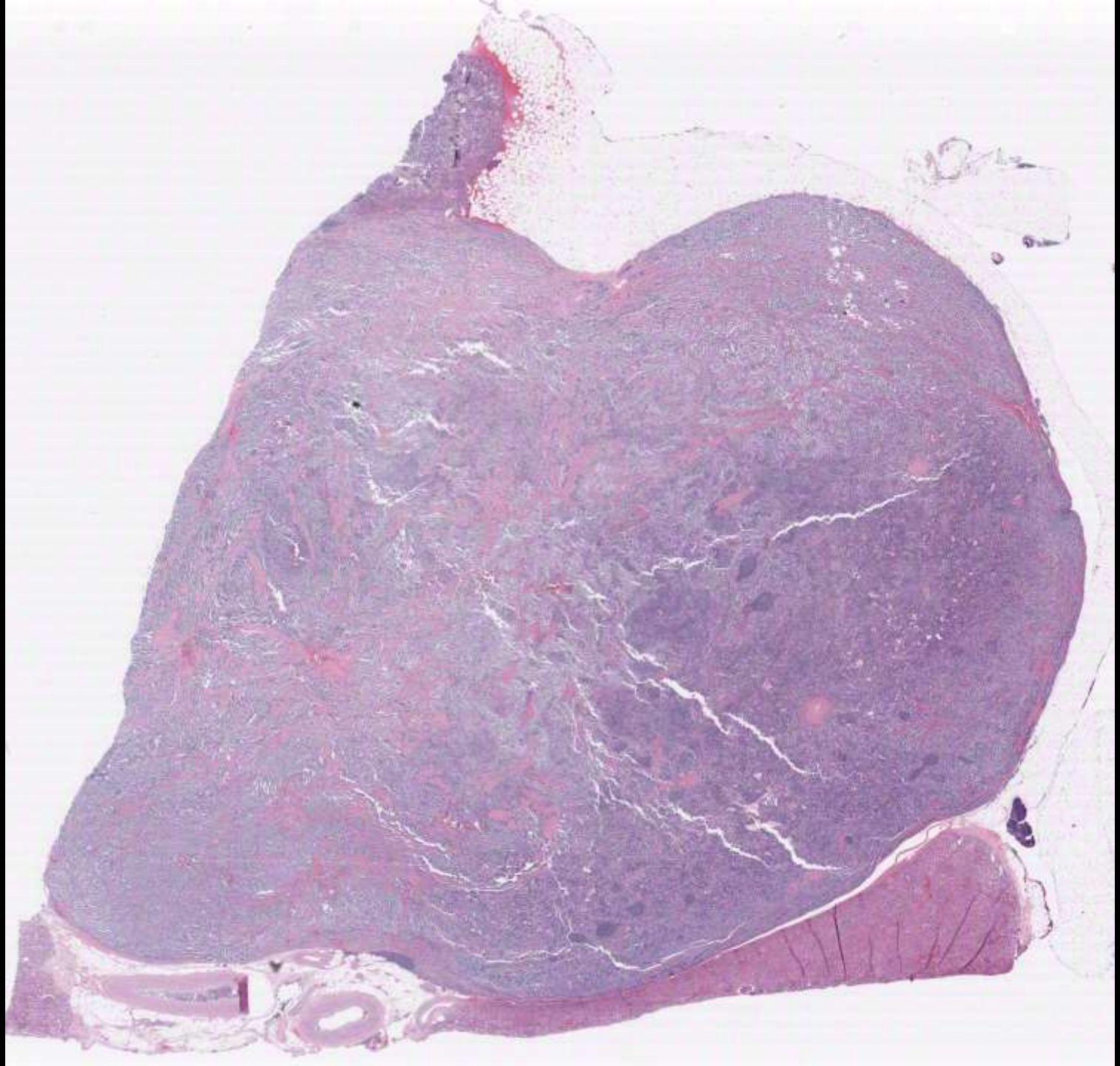

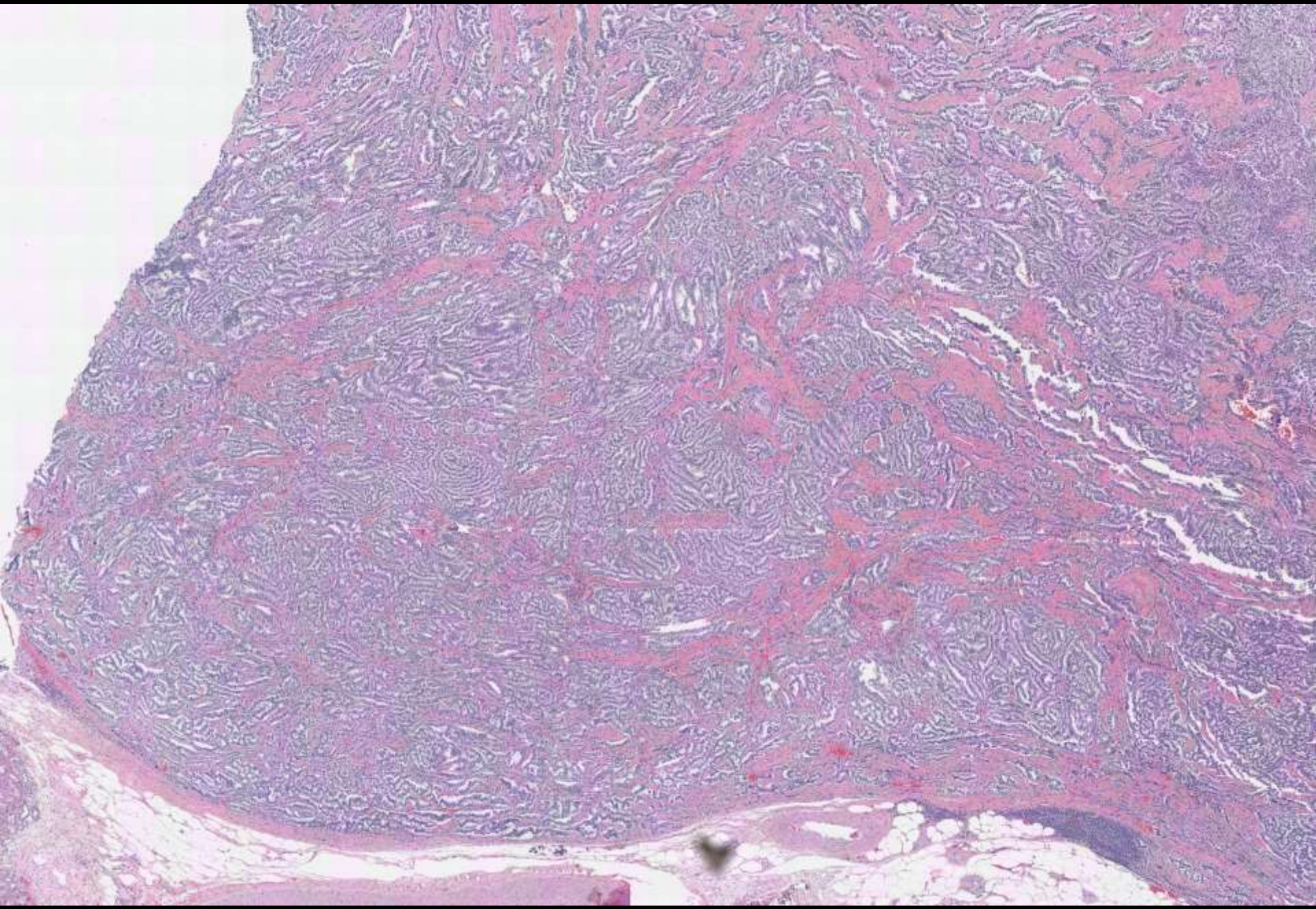

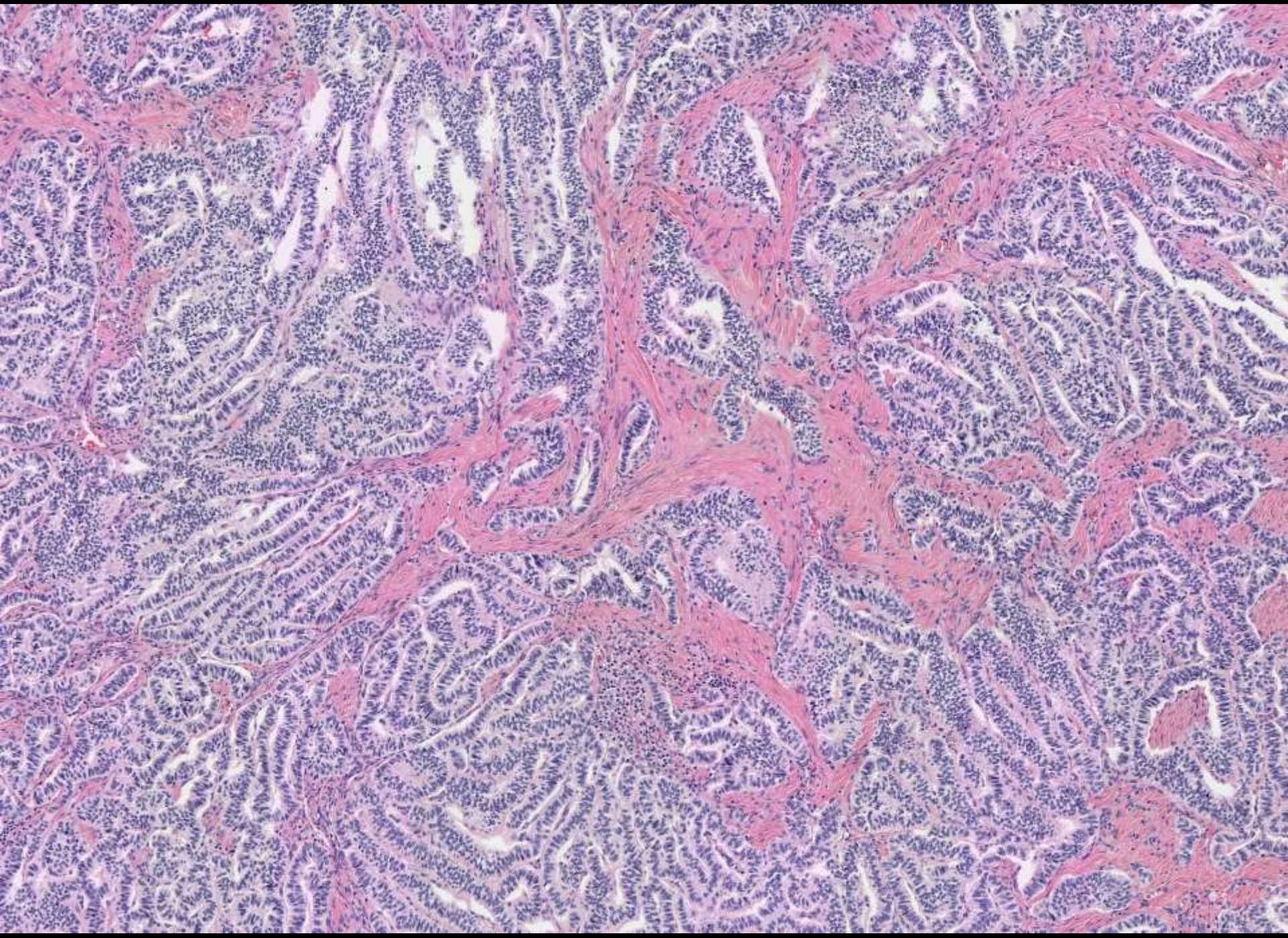

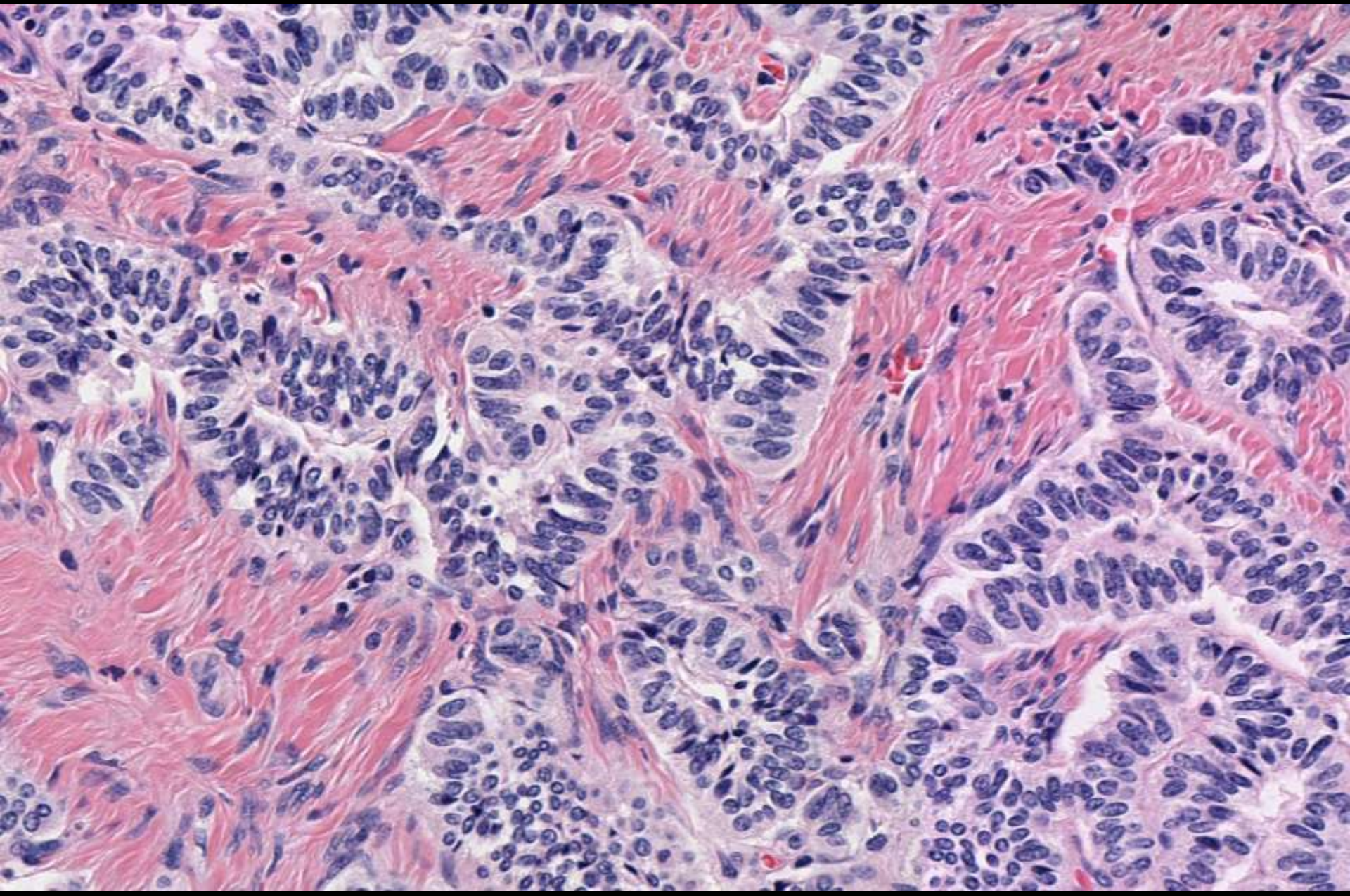

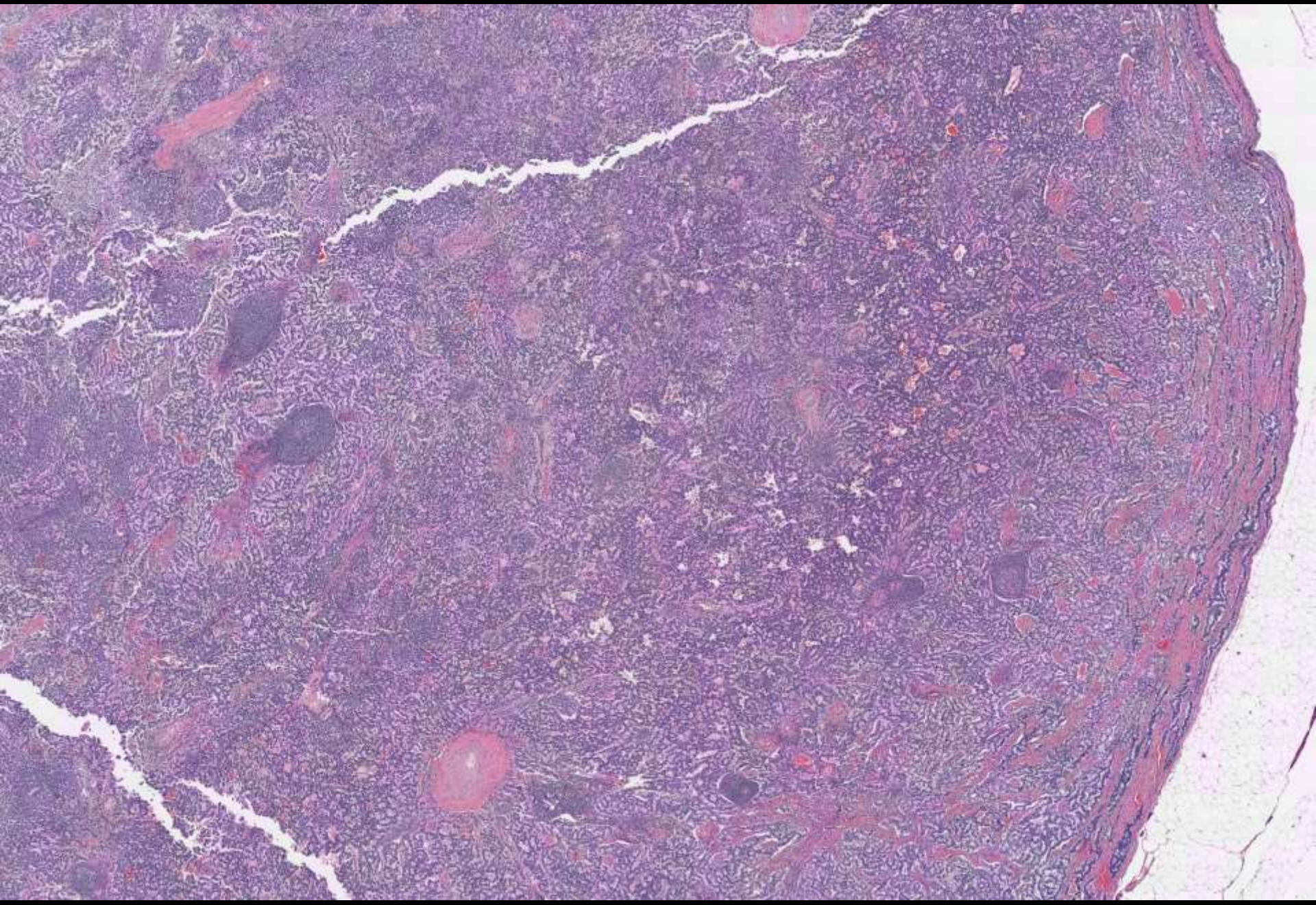

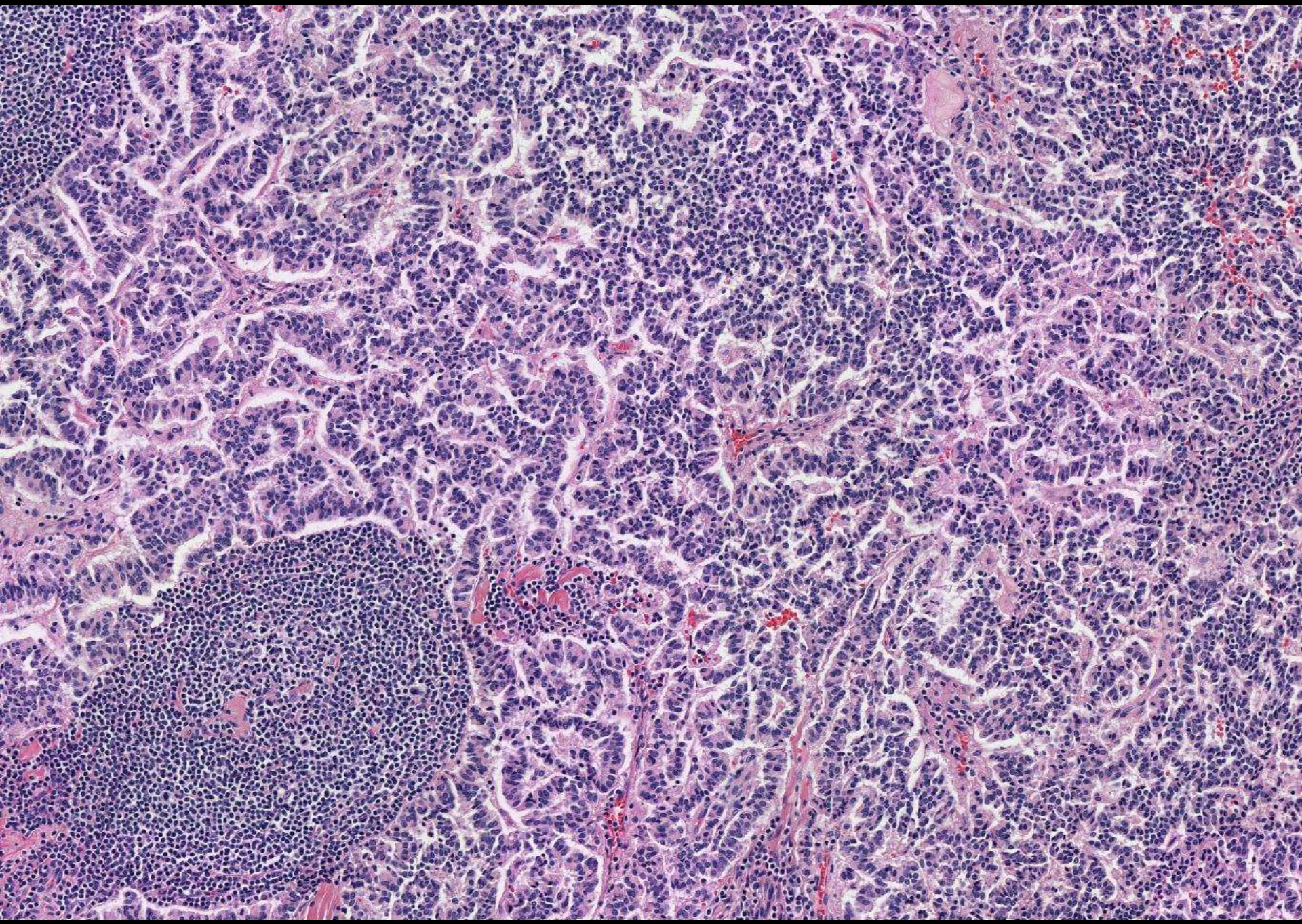

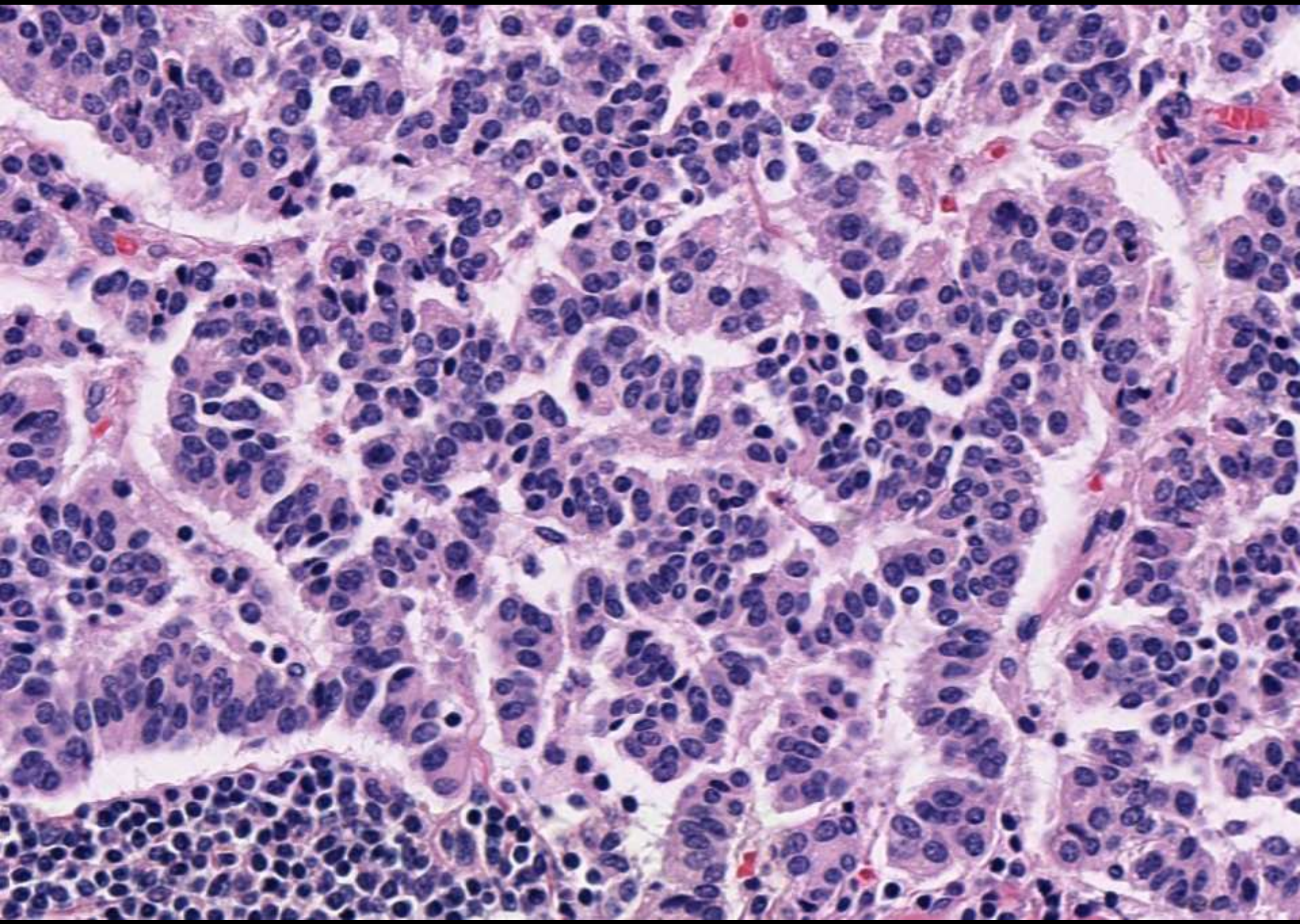

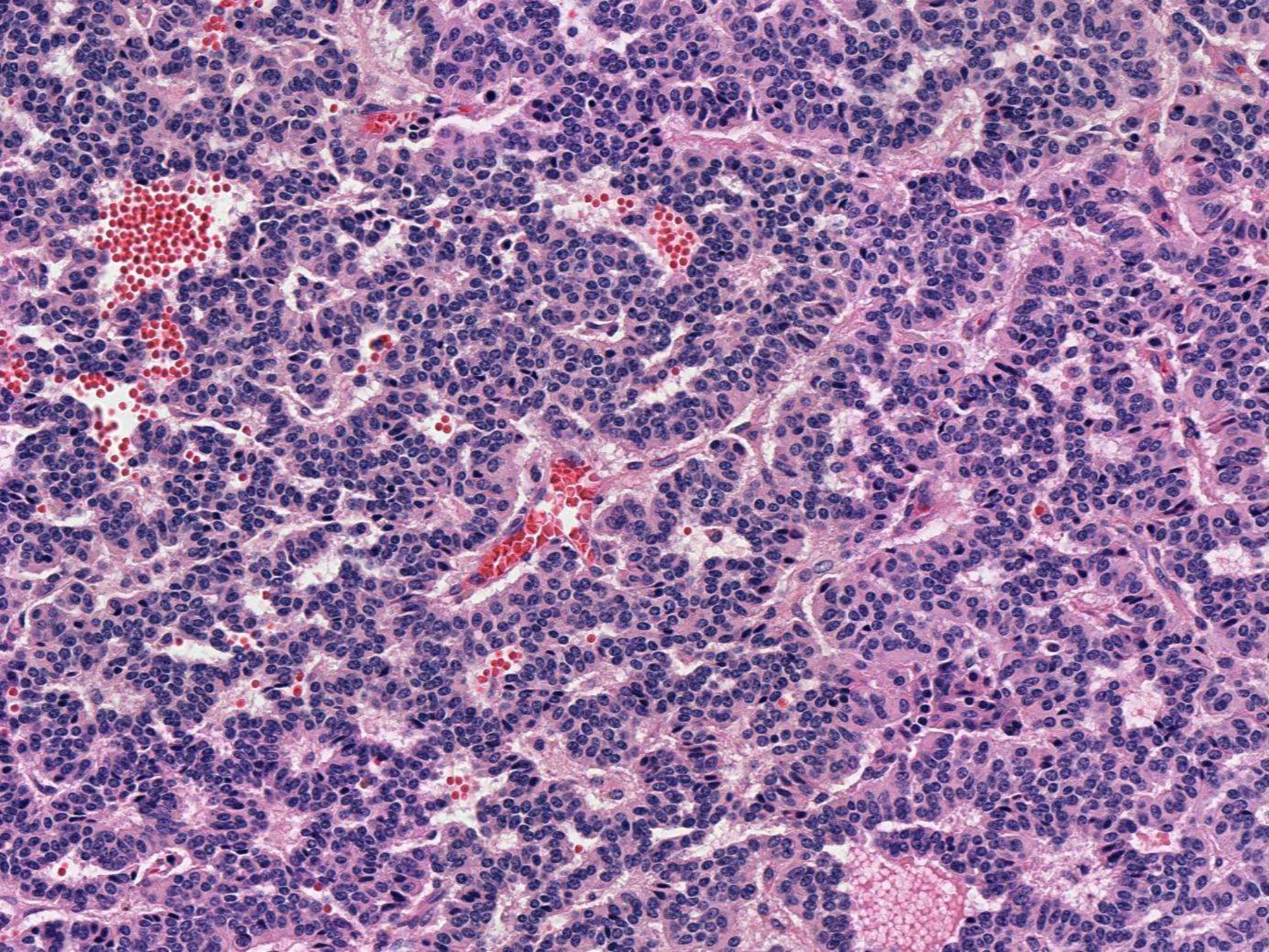

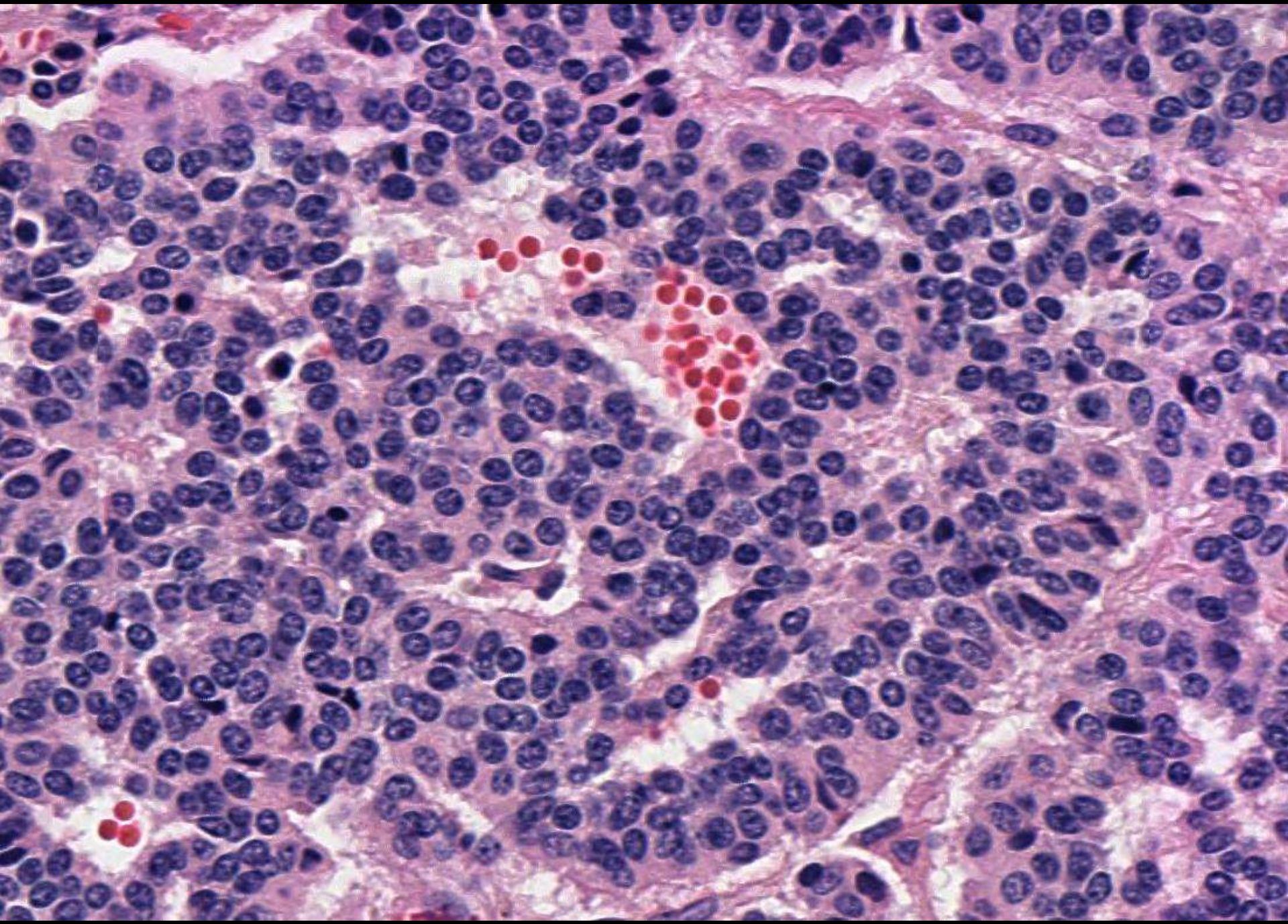

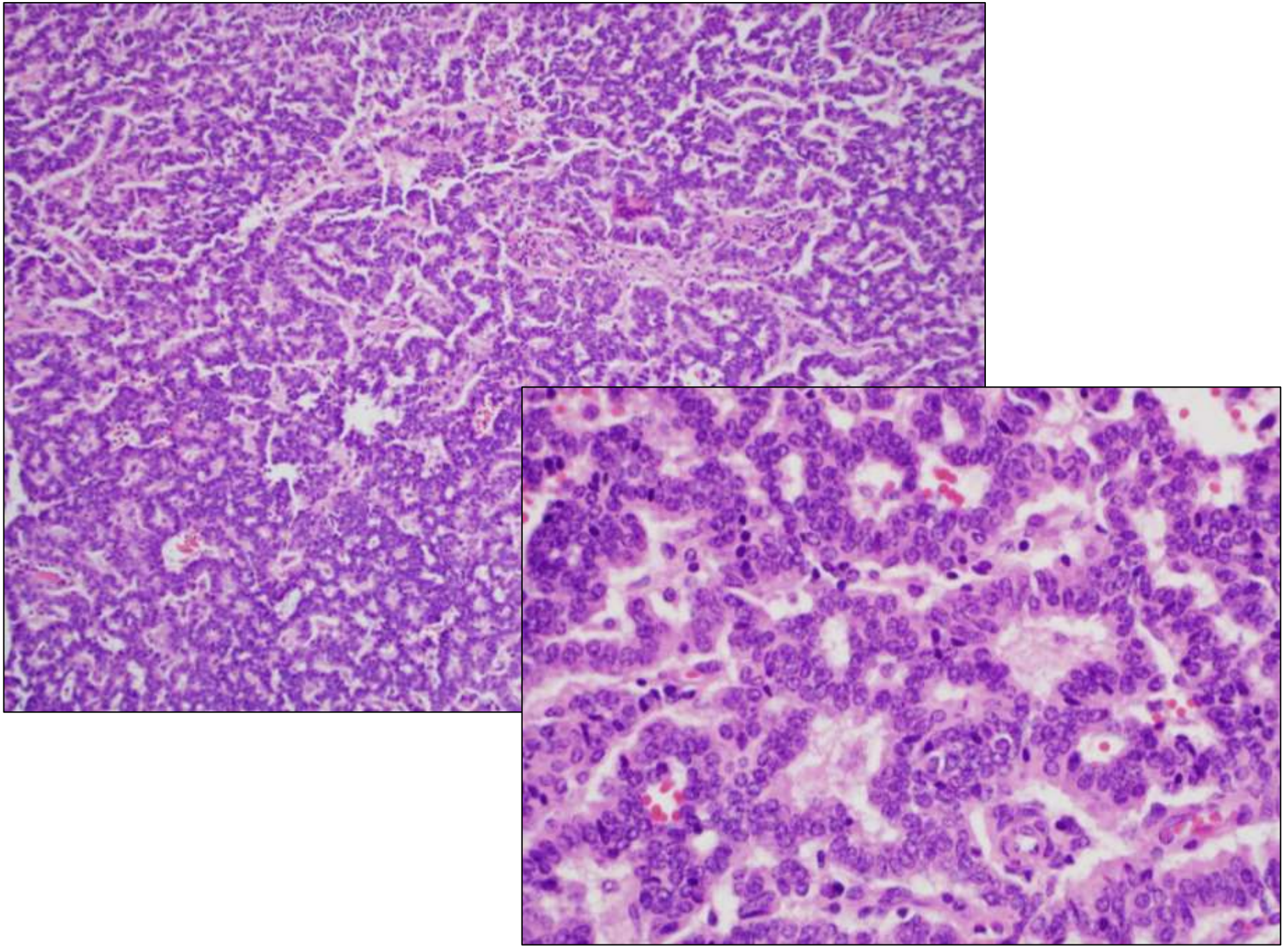

Differential Diagnosis:

- Well-differentiated neuroendocrine tumor
- Metanephric adenoma
- PNET
- Papillary renal cell carcinoma
- Metastasis

IHC

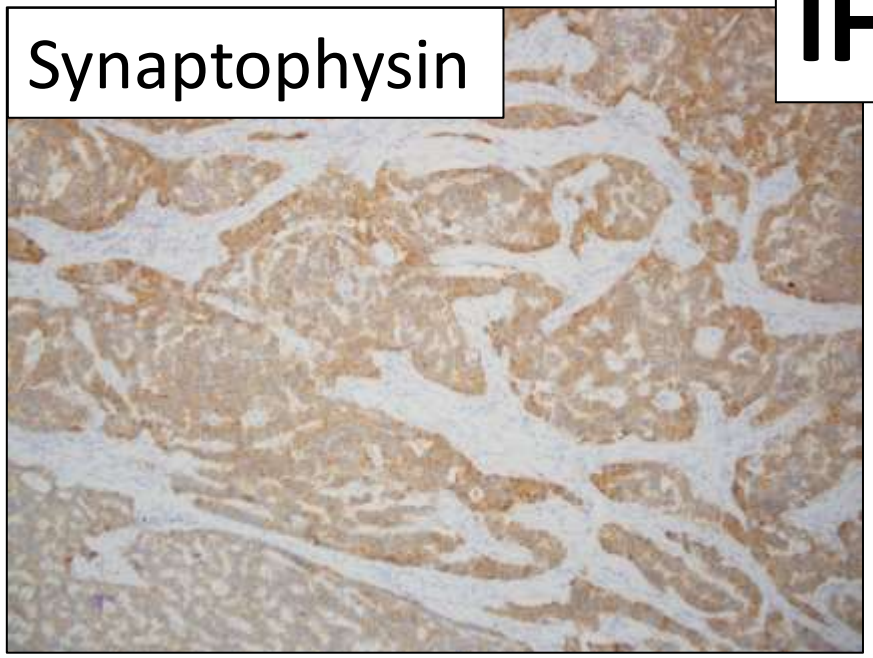

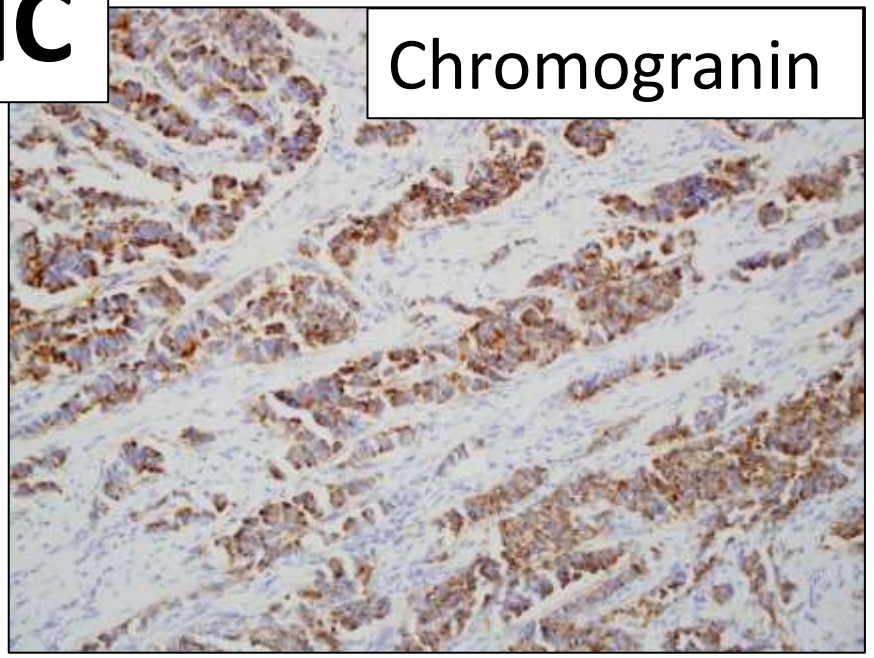

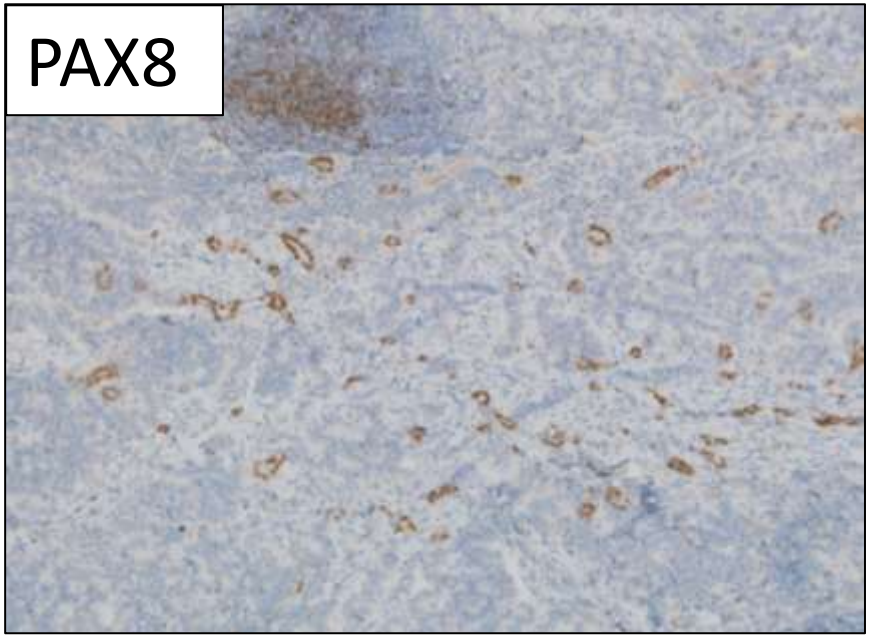

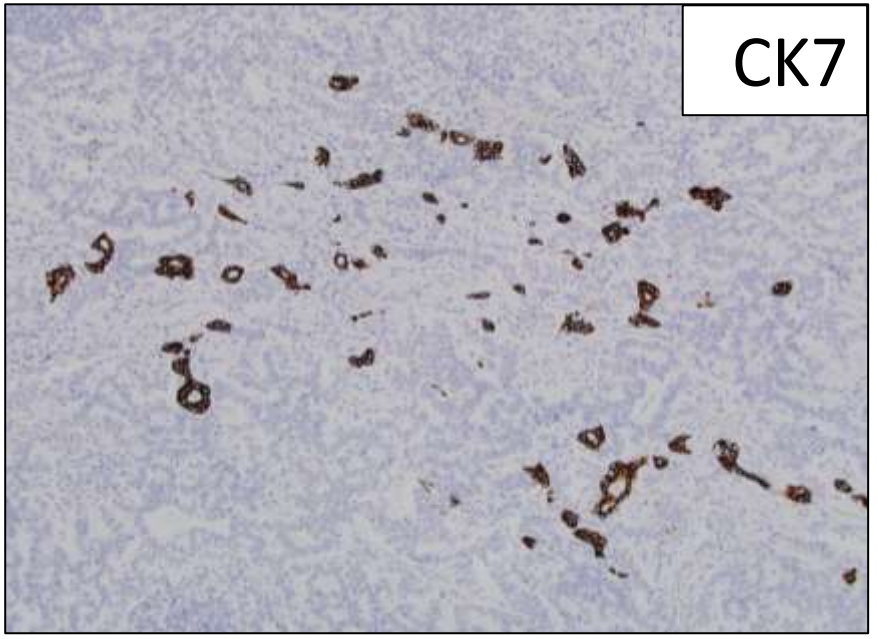

Our diagnosis:

Well-differentiated neuroendocrine tumor

Renal Carcinoid Tumor: A Clinicopathologic Study of 21 Cases

Donna E. Hansel, MD, PhD, Jonathan I. Epstein, MD,†‡§ Ema Berbescu, MD,‖ Samson W. Fine, MD,¶ Robert H. Young, MD,# and John C. Cheville, MD‖**††*

Abstract: Renal carcinoid tumors are exceedingly rare tumors that have been primarily documented as case reports in the literature. In this study, we report a series of 21 renal carcinoid tumors, with emphasis on histopathologic features and clinical outcomes. Patient age ranged from 27 to 78 years (average 52 y). The majority of specimens consisted of radical nephrectomies with or without associated lymph node dissection. Nine tumors were present in the left kidney and 10 were present in the right; location was not available for 2 specimens. No anatomic region of the kidney appeared to be preferentially involved. Twenty tumors were unifocal and ranged in size from 2.6 to 17 cm (average 6.4 cm), and 1 tumor presented as 2 nodules measuring 1 and 2.8 cm. Four patients had a documented history of a horseshoe kidney. Two patients had a history of renal calculi and 1 patient had a history of urothelial carcinoma 8 years prior. Presenting symptoms and clinical findings included back or subset of cases (n = 3/18) and CK20 was positive in 1 case. TTF-1 and WT-1 were negative in all cases examined. Clinical follow-up was available on 15 patients and ranged from 3 months to 11 years. One patient died of disease at 8 months after surgery and 1 patient died without disease at 11 years after surgery. Of the remaining patients, 7 patients were alive without disease and 6 patients were alive with disease. Additional metastases developed in 4 patients and included metastases to the liver and bone.

Key Words: kidney, cancer, carcinoid, neuroendocrine, metastasis

(*Am J Surg Pathol* 2007;31:1539–1544)

Primary carcinoid tumors of the kidney have been reported in the literature primarily as case reports, with

Primary Renal NETs

- Male = Female, ages 27-78
- Size 2.6-17 cm
- Right = Left
- Association with horseshoe kidney
- Metastasis documented in 12/21 patients at time of surgery
- Only one death due to disease

Hansel et al AJSP 2007

Typical histology

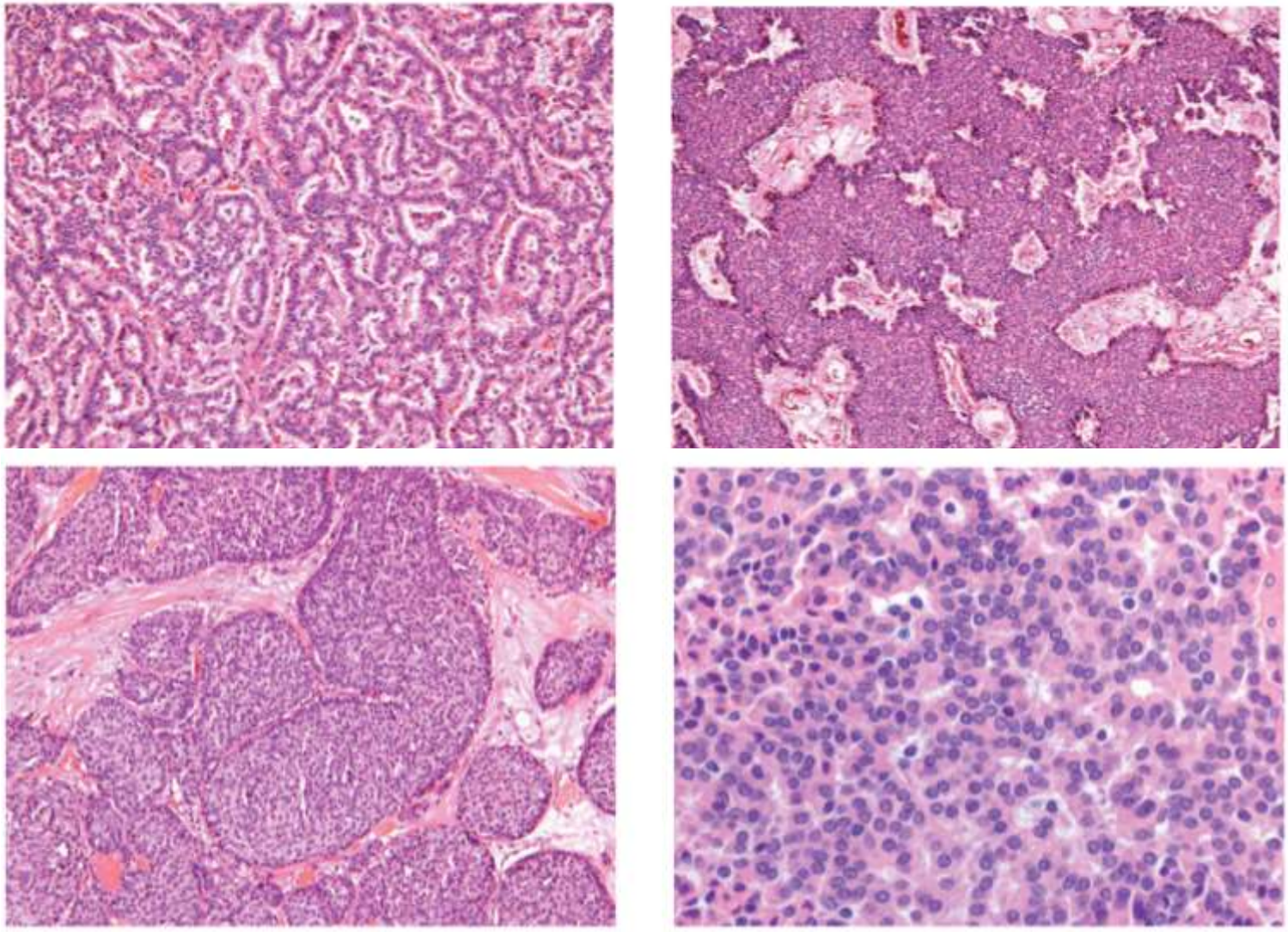

Hansel et al AJSP 2007

Primary Renal NETs

- Exclude other sites of disease with imaging
  - May arise within a teratoma
- Carcinoid terminology falling out of favor
  - No signs or symptoms of carcinoid syndrome
- Use well-differentiated neuroendocrine tumor terminology and report mitotic index and Ki-67

Clinical management and Follow-up

- PET DOTA-TATE scan negative for other sites of disease

19-0308
(scanned slide available)

Ankur Sangoi; El Camino Hospital

71-year-old male with 7.5cm ISUP grade 2 to 3 clear cell renal cell carcinoma, with vascular invasion. Background kidney shows subcapsular 6mm orange lesion within inferior aspect.

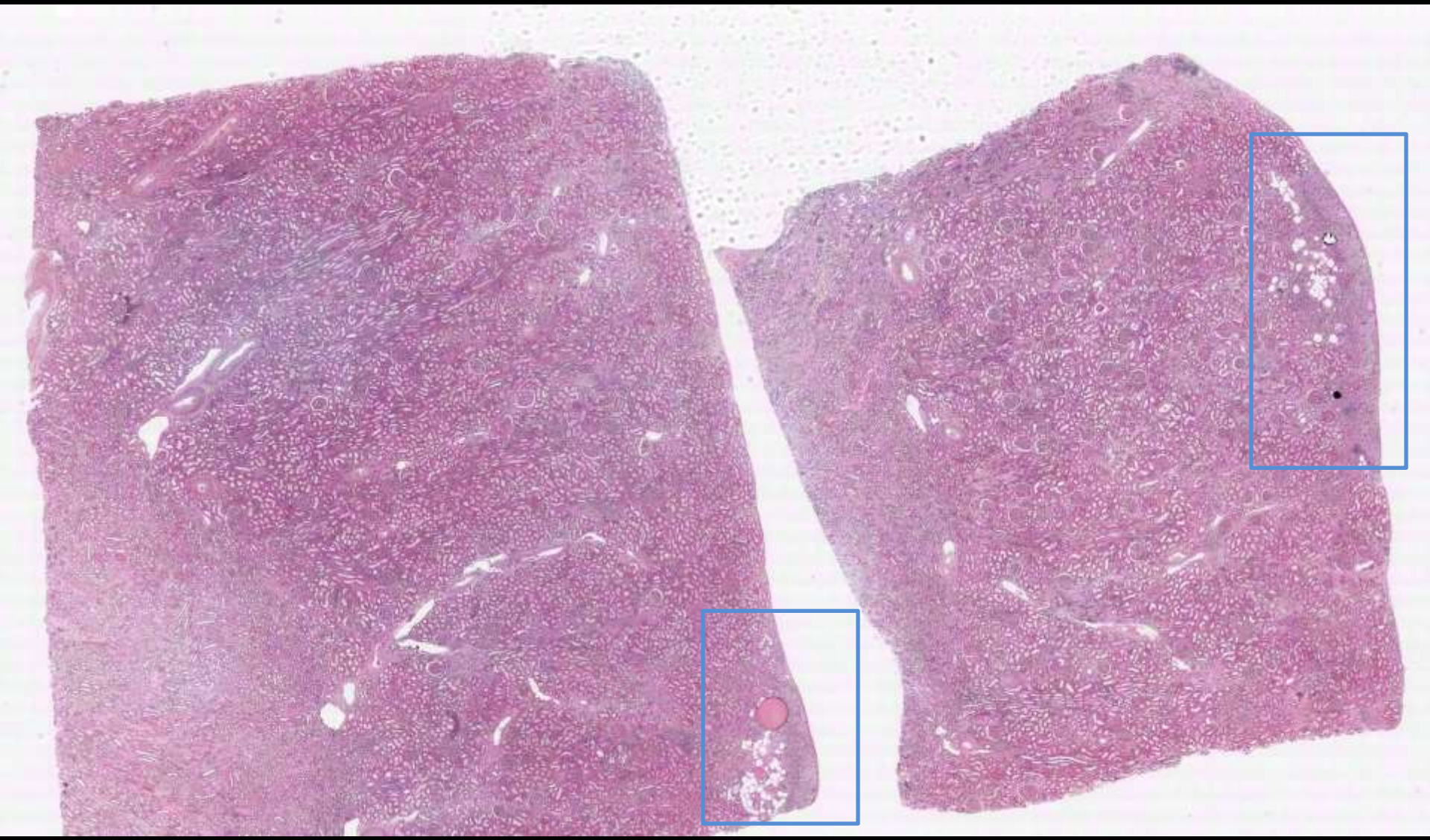

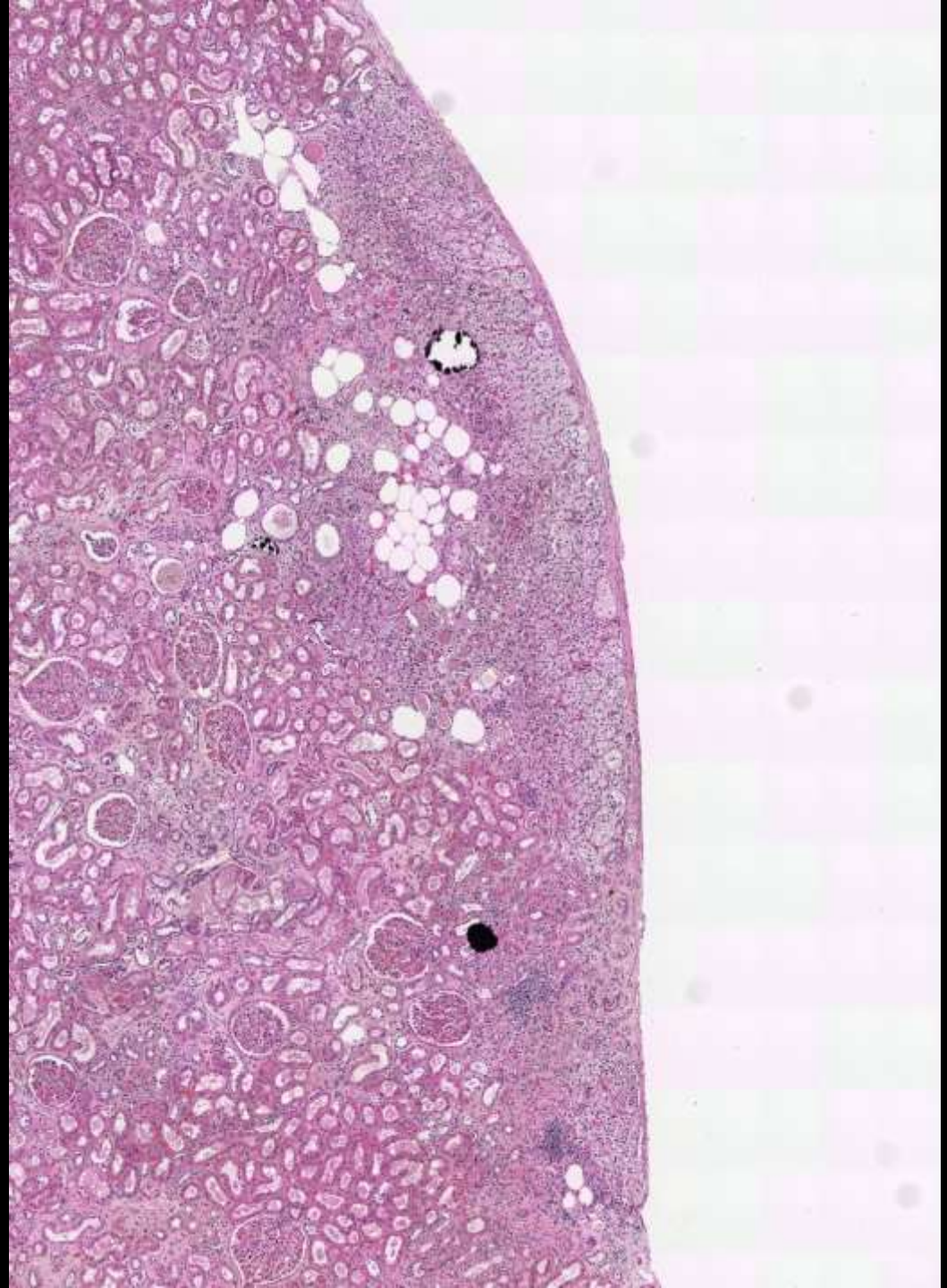

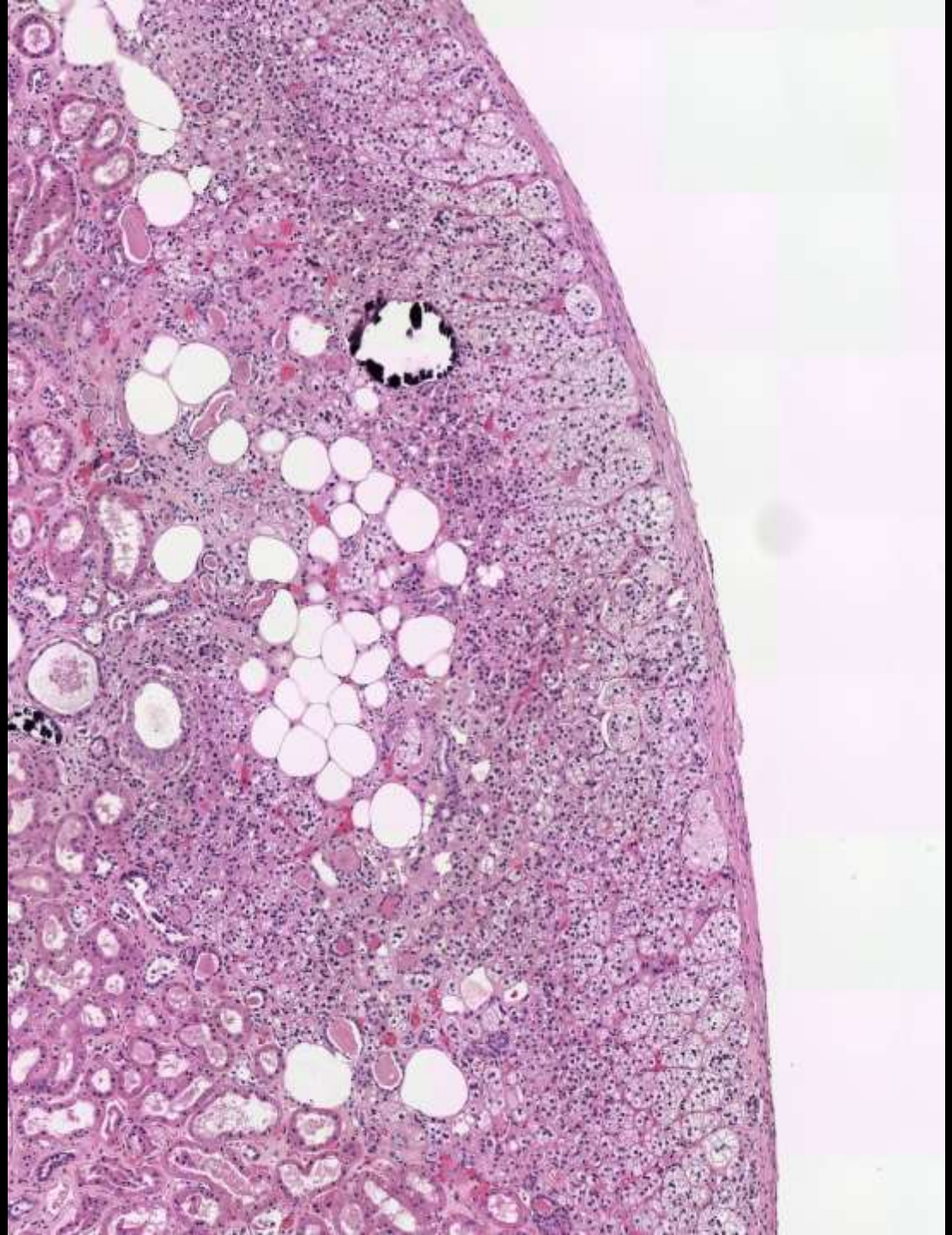

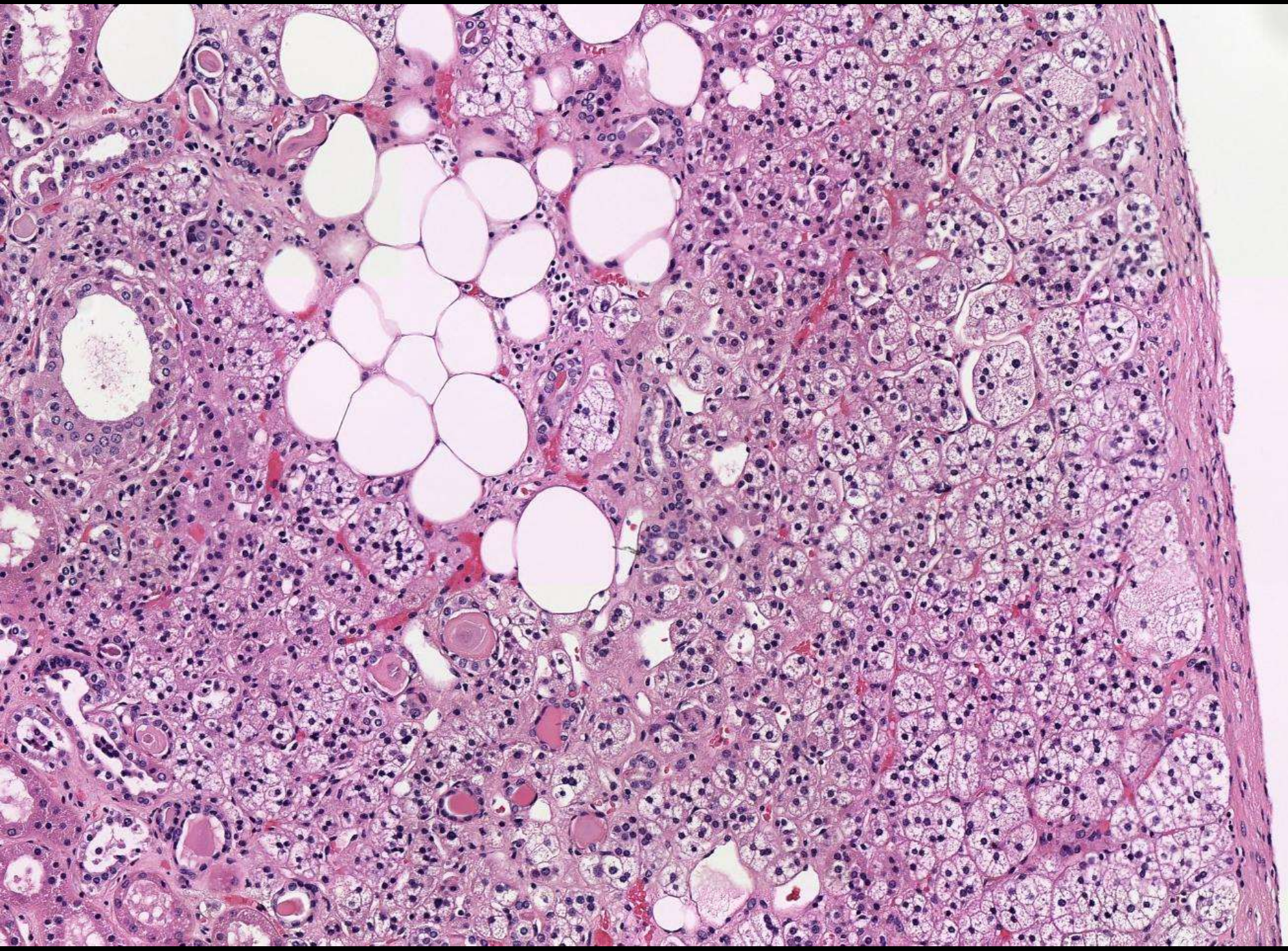

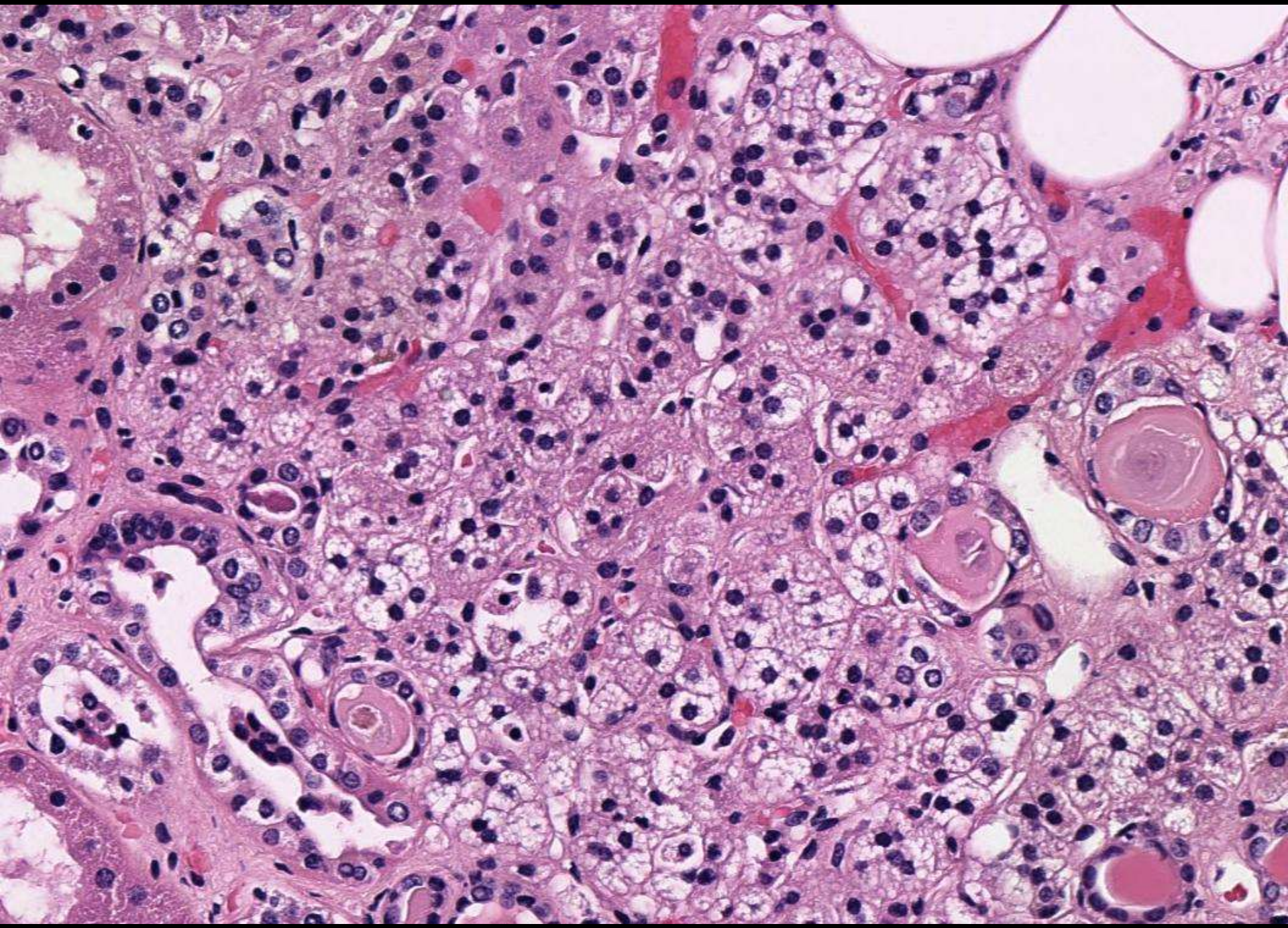

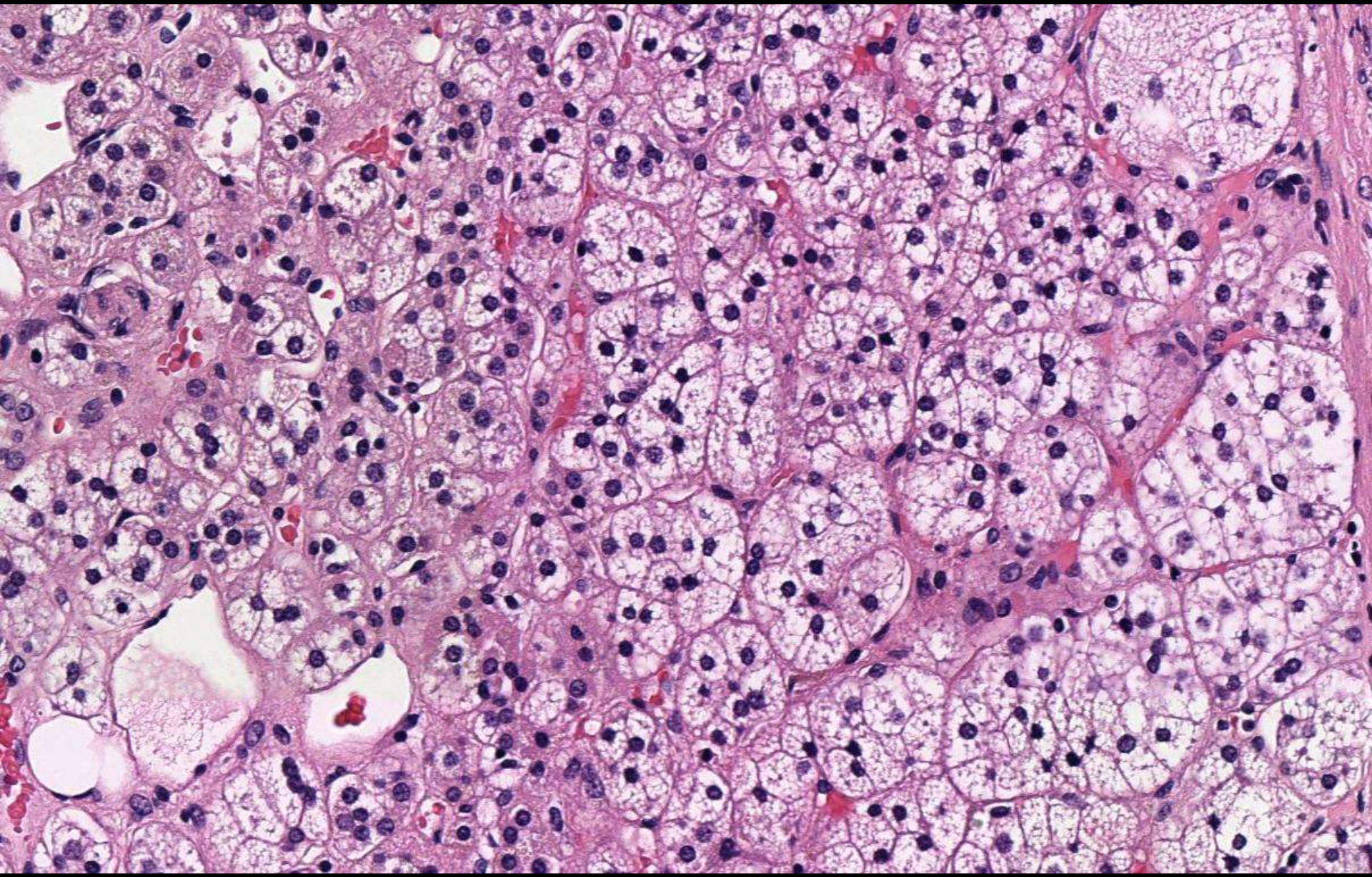

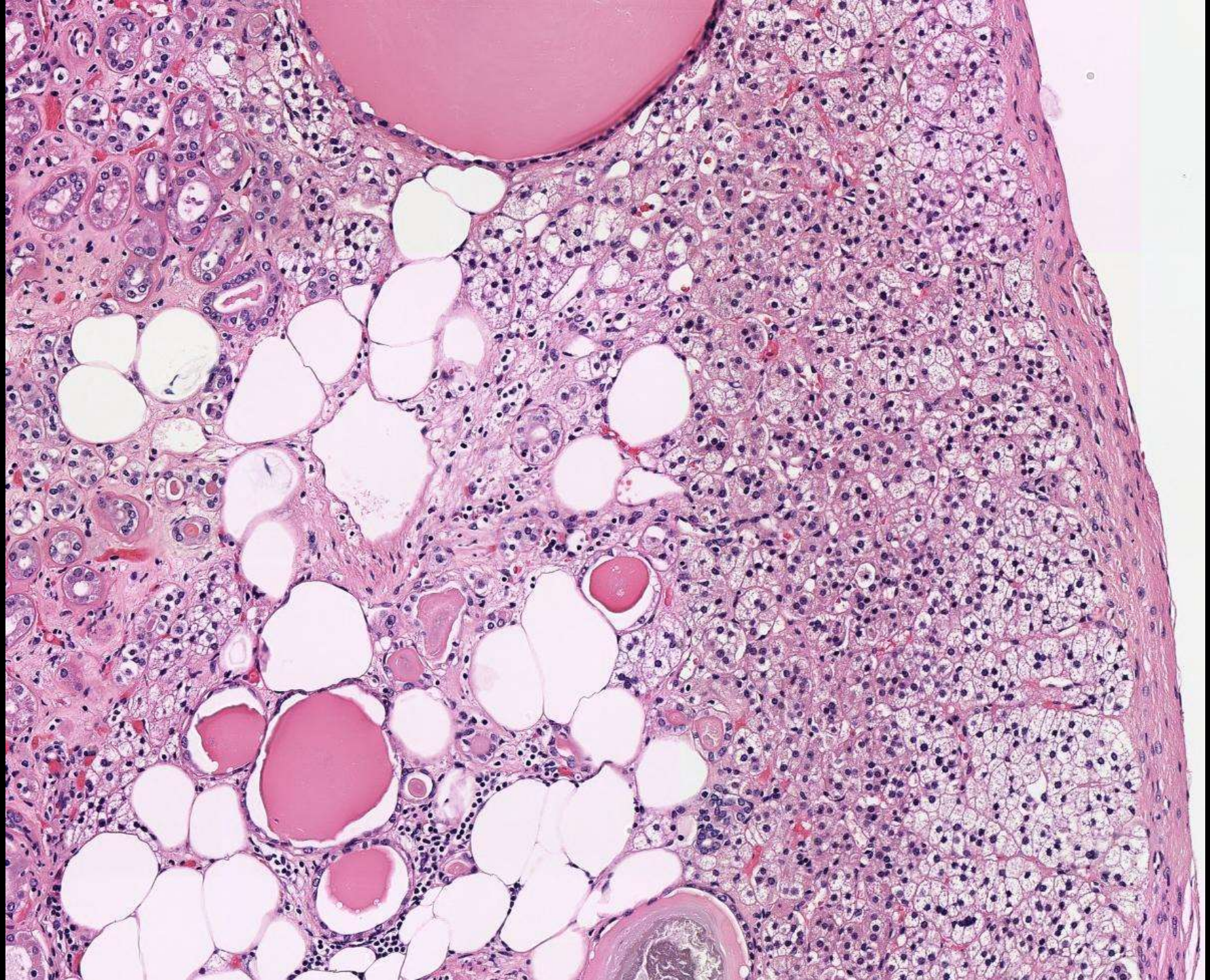

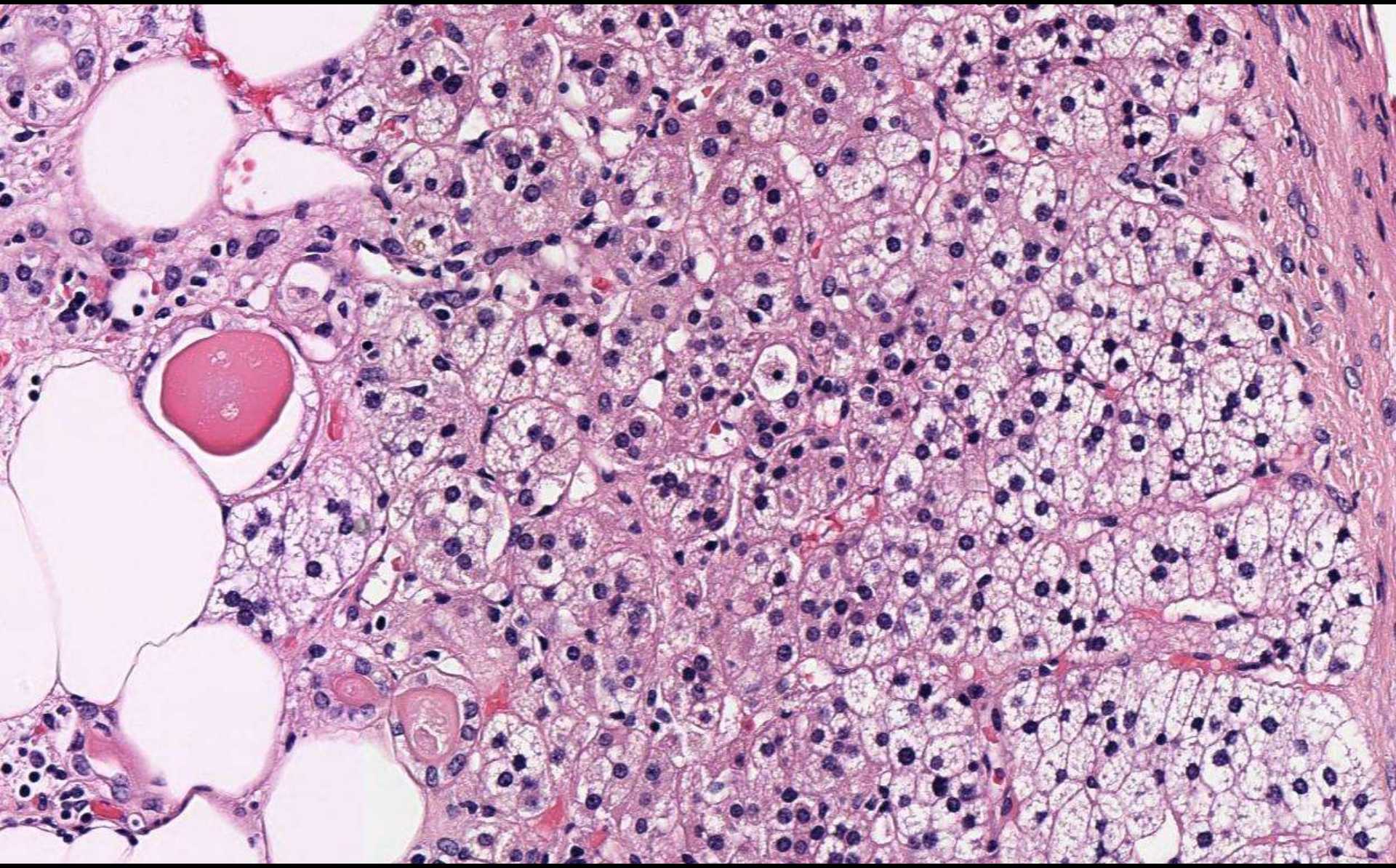

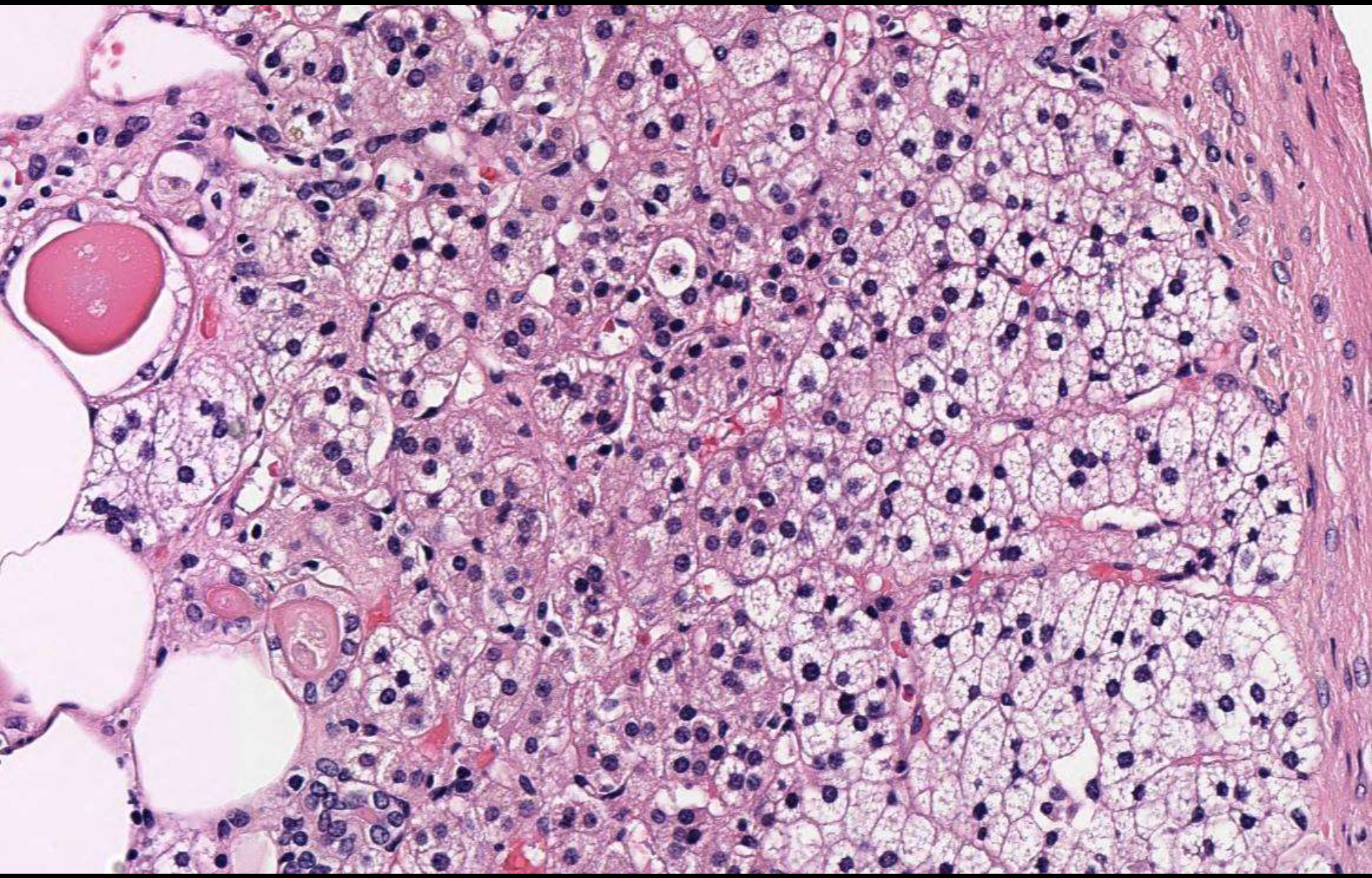

DDx

- Small foci of low grade clear cell RCC
- Small AML/PEComa
- Intrarenal ectopic adrenal tissue
- Renal-adrenal fusion

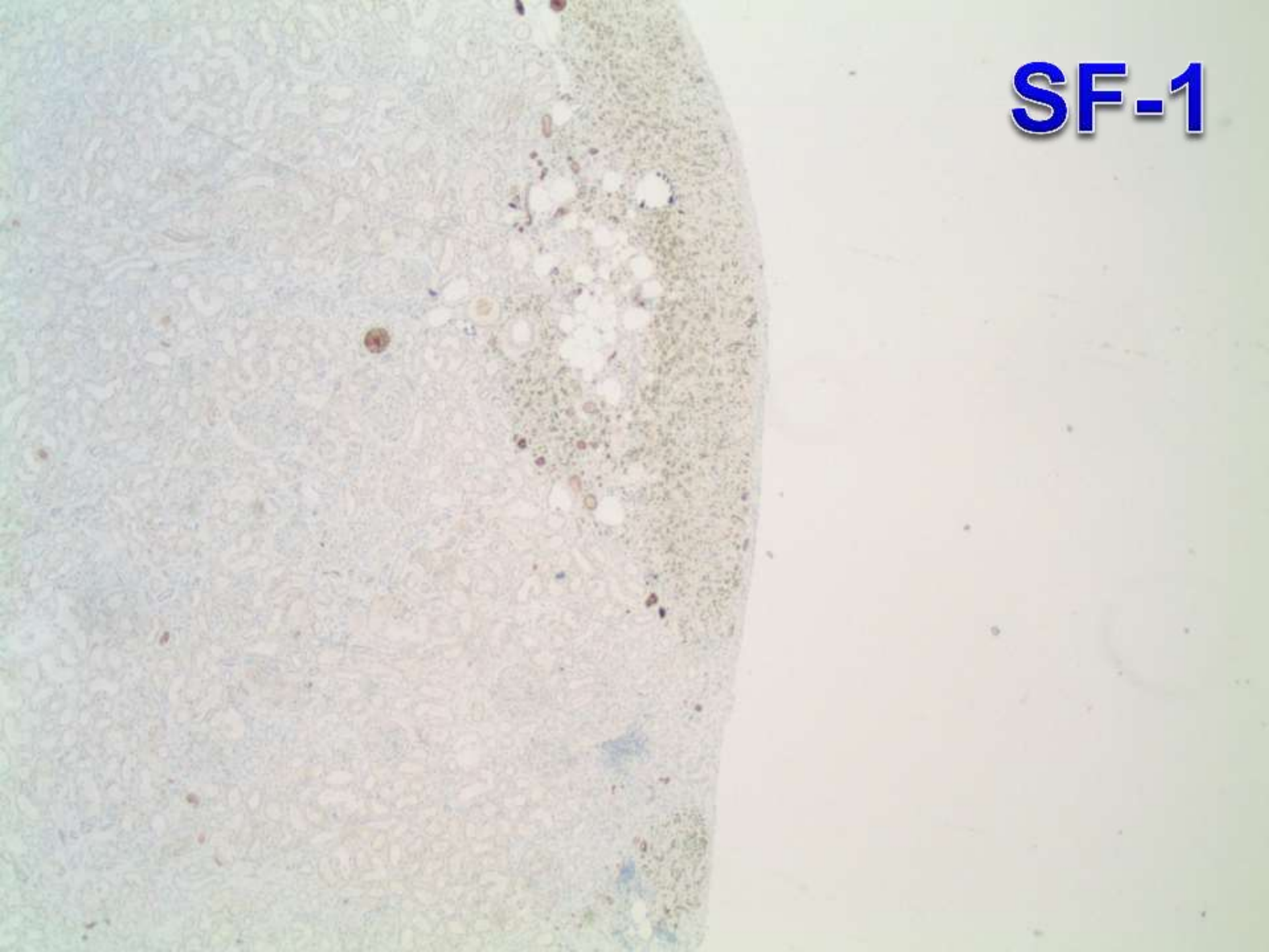
SF-1

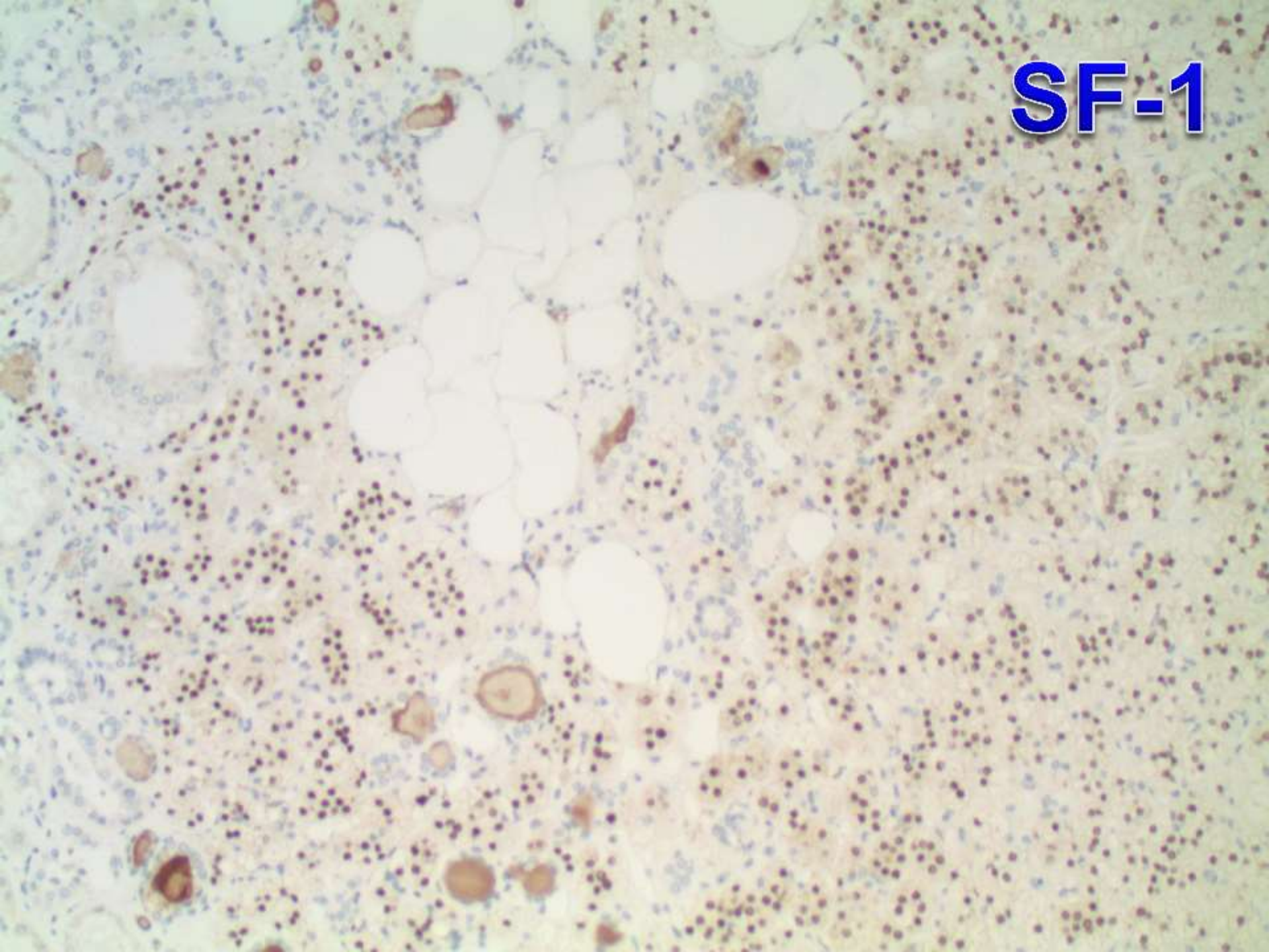
SF-1


SF-1

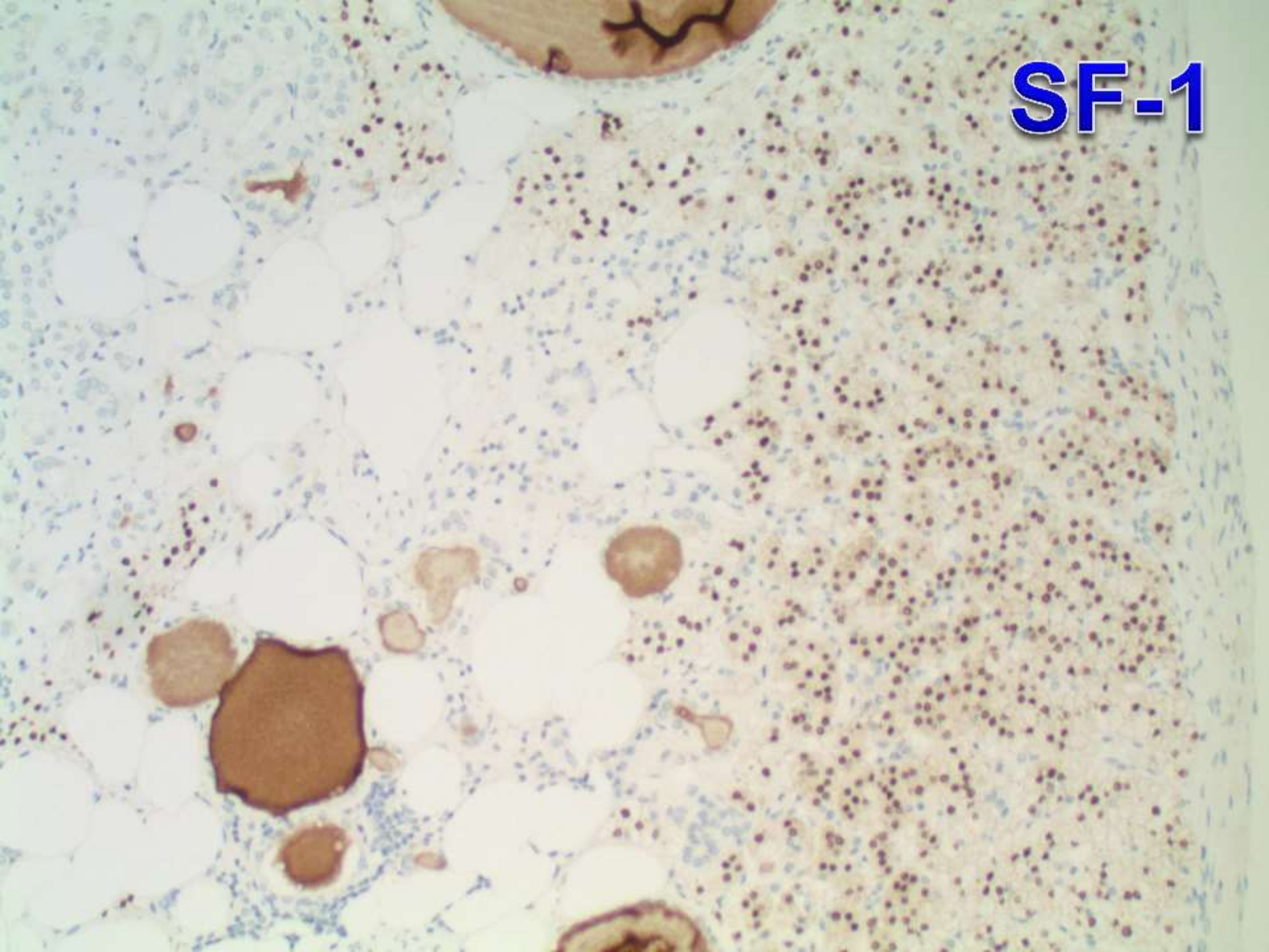
SF-1

Diagnosis

- **Intrarenal ectopic adrenal tissue**
  - Benign, incidental

Intrarenal ectopic adrenal tissue and renal–adrenal fusion: a report of nine cases

Huihui Ye[1], Ghil Suk Yoon[2,3,4] and Jonathan I Epstein[2,3,4]

[1]*Departments of Pathology, New York University Medical Center, New York, NY, USA;* [2]*Department of Pathology, The Johns Hopkins University School of Medicine, The Johns Hopkins Hospital, The James Brady Urological Institute, Baltimore, MD, USA;* [3]*Department of Urology, The Johns Hopkins University School of Medicine, The Johns Hopkins Hospital, The James Brady Urological Institute, Baltimore, MD, USA and* [4]*Department of Oncology, The Johns Hopkins Hospital, The Johns Hopkins University School of Medicine, The James Brady Urological Institute, Baltimore, MD, USA*

Intrarenal ectopic adrenal tissue and renal–adrenal fusion are rare findings in the adult population. We reviewed seven cases of intrarenal adrenal tissue and two cases of renal–adrenal fusion. Patients ranged in age from 35 to 75 years (mean 55). Ectopic adrenal tissue was identified at the superior pole of the kidney in all but one case, which was located in the mid-portion of the kidney. Ectopic adrenal tissue varied in its growth from subcapsular lesions that were plaque-like ($n=3$), wedge-shaped ($n=2$), or spherical ($n=1$) to irregular nests deep in the renal parenchyma ($n=1$). In all nine cases, the adherent and intrarenal adrenal tissue was composed of adrenal cortical tissue, with no adrenal medullary tissue present. In six cases, adrenal tissue focally extended into renal parenchyma in an infiltrative manner. Of the nine cases, two were diagnostic problems for the contributing pathologists. In one case, intrarenal adrenal tissue mimicked low-grade clear cell renal cell carcinoma. In another case, an adrenocortical adenoma adherent to the kidney resembled renal invasion by adrenocortical carcinoma. This study summarizes key morphological features of intrarenal ectopic adrenal tissue and renal–adrenal fusion along with histological pitfalls and its differential diagnoses.

Modern Pathology (2009) **22**, 175–181; doi:10.1038/modpathol.2008.162; published online 26 September 2008

Keywords: renal adrenal fusion; ectopic adrenal; intrarenal adrenal

Table 1 Patient demographics, specimen type, anatomic location, and pathologic diagnosis

Case	*Age*	*Sex*	*Specimen*	*Side*	*Location*	*Size*	*Pathological diagnosis*
1	44	M	Transplant nephrectomy	/	N/A	Microscopic	Cortical necrosis and ATN; ectopic adrenal tissue with focal necrosis
2	35	F	Nephrectomy	R	Upper pole	0.8 cm cyst	Hydronephrosis with chronic pyelonephritis; intrarenal adrenal gland tissue with adjacent simple renal cyst
3	55	F	Donor kidney biopsy	L	N/A	0.3 cm	Intrarenal adrenal rest
4	75	M	Radical nephrectomy	L	Mid-portion	'A small amount'	Clear cell RCC; a small amount of adrenal tissue adherent to the medial renal capsule
5	72	M	Radical nephrectomy	R	Upper pole	0.7 cm	Non-invasive papillary UC; adjacent CIS; A small subcapsular adrenal rest
6	51	M	Radical nephrectomy	L	Upper pole	'A small portion'	Papillary RCC; renal–adrenal fusion
7	52	F	Laparoscopic nephrectomy	L	N/A	Microscopic	End-stage kidney; ectopic adrenal tissue in renal capsule and cortex
8	49	F	Partial nephrectomy	L	Upper pole	$2 \times 2 \times 1$ cm	Cortical adenoma arising in adherent and intrarenal adrenal gland
9	59	F	Radical nephrectomy	R	Upper pole	1.5 cm cyst	Low-grade RCC, NOS; small focus of ectopic adrenal tissue

Table 2 Summary of morphologic findings

Case	*Location*	*Shape*	*Capsule*	*Zonation*	*Aberrant blood vessels*	*Scattered adipocytes*	*Focal infiltrative growth*	*Entrapped renal tubules*
1	Subcap	Plaque	No	None	No	Yes	Yes	No
2	Deep and cystic wall	Irregular	No	None	Yes	No	Yes	Yes
3	Subcap	Spherical	Yes	Maintained	No	No	No	Yes
4	Subcap	Plaque	Focal	None	No	Yes	Yes	No
5	Subcap	Wedge	No	None	Yes	Yes	No	Yes
6	RA fusion	Crescent	Focal	Maintained	No	Yes	Yes	Yes
7	Subcap and extracap	Wedge	No	None	Yes	No	Yes	Yes
8	RA fusion	Spherical	Focal	Partially	No	No	Yes	Yes
9	Subcap and cystic wall	Plaque	Focal	None	No	No	No	No

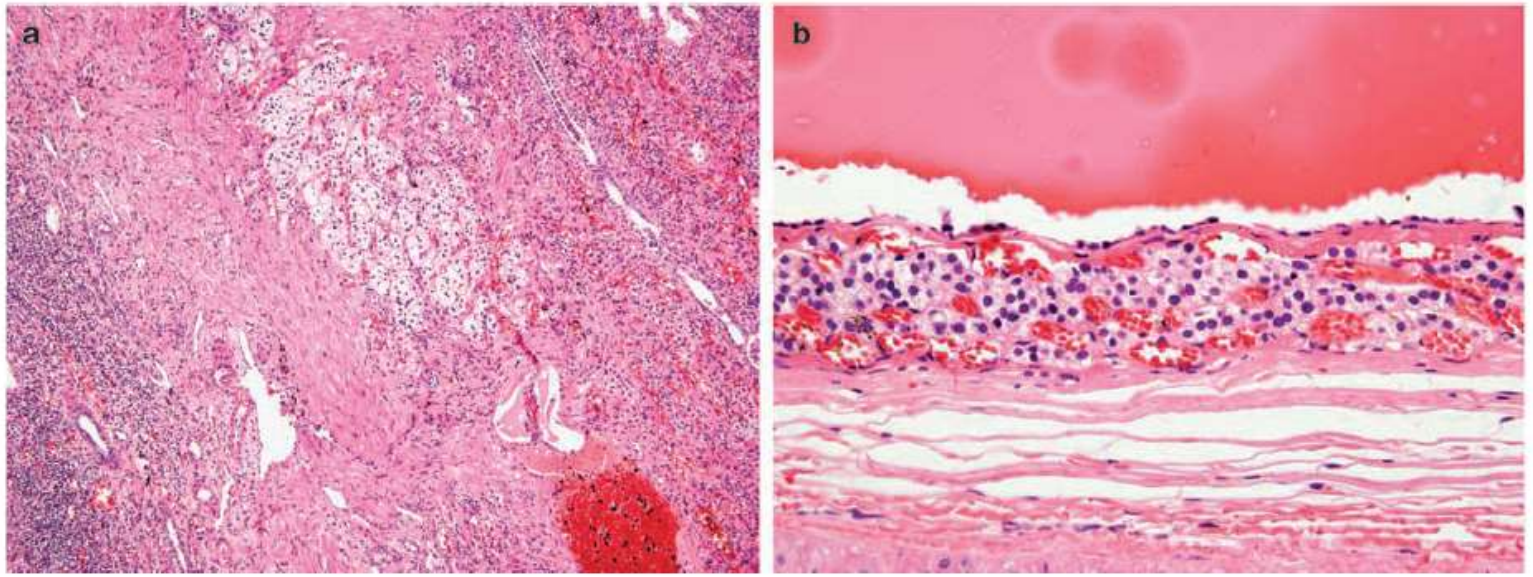

Figure 5 Case 2. irregular solid nests of clear cells deep in renal parenchyma (**a**). Clear cells also noted in the wall of a simple renal cyst, with prominent vascular network similar to that seen in clear cell renal cell carcinoma (**b**).

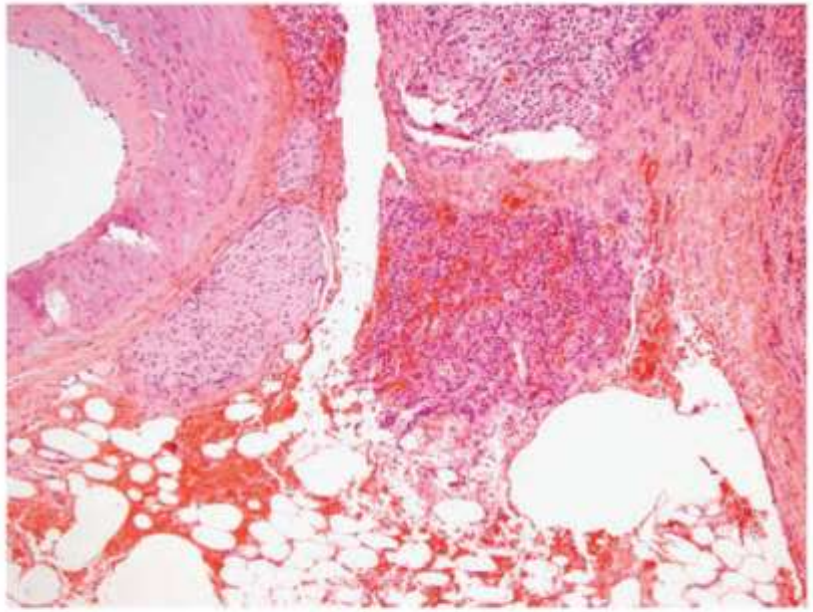

Figure 8 Ectopic adrenal tissue extends from subcaspular region into perirenal adipose tissue without a surrounding fibrous capsule.

RENAL ADRENAL FUSION

- **First described by Rokitansky**
  - Developmental form
    - Failure of retroperitoneal mesenchyme to stimulate capsule formation
  - Post-inflammatory fibrosis type
- **Usually a problem for radiologists, not pathologists**
  - Can be mis-Dx as renal masses


4
5
6
7
8
9
10
11
12
13
14
15

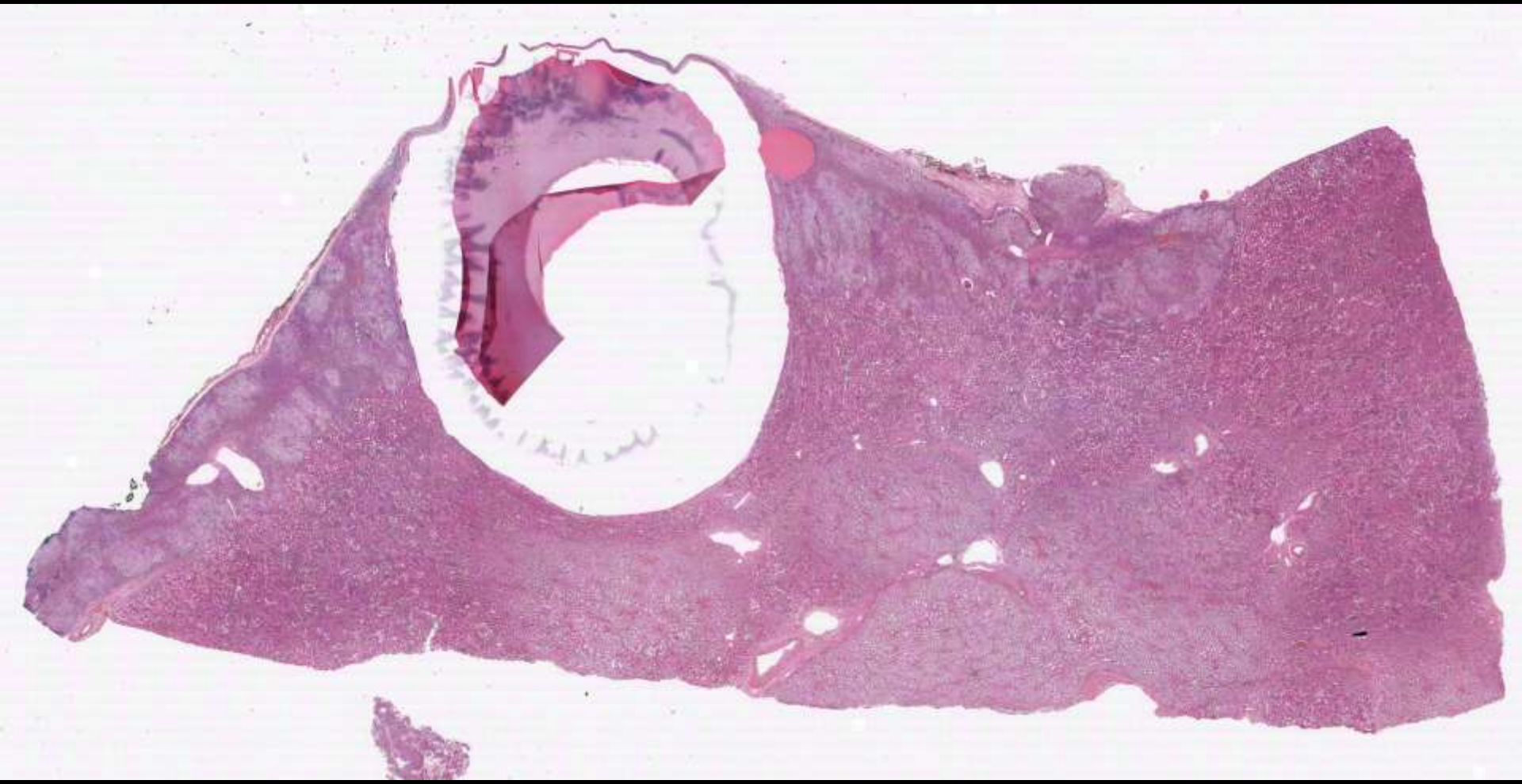

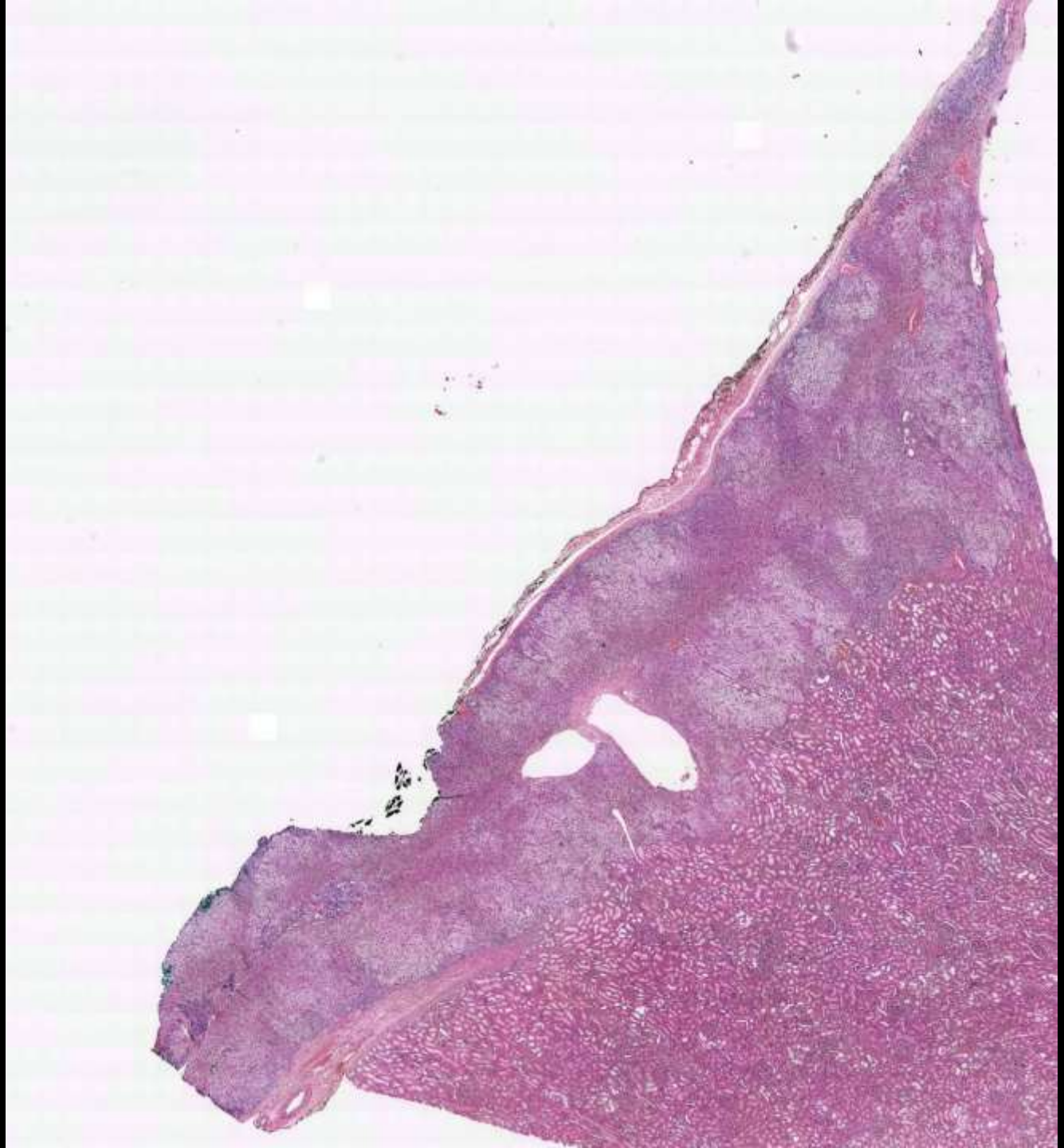

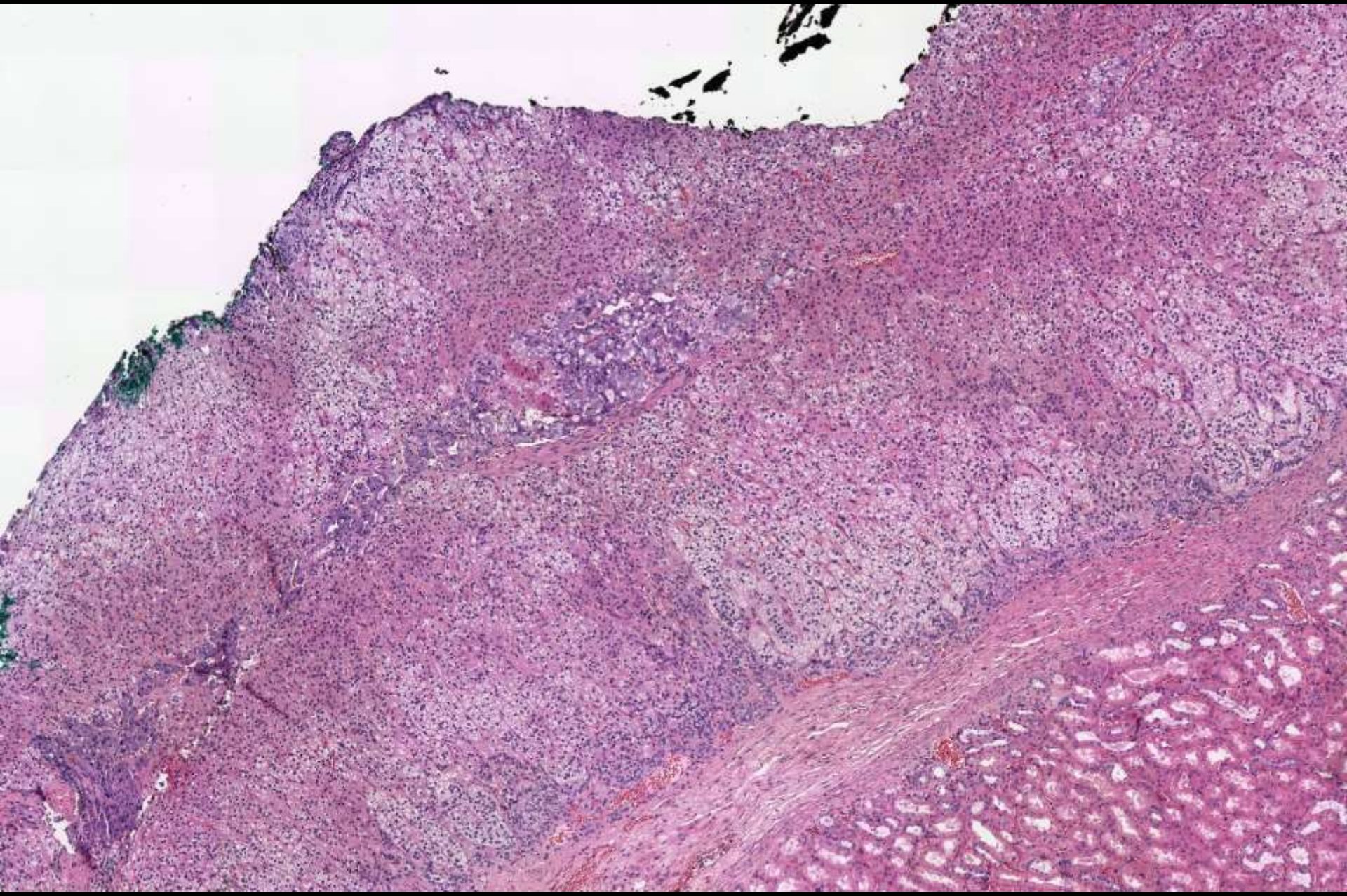

ECTOPIC ADRENAL TISSUE

- **Distinct anomaly from renal-adrenal fusion**
- **1% of adults, 50% neonates**
  - Usually regresses in early infancy
- **Any visceral organ**
  - Kidney, liver, gonads
- **May contain cortex+medulla**

Take home points

- **Ectopic adrenal tissue can be compressed by adjacent cyst**
  - Clear cells in cyst wall → mimic RCC
- **Can extend beyond capsule into perirenal adipose tissue without a capsule**
  - Mimic RCC

19-0309

Ankur Sangoi; El Camino Hospital

34-year-old male without known past medical history, presents with incidentally-found 1.7cm renal tumor. Core biopsy performed before ablation of renal tumor.

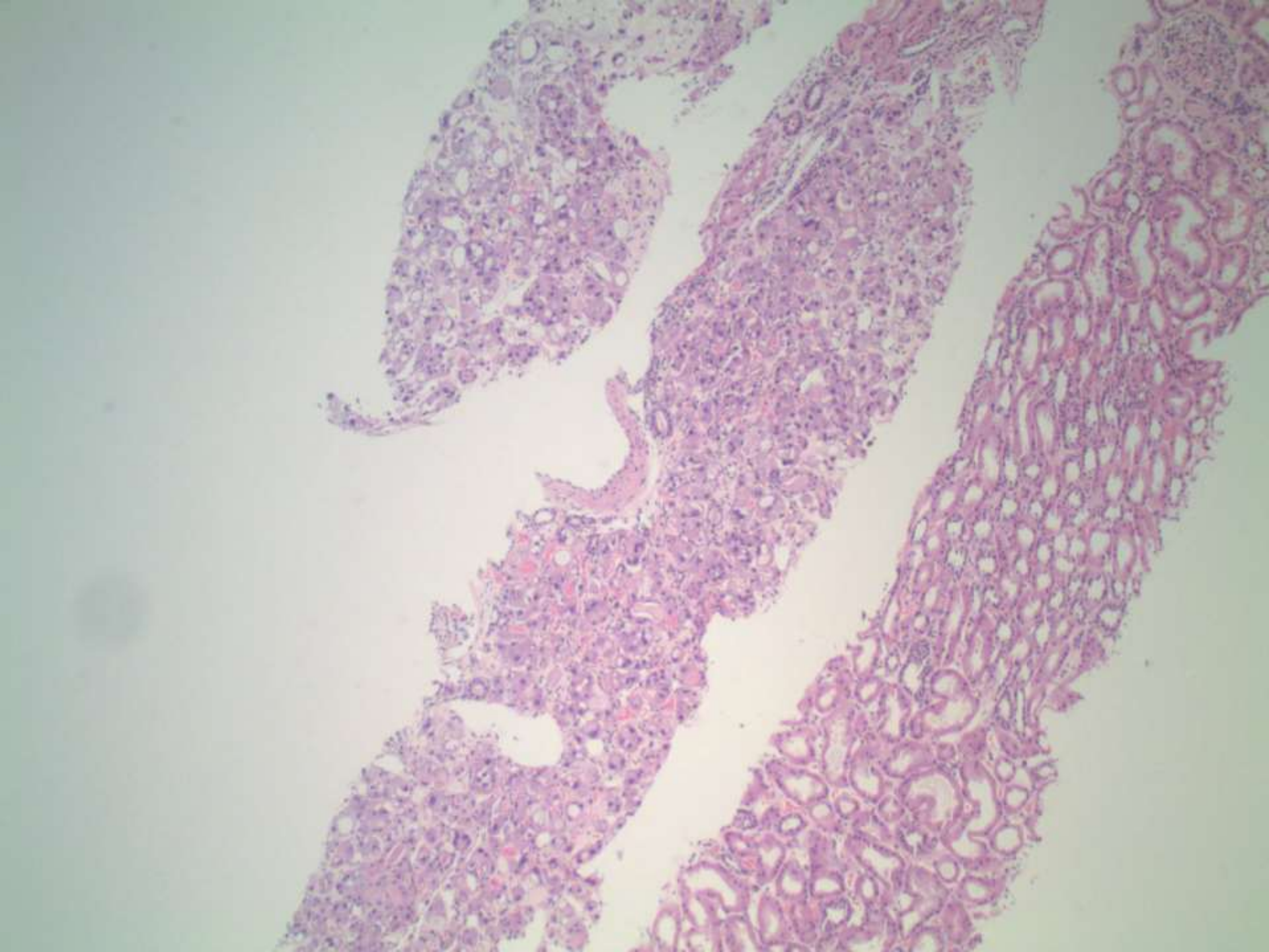

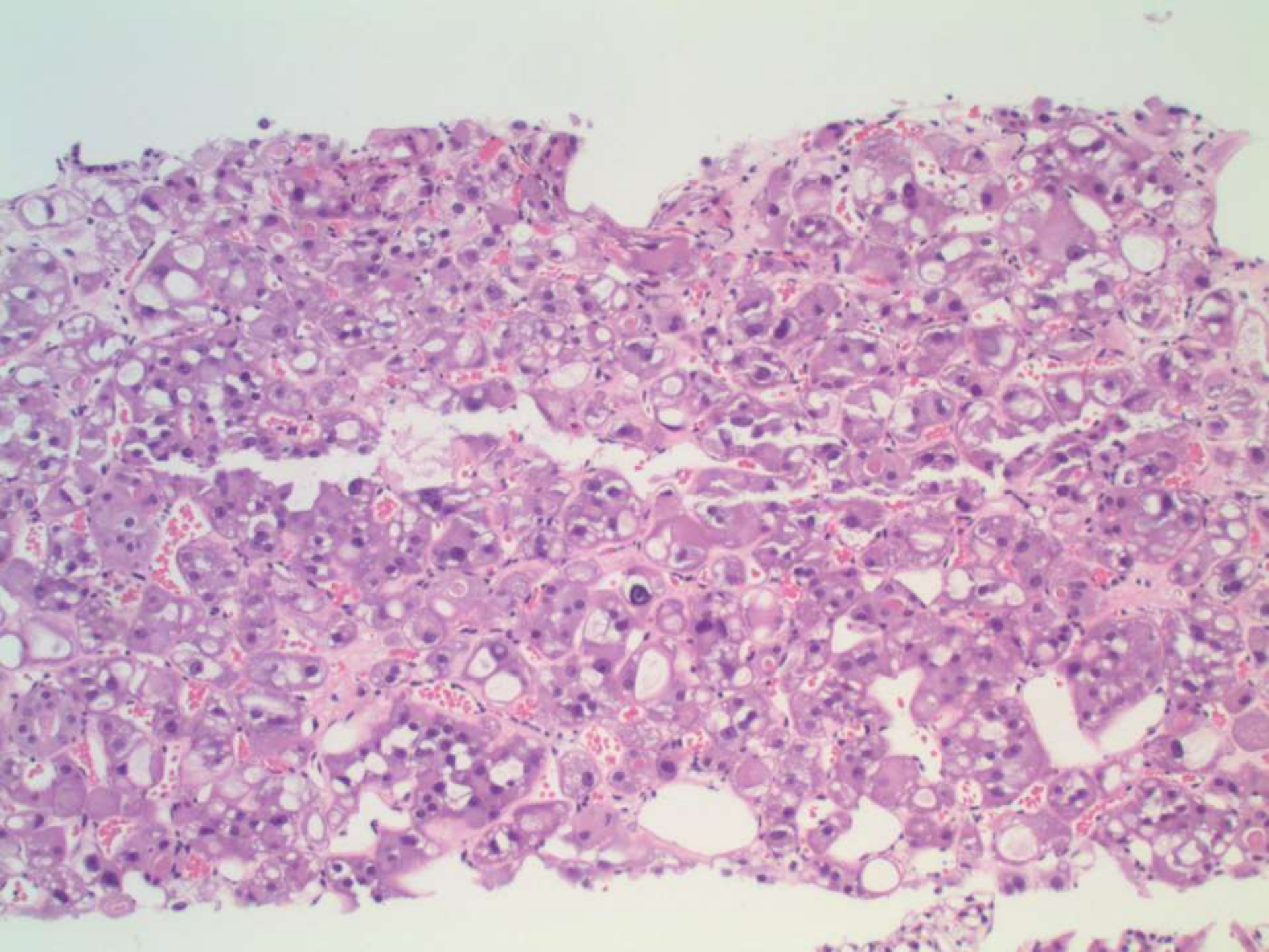

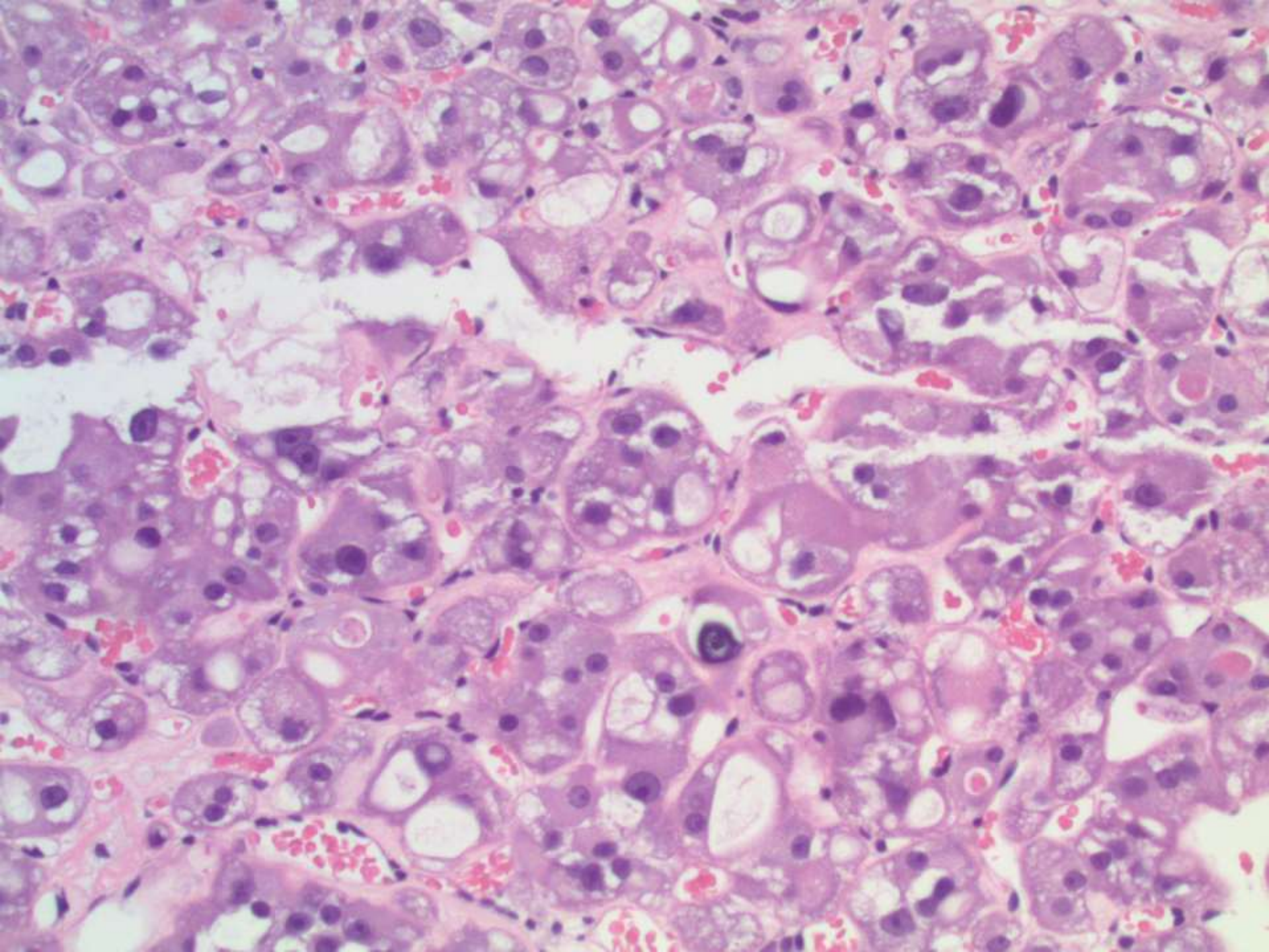

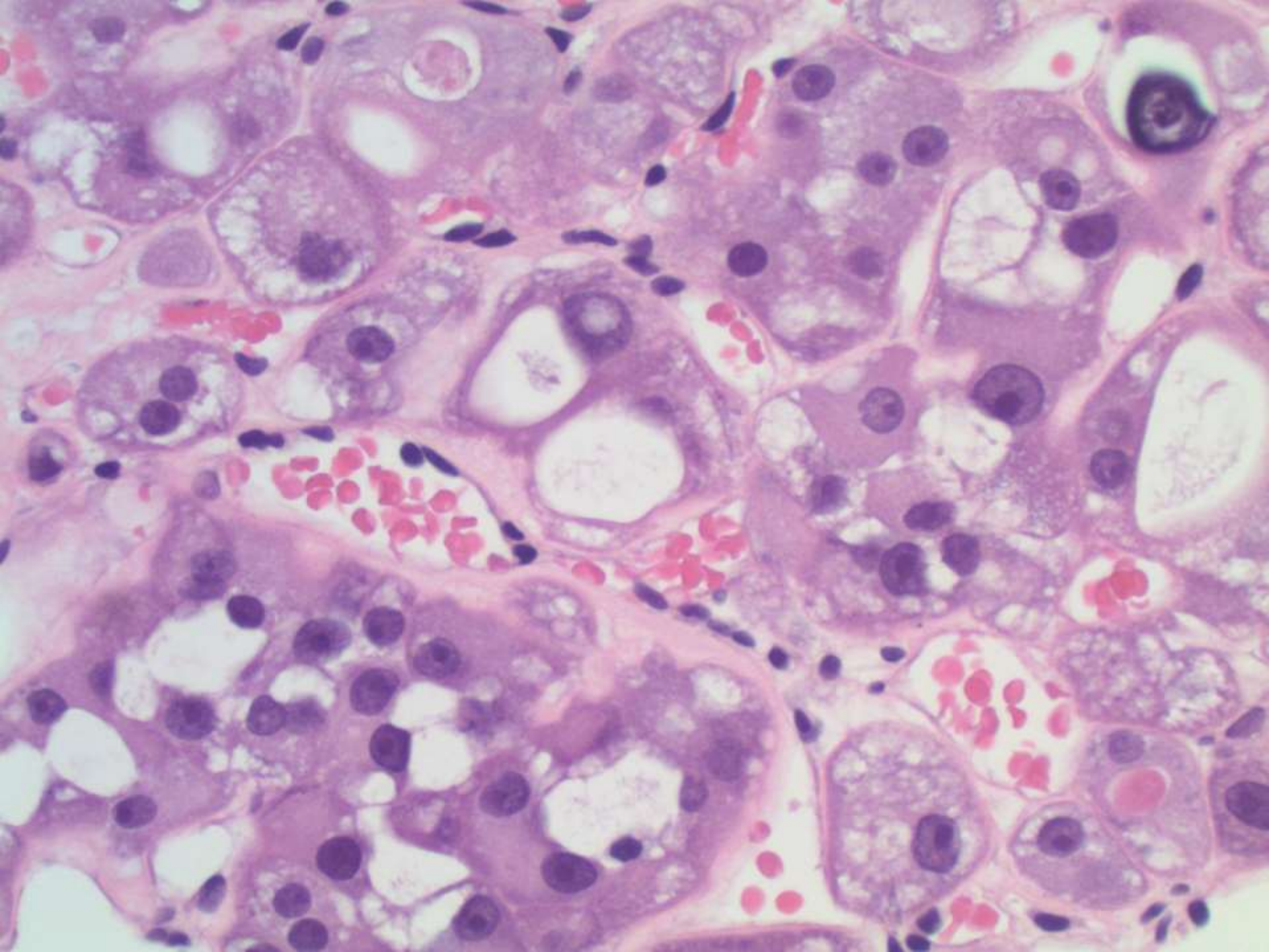

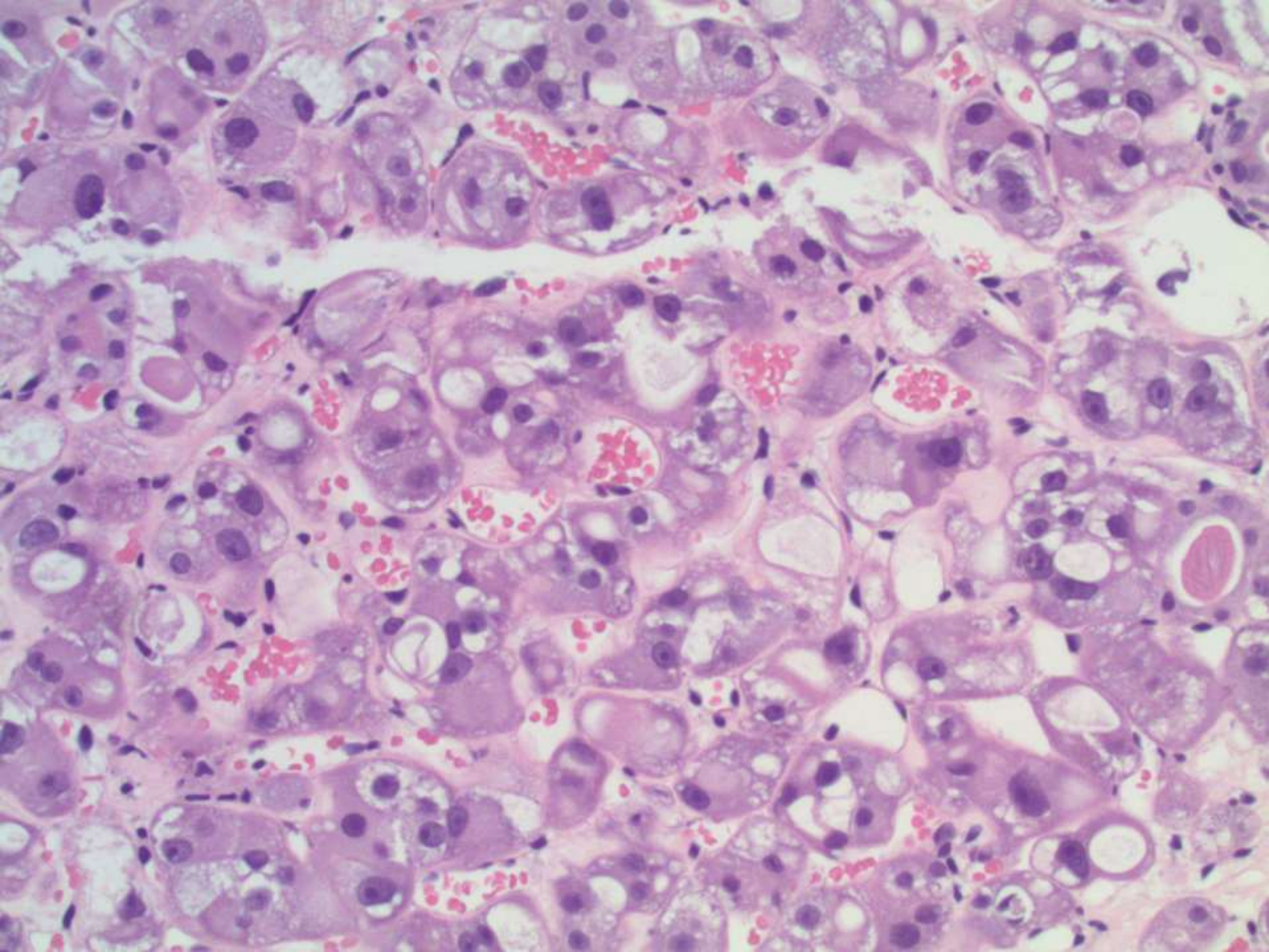

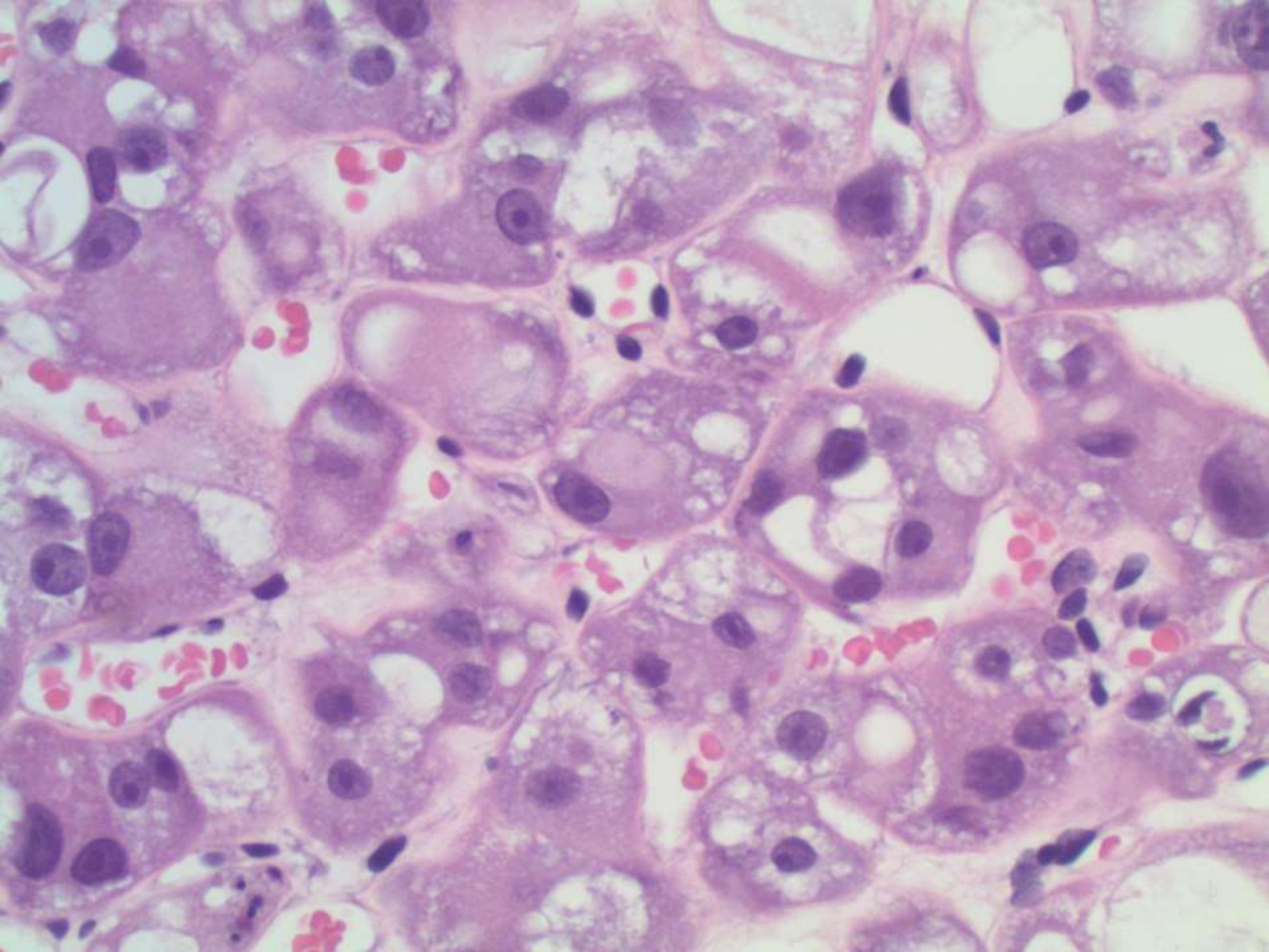

DDx

- Oncocytoma
- Chromophobe RCC (eosinophilic variant)
- Clear cell RCC (eosinophilic variant)
- Xp11 (translocation) RCC
- FH deficient RCC
- ESC RCC
- SDHB RCC
- Epithelioid AML
- Adrenal cortical neoplasm

AE1/AE3

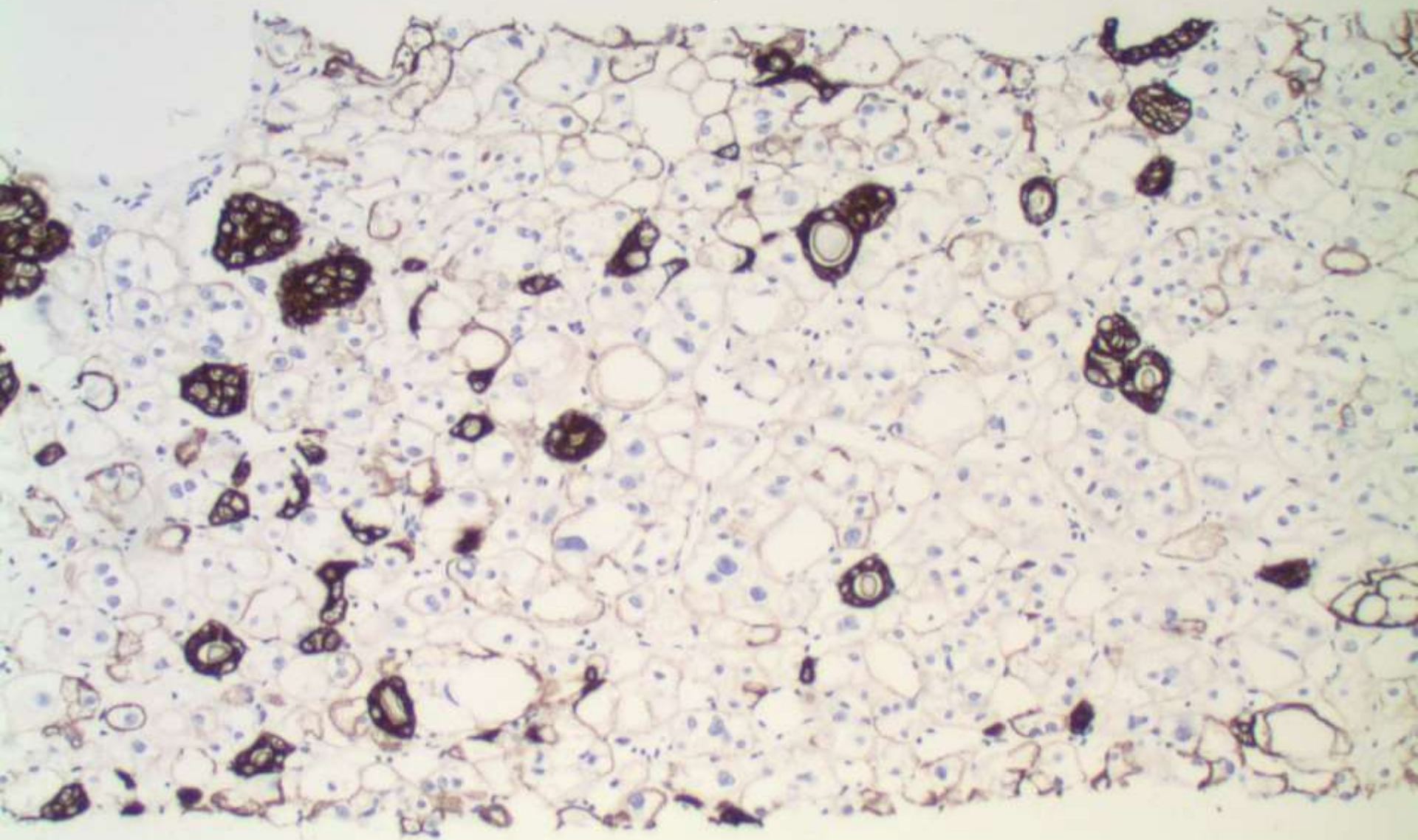

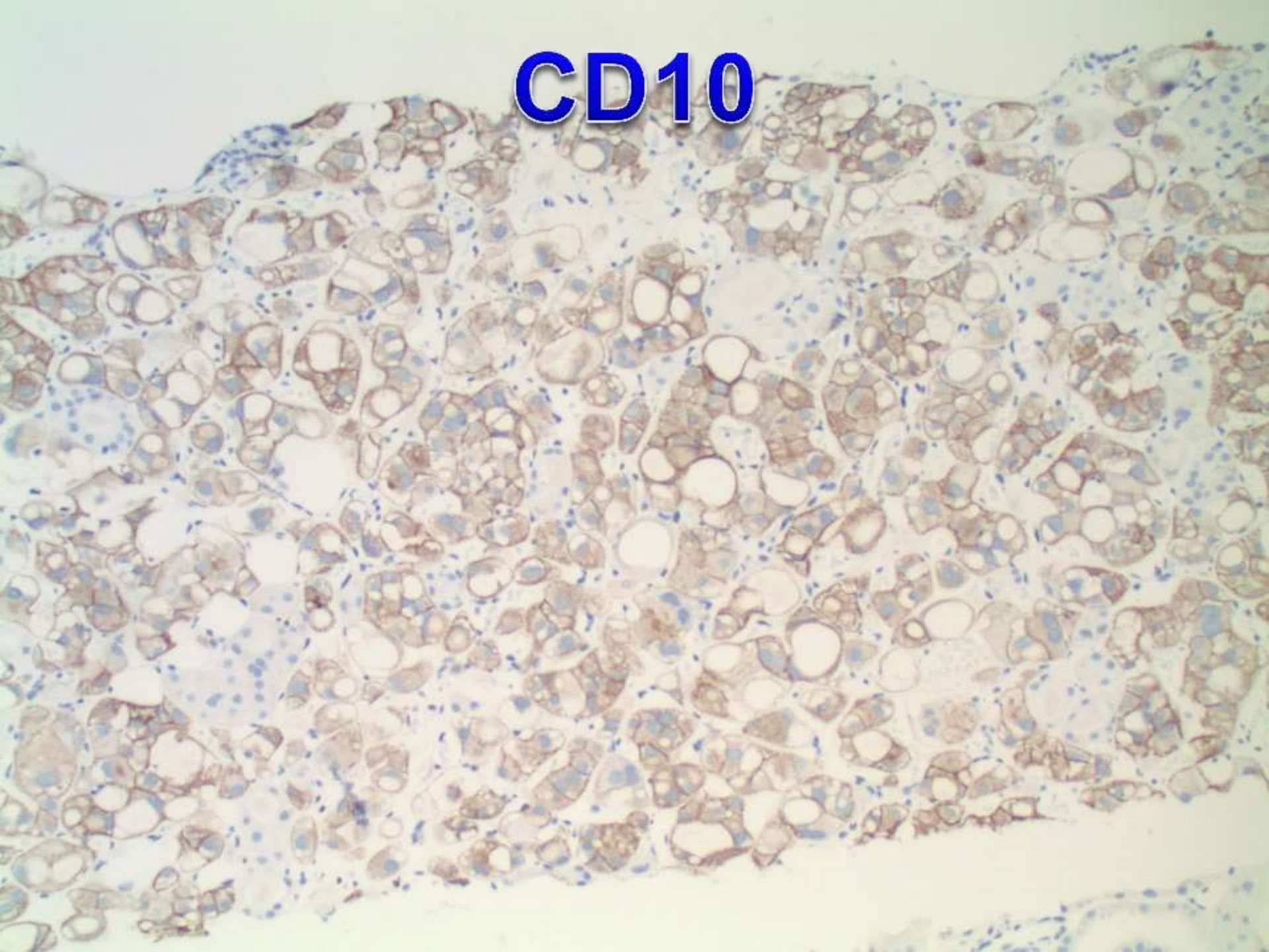
CD10

CK7

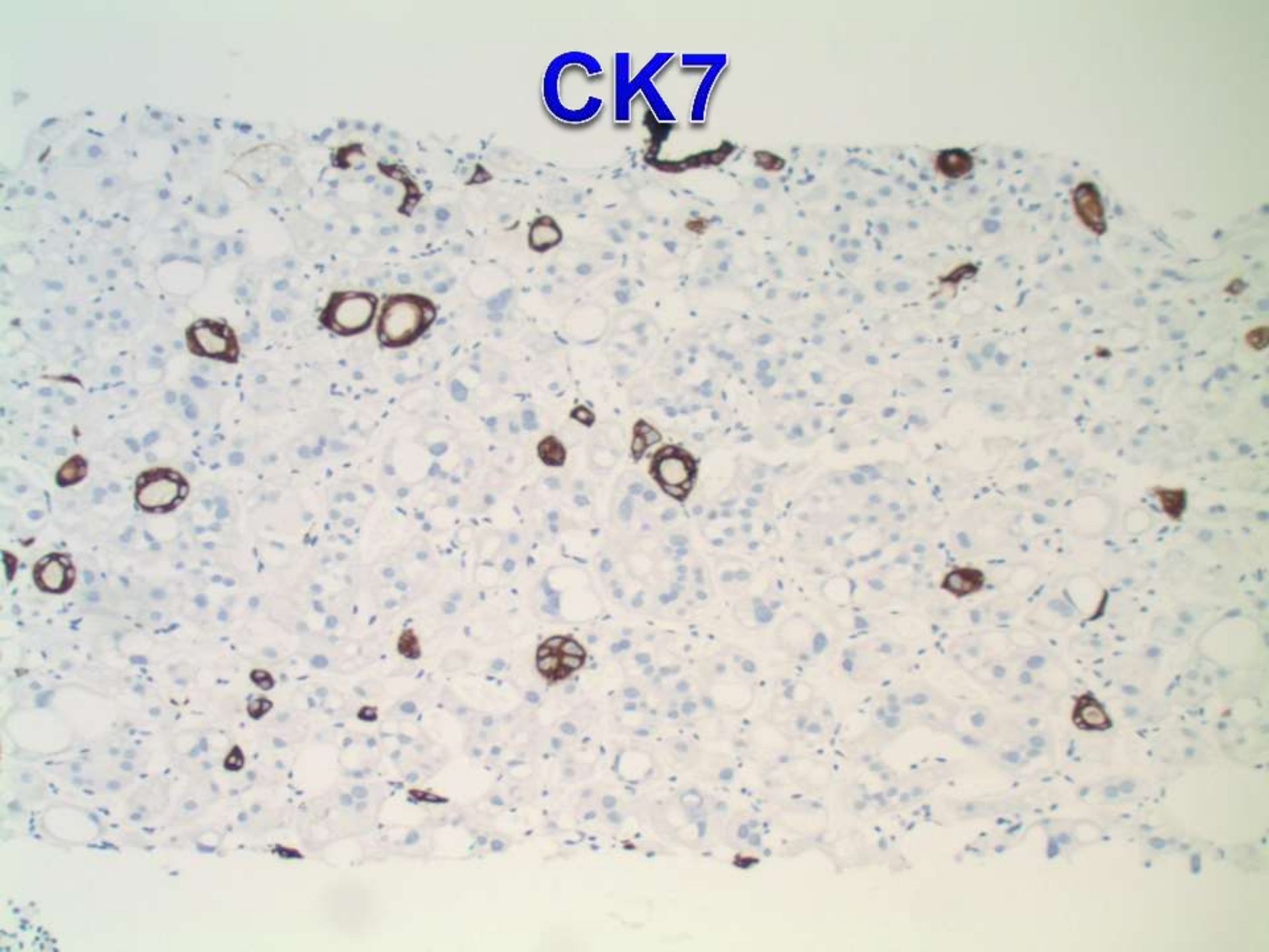

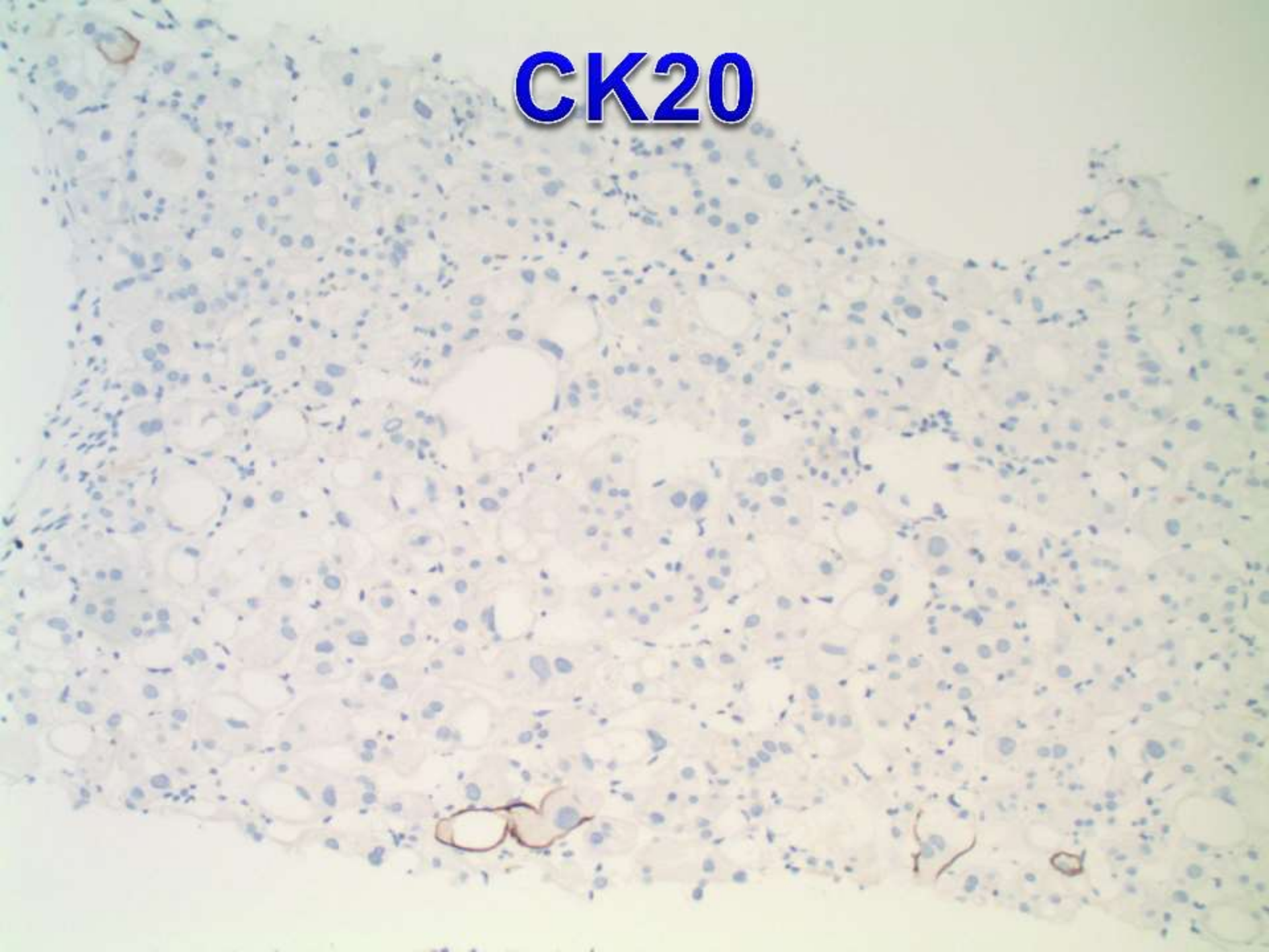
CK20

AMACR

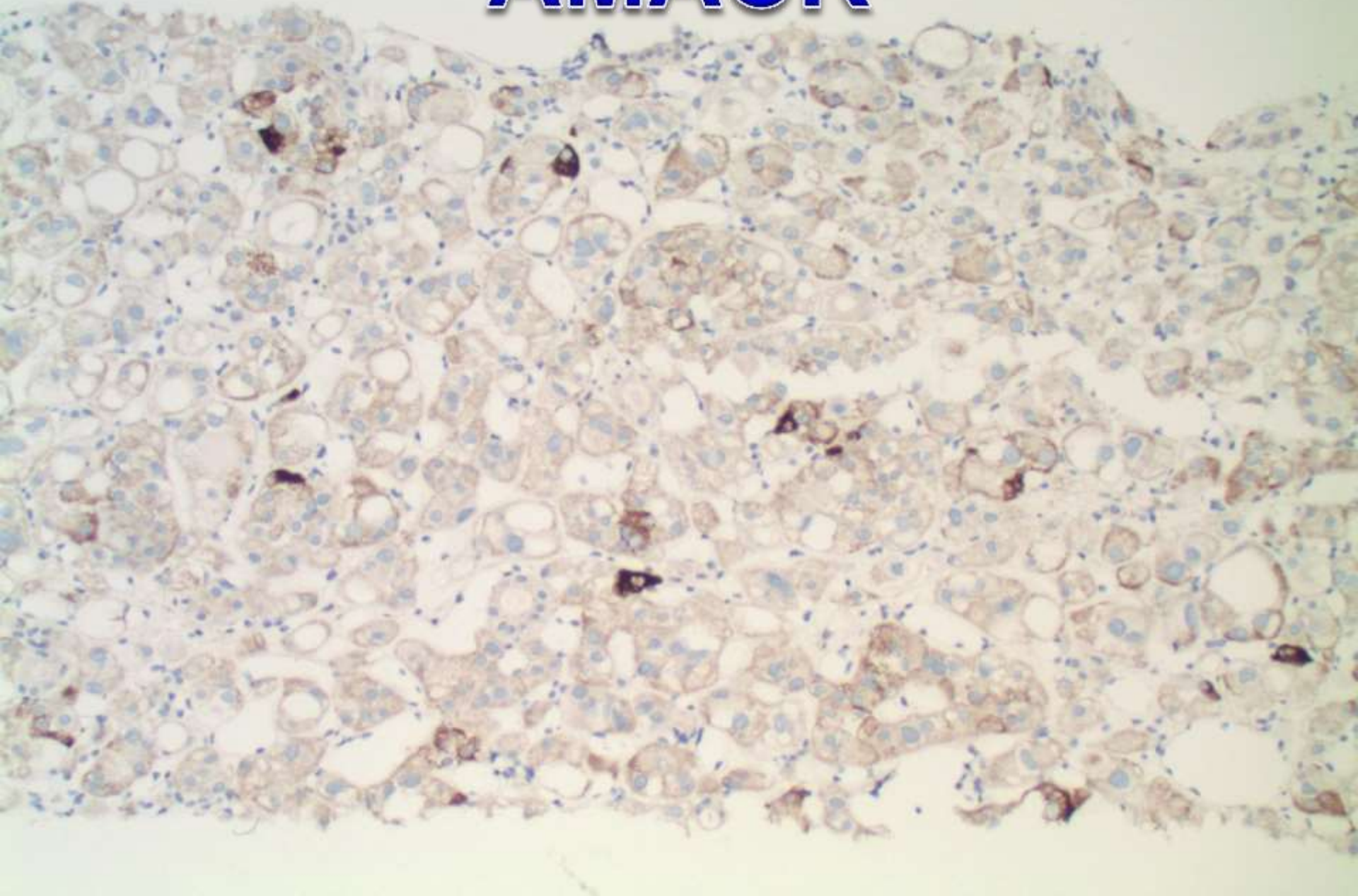

cathepsinK

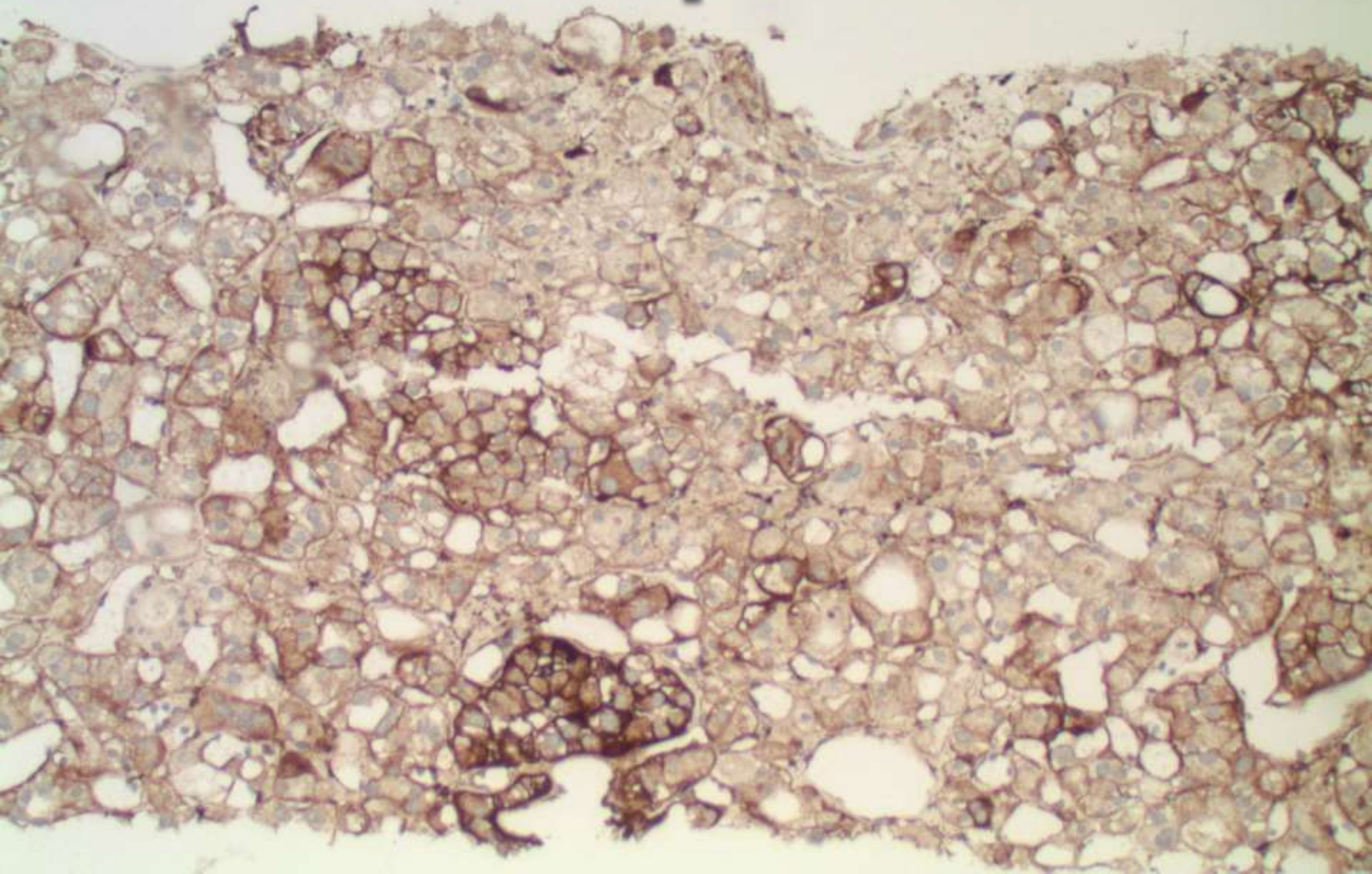

vimentin

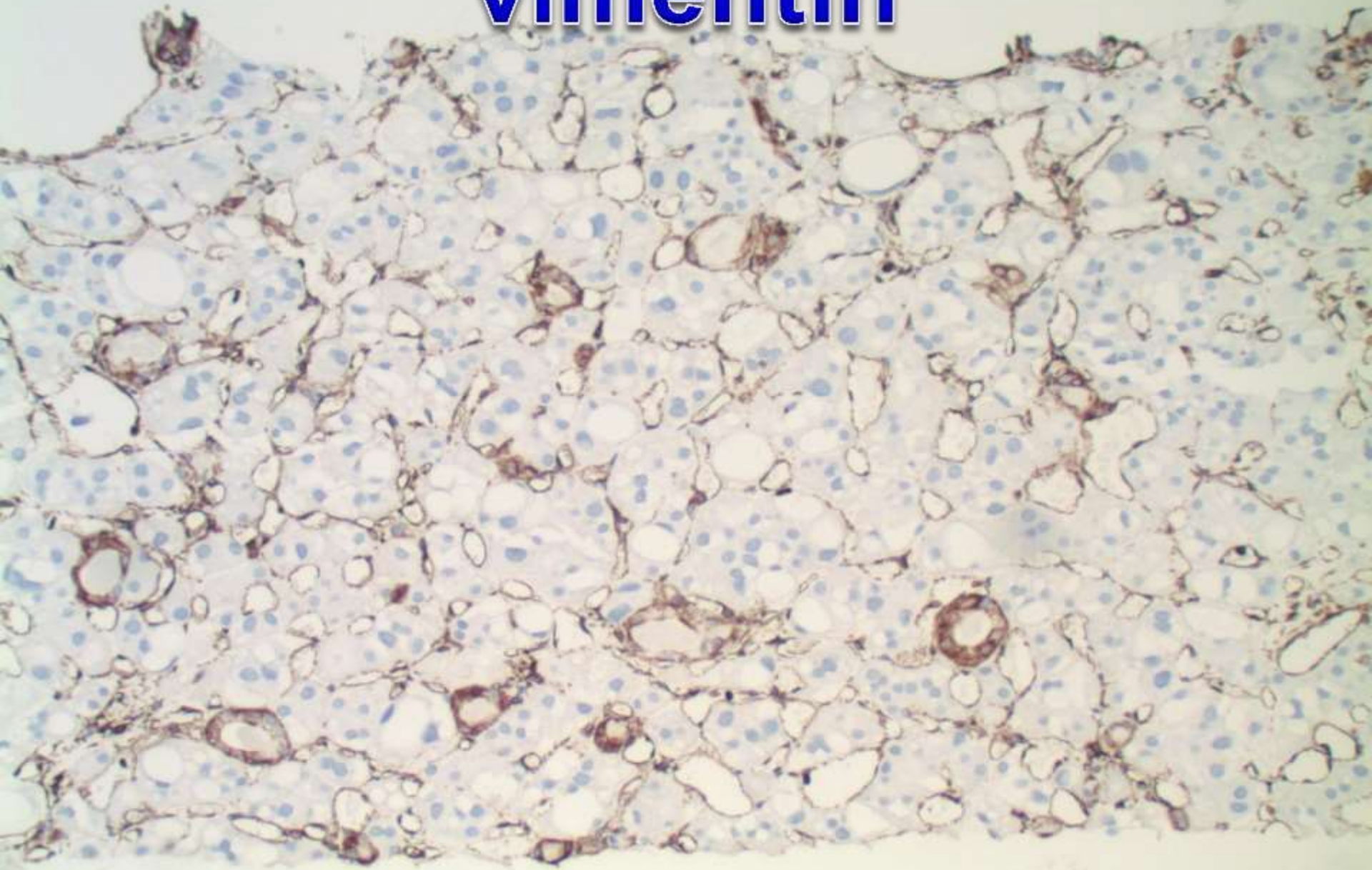

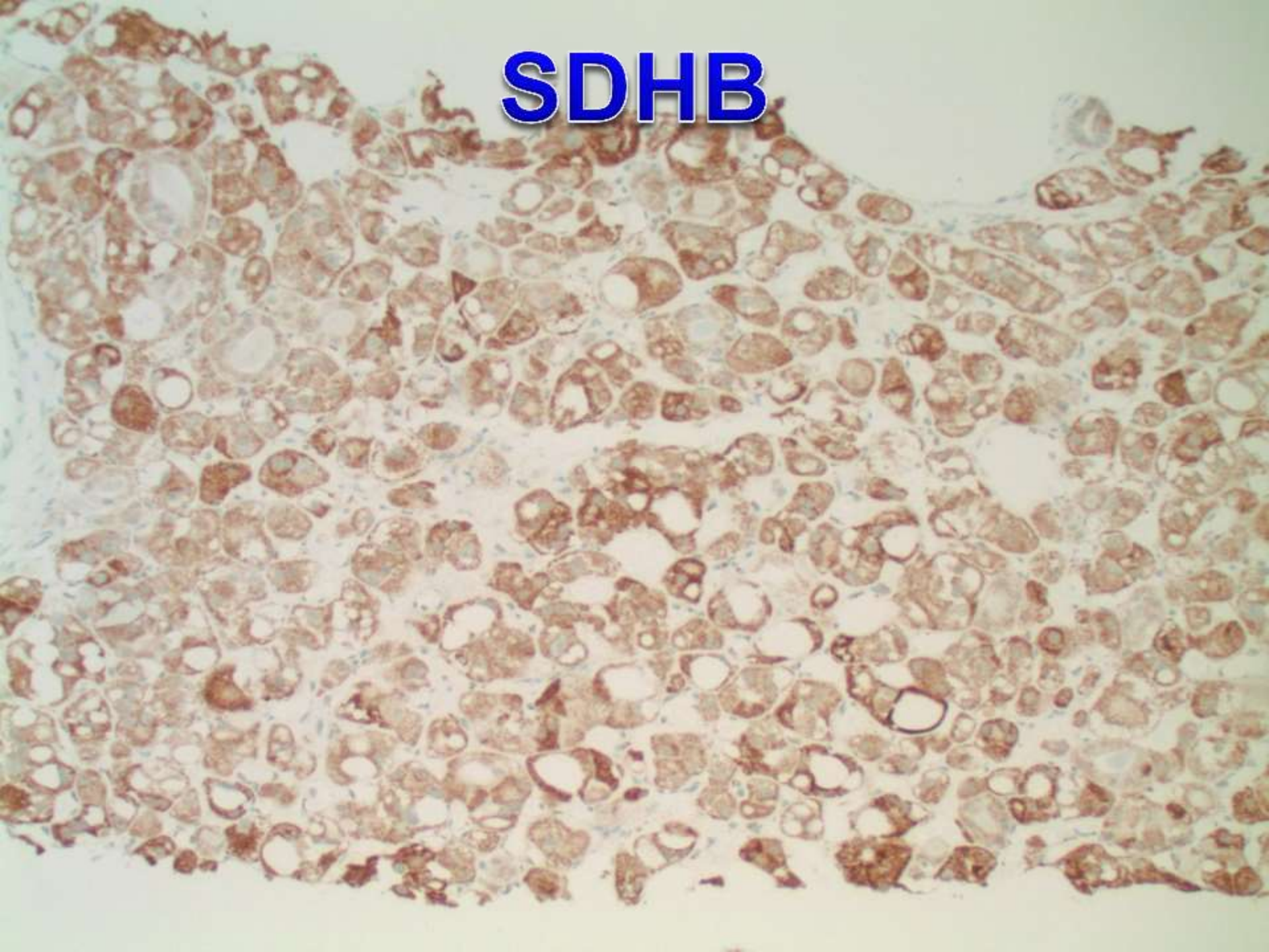
SDHB

HMB45

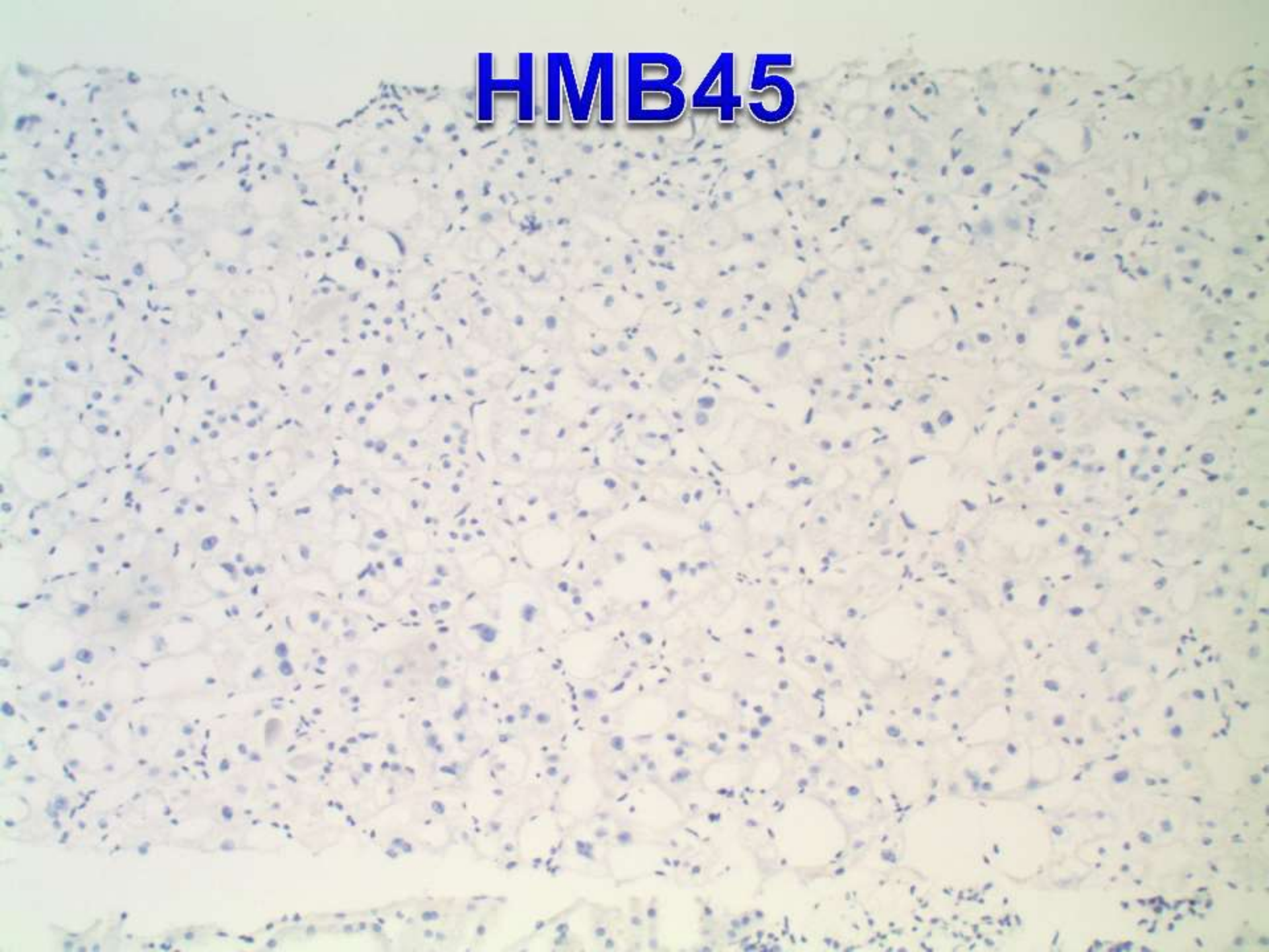

melanA

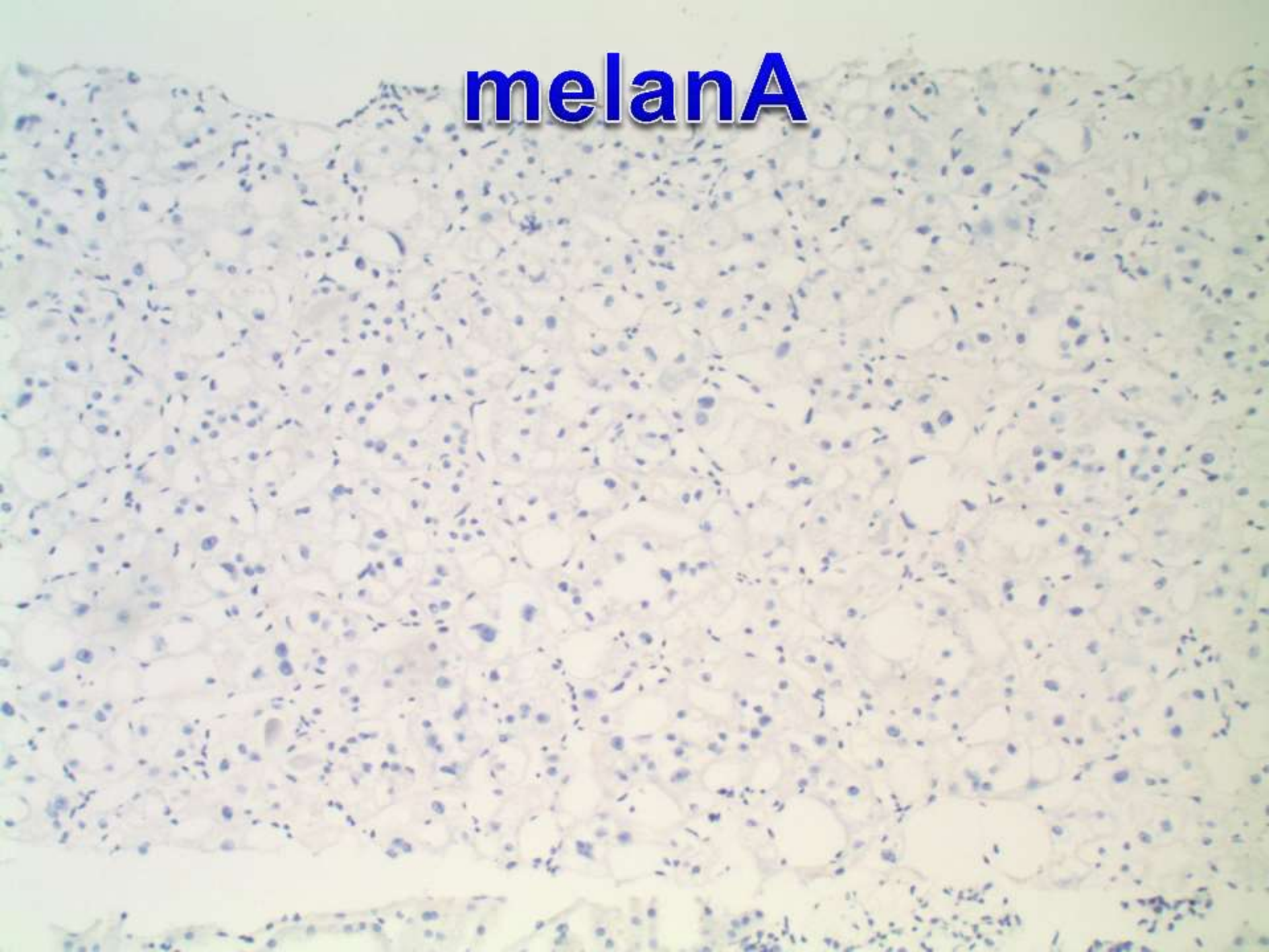

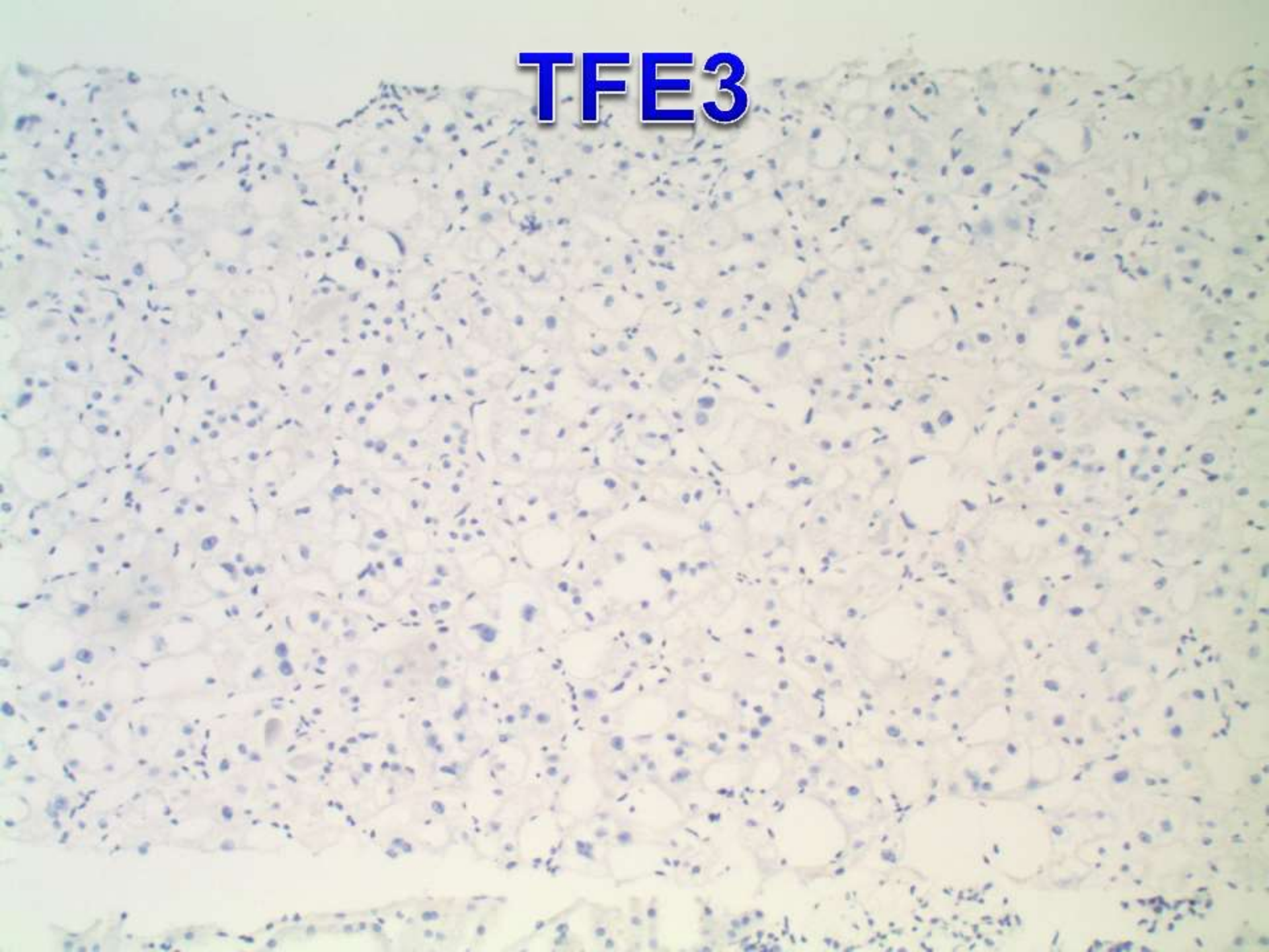
TFE3

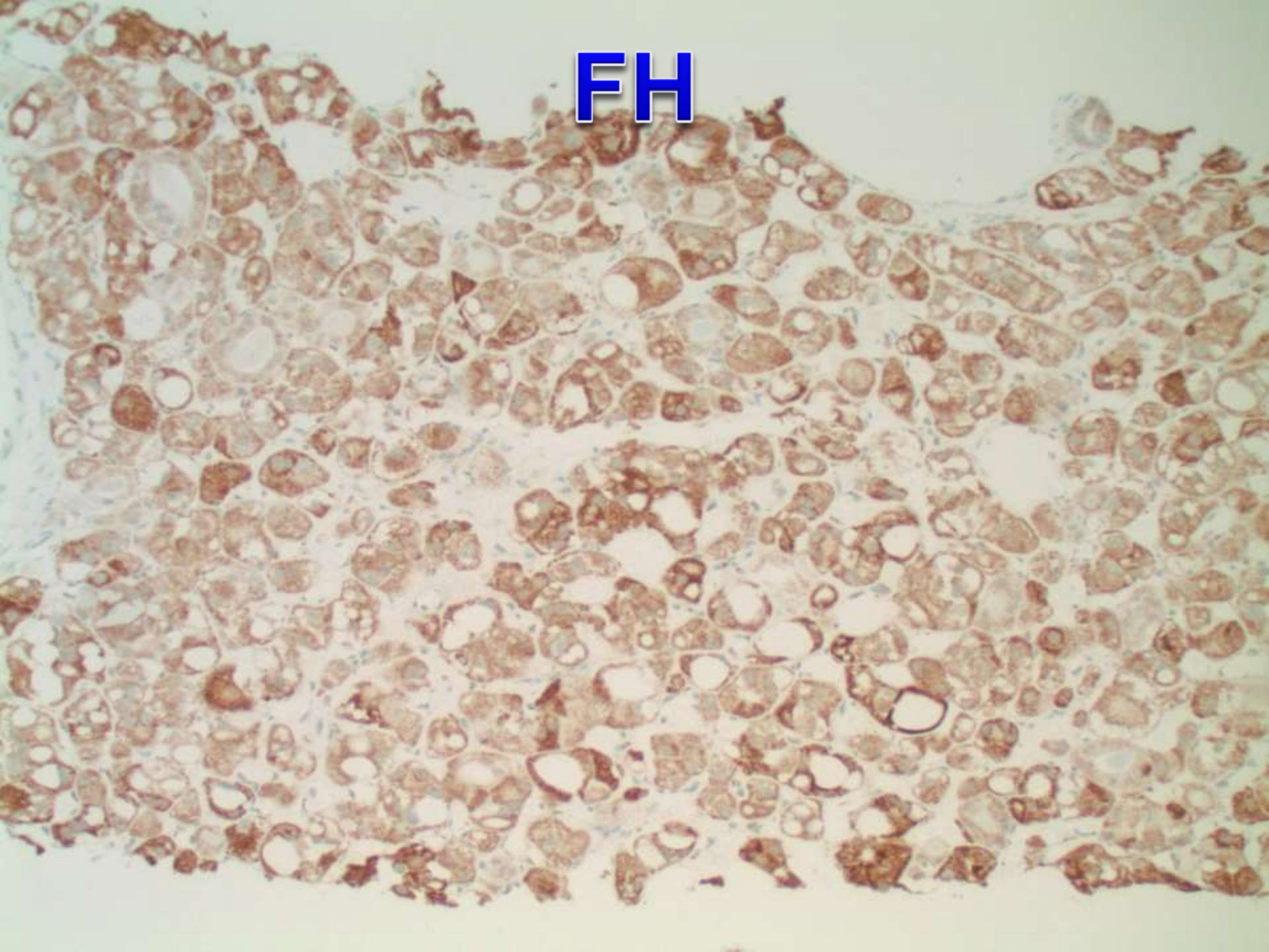
FH

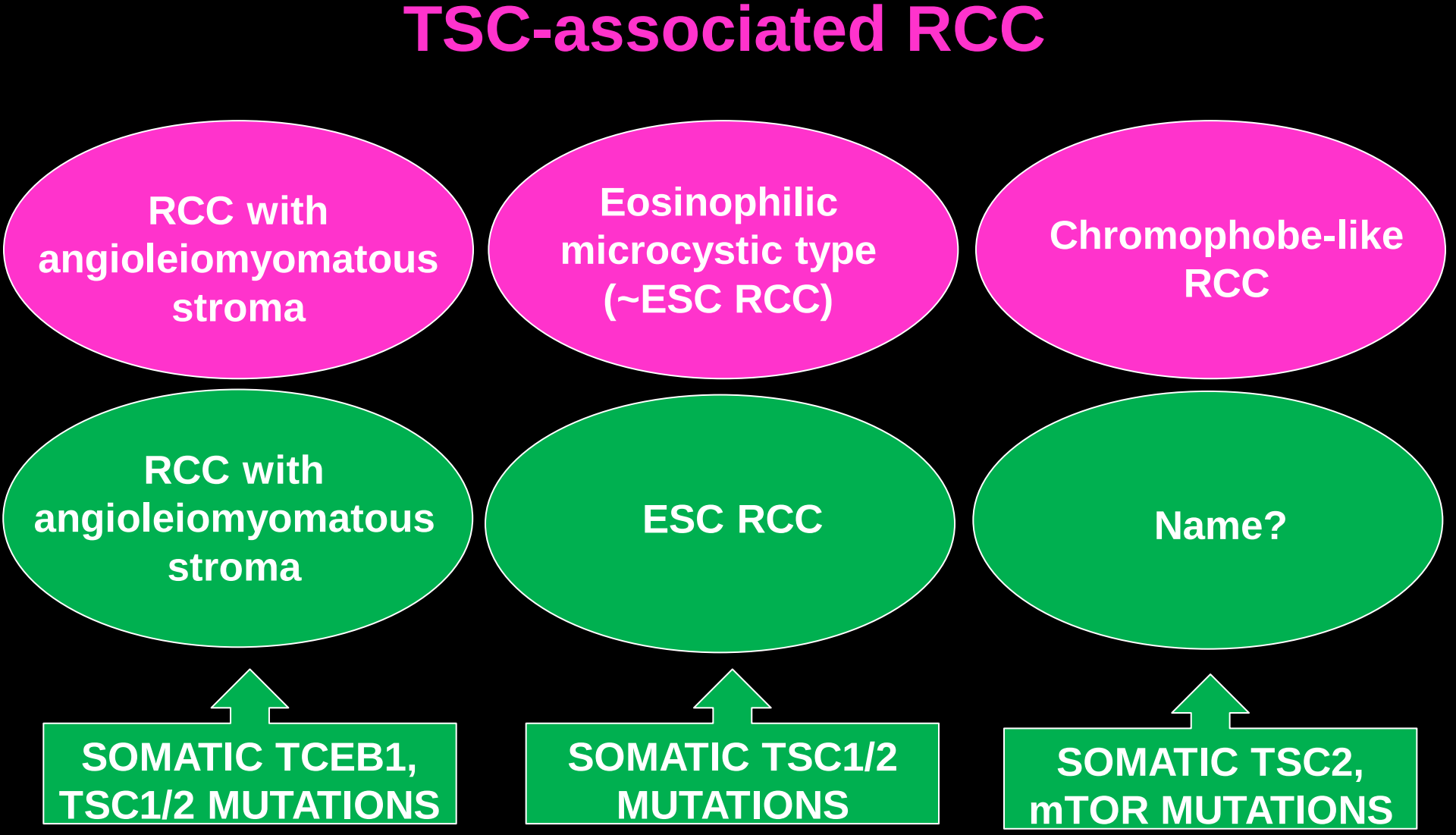
TSC-associated RCC
RCC with angioleiomyomatous stroma
Eosinophilic microcystic type (~ESC RCC)
Chromophobe-like RCC
RCC with angioleiomyomatous stroma
ESC RCC
Name?
SOMATIC TCEB1, TSC1/2 MUTATIONS
SOMATIC TSC1/2 MUTATIONS
SOMATIC TSC2, mTOR MUTATIONS
Sporadic RCC

Platinum Priority – Kidney Cancer

Editorial by Pedram Argani on pp. 487–488 of this issue

Somatic Bi-allelic Loss of *TSC* Genes in Eosinophilic Solid and Cystic Renal Cell Carcinoma

Rohit Mehra [a,b,c,†], Pankaj Vats [a,c,d,†], Xuhong Cao [c,e], Fengyun Su [a,c], Nicole D. Lee [c], Robert Lonigro [a,c], Kumpati Premkumar [c,e], Kiril Trpkov [f], Jesse K. McKenney [g], Saravana M. Dhanasekaran [a,c,‡], Arul M. Chinnaiyan [a,b,c,e,‡,]*

EUROPEAN UROLOGY 74 (2018) 483–486

Eosinophilic Solid and Cystic (ESC) Renal Cell Carcinomas Harbor *TSC* Mutations

Molecular Analysis Supports an Expanding Clinicopathologic Spectrum

Doreen N. Palsgrove, MD, Yunjie Li, MD,* Christine A. Pratilas, MD,* Ming-Tseh Lin, MD, PhD,* Aparna Pallavajjalla, MS,* Christopher Gocke, MD,* Angelo M. De Marzo, MD, PhD,* Andres Matoso, MD,* George J. Netto, MD,*† Jonathan I. Epstein, MD,* and Pedram Argani, MD**

Am J Surg Pathol 2018;42:1166–1181

Somatic Mutations of *TSC2* or *MTOR* Characterize a Morphologically Distinct Subset of Sporadic Renal Cell Carcinoma With Eosinophilic and Vacuolated Cytoplasm

Ying-Bei Chen, MD, PhD, Leili Mirsadraei, MD, Gowtham Jayakumaran, MS, Hikmat A. Al-Ahmadie, MD, Samson W. Fine, MD, Anuradha Gopalan, MD, S. Joseph Sirintrapun, MD, Satish K. Tickoo, MD, and Victor E. Reuter, MD

Am J Surg Pathol 2019;43:121–131

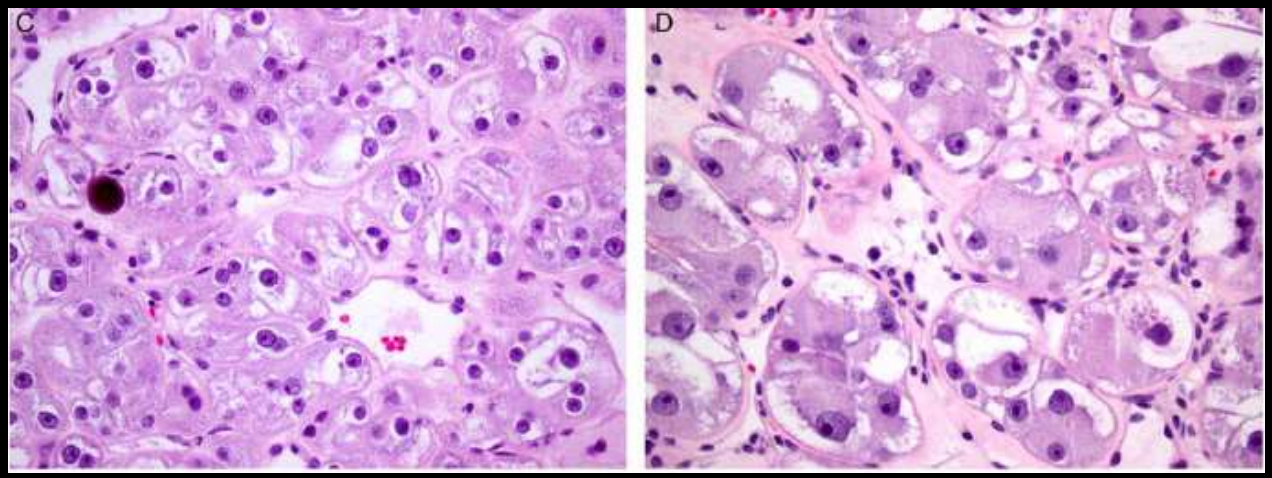

Dx (formal name TBD…):

- **ESC RCC-like carcinoma with somatic TSC2/mTOR mutation**
  - differences vs ESC RCC
    - Unique copy number alterations
    - Nested growth pattern (less cystic)
    - Thick-walled vessels, calcification
    - weak/neg CK20+, cathepsinK+ (often strong)

19-0310

Sharon Wu; El Camino Hospital

81-year-old female with progressive anemia requiring RBC transfusion, cachexia, ataxia, falls, cognitive impairment. Bone marrow biopsy performed.

Clinical History

- WBC 2.6 K/uL
- RBC 2.99 M/uL
- Hb 9.2 g/dL
- Hct 28%
- MCV 94 fL
- RDW 16.7%
- ANC 1.1 K/uL
- ALC 1.1 K/uL

- Neut 43%
- Lymphs 43%
- Mono 11%
- Eos 3%
- Baso 1%

Clinical History

- Fe 73 uL/dL
- Iron sat% 33%
- Ferritin 828 ng/mL
- Vit B12 405 pg/mL
- SPEP normal pattern
- Hep B negative
- Hep C Negative
- ANA Negative

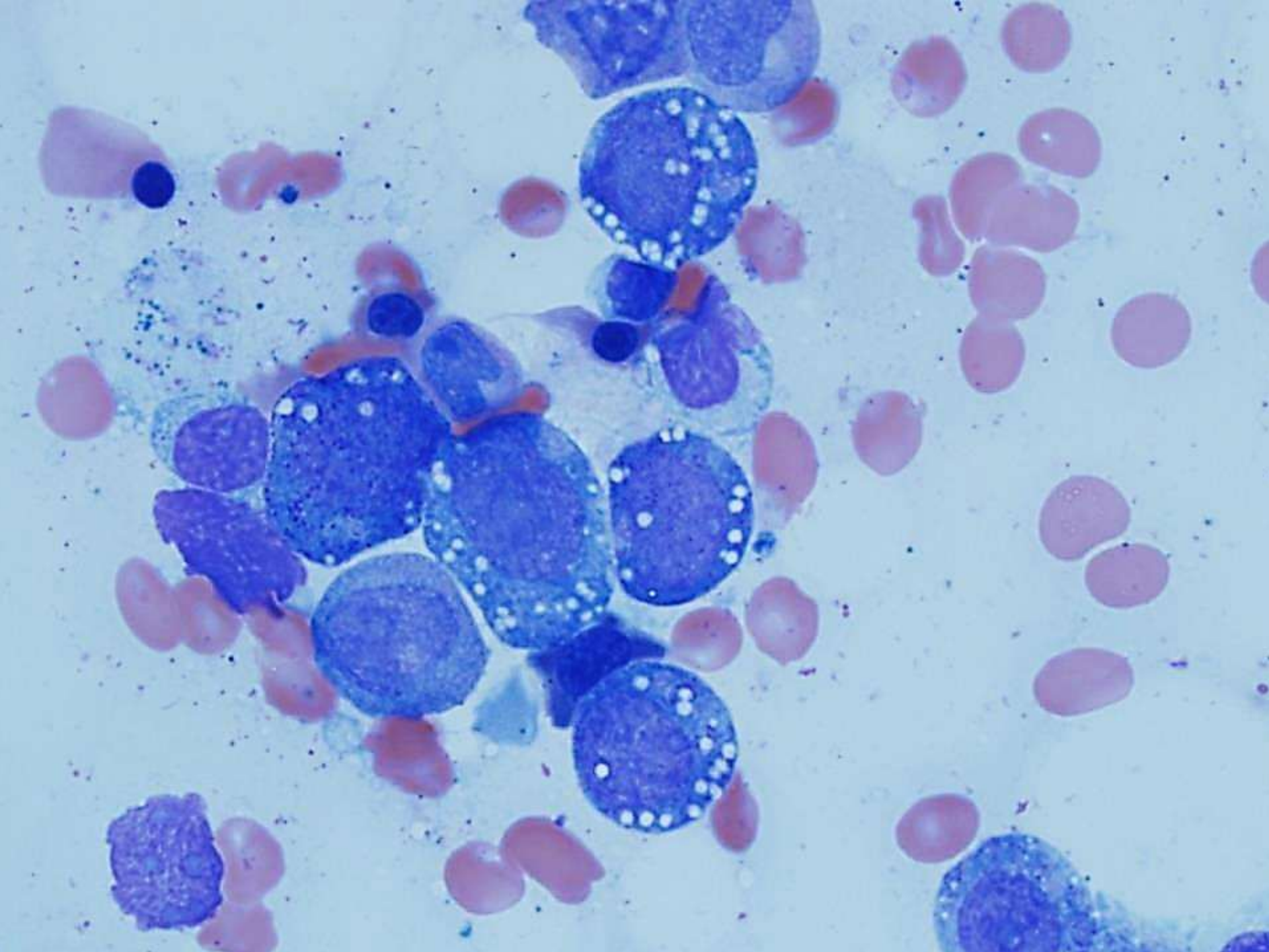

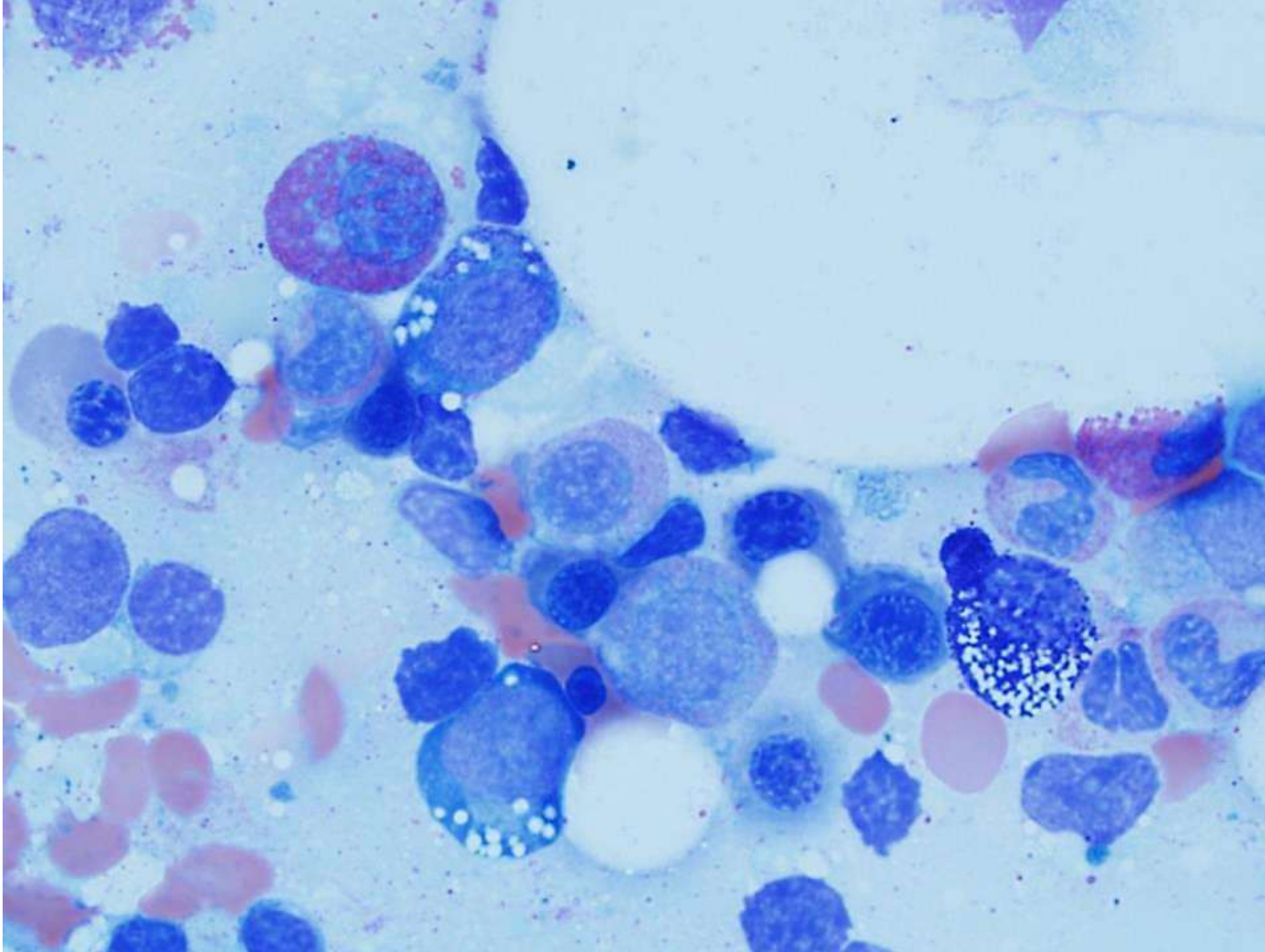

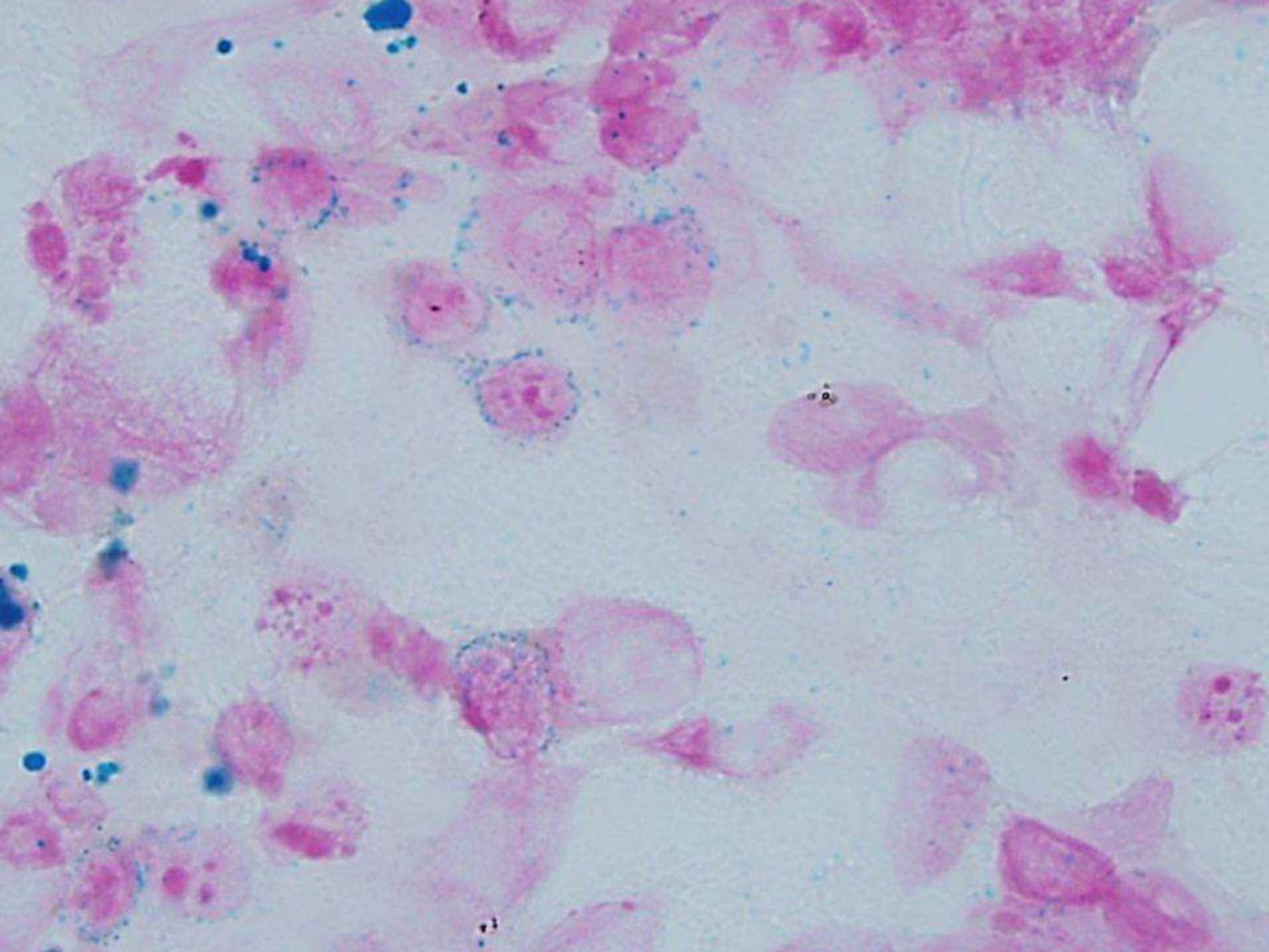

Clinical History

- WBC 2.6 K/uL
- RBC 2.99 M/uL
- Hb 9.2 g/dL
- Hct 28%
- MCV 94 fL
- RDW 16.7%
- ANC 1.1 K/uL
- ALC 1.1 K/uL

- Neut 43%
- Lymphs 43%
- Mono 11%
- Eos 3%
- Baso 1%

Clinical History

- Fe 73 uL/dL
- Iron sat% 33%
- Ferritin 828 ng/mL
- Vit B12 405 pg/mL
- SPEP normal pattern
- Hep B negative
- Hep C Negative
- ANA Negative

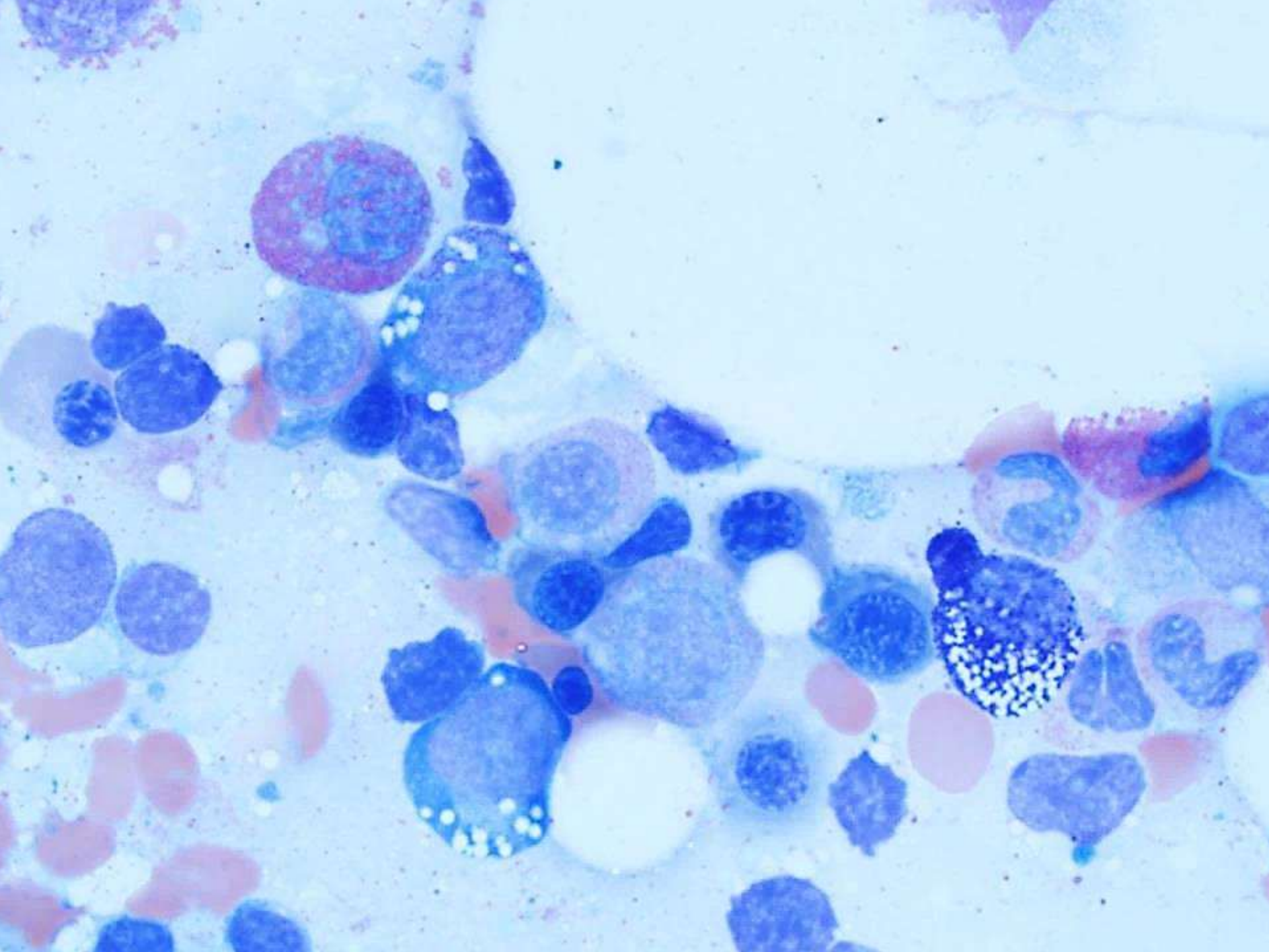

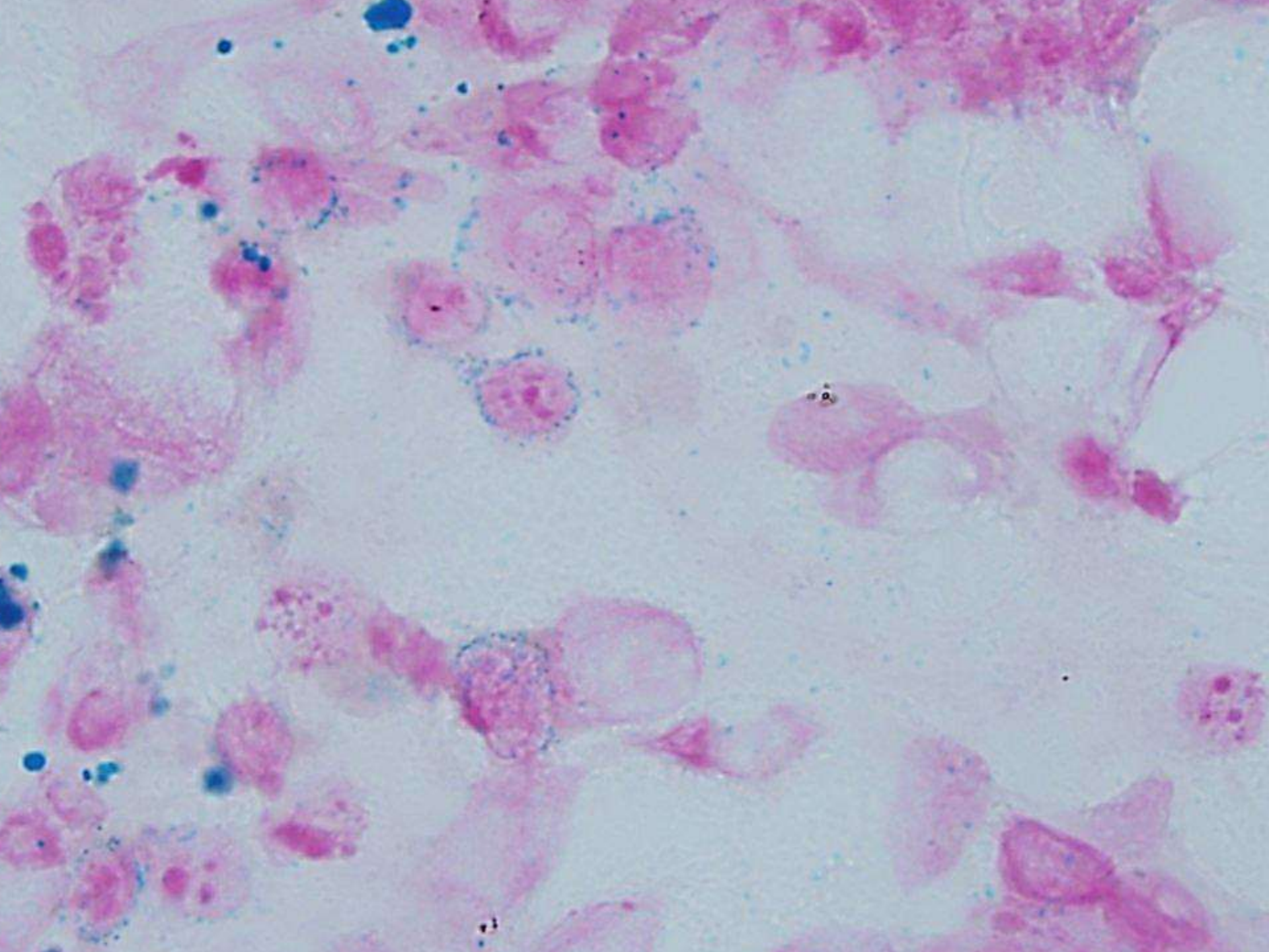

Differential diagnosis

- Cytoplasmic vacuoles within bone marrow cells
  - With ring sideroblasts:
    - **Copper deficiency**
    - **Myelodysplastic syndrome / AML**
  - Without ring sideroblasts:
    - Acute lymphoblastic leukemia
    - Plasma cell myeloma

Differential diagnosis with myelodysplasia

- The overall findings are subtle and nonspecific, and the differential diagnosis includes autoimmune disorders, drug or toxin exposure, hormones or growth factors, vitamin or **essential element deficiencies**, and viral infections, as well as a subtle myelodysplastic syndrome (MDS).

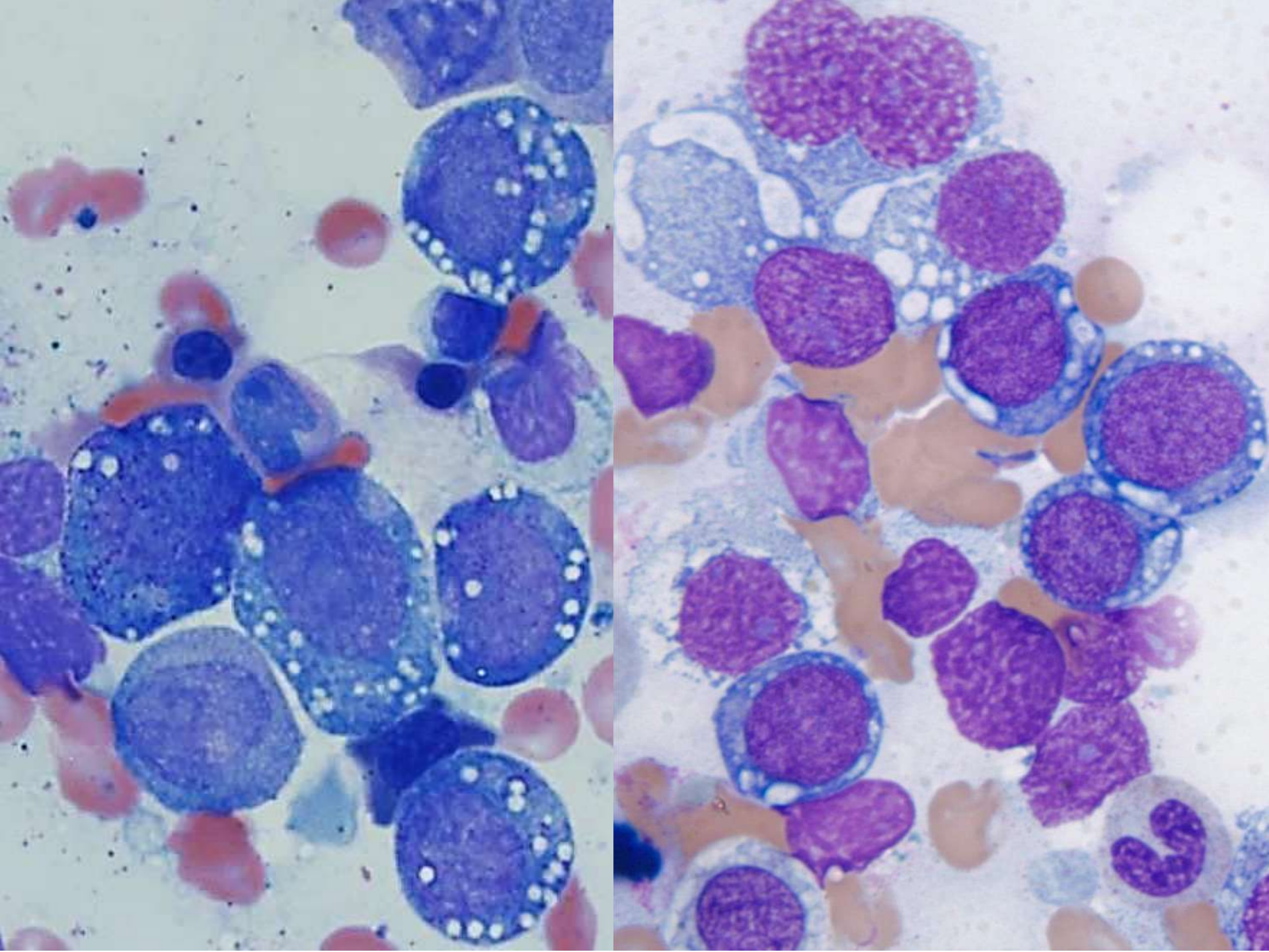

Additional Labs

- Copper, serum 23 (L) (70-175 ug/dL)
- Ceruloplasmin 7.49 (L) (20-60 mg/dL)
- Copper, RBC 0.46 (L) (0.53-0.9 ug/L)

Cytogenetics and FISH

- Normal 46,XX karyotype
- MDS FISH with normal results

Acquired copper deficiency

- Chronic alcoholism
- Parenteral nutrition
- **Prolonged malnourishment**
- Status post gastrectomy
- Zinc supplementation
- Copper chelation
- Premature infants

Effects of copper deficiency

- Normocytic, microcytic or macrocytic anemia
- Neutropenia
- Irreversible myeloneuropathy

Copper and iron metabolism

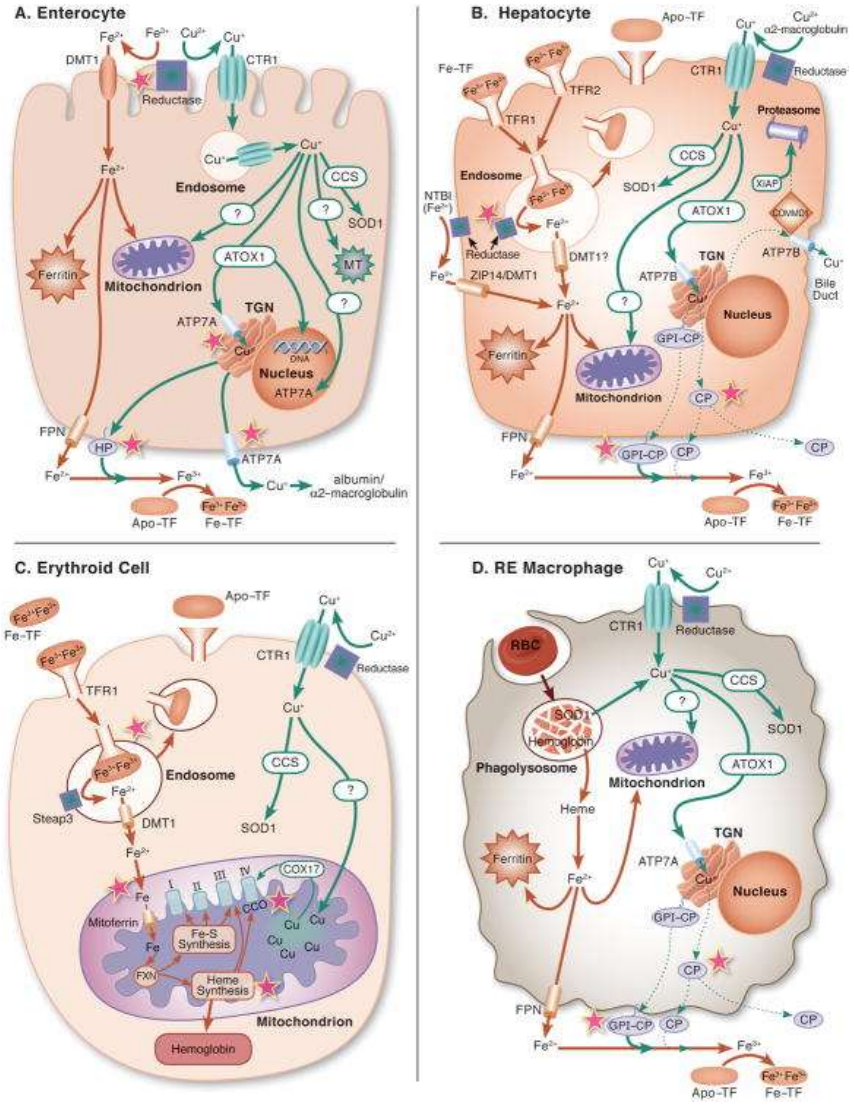

Collins, et al. [Nutr Rev. 2010 Mar; 68(3): 133–147.]

Copper Sources